STUDY ON CHARACTERIZATION, STABILITY AND ENCAPSULATION ACTIVITY OF MONO AND MULTILAYER EMULSION (OIL IN WATER) PREPARED USING CAVITATION

PhD Thesis

JITENDRA CARPENTER

ID No. 2014RCH9505

DEPARTMENT OF CHEMICAL ENGINEERING

MALAVIYA NATIONAL INSTITUTE OF TECHNOLOGY JAIPUR

November, 2019

"Study on characterization, stability and encapsulation activity of mono and multilayer emulsion (oil in water) prepared using cavitation"

Submitted in

fulfillment of the requirements for the degree of

Doctor of Philosophy

by

JITENDRA CARPENTER

(2014RCH9505)

Under the supervision of

DR. VIRENDRA KUMAR SAHARAN

Assistant Professor

DEPARTMENT OF CHEMICAL ENGINEERING

MALAVIYA NATIONAL INSTITUTE OF TECHNOLOGY JAIPUR

November 2019

DECLARATION

I, **Jitendra Carpenter**, declare that this thesis titled **"Study on characterization, stability and encapsulation activity of mono and multilayer emulsion (oil in water) prepared using cavitation***"* and the work presented in it, are my own. I confirm that:

- This work was done wholly or mainly while in candidature for a research degree at this university.
- Where any part of this thesis has previously been submitted for a degree or any other qualification at this university or any other institution, this has been clearly stated.
- Where I have consulted the published work of others, this is always clearly attributed.
- Where I have quoted from the work of others, the source is always given. With the exception of such quotations, this thesis is entirely my own work.
- I have acknowledged all main sources of help.
- Where the thesis is based on work done by myself, jointly with others, I have made clear exactly what was done by others and what I have contributed myself.

Date: 01/11/2019

Jitendra Carpenter

(2014RCH9505)

MALAVIYA NATIONAL INSTITUTE OF TECHNOLOGY, JAIPUR

DEPARTMENT OF CHEMICAL ENGINEERING

JAIPUR-302017, INDIA

<u>CERTIFICATE</u>

This is to certify that the thesis entitled

"Study on characterization, stability and encapsulation activity of mono and multilayer emulsion (oil in water) prepared using cavitation"

being submitted by **Jitendra Carpenter (2014RCH9505)** is a bonafide research work carried out under my supervision and guidance in fulfillment of the requirement for award of the degree of **Doctor of Philosophy** in the Department of Chemical Engineering, Malaviya National Institute of Technology, Jaipur, India. The matter embodied in this thesis is original and has not been submitted to any other University or Institute for the award of any other degree.

Place: Jaipur   **Dr. Virendra Kumar Saharan**

Date: 01 Nov 2019   Assistant Professor

                                                                               Department of Chemical Engineering

                                                                                              MNIT Jaipur

Abstract

In this doctoral thesis, cavitation techniques (ultrasound and hydrodynamic) have been utilized with an intensifying approach for producing oil in water (O/W) emulsions with higher attributes such as minimum droplet size, enhanced stability and higher encapsulation efficiency. This research work aims to advance the understanding of ultrasonic and hydrodynamic cavitation based emulsification process. The motivation of this work was to understand the fundamentals related to the kinetic stability of oil in water emulsions of cavitationally prepared emulsions which are yet to be fully elucidated. This research work deals with the detailed study on the formulation, stability and encapsulation characteristics of mono and multilayer nanoemulsions prepared using ultrasonic and hydrodynamic cavitation. It also considers the impact of ultrasonic and hydrodynamic cavitation parameters on the physicochemical properties of emulsions as well as the significance of the effect of these cavitation process parameters on the emulsion properties such as droplet size, encapsulation stability and chemical stability.

This thesis contains an introduction outlining the background information on the emulsion science and fundamentals of cavitation techniques for the generation of O/W emulsions. The overall study in this research work consists of four major parts which are described as follows:

In the first part of thesis, the mustard oil in water nanoemulsions stabilized by Span 80 and Tween 80 were prepared using ultrasonication with detailed optimization of the various process conditions. Effects of various operating parameters such as HLB (Hydrophilic Lipophilic Balance) value, surfactant volume fraction (φ_S), oil volume fraction (φ_O) and power amplitude were investigated and optimized on the basis of minimum droplet size and stability of nanoemulsions. It was observed that minimum droplet size of about 87.38 nm was obtained within 30 min of ultrasonication at an optimum HLB value of 10, φ_S of 0.08 (8%, v/v), φ_O of 0.1 (10%, v/v) and ultrasonic power amplitude of 40%. The detailed statistical analysis was also conducted using response surface methodology and Analysis of variance technique to describe the significance of the process parameters on the emulsion droplet size. It has been observed that the oil fraction was found to be the most significant factor affecting the droplet size of emulsion. The significance level was found to be in the

order as $\varphi_O > \varphi_S > \%$ Amp $>$ Time $>$ HLB. The stability of the nanoemulsion was measured through visual observation and it was found that the unstable emulsions got separated within 24 hours whereas, stable emulsions never showed any separation until 90 days. In addition to that, the kinetic stability of the prepared nanoemulsions was also assessed under centrifuge and thermal stress conditions. The emulsion stability was found to be unaffected by these forces as the droplet size remained unchanged. The ultrasound prepared emulsion was found to be stable even after 3 months of storage at ambient conditions without any visual evidence of creaming and phase separation and also remained kinetically stable. FTIR analysis of the emulsions at different sonication conditions was carried out to examine the possible impact of ultrasonically induced chemical effects on the oil structure during emulsification and it was found that the oil molecular structure was unaffected by ultrasonication process. This work illustrates the formation and stability of mustard oil in water nanoemulsion using ultrasound cavitation which may be useful in food and cosmetic based applications.

In the second part, nanoemulsions were prepared with the same system but with a different cavitation technique i.e. hydrodynamic cavitation (HC) and compared with ultrasonication process. In this work, detailed geometrical analysis of hydrodynamic cavitating devices was carried out to investigate the effect of geometry (orifice and venturi of different shapes) and geometrical parameters on the formation and stability of mustard oil in water nanoemulsion. The optimization of geometrical parameters was carried out based on the lowest droplet size obtained and droplet size reduced per unit pass. It was observed that the single hole orifice plate of circular shape having lower perimeter and higher flow area than other orifice devices, was found to be an efficient device which produced emulsion of lowest droplet size i.e. 87 nm at an optimum C_V of 0.19 (10 bar optimum operating pressure) in 90 min of processing time. A mathematical correlation was also developed using dimensionless analysis approach for understanding the effect of various operating and geometrical parameters of HC. The mathematical expression to calculate the droplet size was found to be the function of dimensionless numbers such as Reynold number, Weber number and cavitation number. Moreover, the kinetic stability of the nanoemulsion was also assessed under centrifugal and thermal stress conditions and it was found to be unaffected by these forces as no change in the droplet size observed during the assessment. The prepared nanoemulsions were found to be stable up to 3 months indicating the potential of HC over

high energy techniques for producing highly stable nanoemulsion on a large scale. Furthermore HC was found to be 11 times more energy efficient than acoustic cavitation/ultrasonication in the preparation of nanoemulsion.

In the third part, a different kind of emulsion i.e. multilayer O/W emulsion was prepared using layer by layer approach which is a potential system that can be utilized particularly in food and pharmaceuticals for the encapsulation of various nutraceuticals. The ultrasonication method was used for the preparation of multilayer O/W emulsion stabilized with whey protein isolate (WPI) and sodium alginate (SA). Ultrasonication was employed in both batch and recirculating flow configurations. The effect of process parameters such as pH, SA concentration, and sonication time on the droplet size, zeta potential, morphology, physical and oxidative stability of the multilayer emulsion was studied using batch process. It was observed that the emulsion prepared at pH 5, 0.2 wt% SA and 60 sec sonication had good bilayer interaction between WPI and SA molecules. Moreover, it was found that sonication, if given for a controlled time period can improve the physical and oxidative stability of the emulsion. Further, the ultrasonication based recirculating flow configuration (RFC) was utilized for the preparation of multilayer emulsion at the optimum operational conditions obtained in the batch studies. Emulsions prepared using RFC were found to have better physical and oxidative stability than using batch ultrasonication at the optimum flow rate of 0.5 L/min with 6 recirculation passes. RFC was found to be 2.5 times more energy efficient than batch ultrasonication process for the synthesis of multilayer emulsions.

In the fourth part of this thesis, the multilayer emulsion prepared using ultrasonication process was utilized as a carrier system for the encapsulation of a bioactive compound i.e. curcumin. Curcumin is a natural polyphenol compound which is obtained from the turmeric plant, having numerous health promising benefits. In order to deliver the curcumin into the human body, it is necessary to develop an efficient carrier system for its encapsulation such that the physico-chemical properties of curcumin can be preserved during the storage. In this study, the encapsulation stability, antioxidant activity and release properties of curcumin encapsulated in the primary emulsion (PE, stabilized by whey protein isolate) and secondary emulsion (SE, stabilized by double layer of whey protein isolate/sodium alginate) prepared using ultrasonication was analyzed. It was observed that the formation of a double layer

coating of secondary biopolymer over the primary coated droplet enhanced the encapsulation efficiency and antioxidant activity of the curcumin during the storage of 3 weeks. Moreover, the multilayer emulsions were freeze dried in order to see the effect of dehydration of emulsion on the stability of multilayer coated droplets. FTIR analysis indicated the presence of all the constituents including curcumin after the freeze drying of the emulsions. SEM images showed that the microstructure of emulsion droplets was found to be uniformly distributed in case of SE. The antioxidant activity of curcumin encapsulated in SE was found to be higher during storage whereas it was significantly reduced in other encapsulated systems like PE, olive oil and ethanol. In vitro release of curcumin from the multilayer emulsion was carried out under the simulated intestinal conditions of pancreatin enzyme and bile salt. The maximum release of 73% and 64% was obtained in SE and PE, respectively within 2 h of digestion. The different kinetic models such as zero order, first order and Higuchi model were fitted to understand the release kinetic of curcumin. The best fitting was obtained with zeroth order kinetic model based on the regression analysis of the data. Overall this study provided useful information on the formation of multilayer emulsion as a carrier system for better protection and controlled release of curcumin for the food and pharmaceutical applications.

Overall this research work highlights the efficient utilization of both the cavitation techniques i.e. ultrasound and hydrodynamic cavitation for the preparation of different oil in water emulsions which has potential application in food, pharmaceutical and cosmetic industries. Efforts have been made to improve the efficiency of the ultrasonication process not only to get the high stability emulsion but also to improve the throughput capacity of the emulsification process. On the other side, the HC proved its potential for the synthesis of emulsion on a large scale with desired stability and thus can be a good substitute to the other high energy extensive techniques used in the industries. The potential of cavitationally prepared multilayered emulsion for the encapsulation of bioactive compound was thoroughly investigated and it was concluded that the cavitation process is a viable and feasible technique for the production of emulsions as an encapsulating system for the various bioactive compounds that are useful in food, cosmetic and pharmaceutical industries.

Table of Contents

Chapter 5

Curcumin encapsulation in multilayer O/W emulsion: synthesis using   **145**

ultrasonication and studies on stability, antioxidant and release activity

Chapter 6

Conclusions and Scope for future work   **176**

List of Tables

List of Figures

Publications, Conferences and Awards

A) Publications in Journals:

1. **J. Carpenter,** V.K. Saharan, Ultrasonic assisted formation and stability of mustard oil in water nanoemulsion: Effect of process parameters and their optimization, *Ultrasonics Sonochemistry* 35 (2017) 422-430.

2. **J. Carpenter,** S. George, V.K. Saharan, Low pressure hydrodynamic cavitating device for producing highly stable oil in water emulsion: Effect of geometry and cavitation number, *Chemical Engineering and Processing: Process Intensification* 116 (2017) 97-104**.**

3. **J. Carpenter,** S. George, V. K. Saharan, A comparative study of batch and recirculating flow ultrasonication system for preparation of multilayer olive oil in water emulsion stabilized with whey protein isolate and sodium alginate. *Chemical Engineering and Processing: Process Intensification* 125 (2018) 139-149.

4. **J. Carpenter,** S. George, V. K. Saharan, Curcumin encapsulation in multilayer oil in water emulsion: synthesis using ultrasonication and studies on stability, antioxidant and release activity. *Langmuir* 35(33) (2019) 10866-10876.

5. **J. Carpenter,** M. Badve, S. Rajoriya, S. George, V.K. Saharan, A.B. Pandit, Hydrodynamic cavitation: an emerging technology for the intensification of various chemical and physical processes in a chemical process industry, *Reviews in Chemical Engineering* 33 (5) (2017), 433-468**.**

6. S. Rajoriya, **J. Carpenter,** V.K. Saharan, A. B. Pandit, Hydrodynamic cavitation: an advanced oxidation process for the degradation of bio-refractory pollutants, *Reviews in Chemical Engineering* 32 (2016) 379-411**.**

B) Conference Presentations:

1. **J. Carpenter,** V. K. Saharan, Impact of ultrasonication on multilayer oil in water emulsion characteristics: a comparative study between batch and recirculating flow process, *4th International Conference of Chemical Engineering & Industrial Biotechnology (ICCEIB)*, August 1-2, 2018, Kuala Lumpur, Malaysia,.

2. V. K. Saharan, **J. Carpenter,** Hydrodynamic and Acoustic cavitation assisted preparation of Oil in water emulsion stabilized with non-ionic emulsifiers and biopolymers, *3rd Asian Oceania Sonochemical Society (AOSS)*, September 14-16, 2017, Chennai, India,

C) Awards:

1. **CSIR-Senior Research Fellowship Award**, May 2018
2. **SERB-Young Scientist and International Travel Grant Award**, October 2018

DEDICATED TO

MY PARENTS,

MY FAMILY AND

MY LORD GURUDEV

CHAPTER 1

INTRODUCTION AND LITERATURE REVIEW

1.1) Emulsion and its applications

A colloidal dispersion is a two phase system in which one phase (disperse phase) is dispersed into another phase known as continuous phase. The dispersed phase which comprises of colloidal particles may be in the form of solid, liquid or gas phase. When the continuous phase is liquid, the nature of the dispersions describe its form such as if solid particles are dispersed in liquid, the dispersion is called as suspensions, if gas molecules are dispersed in liquid, the dispersion is called as foam and if liquid particles are dispersed in another liquid, the dispersion is called *emulsion.*

Emulsion is a homogenous mixture of two immiscible liquids and the process of mixing two immiscible liquids is called emulsification. In the emulsion, an interface is formed between the oil and water which induces some interfacial tension that separates the two liquids [1]. The force induced between the two liquids is called interfacial tension whereas for the different nature of phases such as when one phase is gaseous then the force induced between them is called surface tension. The interfacial tension is defined as the force per unit length parallel to the interface and measured as mN/m. The thickness of interfacial region is very small. The interfacial region having tension "σ" (mN/m) exhibits some interfacial area. Thus the extent of emulsification increases when interfacial tension reduces which results into increased interfacial area of the region [1].

Emulsions can be classified mainly as (1) oil-in-water, (2) water-in-oil emulsions and (3) multiple emulsions which is combination of both. The kind of emulsion either O/W and/or W/O are basically prepared based on their application. Particularly in most of the chemical processes such as foods, medicinal, pharmaceuticals and cosmetics, O/W emulsions have been utilized for the development of various products. According to the droplet size, one can distinguish emulsions into three categories i.e. (1) macroemulsions, having the droplet size > 1000 nm, (2) miniemulsions with size between 400 and 1000 nm; and (3) nanoemulsion having droplet size of < 300 nm [2, 3].

In food industries, most of the foods ingredients are lipophilic in nature and hence oil in water emulsions are found to be the suitable systems for the delivery of lipophilic compounds such as oils, fatty acids, vitamins, flavors, etc. Also, many natural and processed foods such as milk, creams, beverages, soups, salad dressings, mayonnaise, sauces, deserts, etc. are produced in the form of emulsions. The main advantage of the encapsulation of

foods via emulsification is that they can retain and preserve the properties of these food supplements such as odor, flavor, rancidity, oxidative stability, and essential fats and vitamins for a longer time [1, 4].

In the pharmaceutical industry, many functional and essential drugs are not water soluble and require an alcohol or another organic solvent to form solutions. These solvents may be costly, hazardous to handle and are toxic in nature and thus are not suitable for human health. Through emulsification, these ingredients or drugs become more palatable, and these emulsion based encapsulating media improves the effectiveness and aesthetics of topical drugs such as ointments. Emulsification as an encapsulating medium for the drug is more popular due to their low toxicity, ability to be injected directly into the body, and compatibility with many drug ingredients [5].

In cosmetics applications, emulsions are gaining importance due to their ability to hold the active ingredients for a longer time while maintaining the physico-chemical properties of these ingredients and thus allow the effective delivery of active ingredients into the skin. They are found to be suitable carrier systems for many hair and skin conditioning agents. They are used to deliver various oils and waxes which provide moisturization, smoothness and softness to hair and skin. Emulsions are widely used in cosmetic products such as body creams, bathing oils, sunscreen lotions and many more [4, 6].

In the agricultural industry, emulsions can be used as an encapsulating system for various biocides such as insecticides, pesticides and fungicides. These hydrophobic biocides are usually applied to various crops at very low levels, using spray technique through mechanical devices. An emulsification technique allows the dilution of these biocides to the permissible limit and provides improved sprayability during the application on the crops [4-6]. Similarly in other industries such as paints, bitumen industries etc. various emulsions have been used as the delivery system for either aqueous or oil based actives (or both) [4, 6].

1.2) Stability of emulsions

The significant factor which needs to be considered before the formation of various kinds of emulsion is the stability of the prepared emulsion. Higher the stability of emulsion better would be the shelf life of the materials or products which are encapsulated in the emulsion.

The stable emulsion helps to maintain the physicochemical properties of the nutraceuticals or any bioactive compounds over the longer time. The emulsions (nano and submicron) except microemulsions are usually thermodynamically unstable [2-7]. However, the kinetic stability of the emulsion is affected by various destabilization mechanisms such as creaming, coalescence, flocculation, Ostwald ripening, etc. [6, 7]. The thermodynamic stability gives the information about the processes or changes taking place before and after the emulsification process whereas the kinetic stability gives information about the rate at which these changes or processes occur. The emulsions formed for many applications such as food, pharmaceuticals etc., are usually formed non-spontaneously and destabilizes at varying kinetic rates. Thus the kinetic stability is of great significance in the emulsification process. The emulsion kinetic stability depends on the various breakdown factors such as creaming, flocculation, coalescence, Ostwald ripening etc. as shown in Fig.1.1 [8].
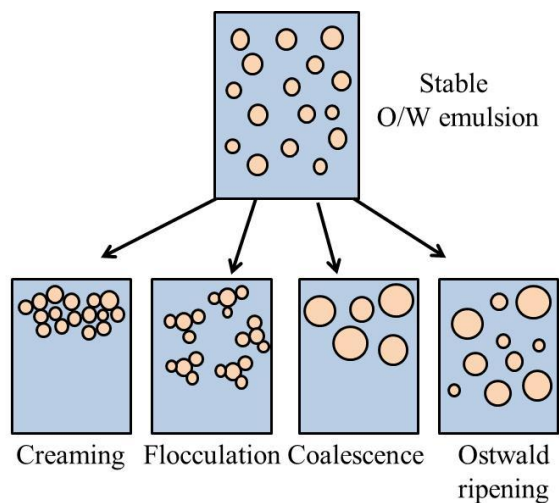
Fig. 1.1 Destabilization mechanism of O/W emulsion

Creaming is basically dependent on the density difference between the dispersed and continuous phases of an emulsion. The flocculated or aggregated droplets may either settle to the bottom (in case of W/O) or gather at the top of a sample (in case of O/W). When higher density droplets settle to the bottom of a vessel, it is known as sedimentation whereas in creaming lower density droplets migrate to the top of the emulsion surface as shown in Fig. 1.1. Whether a droplet undergoes sedimentation or creaming depends on its size, density

and viscosity of the continuous phase. Stoke's law provides an estimate of the rate of sedimentation and creaming [2]:

$$\frac{dx}{dt} = \frac{2r^2(\rho_p - \rho_l)g}{9\eta}$$

(1.3)

Where *dx/dt* is the terminal velocity of the particle/droplet, *r* is the particle/droplet radius, ρ_l is the density of the continuous phase, ρ_p is the density of the particle/droplet, *g* is the gravitational constant and η is the viscosity of the continuous phase.

Flocculation occurs under the effect of Brownian motion in which colloidal droplets below a critical size move randomly and may collide with neighboring droplets depending on the relative magnitude of the attractive and repulsive forces present between the adjacent droplets. If the total attraction energy between droplets/particles is higher than the total repulsion energy then the droplets will adhere to one another as shown in Fig 1.1. Flocculation is a reversible phenomenon where it is possible to re-disperse the clustered droplets by gentle agitation or mixing. However, if the droplets collide with sufficiently high energy then they permanently cluster together which is known as aggregation [9].

Due to random collisions between dispersed droplets, the two possible types of flocculation that can occur are: bridging and depletion flocculation [8, 9]. In bridging flocculation, large surface-active biopolymers (e.g., proteins or polysaccharides) have multiple sites to interact with other molecules, thereby causing the interaction between more than two entities/droplets. Moreover bridging also occurs, when the concentration of biopolymers is insufficient to completely saturate the droplet surface. Conversely, if the free biopolymer concentration in the continuous phase exceeds a critical value, depletion flocculation occurs as the depletion forces overcome the repulsive forces between the droplets. When non-adsorbing biopolymers are added to the aqueous phase of emulsion they increase the attraction between the oil droplets through an osmotic (depletion) effect. If the osmotic attraction generated is sufficiently high then the droplets will aggregate, and depletion flocculation occurs. The process of bridging and depletion flocculation is shown in Fig. 1.2 [9].

(a)   (b)
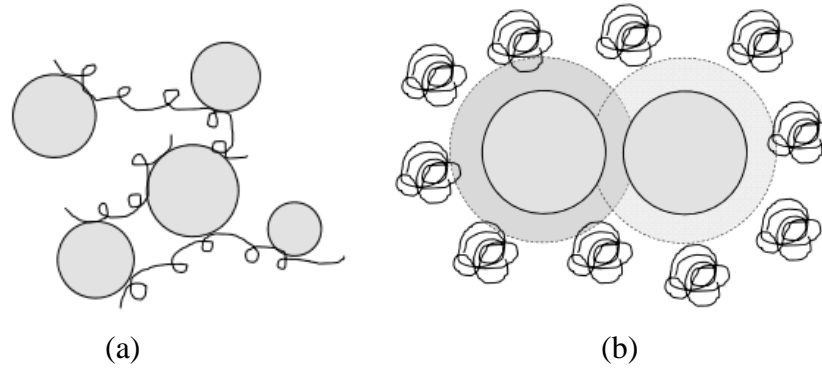
Fig. 1.2 Flocculation (a) Bridging & (b) Depletion flocculation

Coalescence occurs when two or more droplets irreversibly merge into a large droplet. This process can only occur when droplets are in close proximity and the thin film of continuous phase separating them is ruptured. The rate of coalescence depends on numerous factors such as the composition of the adsorbed surfactant layers and the local environmental conditions (e.g., ionic strength, pH, temperature etc.). Contrary to flocculation, this process is irreversible and leads to emulsion breakdown as shown in Fig 1.1 [8, 9].

Ostwald ripening is an emulsion destabilization mechanism whereby emulsion droplets of larger sizes grow by consuming the smaller ones due to the molecular diffusion through the continuous phase. It may happen in polydisperse emulsions, and takes place due to the fact that the solubility of the oil phase increases with decreasing droplet size [2]. In emulsions, which are usually polydisperse, the smaller droplets will have larger solubility when compared with the larger ones (due to curvature effects). As a consequence, the smaller droplets disappear and their molecules diffuse to the continuous phase and reform into larger droplets, thereby leading to a net increase in the droplet size. Ostwald ripening plays a prominent role in emulsion stability where the lipids are more water soluble, such as the case for flavor oils (e.g. limonene, eugenol, etc.), or when the continuous phase contains alcohol, such as cream liqueurs [10]. In O/W emulsions, this process can be inhibited by adding highly water-insoluble hydrophobic materials. The physical basis for Ostwald ripening is described by the Lifshitz-Slezov-Wagner (LSW) theory as follows [10]:

$$\frac{d(R)^3}{dt} = \frac{8}{9}\frac{\gamma V_M}{RT}S(\infty)D \qquad (1.4)$$

Where R is the radius of the emulsion droplet (m), "t" is time (s), $S(\infty)$ is the solubility of the dispersed within the continuous phase for an emulsion droplet with a planar interface (g/L), "D" is the diffusion coefficient of dispersed phase through the continuous phase (m^2/s) and γ is the interfacial tension (N/m), V_M is the molar volume of the dispersed phase (m^3/mol), R is the ideal gas constant and T is temperature in K. It can be noted from Eq. (1.2) that the radius or the oil droplets grows by molecular diffusion in third order with respect to time if other parameters remain constant. Utilization of a dispersed phase with limited solubility in the continuous phase minimizes the mechanism of Ostwald ripening [6-9].

1.3) Stabilization of emulsions

In an emulsion, when two immiscible liquids i.e. oil and water are mixed, two liquid layers are formed separated by a thin interfacial layer possessing some interfacial forces which minimizes the contact area between the two phases. In order to form an emulsion, it is required to change this layer position by bringing some energy into the system. On giving an adequate energy to the system, the disruption of interfacial layer occurs and consequently the interfacial area between the phases increases. But when droplets of oil in continuous phase are formed under agitation, they constantly move, thus collide and may coalesce with each other. After some times, the larger droplets are formed and the two phases get separated as a result of droplets coalescence. The use of an emulsifier is then necessary to avoid the droplets from merging.

The interfacial forces are characterized by the Laplace pressure (ΔP_L), which is the pressure difference between the inside and the outside of the droplet, across the oil-water interface. It can be expressed by the following Eq. (1.5) [8]:

$$\Delta P_L = \frac{2\sigma}{r} \qquad (1.5)$$

Where, σ is the interfacial tension between the two phases, and r is the droplet radius. The above equation clearly indicates that the droplet size depends on the interfacial tension. It is clear from the eq. (1.5) that if the interfacial tension is higher, the droplets formed will be of bigger in size. The Laplace equation indicates that during emulsion formation, the deformation of droplet is opposed by the pressure gradient between the external and the

internal side of an interface. The pressure gradient required for emulsion formation is mostly supplied by agitation and therefore to produce an emulsion of small droplets, very intense agitation/homogenization is required. Therefore, a significant homogenization pressure is required to overcome the interfacial tension and to form emulsion droplets of lower sizes. In addition, when a balance between the interfacial tension and the Laplace pressure is achieved, droplet disruption does not occur and attains the maximum reduction in interfacial tension and droplet size.

As discussed, emulsions stabilize in two ways i.e. by using a suitable emulsifier and by homogenizing the mixture in a homogenizer that provides shear forces for the droplet disruption and their dispersion in the continuous phase. Relying only on one of them (either emulsifier or homogenizer) would pose a great challenge to the techno-economic feasibility of food emulsions. The role of emulsifier is that they adsorb at the oil water interface and increases the interfacial area, thereby reducing the droplet size of the oil phase in emulsion. Apart from that it is also necessary to homogenize the emulsion to uniformly distribute all of the constituents (emulsifier, oil & water) of an emulsion and required for the disruption and dispersions of the droplets in the continuous phase. Thus formation of the emulsion of desired stability in a cost effective manner depends on the choice of emulsifier and a suitable homogenizer.

1.3.1) Emulsifiers

Emulsifiers are amphiphilic molecules with both hydrophilic and lipophilic portions adsorbed at the oil water interface and thus making the emulsion stable. The emulsifier positions itself at the oil/water interface and enhances the interfacial area by reducing the interfacial tension between the phases, and facilitates droplet disruption during homogenization. The emulsifier at the interfacial sites creates a stabilizing film to prevent droplet aggregation. An effective emulsifier has two main functions i.e. (1) it rapidly adsorbs at the oil-water interface during homogenization and (2) it forms an interfacial membrane which provides the steric hindrance between the droplets to prevent their coalescence. There are varieties of emulsifiers or stabilizers available which are classified based upon their molecular structure such as small-molecule surfactants (e.g., monoglycerides, polysorbates,

lecithins and fatty acid salts) and macromolecular emulsifiers (biopolymers e.g., proteins and polysaccharides) [9, 10].

1.3.1.1) Small molecule surfactants

Surfactants molecules possesses a hydrophilic head and a hydrophobic tail group which stabilize the emulsions by adsorbing at the oil water interface with the head group in water and tail group in oil phase. The hydrophilic portions align themselves with the water phase, while the lipophilic portions align with the lipid phase. The molecular mass of the surfactants are relatively smaller than other macromolecular emulsifier (biopolymers), hence they are often called as small molecule surfactants. Also the head size of the surfactants is usually smaller than the head size of macromolecular emulsifiers. These surfactants form relatively thin layer at the interface using the Ewers and Sutherland mechanism [10]. They are characterized by the nature of their head and tail group (Fig. 1.3(a)). The surfactant may be ionic, zwitter ionic and non-ionic in nature and are widely used in the food emulsions. In ionic surfactant, the hydrophilic head is either positively (in case of cationic surfactant) or negatively charged (in case of anionic surfactant) and stabilizes the emulsions based up on the electrostatic interaction with the oil droplets. On the other side, non-ionic surfactants possess no charge and normally stabilize the emulsions mainly by steric interactions [10-11]. Thus they are less sensitive to the pH and ionic strength of the solution. Small molecular surfactants are also likely to form self-assembly in the aqueous solution called micelles, depending on their concentration [10-11]. Some examples of small molecular weight surfactants are Tween, Span, monoglycerides, etc.

The selection of a suitable surfactant to stabilize the emulsion basically depends on their hydrophilic lipophilic balance (HLB). Usually, non-ionic emulsifiers are characterized by the HLB value. The surfactant having a high HLB value contains higher number of hydrophilic groups and is more soluble in water whereas those having a low HLB value contain higher lipophilic groups and thus have higher solubility in oil [11]. An emulsifier that is lipophilic in nature is classified by a low HLB number (< 7) which stabilizes the water in oil emulsion and one that is hydrophilic in nature is classified by a high HLB number (> 7) which stabilizes oil in water emulsions as shown in Fig. 1.3. Moreover, in order to get the desired HLB value, two or more emulsifiers are blended and the resulting

HLB of the blend can be easily calculated. The HLB value of a surfactant can be calculated according to Eq. (1.6) as given below [11].

$$HLB = 7 + \Sigma(Hydrophilic\ group\ numbers) - \Sigma(Lipophilic\ group\ numbers) \quad (1.6)$$
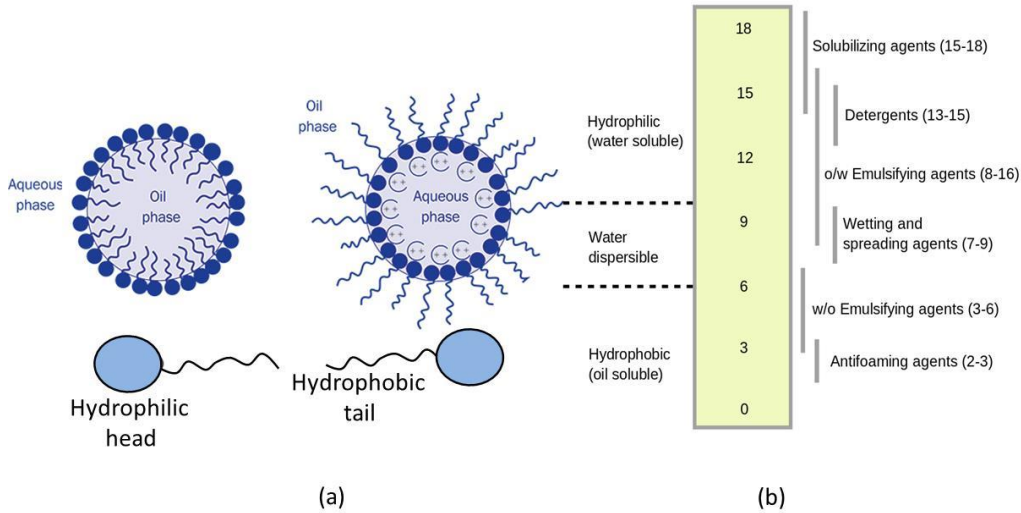
Fig. 1.3 (a) Orientation of head and tail group in O/W and W/O emulsion, and (b) classification of HLB Value

1.3.1.2) Large molecule emulsifiers (Biopolymers)

Biopolymers mainly the polysaccharides and proteins are widely used as functional ingredients for various emulsified food products. Majority of food emulsions are formed and stabilized with polysaccharide and protein combinations. These are the natural and essential food ingredients used in the food emulsion formulations due to their ability to change the texture of food [12]. The protein-polysaccharide complex can form a thick viscoelastic interfacial film at the oil-water interface that improves the stability of emulsions via a combination of electrostatic and steric repulsive forces against various breakdown processes as shown in Fig. 1.4 [1]. Apart from that, the thick interfacial layer of protein-polysaccharide complex prevents the attack of various oxidative compounds such as oxygen molecules, free radicals and transition metal ions, which causes/promote the lipid oxidation. Therefore these biopolymers not only improve the physical stability of emulsions but also improve the oxidative stability of lipid phase of emulsion. Protein and polysaccharide interactions in food emulsions have been studied earlier by many researchers and are being well reviewed in

literature [1, 9, 11, 13. 14]. However, despite the extensive research reported in literature, these biopolymers in food hydrocolloids continue to be one of the most challenging topics to understand.
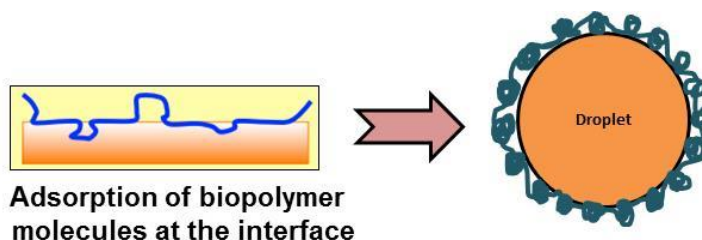
Fig. 1.4 Stabilization mechanism of O/W emulsions by biopolymers

1.3.1.2.1 Proteins

Proteins are naturally-occurring biopolymers that consist of covalently-linked monomers of amino acids. Each amino acid contains at least one primary amino ($-NH_2$), one carboxyl ($-COOH$) group and R-group that strongly influences a protein's capacity to stabilize an emulsion. As a result of their amphiphilic property, proteins are often used as an emulsifier for a variety of food products. From a fundamental perspective, the relationship between protein structure and emulsifying activity depends on a combination of factors such as molecular flexibility, molecular size, surface hydrophobicity, net charge, and amino acid composition. Typically, protein adsorption depends on the surface charge and hydrophobicity as well as the pH and ionic strength of the medium. The molecular weight of proteins ranges from ~5000 to 500000 Da (e.g., myosin, whey protein etc.) [10, 13]. Proteins are a popular choice to stabilize the food emulsions and also help to increase the bioavailability of hydrophobic bioactive compounds encapsulated in emulsions.

1.3.1.2.1 Polysaccharides

Polysaccharides are used in numerous processed foods for emulsification, thickening, stabilization and gelation. These are long-chained, straight or branched polysaccharide-based biopolymers that contain hydroxyl groups capable of hydrogen bonding and thus are used for gelling and thickening the food products. The molecular weight of polysaccharides typically varies between approximately 10 and 10,000 kDa [9, 10]. Their gelling/thickening

ability is highly dependent on composition, concentration, interactions with other components present in the formulation, and also on the local environmental conditions such as pH, ionic strength, and temperature [11]. The effectiveness of surface-active polysaccharides (e.g., derivatives of cellulose such as methylcellulose, carboxymethylcellulose, and hydroxypropylcellulose) as emulsifiers is based on their speed of adsorption at an interface so as to prevent the droplet aggregation [1, 9, 10, 13]. Following their interfacial adsorption, short-range steric repulsive forces help to prevent droplet flocculation. The electrically-charged polysaccharides molecules adsorbed at the oil and water interface, induce the electrostatic repulsion between the droplets and subsequently stabilizes the emulsions against droplet coalescence and aggregation. Ionic strength and pH clearly affect the magnitude of the electrostatic repulsions between droplets stabilized by charged polysaccharides. Some of the polysaccharides which are used for stabilizing the emulsions are shown in Table 1.1 [11].

Table 1.1 Some hydrocolloids/polysaccharides and their functional properties

Hydrocolloids	Carbohydrates	Functions
Starch	Linear chain α-1,4-linked D-glucose	Thickening agent, stabilizer
Cellulose	Linear chain β-1,4-linked D-glucose	Gelling agent, thickener, stabilizer, emulsifier
Gum Arabic	Branched chain β-1,4-linked D-Galactopyranosyl	Emulsifier, stabilizer, thickener
Alginate	Linear copolymer with homopolymeric blocks of β-1,4 linked D-mannuronate (M) & its C-5 epimer α-L-guluronate (G) residues	Emulsifier, stabilizer, thickener
Pectin	Linear chains of α-1,4 linked D-Galacturonic acid	Gelling agent, thickener, stabilizer, emulsifier
Xanthan	D-β-1,4-linked glucose	Stabilizer, thickener, emulsifier, foaming agent

1.3.2 Homogenization of emulsions

As discussed, the emulsifier adsorbs at the oil water interface and subsequently increases the interfacial area by minimizing the interfacial tension between the phases. However, emulsifier molecules are not able to reduce the interfacial forces to a higher extent as required to prepare the uniformly dispersed system. Thus external energy is required to generate intense disruptive forces for the uniform distribution of all ingredients and also to break up bigger oil droplets into the smaller droplets [14]. It can be seen from Fig. 1.5 that initially two immiscible liquids exhibiting an interfacial tension of σ are separated because of differences in the attractive interactions between them. When emulsifiers are added into the solution, they get deposited at the oil water interface because of their amphiphilic behavior but do not completely stabilize the emulsions as they are not uniformly dispersed into the solution. Upon applying some mechanical shear, the generated disruptive forces emulsified the mixture in two ways, first it uniformly disperses the emulsifier molecules in the aqueous phase thereby enhancing the interfacial area between the phases and secondly by the fragmentation of the bigger droplet into the smaller sized droplets [14]. Beyond a certain amount of disruptive force, the interfacial tension would not reduce and droplets of uniform size will be formed as shown in Fig. 1.5.
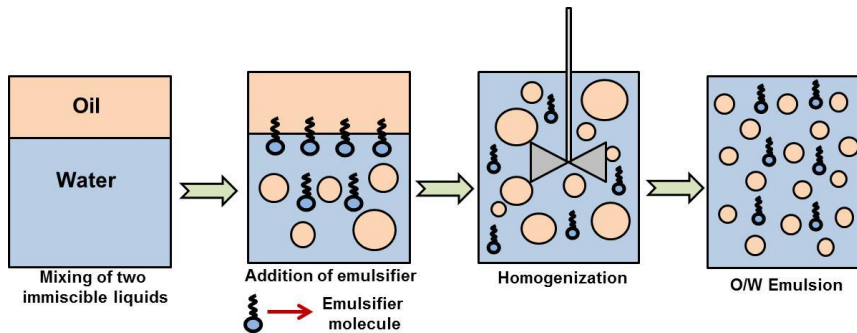
Fig. 1.5 Emulsion homogenization process

The energy required to create interfacial area, A, between the two liquids is "σ A". The relationship between interfacial area and droplet radius is given in Eq. (1.7) [8].

$$A = \frac{6M}{\rho d} \qquad (1.7)$$

13

Where A is interfacial area, M is the mass of oil phase, ρ is the density of oil, and d is the droplet diameter. With a fixed volume fraction of oil phase, A is inversely proportional to d. The emulsions are typically homogenized in mechanical devices known as homogenizers and lots of research work have been carried out for the development of an efficient technique for the emulsification. The most common type of homogenizers that have been used for the production of emulsions on an industrial scale are high pressure homogenizers, microfluidizers, ultrasonic processors and other cavitation based homogenizers. These homogenizers can be categorized in two ways; first the high energy input homogenizers (including high pressure homogenizer and microfluidizers) and second the low energy input homogenizers (including ultrasonication and hydrodynamic cavitation) which are explained in following sections.

1.4 Cavitation

Cavitation is the process of formation, growth and collapse of micro-bubbles or cavities, occurring in a few microseconds at multiple locations in the reactor and thus releases large magnitude of energy in a short span of time [15-17]. The process is initiated with the formation of vapor cavities (bubbles or voids) when liquid enters into the low pressure region and subsequently these cavities attain a maximum size under the conditions of isothermal expansion as shown in Fig. 1.6. In the successive compression cycle, an immediate adiabatic collapse occurs resulting in the formation of supercritical state of high local temperature (1000–10,000 K) and pressure (100–1000 bar) region, known as hot spot [5, 17-18]. The cavitation phenomena can be of two types: stable and transient. Stable cavitation is usually produced at moderate acoustic intensities, and the bubbles inside the liquid oscillate, generally in a nonlinear way, around their equilibrium size and may grow, trapping the dissolved gas. The second type of cavitation, known as transient or inertial cavitation, is generated under high-intensity acoustic fields. During the negative pressure half-cycle, the bubble expands to a size several times higher than its original size. Then, during the compression half-cycle, the bubble collapses violently, forming jets and shock waves. The collapsing bubbles produce very high temperatures and pressures conditions within the liquid which are important in many applications [19]. The high pressures produce

erosion, dispersion, and mechanical rupture while the high temperatures are responsible for sonoluminiscence and sonochemical effects [19].
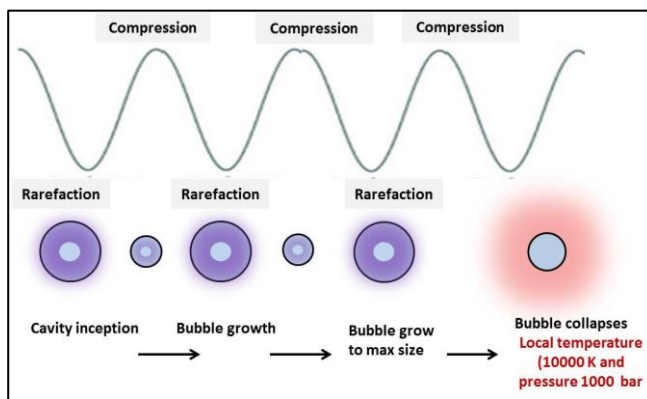
Fig. 1.6 Schematic process of bubble inception, growth and collapse: Cavitation process

Cavitation can also be generated in a liquid medium by flowing the liquid through a suitable constriction such as an orifice, venturi, valve, micro-channels etc. and the process is known as hydrodynamic cavitation. Cavitation can also be generated by passing the ultrasonic waves through the liquid medium known as acoustic cavitation or ultrasonication. From the emulsification point of view, these cavitational techniques can be categorized in two ways viz. high energy input and low energy input devices which are described in following sections.

1.4.1   High pressure/energy input homogenizers

High pressure homogenizers are widely used to produce nanoemulsions in the food industry. Initially the liquid mixture is highly pressurized and forced through a valve that causes a sudden contraction in the flow. During the process, when the liquid passes through the valve as shown in Fig. 1.7, most of the pressure energy is converted into kinetic energy. With sufficient throttling, the kinetic energy increases that subsequently increased the flow velocity through the valve. The vapor bubbles thus formed expand and further collapse, creating shock waves that can break the interface and thus dispersed particles. During homogenization, emulsion experiences a combination of intense disruptive forces such as shear, turbulence and cavitational effects that causes the breakdown of larger droplets into the smaller sizes. The drawback of this method is that it requires high energy inputs i.e. it

usually operates at high pressure ranging from 50 bar to as high as 500 bar which may degrade the emulsion under the extreme high pressure and temperature [20].

Another high pressure system which is known as microfluidization is also used for the production of fine emulsions in food and pharmaceutical industries [21]. In the microfluidizer, two different streams of emulsion mixture are passed at a high pressure in the range of 50 to 1000 bar through a patented fixed geometry interaction chamber (Fig. 1.7) [20]. Two jets of liquid emulsions are accelerated at high velocities from two opposite channels and collide with one another creating tremendous shearing action. In general, inertial forces in turbulent flow induced by high pressure along with cavitation are the predominant factors that cause the disruptions of droplets into fine sizes [22]. These extreme shear rates and impact forces create very fine emulsions. The key element of a microfluidizer is the fixed geometry of chamber where the size reduction occurs. The typical dimension of fluid channels is in the range of 50 - 300 μm where velocities can reach over 400 m/s [20-22]. Although emulsions with smaller droplet sizes can be produced using microfluidization but sometimes it has been found to be unfavorable in specific circumstances, such that higher pressures and longer emulsification time leads to ''over-processing'', which might cause the re-coalescence of emulsion droplets thereby increasing the emulsion droplet size and sometimes the degradation of emulsions [23].
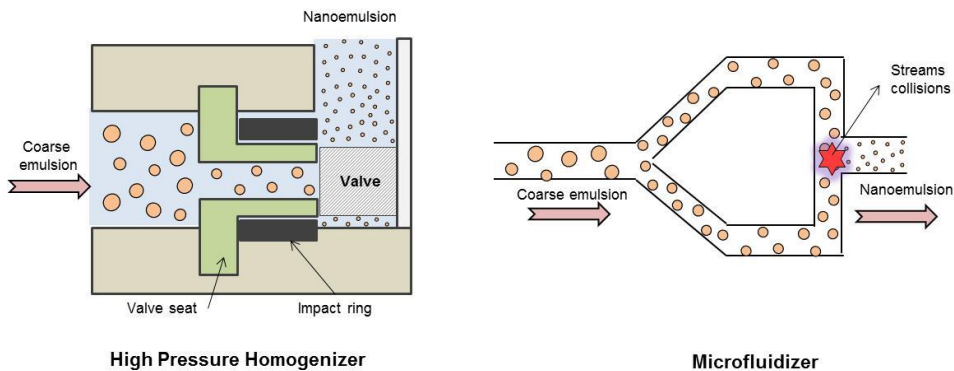
Fig. 1.7 High energy input homogenizers

1.4.2 Low energy input homogenizers

Ultrasonication or ultrasound cavitation is the process of generation of cavitation when the pressure variations in the liquid are affected by passing the ultrasound waves (> 16 kHz)

16

through the liquid. The acoustic energy is generated by the transmission of ultrasound waves that consist of the rarefaction and compression cycles traveling through the liquid medium. The final cavity collapse is adiabatic in nature and thus produces a local high-temperature and pressure conditions. As a result of the extreme cavity collapses, emulsions of smaller droplet size are produced due to the cavitational effects such as mechanical vibrations, acoustic streaming, micro-streaming, shear and high intensity turbulence. Li and Fogler [24, 25] have postulated the two stage mechanism of ultrasonic emulsification. In the first stage, the ultrasonic waves and eddies cause the eruption of the oil-water interface and the dispersion of the oil into continuous phase. In the second stage, the physical effects generated by acoustic cavitation induced the fragmentation of larger droplets into the small droplets. The detail ultrasonic emulsification mechanism is discussed further in section 1.5. Usually ultrasonication processors with frequency in the range of 20 to 40 kHz are proved to produce best dispersion efficiency with smaller droplet size mainly in the nano range and highly stable emulsions [15, 26]. The ultrasonication device is mainly of two types i.e. ultrasonic bath and ultrasonic probe or sonotrode. Some more details on ultrasonication, its emulsification mechanism, reactors configurations and operating parameters are discussed further in Section 1.5.

On the other side, cavitation is also produced by affecting pressure variations in a flowing fluid by allowing the liquid to pass through a constriction typically using an orifice/venturi in a pipe and the process is known as hydrodynamic cavitation (HC) [19]. On passing the liquid through such geometry, the kinetic energy of the liquid increases at the expense of the pressure and this subsequent increase in velocity will cause the pressure at the throat or vena-contracta to be reduced below the vapor pressure of the liquid and thus generates numerous vaporous cavities. Sudden pressure and velocity variations cause dynamic cavity oscillations, and as the cavity collapses, certain physical effects occur in its vicinity which are desired for emulsification. The physical effects generated as a result of cavity collapse i.e. micro streaming, high-pressure shock waves and high local shear forces, lead to the breakage of interface, dispersion of the internal phase into continuous and disruption of the larger droplets into smaller sizes. The desired emulsion droplet size with high stability can be obtained by altering the operating conditions such as geometry of the orifice/venturi and the operating pressure of the liquid. These operating parameters affect the cavitational

17

behavior inside the device mainly the number of cavitational events, cavitational intensity, and the residence time of the cavities, which are the main factors for the disruption of droplets in the emulsion. Venturi devices can be designed in different shapes such as rectangular, elliptical, or circular in shape, whereas in the case of orifice, it can be a single orifice or multiple orifices with throat of different shapes. As the geometry of the device affects the cavitational conditions inside a cavitating device therefore it is important to be considered. Some more details on HC, its emulsification mechanism, reactors configurations and operating parameters are discussed further in Section 1.6.

The comparison between high and low energy methods of cavitation based homogenizers is shown in Fig. 1.8. It can be seen that all of the techniques are able to generate intense cavitational conditions but of different intensities with different mode and geometries. Both the high energy techniques HPH and microfluidizers are capable of producing enormous turbulence and disruptive forces for the desired emulsion droplet size and stability, but the energy required to generate the disruptive forces is high (operating pressure required to be in the range of 50 to 2000 bar) as compared to ultrasonication and HC. Apart from energy intensiveness, these high energy methods have various other disadvantages such as requires high operating pressure, requires premixing, complexity in their geometries, line blockages in the case of microchannels, difficult to clean and high maintenance requirements, etc. [5, 15, 21, 23].

From many decades, ultrasonication has been utilized for the emulsification process because of its potential in producing smaller droplet sizes with superior physical stability. Ultrasonication process offers several advantages over other high energy methods. The operational process is easier, has a smaller foot print, simple geometry, and is easy to clean [15]. Some comparative studies revealed that the ultrasonication was more effective and energy efficient as compared to these high energy methods for achieving the desired droplet size [5, 23, 27]. All these facts make ultrasonication the most effective and promising method for the preparation of emulsions.

On the other hand, hydrodynamic cavitation (orifice/venturi based devices) are proved to generate similar high intensity turbulent conditions but with less energy inputs than ultrasonication. As shown in Fig. 1.8, high energy methods are usually operated at high pressures (>1000 bar), whereas other pressure throttling devices such as orifice and venturi

usually required operating pressures in the range of 5 to 50 bar to achieve the desired emulsion droplet size. Previous studies have reported that the emulsion of desired droplet size can be achieved at low operating pressure in the range of 5 to 55 bar using orifice and venturi based HC devices [28-30]. The cavitational conditions generated inside the orifice/venturi based devices are similar to that of ultrasonication and because of its less energy requirements, orifice/venturi based HC process could be economically feasible for large scale operations. Also there are several advantages of HC which makes it feasible for large scale operations such as its capability in processing larger volume than all other processes, continuous operation, easy scale-up, and low material costs. All these facts proved that both the low energy techniques HC and ultrasonication are the most effective and promising methods for the production of emulsions.

Fig. 1.8 Comparison of high energy and low energy cavitation based homogenizers for emulsification

1.5 Ultrasonication or ultrasound cavitation

In ultrasonication, cavities are generated by passing the sound waves through the liquid medium. The range of sonic spectrum is > 16 kHz, which may be subdivided into three main sections as low-frequency and high-power ultrasound (20–100 kHz), high-frequency and medium-power ultrasound (100 kHz – 1 MHz), and high-frequency and low-power ultrasound (1–10 MHz). Ultrasonic waves consist of rarefaction (expansion) and compression cycles; when these waves are transmitted through liquid, and bubbles/cavities are formed, followed by its rapid growth and finally the collapse of these generated cavities. The average distance between the liquid molecules is larger in rarefaction cycle but smaller in the compression cycle. Cavitation occurs in rarefaction cycles where negative acoustic pressure is sufficiently large to pull apart the liquid molecules from each other, and the distance between the adjacent molecules can exceed the critical molecular distance. At that moment, the voidage is created in the liquid, which causes the formation of cavities. Subsequently, in the compression cycle of the sound wave, acoustic pressure is positive, which pushes the molecules together. The cavities will compress (decrease in size) during the compression cycle of ultrasonic wave, and few of them may collapse in a very small time interval. This final collapse phase is adiabatic in nature, thus producing high local temperature and pressure conditions.

In comparison to the previously discussed high energy homogenizing techniques, ultrasonication offers enhanced level of mixing to produce the emulsions. The implosive collapse of cavities dissipates the energy at the micro level for initiating the droplet disruption process. The detail mechanism is presented in Fig. 1.9 [5]. The first stage showing the generation of primary droplets, where the acoustic field produces the interfacial waves and the instability of which causes eruption of oil phase into the water in the form of droplets. Second stage involves the break-up of primary droplets wherein violent and asymmetric implosion of bubbles cause micro jets which can effectively breaks the primary oil droplets. The break-up of droplets is primarily controlled by the type and amount of shear applied to droplets. Further the stability and coalescence of droplets depend on the rate at which surfactant is adsorbed at the interface of the newly formed droplets and is controlled by the surfactant surface activity and its concentration. Thus, selection of appropriate surfactant is much important in producing highly stable nanoemulsions.
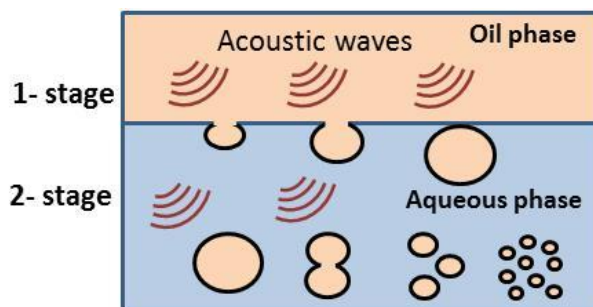
Fig. 1.9 Ultrasonication assisted emulsification process

Ultrasound cavitation is usually produced in two kinds of reactors i.e. ultrasonic bath and ultrasonic horn which are shown in Fig. 1.10. In a bath, the ultrasonic transducers are attached to the bath surface which transmits the waves through the liquid medium whereas an ultrasonic horn consists of a sonotrode or probe which can be immersed in the liquid to be treated. In an ultrasonic reactor, the supplied power converts the line voltage to high frequency electrical energy. This energy is transmitted to the transducer within the converter, where it is changed into the mechanical vibrations. These vibrations generated from the converter are intensified by the ultrasonic probe which subsequently creates the pressure waves in the liquid. This action creates the numerous vaporous cavities, which expand during the negative pressure excursion, and subsequently collapses violently during the positive excursion. Although this phenomenon, known as cavitation, occurs for few microseconds, but it occurs at millions of sites and the cumulative amount of energy generated as a result of these cavity collapse is extremely high. The larger the probe tip, larger will be the volume that can be processed but at a lesser intensity. In both the reactors, cavitation is found to occur near the tip of the horn/transducers, and cavitation intensity decreases exponentially when moving away from the horn tip/transducer surface [17].
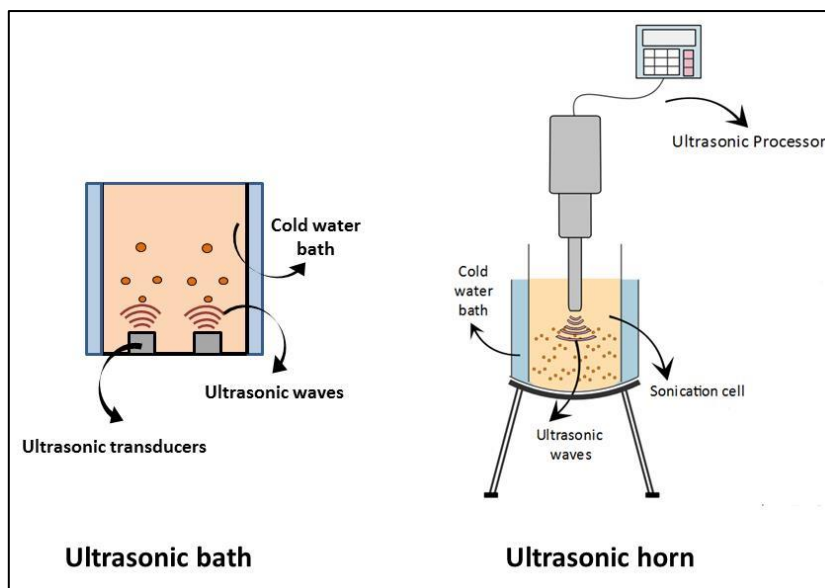
Fig. 1.10 Ultrasonicator; ultrasonic bath and horn

In ultrasonication process, parameters such as ultrasonic frequency, power and processing time are crucial and needs to be optimized to achieve the minimum emulsion droplet size with high stability.

1.5.1 Ultrasonic frequency

Ultrasonic emulsification is typically achieved using low-frequency ultrasound (i.e. 20–100 kHz). The cavitation bubbles formed in this frequency range tend to undergo strong transient cavitation collapse, which produces strong shear forces that can disrupt the large droplets into smaller sizes. The horn-type ultrasonic probe typically delivers ultrasound at a fixed frequency of ~20 kHz, while bath-type equipment can be tuned to provide slightly higher frequency ultrasound. Horn-type transducers are very commonly used as they are more effective for the creation of emulsions of nanosized droplets owing to the high-intensity ultrasound delivered in a narrow cavitation zone. Bath-type ultrasound equipment can be effective in delivering ultrasound across a wider region and is useful for emulsions which require less-intensive size disruption [31].

Additionally, higher frequency ultrasound in the MHz range can also be used to assist in the formation of nanosized emulsion droplets through a process known as tandem acoustic emulsification [15]. In this method, a sequential approach is being utilized for the formation

of the emulsion. The droplets are initially formed at low frequency (20 kHz) and then subsequently exposed to higher frequency ultrasound in the range of MHz which causes the droplets to colloid together and break apart further into smaller droplets with extreme acceleration. The acceleration becomes stronger with increased frequency, which is why the order of the applied frequency is important for tandem acoustic emulsification [15].

1.5.2 Ultrasonic power

The ultrasonic power is a major factor that controls the efficiency of the emulsification process [15]. In general, a higher power delivered will increase the rate at which emulsion droplets are broken up into smaller droplets. However it is necessary to know the limit i.e. to what extent the power can be increased before the effectiveness of cavitation decreases. Sometimes higher processing power gives the droplets greater momentum, increasing the probability of coalescence upon collision and thereby increasing the droplet size [5, 31]. Therefore limited power should be applied in order to avoid the condition of "over processing" which is one of reasons as to why scale up of ultrasonic emulsification process can be a challenge [31]. Determination of optimum power is therefore very important in the ultrasonic emulsification process as the effectiveness of process in reducing the droplet size depends on the power density (W/mL) or energy density (J/mL) i.e. the amount of power or energy required to process a unit volume [15]. Overall, for the fixed power supplied to the solution, the droplet size would reduce only up to its critical size however it can be further reduced by supplying more power to the emulsion mixture for a fixed volume and composition i.e.by increasing the power density (W/mL).

1.5.3 Sonication time

In general, an increase in the sonication time results in a decrease in the droplet size of the emulsion. As the time increases, the amount of ultrasonic energy delivered in the solution also increases, leading to the disruption of more number of droplets and decrease in the size of the emulsion droplets [32]. However, sometimes for a higher sonication time (beyond equilibrium) coalescence of smaller droplets into larger droplets is evident due to the prevalence of a high droplet concentration and collisions among the droplets [34]. Therefore, the emulsion should be exposed to sonication until it attains the minimum interfacial tension

or critical size of the emulsion droplets. However to further reduce the interfacial tension or droplet size, more shear will be required in terms of higher power of sonication. Most of the studies found similar trend which indicated the inefficiency of ultrasonic energy in further reducing the size of emulsion at higher sonication time [23, 33].

1.6 Hydrodynamic cavitation

Hydrodynamic cavitation is simply generated by passing the liquid through constrictions fitted in a conduit. At the constriction, the kinetic energy of the liquid increases at the expense of pressure and with effective throttling, pressure reduces below the vapor pressure of the liquid at the vena-contracta, causing flashing of the liquid and generating numerous vapor cavities. Subsequently as the liquid jet expands, the velocity decreases and the pressure recovers in the downstream section of the cavitating device resulting in the collapse of cavities. A typical pressure profile of an orifice based device is shown in Fig. 1.11. In the downstream section, boundary layer separation occurs and some amount of energy is released in the form of permanent pressure drop. The magnitude of the pressure drop greatly influences the intensity of cavitation and turbulence in the downstream section [35]. Thus, it is necessary to control the operating and geometrical parameters of the devices in order to get the required cavitational intensity.
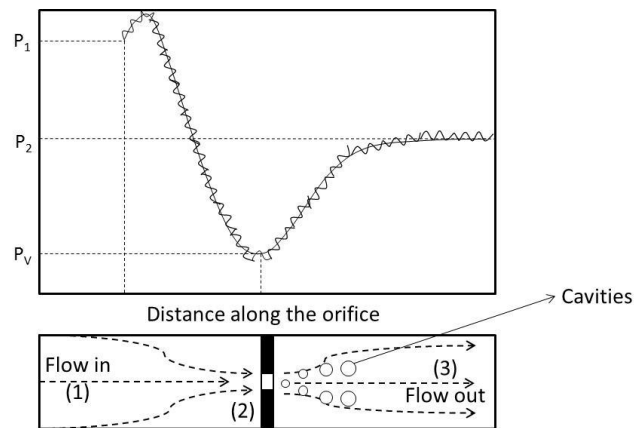
Typical pressure profile in an orifice (1 – upstream of the orifice; 2 - vena contracta; Point 3 - downstream of the orifice)

Fig. 1.11 Typical pressure profile in an orifice (1 – upstream of the orifice; 2 - vena contracta; Point 3 - downstream of the orifice)

24

The dimensionless cavitation number (C_V) represents the hydraulic characteristics of a cavitating device and it characterizes the condition of cavitation inside the cavitating device [36]. It is represented by Eq.(1.8):

$$C_V = \frac{P_2 - P_V}{\frac{1}{2}\rho V_0^2}$$
(1.8)

Where, P_2 is the discharge pressure at downstream section, P_V is the vapor pressure of the liquid, V_0 is the velocity at the throat and ρ is the density of liquid. The C_V at which the inception of cavitation occurs is known as cavitation inception number, C_{Vi}. Ideally, the cavitation inception occurs at C_{Vi} = 1 and there is a significant cavitational effect for C_V values less than 1.

The cavity oscillation and collapse at the liquid-liquid interface effectively delivers high energy by generating the shockwaves, creating high velocity liquid jets and interfacial turbulence. These effects are beneficial for the application that requires the mixing at the molecular level such as emulsification where the interfacial tension between immiscible phases gets reduced. The physical effects such as micro jet streaming and high intensity local turbulence act as the main driving force for the droplet disruption in an emulsion. The energy released as a result of asymmetric cavity collapse dissipates at the micro level which enhances the mixing of two immiscible phases by reducing the interfacial tension and subsequently causes the fragmentation of droplets into smaller sizes in the continuous phase. The mechanism of droplet disruption in hydrodynamic cavitation is shown in Fig. 1.12.
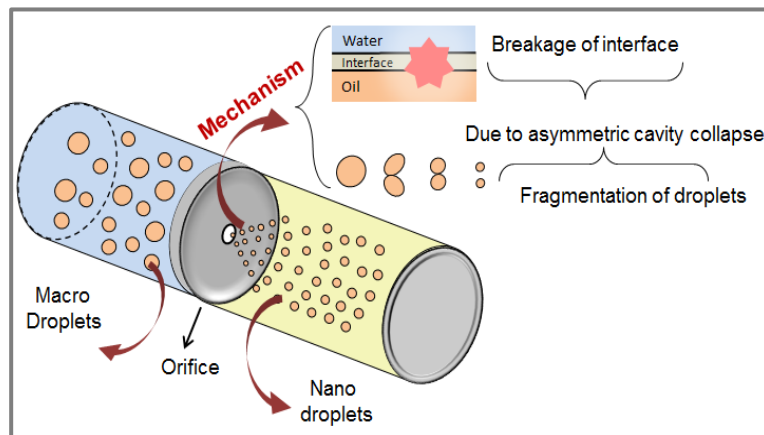
Fig. 1.12 Hydrodynamic cavitation assisted emulsification process

HC is usually generated by providing a suitable constriction in a liquid flow. The throttling can be created using various devices such as venturi, orifice, high speed rotor and homogenizer etc.

Orifice and venturi based HC devices are found to be the most efficient in creating an intense cavitation condition at moderately low pressure than other high pressure devices. The cavitation in an orifice is transient in nature whereas cavitation in a venturi is mostly stable because of its geometrical configuration. In an orifice, the intensity of a cavity collapse very much depends on the area of opening/flow area, size, shape and number of holes. The intensity of cavity collapse in an orifice is also higher due to the generation of more number of transient cavities at the edge of throat which is mainly required for physical transformation such as emulsification. Its geometry could be of different shapes and sizes with single or multiple openings as shown in Fig. 1.13(a). The use of multiple opening orifice plate gives better control over the intensity of cavitation and the number of cavitational events occurring inside the cavitating device [37]. In case of venturi, it consists the convergent section, throat and divergent section in which the flow dynamics vary in a considerable manner, but no sudden contraction and expansion occurs as observed in an orifice. A substantial variation in the flow is found in convergent and divergent section and as a result of this, the flow parameters like pressure and velocity are consistently varied along the length of the venturi. The different size and shape of the throat and divergent section set the criteria for the different cavitational activity such as, it can alter the number of cavitational events, magnitude of the collapse pressure and the residence time of the cavity in low pressure region [19, 37]. The different shapes of venturi such as rectangular and circular as shown in Fig. 1.13(b) can be used to obtain different cavitational conditions inside the reactor. The variation in geometrical parameters of both the devices such as flow perimeter, throat area and divergence angle result into the different cavitational yield and thus it is necessary to consider these factors during the design of a cavitating device [38]. It has been reported that the cavitational properties inside the device can be regulated by varying the operating pressure or cavitation number and geometry of the device. The effect of all these parameters on the emulsification process is discussed in following sections in detail.
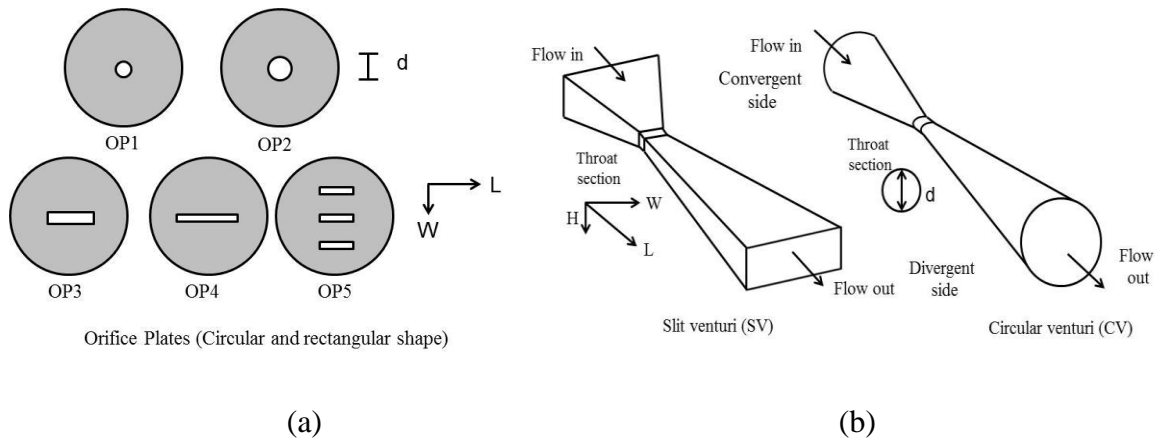
Fig. 1.13 Hydrodynamic cavitating devices of different shapes and sizes, a) orifice plates, and b) venturi

1.6.1 Operating pressure/cavitation number

The operating inlet pressures to the cavitating device and cavitation number are the two important parameters that affect the cavitational intensity generated in the HC reactor. The number of cavities being generated and the pressure/temperature pulse generated due to cavity collapse depends very much on the inlet pressure and the cavitation number. It has been established that on increasing the operating pressure to the device, the velocity at throat increases which causes the reduction in cavitation number. Therefore, the decrease in the cavitation number indicates the generation of more number of cavities. However, a decrease in cavitation number beyond an optimum value leads to the condition of choked cavitation which has no practical utility [19, 38]. Generally, an increase in the inlet operating pressure effectively enhances the rate of emulsion droplet size reduction, which is attributed to the higher cavitational intensity at higher operating pressure. However, beyond an optimum pressure, the droplet size of emulsion would not further reduce at the fixed emulsion compositions. Therefore the optimization of pressure becomes necessary to not only prevent the choking condition but also to maintain the cost effectiveness of the process.

1.6.2   Geometry of the cavitating device

The optimum cavitational yield of HC depends on several operating parameters: number of cavitational events, residence time of cavity in the low-pressure zone, and the rate of pressure recovery in the device [39]. These parameters depend on the geometry and the flow conditions of the liquid, i.e., the scale of turbulence and the rate of pressure recovery. All these parameters need to be optimized considering their interactive effects to get the enhanced cavitational yield and the enhanced emulsification process.

The cavity inception and the number of cavities being generated depend on the size and shape of the constriction. To quantify this dependency, two parameters need to be considered in the analysis first is α, which is the ratio of throat perimeter to the throat area and second is β, which is the ratio of the throat area to the cross-sectional area of the pipe. It has been observed that for orifice plates having the same flow area, it is better to use a plate with a smaller hole size opening, thereby increasing the number of holes in order to achieve a larger extent of the shear layer [19, 40]. The higher α results into the generation of higher frequency of turbulence, leading to the generation of more shear forces required for the droplet disruption. The α value can also be increased by constructing throats of different shapes such as rectangular and elliptical. In case of β value, the area of the throat can be finalized based on the required cavitation number for the desired emulsification process. It is advisable to use a cavitating device having higher β because at lower β value, the pressure drop across the cavitating device as well as energy required for pumping would be higher to achieve the required cavitation number. In case of venturi, the pressure recovers smoothly because of the divergent angle, and cavities get enough time to grow to a maximum size before collapsing, thereby allowing cavities to undergo various cycles of expansion and collapse. Therefore in order to get the higher magnitude of cavity collapse, the divergent angle should be optimized for the desired cavitational intensity.

1.7 Emulsion as an encapsulating & delivery system

Emulsions are the colloidal systems that have been utilized as a delivery vehicle for various nutraceuticals such as fatty oils, vitamins, flavors, drugs and other lipophilic compounds. Emulsions systems have been mainly designed to improve the solubility and bioavailability of lipophilic compounds while incorporating them into the functional foods. Although there

are many other approaches such as liposomes, micelles, hydrogels and other nanodispersons that improves water dispersibility, bioavailability and chemical stability of the lipophilic compounds but emulsification has exceptional advantages particularly in food applications. In food products, O/W emulsions are usually fabricated using food ingredients (including emulsifiers and fatty oils) and also most of the food products are already in the form of emulsions like beverages, sauces, deserts etc. which makes them relatively easy to incorporate the lipophilic constituents. Moreover, the bioactive compounds can also be incorporated in the core (oil phase) of the emulsion matrix that can improve their stability, functionality and facilitates their controlled release in the human body. The formation of an interfacial layer over the oil droplet carrying lipophilic components provides protection against their degradation under the environmental conditions. Emulsification technology has been explored in the context of food applications such as milk, creams, dairy, mayonnaise, beverages, deserts etc. Thus emulsification as a delivery system is represented as a rapidly emerging area in the food, pharmaceutical industries etc.

The significant factors which need to be considered before the formation of emulsion for the perfect encapsulation and the controlled release of bioactives are the selection of the oil phase and a suitable emulsifier. The oil phase acts as a carrier for the lipophilic actives such as flavors, nutrients, vitamins, colors etc. Generally, highly saturated fats can have a negative impact on the health. Oils with high polyunsaturated triglyceride content are mainly considered for dietary intake, and oil containing ω-3 fatty acids are often quoted within nutritional literature as it imparts specific health benefits when consumed regularly. While biopolymers are mainly used for food grade emulsion as they contain food ingredients such as amino acids, carbohydrates, etc. which could be easily digested in GI tract of the body. Also, these type of emulsifiers not only prevent the emulsions against physical instability such as coalescence of droplets but also effectively inhibits the oxidation of lipids present in the emulsion. After fulfilling these two, the main factor which is to be considered is the emulsion stability at the point of application. The higher the emulsion stability, better would be the shelf life of the encapsulating materials. The stable emulsion helps to maintain the physicochemical properties of the nutraceuticals over a longer storage time and also the behavior of emulsion upon their application so as to achieve the controlled release of the compounds.

Thus the main role of a researcher is to design a suitable emulsion system with enhanced stability to improve the shelf life of the encapsulated nutraceutical compounds. The stability of emulsion is a crucial parameter that could be affected by small changes in the emulsion compositions and also by the slight variations in the environmental conditions such as pH, temperature, ionic strength, lipid auto-oxidation etc. Thus it becomes important to select the best operating condition that helps to achieve the desired stability in an energy efficient manner. After obtaining the successful encapsulation of bioactive compounds in food emulsions, it is also necessary to evaluate the release properties for their delivery in the physiological conditions of the body. For mouth, gastric and intestine conditions, the delivery environments will be quite different and thus the release behavior of the compound will also be different.

1.8   Current status of cavitation based emulsification

1.8.1   Ultrasonication assisted emulsification

From many decades, ultrasonication has been utilized for the formation of emulsion because of its potential in getting smaller droplet sizes with superior physical stability. Many studies have been reported on its capability to produce the emulsion with desired stability for various applications such as food, pharmaceuticals and cosmetics. Some of the findings on ultrasonication based studies are discussed below in detail.

Tang et al. [23] reported the comparison between the ultrasonication and microfluidization for the formation of nanoemulsion carrying aspirin. They have tested the energy efficiency of both the process for getting the emulsion of minimum droplet size and uniform size distribution. Initially the coarse emulsion consisting of 10 wt.% Lauroglycol 90, 10 wt.% Transcutol, 3.52 wt.% Cremophor EL, and 76.48 wt.% water was prepared under magnetic stirring before subjecting it to the ultrasonication or microfluidization. In case of ultrasonication, the power amplitude was varied in the range of 50 to 80% whereas in case of microfluidization, the coarse emulsion was passed through a ceramic interaction chamber (75 μm) at different operating pressures (200 to 600 bar). It has been observed that the minimum droplet size of 174 nm was obtained using ultrasonication at 60% amplitude in 100 sec, whereas in case of microfluidization minimum size of 146 nm was obtained at 200 bar after 10 passes. Also, both the techniques were found to produce the fine pharmaceutical

nanoemulsion carrying aspirin with higher long term stability. Moreover the comparison of both the techniques was made based on the applied energy density for achieving the similar droplet size of emulsion. It was observed that in case of ultrasonication, the minimum droplet size of 180 nm was obtained at the delivered energy density of only 11 J/cm$^{3.}$ However microfluidization produced similar size of emulsion but at a higher energy density, which was 12 times greater than ultrasonication. Thus this study showed that the ultrasonication was more energy efficient as compared to microfluidizer for producing the pharmaceutical nanoemulsion.

Ghosh et al., [41] studied the formation of basil oil in water nanoemulsion using ultrasonication process. The system was stabilized with Tween 80 as it has a high hydrophilic–lipophilic balance (HLB-15) and is favorable for oil-in-water emulsion. The nanoemulsion consisting the basil oil (6% v/v) was prepared at different oil to surfactant ratios and at different sonication time. It has been observed that on increasing the surfactant concentration, the droplet size reduces significantly. Nanoemulsion with 1:1, 1:2 and 1:3 (v/v) ratios of oil and surfactant produced droplet sizes of 41, 31 and 29.6 nm respectively after 15 min of sonication. The effect of ultrasonication time on the droplet size of emulsion was evaluated and it was observed that on increasing the sonication time from 5 to 15 min, the droplet size of emulsion was reduced from 58 nm to 41 nm. The ultrasonically prepared nanoemulsions remained stable for a month without any change observed in the droplet size and no phase separation occurred during the storage. The nanoemulsion formed using ultrasonication was found to have an excellent antimicrobial efficiency against the E. Coli microbial species.

Shanmugam & Ashokkumar [42] reported the use of ultrasonication for producing flaxseed oil enriched carrot juice beverage emulsion and studied their characterization. The beverage emulsion was prepared by incorporating 1% (v/v) flaxseed oil in 99% pasteurized carrot juice (PCJ). The mixture was ultrasonically processed at different power and sonication time. The emulsion stability was evaluated by measuring the droplet size and based upon the visual observation for oil separation during the storage period of 8 days. It was observed that at lower sonication time of 3 min, and at all power inputs (88, 132, and 176 W), the emulsion destabilized after 8 days and creaming was observed at the top of the emulsion. Even on further increasing the sonication time to 8 min at 88 and 132 W, there was a slight

creaming phase after 8 days of storage. However, at higher power of 176 W, the emulsion was found to be stable at 4 and 5 min of sonication treatment after 8 days of storage at 4±2 °C. Similar observations were also made with droplet size of emulsion as the size of the emulsion droplets decreased with an increase in power input of ultrasonication. This indicated that the emulsion processed at higher power input have enhanced stability of emulsion because higher power input improved the rate of droplet size reduction by generating more shear forces to produce the finer size of emulsion droplets. The ultrasonication that produced a nutritious beverage emulsion of size 600 nm with enhanced stability of up to 8 days was considered to be the safe technique for the production of food emulsion.

Pongsawatmanit et al. [43] reported the use of ultrasonication for the preparation of multilayer O/W emulsion prepared using palm oil with β-lactoglobulin and sodium alginate. Initially, the multilayer emulsions were produced at various pH (3-7) and alginate concentrations in the absence of ultrasonication in order to see the electrostatic interaction between the primary and secondary biopolymers. The emulsions produced at acidic pH in the range of 3 to 5, showed high interaction between the biopolymers whereas in pH range of 6 to 7, the interaction between them was limited. In absence of ultrasonication, the multilayer emulsion produced at pH 3 and 4 got destabilized as a result of bridging flocculation whereas it showed some good stability at pH 5. However on producing the emulsion with ultrasonication (1 min, 20 kHz, 70% Amp), the emulsion was found to be stable against bridging flocculation even at pH 3 and 4 as depicted in their microscopic analysis. This indicated that high power ultrasonic treatment helps to disrupt the flocs formed by the protein-polysaccharide complex at the interface and thus stabilizes the emulsions formed using functional ingredients such as protein and carbohydrates.

Alzorqi et al. [44] formulated the palm O/W emulsion using ultrasonication for the encapsulation and delivery of β-D-glucan, a natural antioxidant isolated from the fungus *Ganoderma lucidum.* They had formulated the nanoemulsion with an aim to achieve minimum droplet size and higher stability and then evaluated for the antioxidant activity of β-D-glucan encapsulated in the nanoemulsion. In order to form a stable nanoemulsion, the process conditions were optimized using response surface statistical design. It was observed that the nanoemulsion carrying β-D-glucan (loading of 1% and 85% w/w) possessed

minimum droplet size of 263 nm and was found to be stable at 4 and 25⁰C during the storage period of 90 days as there was no change in the droplet size observed. The antioxidant activity of ultrasonically produced emulsions was evaluated and it was observed that at lower concentrations (1-5 % w/w), β-D-glucan-loaded nanoemulsions exhibited higher antioxidant activity (36.9-40.3 % w/w) than free β-D-glucan (15.8-31.2 % w/w). Overall, it was found that the ultrasonically prepared nanoemulsion possesses long term stability of 90 days and also enhanced the antioxidant activity of the β-D-glucan encapsulated in the nanoemulsion.

Likewise there are many other studies on ultrasonic emulsification as shown in Table 1.2 which also provides clear information that ultrasonication is a relatively simple and effective method for the preparation of emulsions under milder conditions. Also it has been established that ultrasound is an efficient technique than other mechanical devices in terms of minimum droplet size and high energy efficiency. Most of the studies used small molecule surfactants, such as Tween 80 and SDS etc. and less work has been reported on the use of biopolymers to stabilize the emulsion using ultrasonication, however still the fundamentals related to the kinetic stability of emulsions under the different conditions are yet to be fully understood. The primary focus of previous studies has been on the formation of nanoemulsions, while the research on long term stability of emulsions under the different stresses such as temperature, pH, composition of emulsion, centrifugation, storage, etc. is lacking in the literature. Therefore, more work is indeed required to be performed both on the theoretical as well as the experimental front for better understanding of the phenomena. The major application of emulsions has been to improve the encapsulation stability and bioavailability of encapsulated lipophilic actives in emulsions. Thus it is necessary to evaluate the desired stability of the emulsion synthesized using ultrasonication for providing the better shelf life of a product as required in food, and pharmaceutical industries.

Moreover previously reported studies were carried out in batch mode only with low processing volume for the synthesis of emulsions using ultrasonication. However for processing larger volume, more energy is required in the form of higher power, amplitude and processing time. Though ultrasonication offers immense cavitational intensity but the use of this technique is lacking for larger scale operations. Therefore, more work is indeed required to intensify the ultrasonic emulsification process with an objective to process larger

volume with minimal amount of energy which would give greater scope for the scale up and commercialization of the process.

Table 1.2 Overview of the ultrasonic emulsification studies reported in literature

Oil phase	Emulsifier/ surfactant	Operating compositions	Ultrasonic operating conditions	Findings	Reference
Sunflower oil	Tween 80, Span 80 & SDS	5.6 wt% surfactant and 15 wt% of sunflower oil	US - 20 kHz, 1000 W, 12 mm probe size	Droplet size: US – 40 nm in 10 min (15 mL volume) at 5.3 wt% Tween 80 and 4.4 wt% Span 80.	Leong et. al. [45]
Paraffin wax	Sodium lauryl sulfate (SDS)	Oil fraction: 0.2 (v/v) SDS fraction: 0 to 10 mg/ml	US: 20 kHz, 750 W 13 mm probe size	Droplet size (average): US – 160 nm in 15 min Stability: 3 month	Jadhav et. al. [46]
Basil oil	Tween 80 (HLB = 15)	6% (v/v) oil, Oil to T80 ratio: 1:4 (v/v)	Ultrasonicator (US): 20 kHz, 750 W, 20 - 40% Amplitude, 13 mm probe size	Droplet size: US – 29 nm in 5 min Stability: 1 month Emulsions had higher antibacterial efficiency against E.Coli	Ghosh et al.[41]
Coconut oil	Span 80 & Tween 80	HLB: 10 Surfactant con.: 0.02 to 0.11 (volume fraction) Oil con.: 0.1 to 0.4	US 1: 20 kHz, 750 W, Surface area: 2120 mm^2 US 2: 20 kHz, 1500 W, 32 mm^2	Droplet size: 116 nm in 5 min at surfactant 0.02 and oil 0.1 volume fraction in US 1 Stability: 1 month	Ramisetty et al. [47]

			US 3: 20 kHz, 1500 W, 32 mm^2		
Lauroglycol 90 and Transcutol mixture	Cremophor EL (HLB = 12–14)	10 wt.% Lauroglycol 90, 10 wt.% Transcutol, 3.52 wt.% Cremophor EL, and 76.48 wt.% de-ionized water	Ultrasonicator (US): 20 kHz, 1000 W, 50-100% Amplitude Microfluidizer (MF): Pressure: 200 bar	Droplet size: US – 174 nm in 100 sec at 60% Amp MF – 146 nm in 10 passes at 200 bar Emulsion was successfully used as carrier for Aspirin loading	Tang et al., [23]
Anatto Seed oil	Gum Arabic	4 wt.% of oil and 16 wt.% of GA	Mechanical stirring: 5 min, 2000 RPM Ultrasonicator (US): 19 kHz, 800 W, 13 mm probe size Power: 160 – 640 W	Droplet size (D$_{32}$): US – 690 nm in 5 min Stability: 1 month Emulsion was found to be a suitable system for the encapsulation of annatto seed oil	Silva et al. [48]
Flaxseed oil in pasteurized carrot juice	-	1% (v/v) oil in PCJ	US – 20kHz, 450W 12-mm diameter	Droplet size (D$_{43}$): 500 nm in 8 min (50 ml) Stability: 8 days	Shanmugham & Ashokkumar [42]
Eucalyptus oil	Tween 80	16.66% (v/v) Oil, 16.66% (v/v) Tween 80, and	Mechanical stirring: 10 min, 250 RPM US – 20kHz, 750W,	Droplet size: 3.8 nm in 30 min The wound healing potential of nanoemulsion was tested on	Sugumar et al. [49]

		66.68% (v/v) Water	40% Amplitude, 0-30 min	Wistar rats and obtained higher wound contraction rate	
Clove oil	Tween 80/Span 80	HLB = 9, Surfactant: 5 wt% Oil: 2.5 to 10 wt%	US – 24kHz, 400 W, 14 mm probe diameter	Droplet size: 36 nm at 15 wt% oil in 5 min sonication (0.75% duty cycle, and 208 W/cm^2 intensity) The emulsion size increased from 36 nm to 100 nm owing to Ostwald ripening after 6 months	Shahavi et al. [50]
Wheat bran oil	Tween 80/Span 80	HLB = 11, 1% of WBO and 7.3% surfactant	High speed blender: 5 min before US. US – 20kHz, 500 W, 3 mm micro tip probe, 20% Amplitude, Process optimized using response surface methodology	Droplet size: 39 nm in 50 sec sonication after premixing with high speed blender Stability: 2 months storage at 4°C without any change in droplet size Nanoemulsion showed relevant antioxidant activity.	Rebolleda et al. [51]

1.8.2 Hydrodynamic cavitation assisted emulsification

In the last decade, hydrodynamic cavitation has been applied in the emulsification process for the formation of different emulsions. Studies reported in literature proved the potentiality of this technique for the preparation of various emulsions with nano and submicron range of droplet sizes. There is not much work reported in literature on the applications of hydrodynamic cavitation for oil in water emulsification process until now. Only few studies, which are explained below, have been reported on the use of hydrodynamic cavitation for the preparation of O/W emulsion.

Parthasarathy et al. [28] developed a liquid whistle hydrodynamic cavitation reactor (LWHCR) for the preparation of palm oil based submicron emulsion using Tween 80 as an emulsifier and used it for the encapsulation of curcumin. The LWHCR comprised an orifice and a blade which was kept at some distance away from the orifice plate. The minimum droplet size was obtained to be 415 nm at 800 psi using the combination of orifice and blade with orifice plate-blade distance of 0.5 cm. The distance between orifice and blade was optimized for obtaining sufficient back pressure to maximize the collapse intensity. The effect of cosurfactant i.e. span 80 was also studied and no significant reduction in the final droplet size was observed. Additionally the curcumin encapsulation efficiency was also evaluated in the formulated emulsion using LWHCR and it was found that the maximum efficiency of 88% was achieved indicating the superiority and potential of hydrodynamic cavitation for encapsulation of various active pharmaceutical and food ingredients.

Ramisetty et al. [29] investigated the use of HC reactor for the preparation of coconut oil in water nano emulsion using Tween 80 and Span 80 surfactants. The effect of inlet pressure in the range of 5 to 20 bar, number of passes and geometry of a venturi (slit and circular) on the emulsion droplet size was investigated. It was observed that the droplet size reduced from 711 nm to 332 nm on increasing inlet pressure from 5 to 10 bar after 10 min of treatment using circular venturi and further no reduction was observed beyond 10 bar. However, the minimum droplet size of 200 nm was obtained at the end of 30 min at 10 bar (Cv = 0.08) using circular venturi. Though the minimum droplet size was obtained in case of circular venturi but the slit venturi showed more pronounced effect on the rate of droplet size reduction as compared to circular venturi. With the advantage of high flow area in slit

venturi and the subsequent high energy dissipation, the maximum reduction in the droplet size per unit pass at 5 bar inlet pressure was obtained as compared to circular venturi. This indicates that higher cavitational yield can be obtained in slit venturi as compared to circular venturi and that too with lesser pressure drop and minimum use of energy. This study successfully demonstrated the effectiveness of venturi based HC process in the production of emulsions.

As discussed earlier and shown in Table 1.3, it can be seen that, these reported works were focused only on the preparation of O/W emulsion using either single hole orifice or venturi based HC devices. These studies were emphasized on the optimization of the process parameters such as operating pressure, emulsion composition (oil and surfactant concentration) for getting the desired droplet size. However there is no work reported in the literature on the design and optimization of different cavitating devices such as orifice plate and venturi for the preparation of nanoemulsion. It is only recently that Ramisetty et al. [29] reported the effect of geometry of venturi (slit and circular) on the extent of coconut oil in water emulsification but the design of orifice plates based on several parameters such as α (ratio of throat perimeter to its cross sectional area) and β (throat area to pipe cross sectional area) are not yet reported. Moreover the significance of cavitation number in the design and operation of a cavitating device was not discussed in any of the reported studies. Therefore all these parameters needs to be studied and optimized to get enhanced cavitational yield from the hydrodynamic cavitation device because considering only one parameter in the design of a cavitating device would not result in the possible explanation of all the cavitational conditions for the desired effects.

Table 1.3 Overview of the hydrodynamic cavitation emulsification studies reported in literature

Oil phase	Emulsifier/ surfactant	Operating compositions	HC device	Operating conditions	Findings	Reference
Palm oil	Tween 80	Surfactant: 1% (w/w) Oil: 20% (w/w)	An LWHCR consisting orifice with a blade placed at different distance (0.5 to 0.8 cm)	Orifice size = 0.16 mm, Flow area = 0.02 mm^2 Pressure = 55.15 bar	Droplet size: 476 nm Device: orifice Pressure: 55.15 bar. Passes: 10	Parthasarathy et al., [28]
Coconut oil	Span 80 & Tween 80	HLB = 10, surfactant: 11% (v/v) Oil: 10% (v/v)	Slit venturi : Flow area: 11.4 mm^2 Circular venturi: 3.14 mm^2	Flow area: Slit venturi: 11.4 mm^2, circular venturi: 3.14 mm^2, Pressure = 20 bar	Droplet size: 170 nm Device: circular venturi Pressure: 20 bar. Time = 20 min	Ramisetty et al. [29]
Water containing ascorbic acid and gelatin (W/O/W)	Span 80 in Maisin and Capryol (oil phase)	40 wt% water phase in W/O emulsion, In W/O/W emulsion: 30% W/O emulsion + 70% Water	An LWHCR consisting orifice with a blade placed at distance of 0.6 cm	Orifice size = 0.16 mm Flow area = 0.02 mm^2 Pressure = 6.9 bar to 13.79 bar	Droplet size: 565 nm Device: orifice Pressure: 13.79 bar. Passes: 20	Tang & Sivakumar [30]

1.9 Objectives of this research work

The overall aim of this thesis work was to develop a mechanistic understanding of the ultrasound and hydrodynamic cavitation assisted emulsification processes, emulsion stabilization mechanisms of small molecule and large molecule emulsifiers and the utilization of emulsion for the encapsulation and delivery of the bioactive compound. The aims and objectives set at the beginning of this investigation has been summarized as follows:

- Formation and stability of oil in water (O/W) nanoemulsion with a non-ionic surfactant using ultrasound and hydrodynamic cavitation

- Investigation on the effect of process parameters (oil concentration, surfactant concentrations), ultrasound parameters (power amplitude, sonication time) and external shear (thermal stress and centrifugation) on the droplet size and stability of nanoemulsion.

- Development of novel hydrodynamic cavitating devices such as venturi and orifice plates and the investigation on the effect of geometrical parameters such as throat perimeter, throat size and area on the droplet size and stability of nanoemulsion.

- Formation and stability of mono and multilayer (O/W) emulsion with protein and polysaccharides based biopolymers using ultrasound cavitation

- Characterization of Multilayer (O/W) emulsion (droplet size, droplet charge, morphology, physical and chemical stability) in the presence of protein and polysaccharide based emulsifier (biopolymers).

- Investigation on the effect of ultrasound cavitation on the physical and oxidative stability of mono and multilayer emulsion

- Investigation on the formation of multilayer emulsion as an encapsulating and carrier system for the lipophilic bioactive compound (curcumin) with an aim to study the effect on the encapsulation stability, antioxidant activity and controlled release of compound.

- Characterization and evaluation of stability of multilayer O/W emulsion carrying bioactive compound after the drying of emulsion.

- Evaluation of release activity of encapsulated bioactive compound under the simulated intestinal condition of the human body.

1.10   Thesis Layout

This dissertation is mainly composed of six chapters: The first chapter is about the introduction and literature review, thereafter four successive chapters are about the results and discussions on different research studies conducted and a final chapter is on the conclusion along with the scope for future work.

Chapter 1 is an introduction outlining background information, fundamentals of emulsions, stability, methods for homogenization, cavitation process and also a summary on the scientific knowledge found in the literature related to the topics mentioned in this thesis.

Chapter 2 is about the formation and stability of O/W nanoemulsion prepared using ultrasonication. This study includes the detail investigation on the process optimization of ultrasonically prepared nanoemulsion using mustard oil with Tween 80 and Span 80 surfactants. The kinetic stability of produced nanoemulsion was assessed under the influence of high temperature, centrifugation and normal storage conditions.

Chapter 3 is on the formation and stability of O/W nanoemulsion using hydrodynamic cavitation. This study reports the detail investigation on the geometrical analysis of various hydrodynamic cavitating devices for the generation of nanoemulsion. The effects of various geometrical parameters (throat area, and throat perimeter) on the emulsification process were studied. The long term stability of the nanoemulsion was also evaluated. The energy efficiency of ultrasonication and hydrodynamic cavitation was also compared.

Chapter 4 is on the preparation of multilayer O/W emulsion stabilized with whey protein isolate and sodium alginate (SA) using ultrasonication. In this study, effects of process parameters such as pH, SA concentration, and sonication time on the droplet size, zeta potential, morphology, physical and oxidative stability of the multilayer emulsion were studied. The ultrasonication process was employed in both batch and recirculating flow configurations and the energy efficiency comparison was made between them.

Chapter 5 is about the utilization of ultrasonically prepared multilayer emulsion for the encapsulation of curcumin, a bioactive compound. In this work, the detail investigation on the encapsulation stability, antioxidant activity and release properties of curcumin encapsulated in multilayer emulsion is reported.

Chapter 6 summarizes the conclusions of the thesis and provides necessary recommendations for future work.

References

1. D.J. McClements, Food Emulsions Principles, Practices, and Techniques Second Edition, Food Emulsions Principles, Practices, and Techniques. (2005) CRC Press.

2. R. Pichot, "Stability and characterisation of emulsions in the presence of colloidal particles and surfactants." PhD diss., University of Birmingham, 2012.

3. A Bhushani, C. Anandharamakrishnan, Food-Grade Nanoemulsions for Protection and Delivery of Nutrients. In Nanoscience in Food and Agriculture 4, (2017). 99-139. Springer, Cham.

4. N. Dasgupta, and S. Ranjan, Food Nanoemulsions: Stability, Benefits and Applications. In An Introduction to Food Grade Nanoemulsions, Springer, Singapore (2018) 19-48.

5. M. Sivakumar, S. Y. Tang, K. W. Tan, Cavitation technology – A greener processing technique for the generation of pharmaceutical nanoemulsions, Ultrason. Sonochem. 21 (2014) 2069–2083.

6. C. Solan, P. Izuierdo, J. Nolla, N. Azemar, M.J. Garcia, Nanoemulsions. Curr. Opin. Colloid. Interface Sci.10 (2005) 102-110.

7. I. A. Appelqvist, M. Golding, R. Vreeker, N. J. Zuidam, Emulsions as delivery systems in foods. Encapsulation and controlled release technologies in food systems, (2007). 41-81.

8. J. Zhang, "Novel emulsion-based delivery systems." (2011), PhD Diss.

9. D. Guzey, D.J. McClements, Formation, stability and properties of multilayer emulsions for application in the food industry, Adv. Colloid Interface Sci. 128–130 (2006) 227–248.

10. L. Li, "In vitro gastrointestinal digestion of oil-in-water emulsions, PhD Diss. (2012). Food Technology at Massey University, Auckland, New Zealand.

11. M. Ray, R. Gupta, D. Rousseau, Properties and applications of multilayer and nanoscale emulsions. In book: Nanotechnology and Functional Foods: Effective Delivery of Bioactive Ingredients, In (2015), 175-190.

12. C. Schorsch, M.G. Jones, I.T. Norton, Thermodynamic incompatibility and microstructure of milk protein/locust bean gum/sucrose systems. Food Hyd. 13(2) (1999) 89-99.

13. D.J. McClements, Protein-stabilized emulsions, Current Opinion in Colloid and Interface Science. 9 (2004) 305–313.

14. O. Sullivan, J. Jonathan, Applications of ultrasound for the functional modification of proteins and submicron emulsion fabrication. PhD diss. (2015) University of Birmingham.

15. A. Shanmugam, and M. Ashokkumar, Ultrasonic Preparation of Food Emulsions. Book: Ultrasound in Food Processing: Recent Advances (2017) 287-310.

16. A, Mahulkar A. B. Pandit Analysis of Hydrodynamic and Acoustic Cavitation reactors; numerical and experimental analysis, applications, operations and scale-up. (2010) VDM Verlag Dr. Müller.

17. P. R. Gogate, Cavitational reactors for process intensification of chemical processing applications: A critical review. Chem Eng Process 47 (2008) 515–527.

18. P. R. Gogate, Hydrodynamic Cavitation for Food and Water Processing, Food Bioprocess Technol 4 (2011) 996–1011.

19. J. Carpenter, M. Badve, S. Rajoriya, S. George, V.K. Saharan, A.B Pandit, Hydrodynamic cavitation: an emerging technology for the intensification of various chemical and physical processes in a chemical process industry. Rev. Chem. Eng. 33(5), (2017) 433-468.

20. N. Dasgupta, S. Ranjan,. Fabrication of Nanoemulsion: A Brief Review. In An Introduction to Food Grade Nanoemulsions, Springer, Singapore (2018) 49-62..

21. Y.F. Maa, C.C. Hsu. "Performance of sonication and microfluidization for liquid–liquid emulsification." Pharmaceutical development and technology 4(2) (1999) 233-240.

22. S.M. Jafari, Y. He, B. Bhandari, Optimization of nano-emulsions production by microfluidization. European Food Research and Technology, 225 (2007) 733-741.

23. S.Y. Tang, P. Shridharan, M. Sivakumar, Impact of process parameters in the generation of novel aspirin nanoemulsions–comparative studies between ultrasound cavitation and microfluidizer. Ultrasonics Sonochemistry, 20 (2013) 485-497.

24. M.K. Li, H.S. Fogler, Acoustic emulsification. (Part 1) The instability of the oil-water interface to form the initial droplets, J. Fluid Mech. 88 (3) (1978) 499–511.

25. M.K. Li, H.S. Fogler, Acoustic emulsification. (Part 2) Break-up of the larger primary oil droplets in a water medium, J. Fluid Mech. 88 (3) (1978) 513–528.

26. J. Canselier, H. Delmas, A. Wilhelm, Ultrasound emulsification – an overview. Journal of Dispersion Science and Technology 23 (2002), 333–349.

27. B. Abismail, J.P. Canselier, A.M. Wilhelm, H. Delmas, C. Gourdon, Emulsification by ultrasound: droplet size distribution and stability, Ultrason. Sonochem. 6 (1999) 75–83.

28. S. Parthasarathy, S. Y. Tang, S. Manickam, Generation and optimization of palm oil-based oil-in-water (O/W) submicron-emulsions and encapsulation of curcumin using a liquid whistle hydrodynamic cavitation reactor (LWHCR), Ind. Eng. Chem. Res. 52 (34) (2013) 11829–11837.

29. K. A. Ramisetty, A. B. Pandit, P. R. Gogate, Novel approach of producing oil in water emulsion using hydrodynamic cavitation reactor, Ind. Eng. Chem. Res. 53(42) (2014) 16508-16515.

30. S. Y. Tang, M. Sivakumar, A novel and facile liquid whistle hydrodynamic cavitation reactor to produce submicron multiple emulsions. AIChE J. 59(1) (2013), 155-167.

31. T.S.H. Leong, S. Manickam, G.J. Martin, W. Li, M. Ashokkumar, Ultrasonic Production of Nano-emulsions for Bioactive Delivery in Drug and Food Applications. (2018) Springer.

32. A. Shanmugam, M. Ashokkumar, Ultrasonic preparation of stable flax seed oil emulsions in dairy systems – Physicochemical characterization. Food Hyd. 39 (2014) 151–162.

33. S. Kentish, T.J. Wooster, M. Ashokkumar, The use of ultrasonics for nano emulsion preparation. Innovative Food Science and Emerging Technologies 9 (2008) 170–175.

34. K. Chalothorn, W. Warisnoicharoen, Ultrasonic emulsification of whey protein isolate-stabilized nanoemulsions containing omega-3 oil from plant seed. American Journal of Food Technology 7 (2012) 532–541.

35. V.S. Moholkar, A.B. Pandit, Bubble behavior in hydrodynamic cavitation: effect of turbulence. AIChE J (1997) 43: 1641.

36. Saharan VK, Badve MP, Pandit AB. Degradation of reactive red 120 dye using hydrodynamic cavitation. Chem Eng J 178 (2011) 100–107.

37. P.R. Gogate, A.M. Kabadi, A review of applications of cavitation in biochemical engineering/biotechnology. Biochem Eng J 44 (2009) 60–72.

38. V.K. Saharan, M.A. Rizwani, A.A. Malani, A.B, Pandit, Effect of geometry of hydrodynamically cavitating device on degradation of orange-G. Ultrason Sonochem 20 (2013) 345–353

39. T.A. Bashir, A.G. Soni, A.V. Mahulkar, A.B. Pandit, The CFD driven optimization of a modified venturi for cavitation activity. Can J Chem Eng. 89 (2011) 1366–1375.

40. M. Sivakumar, A.B. Pandit, Wastewater treatment: a novel energy efficient hydrodynamic cavitational technique. Ultrason Sonochem 9 (2002) 123–131.

41. V. Ghosh, A. Mukherjee, N. Chandrasekaran, Ultrasonic emulsification of food-grade nanoemulsion formulation and evaluation of its bactericidal activity, Ultrason. Sonochem. 20 (2013) 338–344.

42. A. Shanmugam, M. Ashokkumar, Characterization of Ultrasonically Prepared Flaxseed oil Enriched Beverage/Carrot Juice Emulsions and Process-Induced Changes to the Functional Properties of Carrot Juice, Food Bioprocess Technol. 8 (2015) 1258–1266.

43. R. Pongsawatmanit, T. Harnsilawat, D.J. McClements, Influence of alginate, pH and ultrasound treatment on palm oil-in-water emulsions stabilized by β-lactoglobulin, Colloids and Surfaces A: Physicochemical and Engineering Aspects. 287 (2006) 59–67.

44. I. Alzorqi, M.R. Ketabchi, S. Sudheer, S. Manickam, Optimization of Ultrasound Induced Emulsification on the Formulation of Palm-olein based Nanoemulsions for the Incorporation of Antioxidant β-Dglucan polysaccharides, Ultrason. Sonochem. 31 (2016) 71-84.

45. T.S.H. Leong, T.J. Wooster, S.E. Kentish, M. Ashokkumar, Minimising oil droplet size using ultrasonic emulsification, Ultrasonics Sonochemistry 16 (2009) 721–727.

46. A. J. Jadhav, C. R. Holkar, S. E. Karekar, D. V. Pinjari, A. B. Pandit, Ultrasound assisted manufacturing of paraffin wax nanoemulsions: Process optimization, Ultrasonics Sonochemistry 23 (2015) 201–207.

47. K. A. Ramisetty, A. B. Pandit, P. R. Gogate, Ultrasound assisted preparation of emulsion of coconut oil in water: Understanding the effect of operating parameters and comparison of reactor designs, Chemical Engineering and Processing 88 (2015) 70–77.

48. E. K. Silva, G. L. Zabot, M. A. Meireles, Ultrasound-assisted encapsulation of annatto seed oil: Retention and release of a bioactive compound with functional activities, Food Research International 78 (2015) 159–16.

49. S. Sugumar, V. Ghosh, M. J. Nirmala, A. Mukherjee, N. Chandrasekaran, Ultrasonic emulsification of eucalyptus oil nanoemulsion: Antibacterial activity against Staphylococcus aureus and wound healing activity in Wistar rats, Ultrason. Sonochem. 21 (2014) 1044-1049.

50. M.H. Shahavia,M. Hosseini, M. Jahanshahi, R.L. Meyer, G.N.Darzi, Evaluation of critical parameters for preparation of stable clove oil nanoemulsion, Arabian Journal of Chemistry (2015).

51. S. Rebolleda, M.T. Sanz, J.M. Benito, S. Beltrán, I. Escudero, L.G. San-José, Formulation and characterization of wheat bran oil-in-water nanoemulsions, Food Chemistry 167 (2015) 16-23.

CHAPTER 2

FORMATION AND STABILITY OF O/W NANOEMULSION USING ULTRASONICATION: EFFECT OF PROCESS PARAMETERS

2.1 Introduction

Nanoemulsions are gaining more interest due to their wide applications in food industries, pharmaceuticals, cosmetics, etc. because of their several benefits. Due to the nano droplet size, nanoemulsions retain long term stability i.e. up to several months and years [1] as compared to other conventional emulsions. Prior to the application of nanoemulsions, their characteristics and stability are to be well established. Mainly the emulsion stability against the various breakdown processes including coalescence, flocculation, creaming and Ostwald ripening, pose a great limitation against its use and synthesis [2].

In food applications, nanoemulsions are found as a novel system for delivery of various nutraceuticals. Nanoemulsions have potential to improve the solubility and bioavailability of many food active compounds and therefore serve as a carrier for the delivery of lipophilic active compounds in food applications [3, 4]. In pharmaceuticals, nanoemulsion is suitable for drug delivery because of its ability in solubilizing the non-polar active compounds [5-7]. In cosmetics, nanoemulsions can be used for synthesis of skin and hair care products.

A nanoemulsion is a non-equilibrium system (i.e. thermodynamically unstable) and hence cannot be formed spontaneously [2]. Also, large amounts of emulsifiers are avoided in food, pharmaceuticals, and cosmetics based nanoemulsions. Therefore nanoemulsions require some desired amount of energy either in the form of agitation or mechanical disturbances to assist the emulsification process thus breaking the interface and reducing the emulsion droplet size [8]. Generally, high speed agitators and high pressure homogenizers are preferred for the preparation of nanoemulsions but these techniques consume high energy and have less control over the particle size distribution and stability of emulsions [8, 9]. On the other side, Ultrasonication is found to be an efficient technique for the preparation of nanoemulsions that has better control over the characteristics of emulsions [9-12]. When ultrasound waves are transferred through the liquid medium, they create cavitation phenomena which comprise of the formation, growth and implosive collapse of microbubbles/cavities in the liquid medium. This transient collapse conditions generate a localized hot spot region consisting of very high temperature up to 5000 K and pressure up to 1000 bar [13]. Such intense cavitation conditions can initiate the desired physical transformation during emulsification. Ultrasound based emulsification occurs in two ways [14, 15], first the generation of droplets in the acoustic field and second the creation of

intense turbulence and microjets during asymmetric cavity collapse which cause the break up and dispersion of droplets in the continuous phase. Many studies proved the capability of ultrasound for producing the nanoemulsion of droplet sizes below 100 nm [8, 9, 16-18]. The emulsion having lower droplet size possesses long term stability. Therefore ultrasound can effectively control the particle size distribution as well as improve stability of the emulsions. Moreover, many studies have reported that ultrasound assisted nanoemulsions are proven to be suitable systems for the encapsulation and delivery of various drugs and food active compounds [8, 17, 19 - 23].

In the last decade, many studies have reported the use of ultrasound cavitation for the formation of Oil in water nanoemulsions using different essential edible oils such as coconut oil [9], sunflower oil [16], flaxseed oil [8, 17], basil oil [18] etc. These oils mainly consist of the essential fatty acids, vitamins, etc. and therefore emulsions derived from these oils can be used to deliver bioactive compounds in food applications. As per the author's knowledge, few studies have been reported on the formation of mustard oil in water nanoemulsions using ultrasonication [24-26] however analysis of the kinetic and long term stability of this nanoemulsion system have not been studied which is the novel aspect of this work. Therefore, in the present study, the point of interest was the evaluation of kinetic stability of ultrasonically prepared mustard oil in water nanoemulsions under centrifugal and thermal stress conditions which is not reported in the literature. Another aim of the study was to evaluate the influence of ultrasound induced chemical effects on the prepared nanoemulsions.

Mustard oil is mainly obtained from the mustard seeds at low temperature (40-60°C). It is widely used as cooking oil in India and is being considered as heart friendly oil. This oil protects against heart diseases which may be attributed to the presence of omega 3 polyunsaturated fatty acids. Like other edible oils, mustard oil is also rich in alpha-linolenic acid which reduces the cholesterol levels and consequently the risks of heart diseases. Alpha-linolenic acid is an essential fatty acid that is known to support cell, nerve & cognitive skills development in children and cardiovascular functions in humans [17, 27]. Hence mustard oil is considered to be a safe and healthy edible oil. Moreover, mustard oil based cosmetics are found to be more favorable and protective for skin, as the oil contains high level of Vitamin E which protects against UV rays and other pollutants. Also, mustard

oil possesses anti-bacterial and anti-fungal properties that effectively prevent skin infections [28]. Therefore, mustard oil based nanoemulsion can be better utilized in cosmetics and food applications.

In the present study, mustard oil in water nanoemulsions were prepared using ultrasound cavitation and stabilized by combination of Span80 (S80) and Tween 80 (T80) surfactants. The main objective of the present study was to evaluate the kinetic stability of the emulsions formed at the optimum operating condition and to study, the effect of various parameters such as HLB, surfactant fraction (φ_S), oil volume fraction (φ_O) and ultrasound power on emulsion properties. The kinetic stability of prepared emulsions has been evaluated under the centrifugal and thermal stress conditions. The present work also report the role of ultrasound induced chemical effects on the oil molecular structure of prepared nanoemulsion using FTIR analysis.

2.2 Materials and Methods

2.2.1 Materials

Refined mustard oil was obtained from the local market. The surfactants Span 80 and Tween 80 were obtained from TCI Chemicals, India. Deionized water (Ultrapure, Thermofisher) was used for the preparation of all formulations. All the materials were used in experiments without any further purification.

2.2.2 Preparation of emulsion

The nanoemulsion was prepared using mustard oil as an internal phase in deionized water and the formulations were stabilized by the addition of surfactants Tween 80 and Span 80. Primarily the surfactants Tween 80 and Span 80, at the required HLB were premixed with deionized water and the mixture was heated up to 45 °C for the complete dissolution of surfactants. After cooling the mixture to room temperature, mustard oil was added dropwise into the mixture for the formation of an emulsion in a complete batch of 100 ml. The prepared formulations were further subjected to sonication for 30 min using Ultrasonic processor (VCX 750, Sonics, USA) that operated at 20 kHz with a maximum power output of 750 W. The schematic of experimental set up is shown in Fig. 2.1. The tip of ultrasonic horn having diameter of 13 mm was immersed up to 25 mm depth in the emulsion mixture.

To prevent overheating and temperature rise during the ultrasonication process, an ice bath was used to maintain the temperature difference (before and after sonication) at ≤ 5°C. The experiments were conducted at different HLB values (8, 9, 10, and 11) for getting the minimum droplet size and a stable emulsion. The desired HLB values can be calculated as given in Eq. (2.1):

$$HLB_{RESULTANT} = (HLB_{T80} \times V_T) + (HLB_{S80} \times V_S) \qquad (2.1)$$

Where $HLB_{RESULTANT}$, HLB_{T80} and HLB_{S80} are the HLB of mixed surfactant, Tween 80 (HLB:15.0) and Span 80 (HLB:4.3) respectively and V_T and V_S are the volume percentage of T80 and S80. Therefore in order to obtain higher extent of stability of the prepared oil in water nanoemulsions, HLB value was varied from its lower to higher value i.e. from 8 to 11.The required HLB was obtained by mixing Tween 80 and Span 80 at desired ratio. After optimization of HLB value, the effect of surfactant volume fractions (φ_S) in the range of 0.02 to 0.10 was investigated. The surfactant volume of lower and higher range was used to investigate their effect on physico-chemical properties and stability of the emulsions. Mustard oil (disperse phase) volume fraction (φ_O) was also varied in the range of 0.10 to 0.40 and their effect on the droplet size and stability of emulsion was investigated. Sonication time and power amplitude were also varied to investigate the effect of cavitation conditions on the quality and physico-chemical properties of the emulsion. All the experiments were repeated three times and the average value was reported with an experimental error of ±2 %.
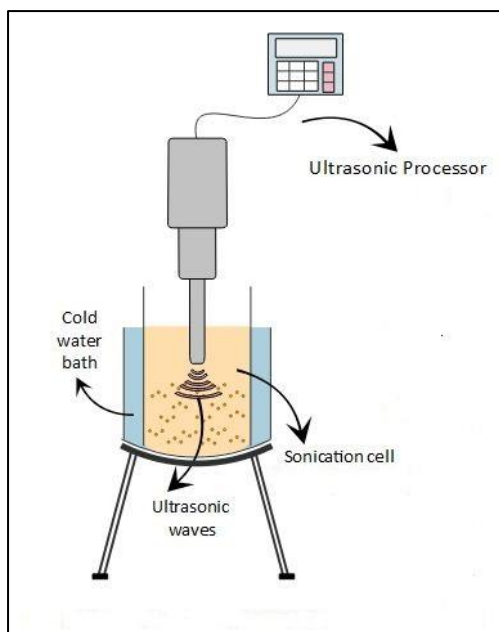
Fig. 2.1 The schematic of experimental set up (Ultrasonic processor)

2.2.3 Statistical analysis of process parameters using response surface methodology

Response surface methodology (RSM) was used to study the effects of independent variables such as HLB, oil fraction, surfactant fraction, power amplitude and sonication time and their interactions on the droplet size of emulsion. The RSM and Analysis of variance (ANOVA) were conducted in Minitab (Trial version) to develop an empirical second order polynomial regression model to predict the droplet size of emulsion. The statistical significance of the model parameters was studied using Fischer's F-test and Probability (P-value) test, and the quality of the polynomial equation was checked by determining the regression coefficient (R^2). The contour plots of the model-predicted responses were utilized to specify the interactive relationships between the significant variables.

2.2.4 Droplet size and Zeta potential measurements

Droplet size and zeta potential of the emulsions were determined using Zetasizer Nano ZS (Malvern Instruments, UK) which is provided with dynamic light scattering and electrophoresis facility for the analysis. Before carrying out the measurements, all the formulations were diluted to the ratio of 1:1000 in deionized water to prevent multiple scattering effects during size analysis. A refractive index of 1.59 and absorbance of 0.01 was used. The Zetasizer gave the Z-average diameter which was represented as droplet size (nm)

in this study. Duplicate samples along with three measurements were considered for ensuring repeatability of the analysis.

2.2.5 Interfacial tension and density measurement

The interfacial tension of the various formulations was determined using Goniometer (Kruss, Germany). Pendant drop method was used to determine the interfacial tension [29] in which the emulsion sample was taken in a syringe that comprised of a needle with diameter as 1.835 mm and a drop was formed into pure mustard oil placed in an optical glass cuvette. The interfacial tension was measured after the drop became stable in the oil medium inside the cuvette. Three measurements of the duplicate samples were performed along with estimation of standard deviations. All the measurements were conducted at room temperature. The density of the nanoemulsion samples were measured using a density-meter (Kruss, Germany). All the measurements were conducted at room temperature.

2.2.6 Creaming Index measurements

Creaming Index measurement represents the extent of separation of phases. The measurement of separation was done using Eq. (2.2) as follows [30]:

$$\% \, CI = \frac{H_S}{H_T} \, X \, 100, \qquad H_S = H_T - H_C \qquad (2.2)$$

Where % CI is the Creaming Index, H_S represents the height of stable phase, H_C represents the height of cream layer at the top of emulsion and H_T represents the total height of emulsion or solution. The CI as 100% denotes that the emulsion is stable i.e. no separation occurs. The % CI of all the formulated emulsions was measured after 24 hour storage at room temperature. The emulsions were considered unstable if the separation occurred within 24 hours and stable if it never showed any separation up to 90 days of storage.

2.2.7 Kinetic stability analysis

In order to determine for possible breakage in emulsions due to creaming and coalescence, the kinetic stability were evaluated using the centrifuge and thermal treatment tests. All the formulations were initially centrifuged at 5000 rpm (3520 RCF (relative centrifugal force))

for 15 minutes and further subjected to heating cycles at 40°C, 60°C and 80°C. The kinetic stability tests were carried out after 7, 30, and 90 days storage of emulsions. The stability of the emulsion after these tests were evaluated based on the % CI and size measurement. The stability of emulsion was confirmed when no change was observed in the droplet size after a predetermined period.

2.2.8 Long term stability

The long-term stability of nanoemulsion was evaluated by measuring the droplet size as a function of time. The sample prepared at the optimum condition was stored at room temperature for up to 3 months and droplet size was measured at different intervals of time during the storage.

2.2.9 Physico-chemical properties of nanoemulsions

Fourier transform infrared spectroscopy (FTIR, Perkin Elmer) was used to evaluate the change in chemical bonds of oil molecules present in the emulsions. The FTIR spectrum of pure oil and the ultrasonically prepared oil emulsions at different conditions were studied in the range varying from 4000 to 400 cm^{-1}. The purpose of this analysis was to investigate the structural and bonding changes in oil molecules as a result of ultrasound induced chemical effects during emulsification.

2.3 Results and Discussions

2.3.1 Optimization of HLB value

To produce stable emulsions, surfactants or various combinations of surfactants can be used to reduce the interfacial tension which controls the deformation of emulsion droplet. The synergy between surfactant and co-surfactant can alter the droplet size and helps to achieve a higher degree of emulsion stability [16]. In the present study, Tween 80 (hydrophilic) and Span 80 (lipophilic) surfactants were used as they exhibited better synergetic properties, forming a rigid and strengthened emulsifier film at the interface and are also safe, cheap and non-toxic in nature [16, 31]. These surfactants are mainly used in cosmetic and food applications. Initially, emulsions were prepared with oil fraction (φ_O) of 0.10 and surfactant fraction, (φ_S) of 0.08 using a blend of Tween 80 and span 80 having

HLB values ranging from 8 to 11 in order to optimize the desired HLB value. The prepared formulations were subjected to sonication in an ultrasonic processor for a period of 30 min. The effect of HLB values on droplet size is shown in Fig. 2.2. It was observed that on increasing the HLB value from 8 to 10, the droplet size decreased from 128.5 nm to 87.38 nm after 30 min of sonication. This was attributed to the favorability of higher HLB values towards the formation of oil in water emulsion due to the strong packing of surfactant molecules around the interface which consequently reduced the interfacial tension and droplet size. At lower HLB values, the volume fraction of S80 was high as compared to T80 in the emulsion which increases hydrophobicity of the surfactant system resulting in a weak packing of surfactant molecules around the interface due to imbalance conditions of hydrophobicity and hydrophilicity. Therefore, the droplet size obtained was high at lower HLB as compared to higher HLB values. However, no further reduction was observed in droplet size with an increase in HLB value from 10 to 11. This indicated that the packing strength of T80 and S80 at the droplet interface had reached its saturation state at HLB 10 and hence no further reduction in droplet size was observed. At higher HLB, T80 molecules are present in excess and therefore will occupy maximum active sites. The interfacial molecular area of T80 (2.48 nm^2) is higher than S80 (0.46 nm^2) [1, 16] and therefore there is no decrease in droplet size after HLB 10. In all the prepared nanoemulsions, no phase separation was observed as % CI was 100% for all HLB values after 24 hours storage at room temperature. Hence, HLB value of 10 was found as an optimum value and all further experiments were conducted at HLB 10.

The results obtained are found to be in accordance with the literatures [9, 16, 31]. Ramisetty et al. [9] reported the use of T80 and S80 to stabilize coconut oil in water emulsion system. It was observed that at HLB 10, the emulsion was more stable against the electrolyte and freeze thaw destabilization test. Li et al. [31] investigated the influence of HLB values on droplet size for the preparation of paraffin wax emulsion stabilized by T80 and S80 emulsifiers. They observed that droplet size decreased from 3.5 μm to below 700 nm on increasing HLB values from 9.1 to 10.3. The droplet size obtained at HLB 9.5 to 10.2 was almost same. Based on the stability and droplet size analysis, HLB 10.1 was found as an optimum value for paraffin wax emulsion. Leong et al. [16] investigated the effects of addition of S80 in T80 stabilized sunflower oil in water emulsions. It was found that on

addition of S80 at concentrations varying from 0% to 6% (wt%), the droplet size reduced from 180 nm to almost 150 nm but beyond 6%, the emulsion became hydrophobic and unfavorable for stabilizing the oil in water emulsion and as a consequence the droplet size increased.
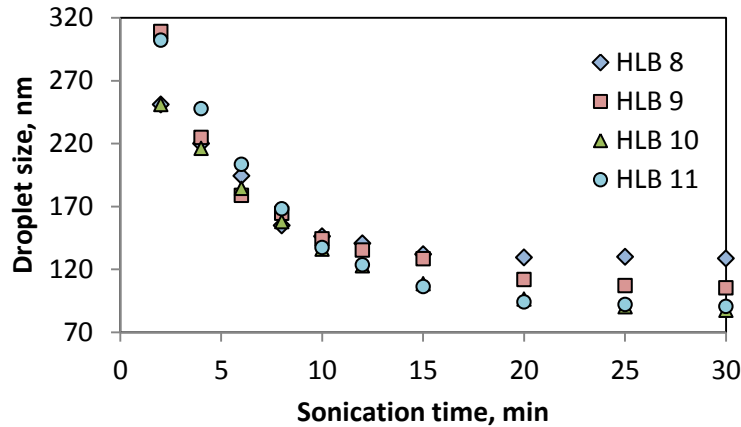
Fig.2.2 Effect of HLB values on droplet size of emulsion

(Condition: φ_O - 0.10, φ_S - 0.08, at 40% amplitude)

2.3.2 Influence of surfactant fraction

The role of surfactant is most significant during the formation of nanoemulsion as it decreases the extent of free energy, reducing the interfacial tension and droplet size. In present study, φ_S was varied in the range from 0.02 to 0.10 at fixed oil fraction (φ_O) of 0.10. It was observed that surfactant concentration significantly affect the droplet size. From Fig. 2.3, it was observed that on increasing φ_S from 0.02 to 0.08, the droplet size decreased from 176.1 nm to 87.38 nm after 30 min of sonication. But on increasing φ_S from 0.08 to 0.10, no further reduction in the droplet size was observed. Since the number of interfacial sites for the adsorption of surfactant was limited, excess surfactant concentration beyond an optimum value resulted in no further reduction in the droplet size. The emulsion prepared at φ_S value of 0.08 was found to be translucent, whereas at higher fractions (>0.08) the emulsions became more turbid. This indicates that beyond the optimum value (φ_S>0.8), the number of interfacial sites were insufficient for the large number of surfactant molecules and additional molecules lead to the micellisation in aqueous phase which caused increased turbidity of the emulsion.

It was also observed in these experiments that on increasing the sonication time, the droplet size reduced at all surfactant fraction. It can also be seen that for all sonication time i.e. from 15 to 30 min, the droplet size was almost constant for φ_S values greater than 0.08, which indicate that complete dispersion and adsorption of surfactant molecules was achieved at φ_S of 0.08. Therefore, φ_S value at 0.08 was considered to be an optimum fraction for prepared emulsions.

Furthermore, increase in the surfactant concentration also affected other emulsion properties such as PDI, interfacial tension, zeta potential, and density (Table 2.1). It was found that with an increase in the φ_S from 0.02 to 0.10, the droplet size range becomes narrow as PDI was reduced from 0.204 to 0.129. On increasing φ_S from 0.02 to 0.10, the interfacial tension decreased from 40.07 to 23.95 mN/m due to an increase in the interfacial area, thus providing more area for the adsorption of surfactant molecules. Also, an increase in the surfactant fraction marginally increased the density of the emulsions as effective volume fraction was increased due to surfactant molecular layer formation around the droplet. On increasing φ_S from 0.02 to 0.10, the zeta potential varied from -23.7 to -40 mV which also indicates that the formulations prepared at lower φ_S were less stable. The increased stability of emulsions with higher φ_S is due to increased surface charges that occurred at higher φ_S and thus maintained the repulsion between the droplets.
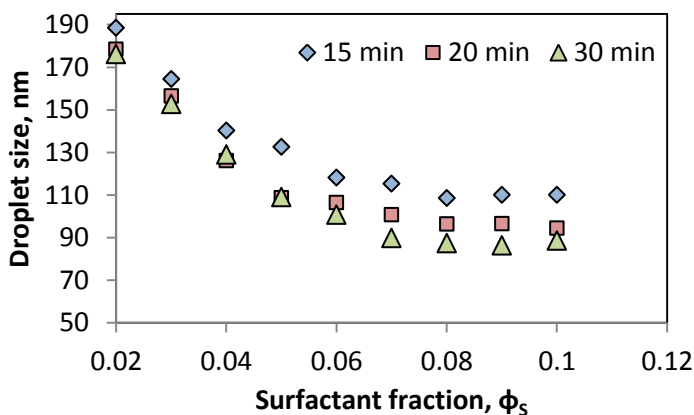
Fig. 2.3 Effect of surfactant concentration on droplet size as a function of sonication time (Condition: φ_O – 0.10, HLB – 10, 40% power amplitude)

Table 2.1 Effect of surfactant fractions on physico-chemical properties of prepared emulsion after 30 min of sonication

Surfactant fraction, φ_S	Droplet size, nm	PDI	Interfacial tension		Zeta potential, mV	Density, g/cc
			σ, mN/m	Std. deviation		
0.02	176.10	0.204	40.07	± 0.58	-23.5	0.988
0.03	152.70	0.209	35.45	± 1.72	-29.1	0.990
0.04	129.00	0.166	29.57	± 1.94	-30.2	0.989
0.05	109.00	0.137	27.45	± 2.57	-34.3	0.990
0.06	100.80	0.125	26.98	± 0.91	-36.8	0.991
0.07	89.73	0.112	26.14	± 1.76	-37.4	0.991
0.08	87.38	0.129	25.01	± 2.04	-37.9	0.993
0.09	86.31	0.131	24.06	± 0.17	-39.3	0.992
0.10	88.52	0.122	23.95	± 1.81	-40.4	0.993

2.3.3 Influence of oil fraction

The droplet size and stability of the emulsion also depends on the concentration of oil phase. In this study, emulsions were prepared with varying oil fraction, φ_O in the range of 0.10 to 0.40 (10% to 40%, v/v) at fixed HLB of 10 and φ_S at 0.08 and then subjected to sonication for a time up to 30 min. Variation in droplet size and stability of the emulsion w. r. t. sonication time is shown in Figs. 2.4 (A) & (B). It was observed that at sonication time of 30 min, on increasing the fraction, φ_O from 0.10 to 0.40, droplet size was increased from 87.38 nm to 212.8 nm. Higher φ_O resulted in higher droplet size due to increase in the rate of droplet coalescence. When the same amount of energy was supplied, the number of oil droplets formed was found likely to increase on increasing the oil fraction φ_O and thus resulted into more naked interfacial sites [32, 33]. As a result, the number of interfacial sites would be more for fixed surfactant fraction (φ_S) which increase the chances of coalescence and thereby the droplet size. The emulsions prepared at φ_O of 0.10 were found to be the most stable against creaming at all sonication times measured after 24 hour of storage as shown in Fig. 2.4B. Whereas the emulsions prepared at φ_O of 0.20 and 0.30 were completely stable against creaming after 15 and 25 min of sonication time respectively. It indicated that

emulsions of higher oil fraction require higher power dissipation to get the same reduction in droplet size. On further increasing φ_O from 0.30 to 0.40, the %CI was reduced to 96% which indicated that the rate of coalescence was higher at higher φ_O for fixed amount of energy supplied. Thus it can be concluded that higher fraction of oil up to 0.30 can be used to prepare the stable emulsion with increased sonication time and therefore benefits of higher oil fraction can be utilized for selected applications such as food and cosmetics using ultrasonication. Therefore based on the droplet size obtained, the fraction φ_O - 0.10 was found to be the optimum as the emulsion exhibited long term stability as compared to emulsions prepared at higher φ_O (>0.10).
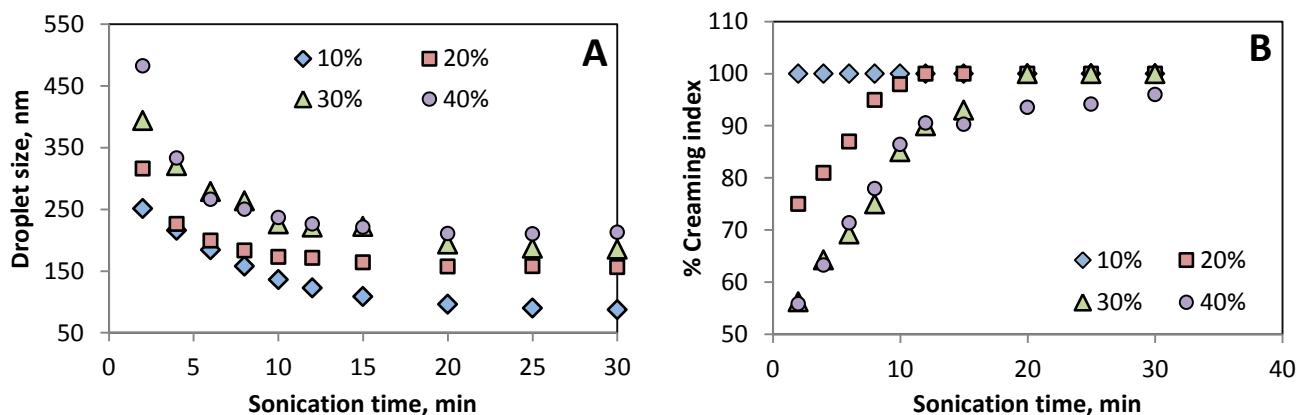
Fig. 2.4 Effect of oil fraction on (A) droplet size and (B) creaming index of emulsions
(Condition: φ_S − 0.08, HLB − 10 at 40% power amplitude)

2.3.4 Influence of operating parameters of ultrasonication on emulsification

2.3.4.1 Effect of power amplitude

To achieve high extent of dispersion of oil phase in continuous phase, high energy is required in order to break the oil-water interface and thereby cause the maximum extent of emulsification. As discussed earlier, ultrasonic cavitation induces shear forces which cause the disruption of larger droplets into smaller ones. Thus to analyze the effect of ultrasonic power on the droplet size, the power amplitude was varied at 20%, 30% and 40%. To evaluate the effectiveness of ultrasonic device, actual energy dissipated to emulsion was calculated, as it is lower than the rated power [9]. The actual energy dissipated to the system was calculated using calorimetric method [9, 30, 34]. The calculated energy dissipation is

presented in Table 2.2. It can be seen that energy dissipation increased with increase in the power amplitude. Fig. 2.5 (A) shows droplet size measurements as a function of sonication time at different ultrasonic amplitude. It was observed that the droplet size decreased with increasing power amplitude. This can be understood by the fact that at higher amplitude more energy was dissipated into the system which significantly produced higher cavitational collapse pressure at the end of asymmetric cavity collapse [33]. The minimum droplet size was obtained around 87 nm at 40% amplitude as compared to 93 nm and 121 nm obtained at 30% and 20% amplitude respectively after 30 min sonication. Therefore, 40% amplitude was found to be the optimum value for reduction in the droplet size to the maximum extent. Moreover, emulsion stability against creaming (% CI) was also increased due to the high energy dissipation at higher amplitude. From Fig. 2.5 (C), it was observed that at 40% amplitude, the emulsion was completely stable even after 5 min of sonication time, whereas at 30% and 20% amplitude, the emulsion became stable only within 10 and 15 min of sonication time respectively. Thus it can be concluded that operating the ultrasonic horn at 40% amplitude can efficiently reduce the droplet size and improve the stability of the emulsion against creaming and coalescence. Moreover it can be seen from Table 2.2 that there is not a significant change in the droplet size between 30% and 40% amplitude as well as %CI was found to be 100 % at all the sonication time studied for the 40% amplitude and therefore it was decided not to increase the % amplitude beyond 40% as it will unnecessary consumed more energy.

Similar trend was also observed by Jadhav et al. [30] for paraffin wax based nanoemulsion and by O'Sullivan et al. [34] for rapeseed oil based emulsions both prepared through ultrasonication.

Table 2.2 Energy dissipated supplied to emulsion and their effect on droplet size

Amplitude	Sonication time, min	Energy dissipated, kJ	Droplet size, nm	PDI
20%	30	9.57	121.0	0.301
30%	30	13.53	93.47	0.276
40%	30	17.07	87.38	0.129
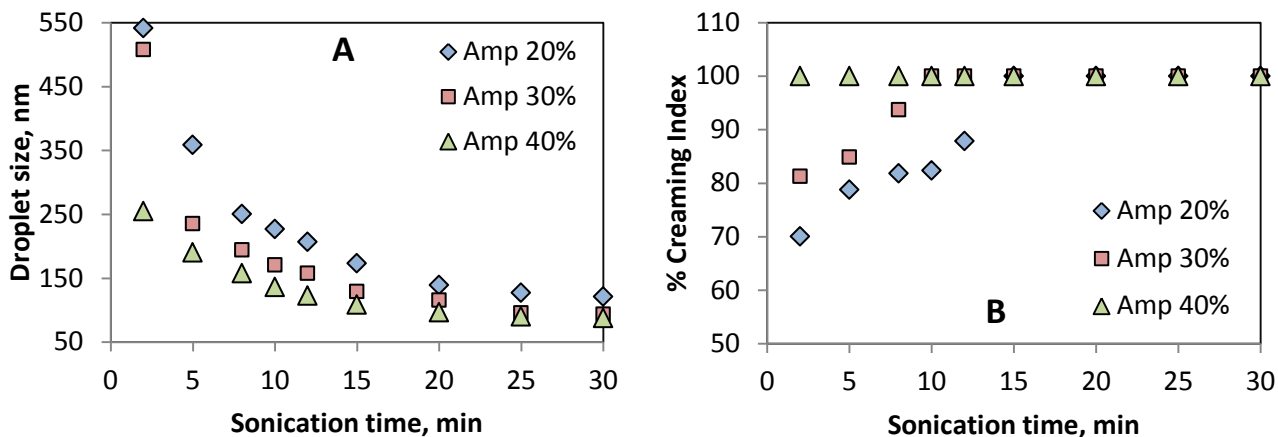
Fig. 2.5 Effect of different power amplitude on (A) droplet size and (B) Creaming Index of emulsion (Process condition: HLB – 10, φ_O – 0.10 and φ_S – 0.08).

The effect of energy density (J/ml) on droplet size was also investigated and is shown in Fig. 2.6. Droplet size also depends on the processing volume since the cavitational yield very much depends on the energy density (J/ml). At constant sonication time, the droplet size would generally be high at higher processing volume because of low energy dissipation that occurs at higher volume [34 - 36]. The ultrasonic emulsification in smaller volume is more efficient than large volume as acoustic energy is extensively distribute throughout the liquid resulting into more rapid reduction in droplet size [34]. However, at higher operating volume, minimum droplet size can be attained by increasing the exposure time of emulsion in acoustic field. The present investigation as shown in Fig. 2.6 has been done at constant sonication time of 30 min by preparing emulsion at optimal operating condition. The operating batch volume of emulsion was varied from 100 ml to 300 ml and the respective droplet size was found in range of 86 nm to 128.6 nm. An increase in droplet size with an increase in solution volume is attributed to lower energy dissipation at fixed sonication time. The droplet size data w. r. t. energy density was fitted in the model equation, $d \propto E_V^{-0.4}$, presented by Walstra [37] where E_V is energy dissipation (J/mL). It can be seen from Fig. 2.6 that the power law model is fitted well in experimental data with regression coefficient of 0.987. The constant and exponent were obtained as 925.13 and 0.4, respectively as shown in Eq. (2.3). Similar observation were also reported by Leong et al. [16] for the ultrasonic

emulsification of sunflower oil stabilized by sodium dodecyl sulfate and polyethylene glycol at atmospheric pressure using different sonication conditions.

$$d = 925.13 \, E_V{}^{-0.4} \hspace{3cm} (2.3)$$
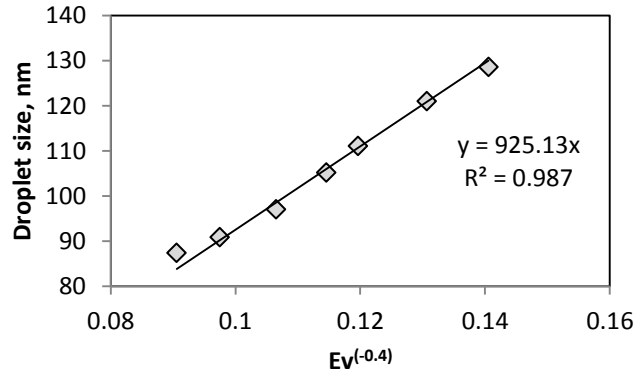
Fig. 2.6 Effect of energy density (E_V) on droplet size of emulsion (Condition: $\varphi_O - 0.10$, $\varphi_S - 0.08$, HLB $- 10$, 40% amplitude, and 30 min)

2.3.4.2 Effect of sonication time on emulsification

The sonication time has significant importance during ultrasonic emulsification. The sonication time indicates the residence time of emulsion under the extreme turbulence conditions of the acoustic field. At higher sonication time, the amount of energy dissipated would be more which resulted in lower droplet size. An increase in sonication time not only reduced the droplet size but also improved the uniformity of the droplets size distribution in the emulsion. It was observed that after sonication time of 20 to 25 min there was no or only a marginal change in droplet size in all the cases as discussed in previous sections (Figs. 2.2-2.5). The creaming stability was also improved after a certain sonication time depending on the other process parameters (Figs. 2.4-2.5). This showed that at higher sonication time the chances of droplet coalescence was reduced as more energy was dissipated into the emulsion causing no separation i.e. 100% CI. Apart from that, the cavitational effects also control the droplet size distribution. It was observed that on increasing the sonication time from 5 to 30 min, the PDI value decreased from 0.3 to 0.12 which indicates that the droplet size distribution became narrow at higher sonication time as shown in Fig. 2.7. At sonication time of 5 min, the droplet size distribution was bimodal and polydisperse which shifted to a unimodal and narrow distribution after 15 min of sonication time as shown in Fig. 2.7.
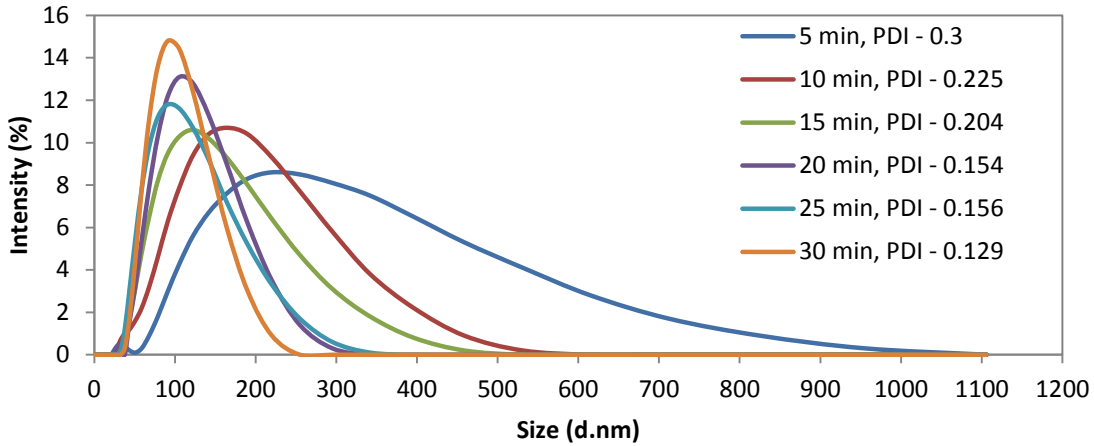
Fig. 2.7 Effect of sonication time on particle size distribution of nanoemulsion

2.3.5 Statistical analysis of process parameters using Response surface methodology

The RSM optimization technique was used in the statistical analysis of the observed data to analyze the individualistic and interactive effects of various process and operational parameters on the emulsion droplet size. The experimental data were used to derive the quadratic polynomial equation for the prediction of droplet size of nanoemulsions which is given in Eq. (2.4). This equation can be used to predict the droplet size of nanoemulsions and it was found that the predicted values agreed well with the experimental values. The mathematical equation for the droplet size shows the first-order effects (terms denoted by X_1, X_2, X_3, X_4, X_5), second-order effects (denoted by X_1^2, X_2^2, X_3^2, X_4^2, & X_5^2) and interaction effects (terms denoted by X_1X_5, X_2X_5, X_3X_5, and X_4X_5).

Model Equation:

$$Y = 992 - 98.6\,X_1 - 2378X_2 + 801.7X_3 - 10.65X_4 - 8.83X_5 + 5.34X_1^2 + 17807X_2^2 - 1031X_3^2 + 0.073X_4^2 + 0.1994X_5^2 - 0.641X_1X_5 - 34.43X_2X_5 + 4.91X_3X_5 + 0.176X_4X_5$$

$$\ldots\ldots\ldots (2.4)$$

Where, Y is the droplet size as response, X_1 is HLB, X_2 is surfactant fraction, X_3 is oil fraction, X_4 is % Amplitude, and X_5 is sonication time.

The results of ANOVA for the fitted quadratic polynomial model of droplet size are shown in Table 2.3. Analysis of variance (ANOVA) showed that the resultant quadratic polynomial model adequately represented the experimental data with the coefficients of regression (R^2) as 0.96. The parameter significance is described by the F-values and p-values, where higher

value of F and lower value of p (< 0.05) indicates the higher significance level of the coefficients in the equation. As shown in Table 2.3, the corresponding P-values indicate that all parameters such as HLB, φ_O, φ_S, % Amplitude and time had significant effect on the droplets size ($P < 0.05$).

Table 2.3 ANOVA for the fitted quadratic polynomial model of emulsion droplet size.

Source	Degree of Freedom	Sum of squares	Mean square	F-Value	P-Value
Model	14	221713	15836.7	196.70	0.000
X_1-HLB	1	2276	2276.1	28.27	0.000
X_2-SF (φ_S)	1	26973	26973.2	335.02	0.000
X_3-OF (φ_O)	1	67892	67891.8	843.24	0.000
X_4-% Amp	1	20615	20615.0	256.05	0.000
X_5-Time	1	10316	10316.4	128.13	0.000
Squares					
X_1^2	1	995	995.1	12.36	0.001
X_2^2	1	5962	5961.6	74.04	0.000
X_3^2	1	3255	3254.9	40.43	0.000
X_4^2	1	249	249.3	3.10	0.082
X_5^2	1	15766	15765.6	195.81	0.000
2-Way Interaction					
$X_1.X_5$	1	1000	1000.1	12.42	0.001
$X_2 X_5$	1	3575	3574.7	44.40	0.000
$X_3.X_5$	1	1137	1137.4	14.13	0.000
$X_4. X_5$	1	5613	5613.3	69.72	0.000
Error	87	7005	80.5		
Total	101	228718			

$R^2 = 96.94\%$; R^2 (adj.) = 96.44%

It has been observed that F-value (843.24) was higher in the case of X_3 (oil fraction) as compared to that obtained with other variables. This indicated that the individual influence of oil fraction on the emulsion droplet size was more than that of other variables such as HLB, φ_S, Amplitude, time and other interaction effect. It can be seen from the contour plots in Fig. 2.8A that droplet size increased as oil fraction was increased. This could be attributed to many reasons such as, higher oil content leads to increase in emulsion viscosity and thereby making the droplet disruption more difficult. Also, at higher oil fraction, oil to surfactant ratio increased which ultimately caused increased interfacial

tension at the oil-water interface and thereby required higher sonication time to achieve the higher droplet size reduction.

The second most significant parameter is surfactant fraction (φ_S). It can be observed from Fig. 2.8C that the droplet size reduced as the surfactant concentration increased. The oil surfactant ratio reduced with an increase in the surfactant fraction and thereby caused lower droplet size as sufficient amount of surfactant molecules were available at the oil water interface at higher φ_S. The individual influence of HLB was found to be lower as compared to all other variables as the F-value (28.27) of HLB was lower as shown in Table 2.3. Since, the selected values of HLB (varied between 8 to 12) were found to be the most favorable conditions for the preparation of oil in water emulsion, therefore the effect of HLB was found to be less significant in the selected range. This can also be understood from the fact that for all HLB values, the droplet size was found to be below 160 nm even at the lower sonication time of 15 min as shown in Fig. 2.8B. However, at higher oil fraction, $\varphi_O > 0.3$, emulsions possess minimum droplet size in the range of 200-220 nm even at higher sonication time (>20 min) as shown in Fig. 2.8A. Therefore oil and surfactant fractions were found to affect the droplet size most significantly than other individual parameters and their interaction effects. The significance level was found to be in the order as $\varphi_O > \varphi_S > \%$Amp > Time > HLB.

2.3.5.1 Interpretation of residual plots

The model estimation is based on its ability to explain the experimental data. The residuals investigate how well the model predicts the observed data [43]. The normal % probability versus residuals is presented in Fig. 2.9. The residuals fall on a straight line indicating the normal distribution of errors, therefore the adequacy of the least square fit was obtained [43, 44]. In Fig. 2.9, the plot of residuals versus fitted response values of the droplet size shows equal scatter of the points above and below the x-axis which indicated that the residuals satisfy the independency and constant variance. This reveals that the suggested model is adequate in describing the dependency of the droplet size on the selected regressors (independent variables) applied for the emulsification process.
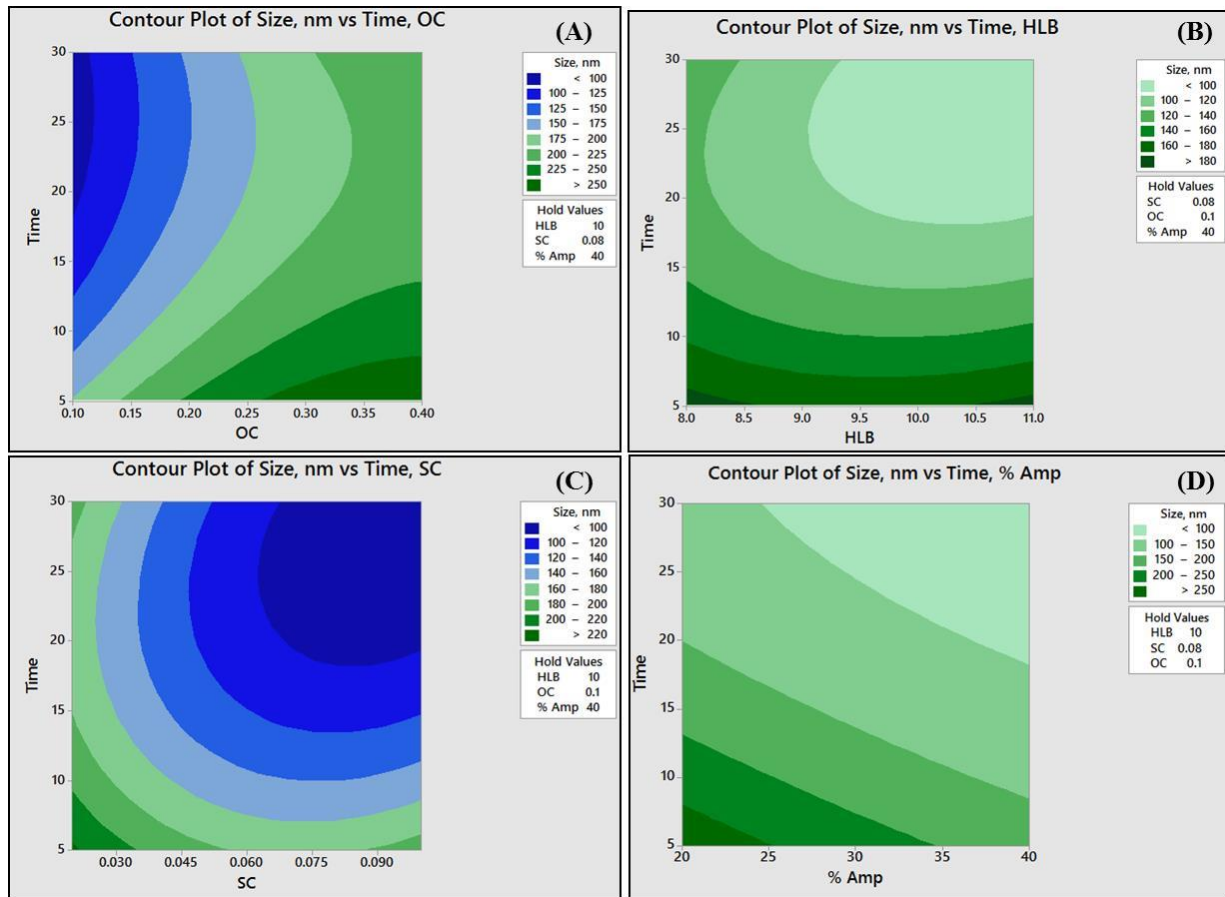
Fig. 2.8 Contour plots of combined effects of (A) Oil fraction (OC) with time, (B) HLB with time, (C) surfactant fraction (SC) with time, and (D) % Amplitude with time, on the droplet size of nanoemulsion
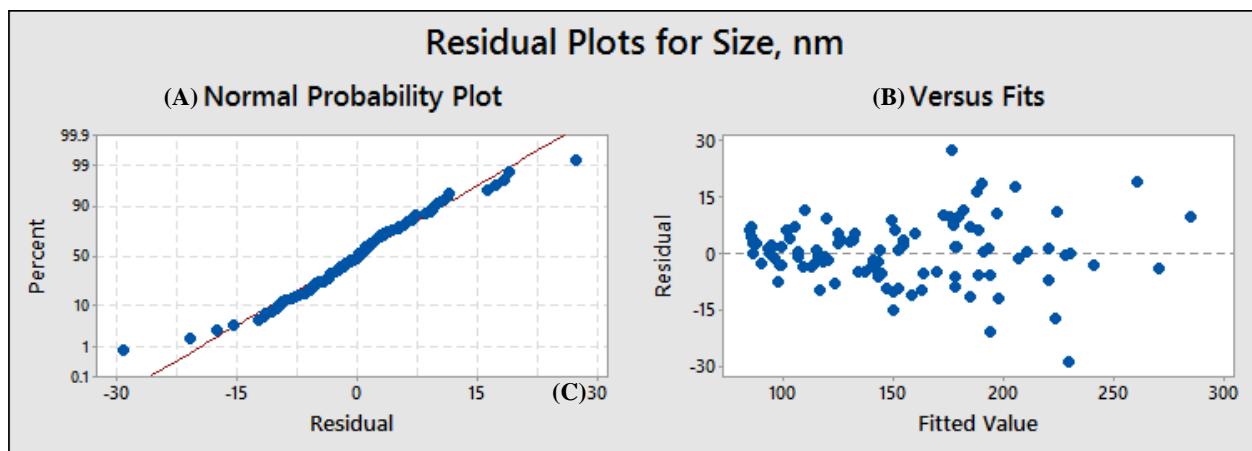
Fig. 2.9 Residual plots for droplet size of nano-emulsion (A) Normal probability; and (B) residuals versus predicted response

67

2.3.6   Effect of ultrasonication on molecular structure of oil

As proven in many studies, ultrasonically assisted emulsions are produced by the physical effects induced in liquids such as liquid microjets, mechanical vibrations, and extreme turbulence as a result of violent cavity collapse [38, 39]. However, it was also established that acoustic cavitation through ultrasound can effectively generate highly reactive free radicals due to the dissociation of molecules under extreme conditions of cavity collapse which are capable to oxidize lipids and fatty oils [40- 42]. A study conducted by Pandit and Joshi [40] reported that the cavitational (chemical) effects can initiate the hydrolysis of fatty oils under the ambient conditions. Chemat et al. [41] observed the oxidation of sunflower oil due to the presence of extraneous free radicals produced during ultrasound treatment. Thus to find out the possible impact of ultrasound induced chemical effects on mustard oil in nanoemulsion, FTIR analysis of emulsion was performed and compared with pure mustard oil. Fig. 2.10 shows FTIR spectra of pure mustard oil and sonicated nanoemulsion at different sonication time. It was assumed that at higher sonication time, the degree of cavitational activity in terms of chemical effects would be high and would attack the oil molecules for a longer time and may degrade it more. Thus, to compare the effect of sonication time on emulsion quality/structure of oil, FTIR spectra were performed for a low sonicated (5 min) and one for higher sonicated emulsion (30 min) as shown in Fig. 2.10. It was found that all of the peaks were same as obtained in pure mustard oil except the first peak observed in case of nanoemulsion at 3349.35 cm^{-1}which is corresponding to H-OH stretching indicating the presence of water in emulsion. The other major peaks observed at 1743.53 cm^{-1} and 1640.96 cm^{-1} corresponding to C=O stretch indicate the presence of esters in oil which was same as that of the spectra of pure oil. Therefore presence of no extra peaks except the peak of H-OH bond confirmed that no chemical changes occurred by ultrasonication during emulsification which means only physical effects were induced during the ultrasonically prepared emulsion. Moreover, the spectra of emulsion prepared at 5 min and 30 min were identical indicating the absence of chemical effects during emulsification and proved that the oil structure remain unchanged even at the higher sonication time. The FTIR analysis indicated no disintegration of the oil molecular structure even though some previous studies report on the hydrolysis of oil during the ultrasonic emulsification at higher sonication time [40]. Previous study by Pandit and Joshi reported that the hydrolysis of

Castor and kerdi oil occurred when subjected to sonication beyond 100 min which resulted in an increase in the free fatty acid content. However, in the present study, sonication was applied only for a period of 30 min and the hydrolysis of oil may not have occurred within 30 min of sonication. Therefore, it was concluded that oil molecules have not been hydrolyzed or deteriorated under ultrasonication conditions as depicted in the FTIR analysis. Apart from that, there was no evidence of any burnt metallic odor during emulsification after sonication time of 30 min, indicating no oxidative breakdown of lipids in the oil. This may be due to the presence of oil molecules inside the emulsion droplets which are in nano scale and therefore oil molecules were not exposed directly to the ultrasonication effects and free radicals. Thus from these aspects, it can be concluded that the oil molecular structure was unaffected by ultrasonication.

The FTIR spectrum of mustard oil nanoemulsion was found consistent with the spectra of mustard oil based microemulsion provided by Ghosh et al. [28]. Jadhav et al. [30] had also observed similar results for the preparation of paraffin wax nanoemulsion using ultrasonication. The FTIR spectra of the prepared nanoemulsion indicated only the presence of H-OH bond and they had concluded that chemical effects were not affecting the chemical structure of paraffin wax during ultrasonically prepared emulsion.
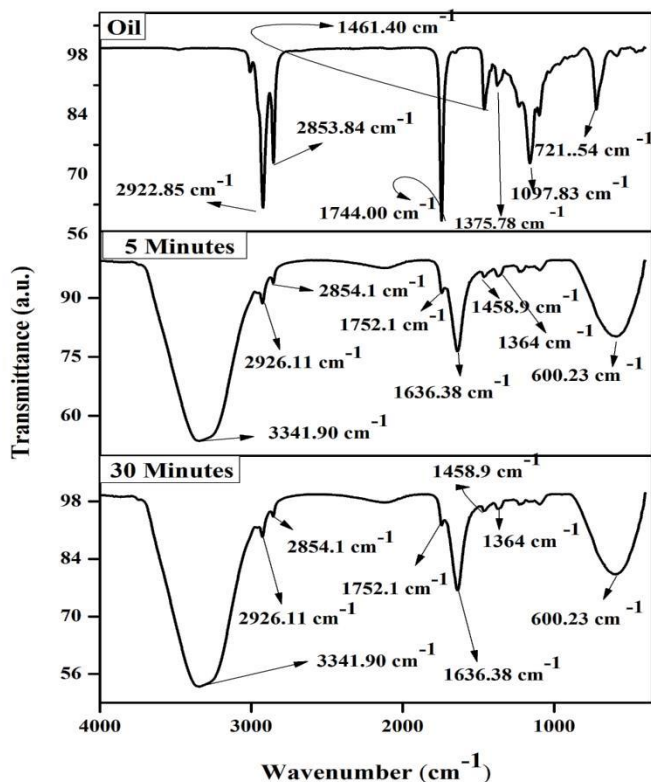
Fig. 2.10 FTIR Spectra of pure mustard oil and nanoemulsion prepared at different sonication time

2.3.7 Kinetic stability analysis

It is necessary to evaluate the stability of emulsion before their applications in the required field. In present study the kinetic stability test was carried out not only to evaluate the instability of emulsions against the breakdown process such as creaming and coalescence but also for predicting their long term stability. Under the influence of centrifugal force and high temperature, the Brownian motion of droplets increases and as a result the droplets may approach each other [33, 45, 46] which consequently increases the rate of coalescence and droplet size. An emulsion is said to be physically stable if their dispersed state remain unchanged i.e. if the droplets size remains constant even at the input of centrifugal force and high temperature. The kinetic stability of emulsions under the centrifugation and thermal stress was confirmed based on size and % CI measurement. An emulsion is said to be stable if it possess similar droplet size after the stability test whereas the instability is confirmed if there is a large difference in droplet size along with any decrement in % CI value.

In the present study, the emulsion formulations prepared at 15 min and 30 min sonication time and which showed 100 % creaming index after sonication were subjected to the centrifuge and high temperature cycle after 7, 30, and 90 days of storage and the their kinetic stability was confirmed based on no change found in the droplet size after the analysis. Before the stability test was conducted, the samples were kept in a dark place at room temperature for 7 days.

2.3.7.1 Centrifuge test

For the formulations prepared at optimum condition i.e. at HLB 10, φ_O – 0.10, φ_S – 0.08 and 40% amplitude after 15 min and 30 min sonication, it was observed that on conducting the centrifuge test at 5000 RPM (3520 RCF) for 15 min, there was no evidence of creaming or separation and no significant difference was found in droplet size even after 90 days of storage as shown in Table 2.4. Steric hindrance provided by the surfactants maintains the repulsion between the droplets and sonication effect reduces the droplet size and controls the size distribution. The combined effect of ultrasonication and surfactant helps in maintaining the stability of emulsion under the shear of centrifuge. However, the formulations prepared at lower power amplitude of 20% and 30% for 15 min sonication showed some breakdown whereas the formulations at 40% amplitude after 15 min sonication doesn't show any breakdown and remained stable. The % CI of emulsion at 20% and 30% amplitude decreased to 96% and 98% respectively and also the droplet size increased from 180.7 nm to 210.5 nm (20% amplitude) and 138.8 nm to 146.3 nm (30% amplitude). The higher droplet size at lower % amplitude can be attributed to the reduced energy dissipation. The energy dissipation at 40% amplitude was 14.5 kJ which was higher than 11.2 kJ and 7 kJ obtained at 30% and 20% amplitude, respectively. Therefore, at lower amplitude (20%), droplets of larger size were obtained which subsequently coalesced with each other under the influence of centrifugal force of 3520 RCF (5000 RPM) which resulted into an increased droplet size of the nanoemulsion and thereby caused reduced stability. But the formulation prepared at sonication time of 30 min did not show any instability and droplet size remained constant after the centrifuge test indicating that higher sonication time was required at lower amplitude for obtaining better stability of emulsion. Similar observation was also reported by Silva et al. [33] in their study during the centrifugation of triglyceride oil based emulsion

stabilized by anionic (SDS), cationic (DTAB) and nonionic surfactant (Tween 20). It was found that there was no significant change in droplet size under the effect of centrifugation and emulsion was found to be stable during storage of 1 year.

Thus in all, it can be concluded that, under the centrifugal effects, the stability of the emulsion was not disturbed and emulsions were found to be kinetically stable due to perfect dispersion and minimum droplet size was attained using ultrasonication.

2.3.7.2 Thermal stress test

Thermal stability of the emulsions prepared at the optimum condition was performed after periods of 7 days, 1 month and 3 months as shown in Table 2.4. Emulsions were subjected to heating at 40°C, 60°C and 80°C to check the possible instability phenomena under the thermal stress conditions. To confirm the stability of the emulsion under the heating cycle, size measurements were conducted immediately after heating the sample for 30 min at each temperature. It was observed that formulations prepared at the optimum condition i.e. HLB 10, φ_S – 0.08, φ_O – 0.10 and 40% amplitude after 15 min and 30 min sonication, were found to be stable after heating the sample at 40 to 80°C. Increase in temperature did not have any significant effect on the emulsion characteristics as there was no evidence of phase separation or any significant change in the droplet size. For formulations that were prepared with φ_O – 0.20 at 30 min sonication, when heated at 80°C, the droplet size increased from 156.1 nm to 179.2 nm, whereas on heating at 40 and 60°C, samples were stable as the droplet size remained same. This indicated that emulsion with higher oil fraction ($\varphi_o > 0.10$) undergoes coalescence when heated to 80°C and this caused instability and phase separation within the prepared emulsions. Similar observation was also found in case of the formulations prepared at 20% amplitude after 15 min sonication. It was observed that the droplet size increased from 180.7 nm to 202.2 nm, 209.5 nm and 216.6 nm at 40°C, 60°C and 80°C respectively. This was due to the inadequate shear applied during the preparation of emulsion at 20% amplitude and 15 min sonication time. When formulations prepared at extended sonication of 30 min were subjected to heating at 40 to 80°C, the droplet size remained constant. This indicated that adequate amount of energy was provided in 30 min sonication that maintained the dispersion and stability of emulsion under the heating conditions for lower amplitude.

Thus, based on the results obtained at optimum conditions as shown in Table 2.4, it was concluded that the nanoemulsions of smaller droplet size (<150 nm) were less sensitive under the influence of heating effects even after 3 months and hence proved to be kinetically stable.

Table 2.4 Droplet size of nanoemulsion produced with optimum condition (HLB – 10, φ_O - 0.10, φ_S – 0.08, Amplitude – 40%) at 15 min sonication after kinetic stability tests.

Droplet size, nm			
After production	108.6 ± 7.02		
No. of days	7	30	90
After centrifuge	110.6 ± 1.69	110.8 ± 3.06	111.4 ± 3.88
After thermal stress			
40°C	109.6 ± 4.52	108.8 ± 5.79	109.2 ± 1.97
60°C	110.5 ± 3.06	110.7 ± 5.62	110.2 ± 6.92
80°C	108.9 ± 2.19	109.7 ± 7.99	111.0 ± 3.53

2.3.7.3 Long term stability

Droplet size and PDI of nanoemulsion as a function of storage time are shown in Fig. 2.11. The emulsion prepared at optimum HLB – 10, φ_O – 0.10, φ_S – 0.08, Amplitude – 40% after 15 min sonication was stored up to 3 months in order to check any change in droplet size and instability phenomena. It can be observed from Fig. 2.9 that the droplet size and size distribution in nanoemulsion were found to be uniform for the period up to 3 months and emulsion prepared at optimal conditions exhibit good stability against creaming for 3 months. Similar results were also reported in literature [8, 18, 25, 28]. Shanmugam and Ashokkumar [6] have reported the stability of ultrasonically prepared flaxseed oil emulsion against creaming up to 9 days and found that % CI was 100% at different sonication conditions. Ghosh et al. [18] reported no change in the droplet size and phase characteristics of ultrasonically prepared basil oil emulsion during 1 month of storage and concluded that the emulsion was kinetically stable for 1 month. Jadhav et al. [30] also observed that the ultrasonically prepared paraffin wax nanoemulsion stabilized by SDS was found kinetically stable up to 3 months. Silva et al. [33] found that the emulsion of triglyceride oil stabilized

by an anionic (SDS), cationic (DTAB) and nonionic surfactant (Tween 20) were found to be kinetically stable up to 35 days as the droplet size of each formulation obtained was same throughout the period of 35 days.

Thus it can be concluded from the present study that ultrasonication is an efficient technique for the formation of mustard oil based nanoemulsions as the emulsion was found to be kinetically stable up to 3 months against creaming and also at the different shear conditions (centrifuge, thermal stress and storage stability).
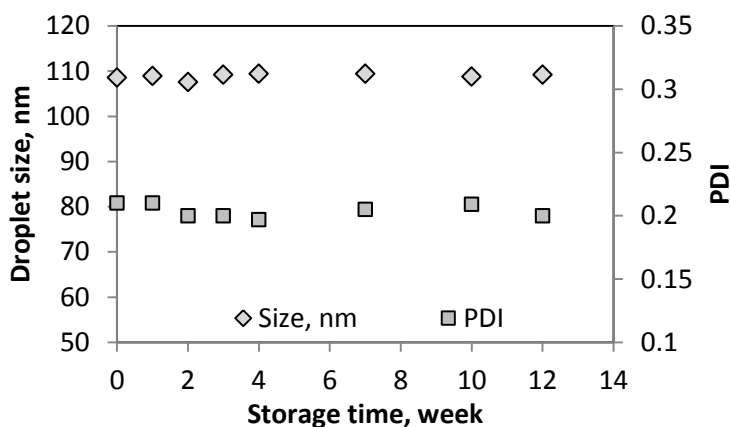
Fig. 2.11 Droplet size and PDI value of emulsion as a function of storage time
(Condition: HLB − 10, φ_O − 0.10, φ_S − 0.08, 15 min, 40 % Amplitude)

2.4 Summary

It has been studied that ultrasound cavitation is a viable and efficient technique for the formation of mustard oil in water nanoemulsions of droplet size in nano range. The present work is summarized as below:

1. The size of emulsion droplets decreased with an increase in the HLB value from 8 to 10 but beyond HLB 10, the droplet size remained constant.

2. The surfactant fraction (φ_S) was studied in the range of 0.02 to 0.10 and, it was observed that droplet size decreased up to an optimum φ_S of 0.08 and then remained constant. However, the droplet size was observed to be in nano range between 87 to 150 nm for φ_S varying from 0.03 to 0.08 which indicate that less surfactant can be used in combination with ultrasonication. The minimum droplet size was found at φ_S − 0.08 which was considered to be the optimum volume fraction.

3. Increase in droplet size as well as some extent of creaming was observed with an increase in the oil volume fraction (φ_O) of emulsion. Minimum droplet size was

74

obtained for volume fraction (φ_O) of 0.10. However, the droplet size of emulsion at φ_O of 0.20 was also in nano ranges i.e. 156 nm and was also found kinetically stable as % CI was 100%. This indicates that higher volume fraction can also be used to prepare stable emulsions with the help of ultrasonication and thus make it a viable option for food industries.

4. The power amplitude of 40% was found to be efficient as the droplet size obtained was lowest and emulsion was more stable against creaming as compared to the emulsions prepared at 20% and 30% amplitude.

5. The statistical analysis was conducted using RSM technique to develop an empirical second order polynomial regression model that predicted the droplet size of emulsion under the influence of independent process variables and their interactive effects. The results showed that there was a significant effect of all parameters on the droplet size but the influence of oil fraction was found to be more as compared to others.

6. The fitted polynomial model adequately represented the experimental data with the coefficients of regression (R^2) at 0.96. The residuals indicated the behavior of the model equation in which the predicted values agreed well with the experimental values of the study.

7. The ultrasound cavitation effects did not affect the oil structure which was confirmed using FTIR analysis. This indicated that only physical effects of ultrasonication were contributing and the molecular structure of oil in emulsion was not disturbed.

8. The stability of the emulsion was demonstrated by the centrifuge and thermal stress tests whereby the emulsion exhibited good stability against creaming under the shear of centrifugal force and high temperature conditions. The droplet size was found to be unchanged after the kinetic stability analysis.

9. Also the emulsion prepared through ultrasonication was found to be stable for up to 3 months as there was no evidence of phase separation and any increment in droplet size.

Thus in overall it can be concluded that ultrasonically prepared mustard oil based nanoemulsion can be applicable for many practical applications in food and cosmetics industry.

References

1. W. Liu, D. Sun, C. Li, Q. Liu, J. Xu, Formation and stability of paraffin oil-in-water nano-emulsions prepared by the emulsion inversion point method, Journal of Colloid and Interface Science 303 (2006) 557–563.

2. C. Solan, P. Izuierdo, J. Nolla, N. Azemar, M.J. Garcia, Nanoemulsions. Curr. Opin. Colloid. Interface Sci.10 (2005) 102-110.

3. Wang, X.Y.; Wang, Y.W; Huang, R. Enhancing stability and oral bioavailability of polyphenols using nanoemulsions. In: Micro/Nanoencapsulation of Active Food Ingredients. Q. R. Huang, P. Given and M. Qian (Editors). (2009) ACS Symposium Series 1007. Washington, DC.

4. T. Mahmood, N. Akhtar, S. Manickam, Interfacial film stabilized W/O/W nano multiple emulsions loaded with green tea and lotus extracts: systematic characterization of physicochemical properties and shelf-storage stability. Journal of Nanobiotechnology 12(1) (2014) 1-8.

5. S. Parthasarathy, S. Y. Tang, S. Manickam, Generation and optimization of palm oil-based oil-in-water (O/W) submicron-emulsions and encapsulation of curcumin using a liquid whistle hydrodynamic cavitation reactor (LWHCR), Ind. Eng. Chem. Res. 52 (34) (2013) 11829–11837.

6. J. Gutierrez, C. Gonzalez, A. Maestro, I. Sole, C. Pey, J. Nolla, Nano-emulsions: new applications and optimization of their preparation. Curr. Opin. Colloid Interface Sci. 13 (2008) 245-251.

7. D.K. Sarker, Engineering of nanoemulsions for drug delivery. Current Drug Delivery.2 (2005) 297-310.

8. A. Shanmugam, M. Ashokkumar, Ultrasonic preparation of stable flax seed oil emulsions in dairy systems physicchemical characterization, Food Hydrocolloids 39 (2014) 151-162.

9. K. A. Ramisetty, A. B. Pandit, P. R. Gogate, Ultrasound assisted preparation of emulsion of coconut oil in water: Understanding the effect of operating parameters and comparison of reactor designs, Chemical Engineering and Processing 88 (2015) 70–77.

10. S. Y. Tang, P. Shridharan, M. Sivakumar, Impact of process parameters in the generation of novel aspirin nanoemulsions–comparative studies between ultrasound cavitation and microfluidizer. Ultrasonics Sonochemistry, 20(1) (2013) 485-497.

11. S. Y. Tang, M. Sivakumar, B. Nashiru, Impact of osmotic pressure and gelling in the generation of highly stable single core water-in-oil-in-water (W/O/W) nano multiple emulsions of aspirin assisted by two-stage ultrasonic cavitational emulsification, Colloids and Surfaces B: Biointerfaces102 (2013) 653-658.

12. S. Y. Tang, S. Manickam, T. K. Wei, B. Nashiru, Formulation Development and Optimization of a Novel Cremophore EL-based Nanoemulsion using Ultrasound Cavitation, Ultrasonics Sonochemistry 19(2) (2012) 330-345.

13. M. Sivakumar, S. Y. Tang, K. W. Tan, Cavitation technology – A greener processing technique for the generation of pharmaceutical nanoemulsions, Ultrasonics Sonochemistry 21 (2014) 2069–2083.

14. M.K. Li, H.S. Fogler, Acoustic emulsification. Part 1. The instability of the oilwater interface to form the initial droplets, J. Fluid Mech. 88 (3) (1978) 499– 511.

15. M.K. Li, H.S. Fogler, Acoustic emulsification. Part 2. Break-up of the larger primary oil droplets in a water medium, J. Fluid Mech. 88 (3) (1978) 513–528.

16. T.S.H. Leong, T.J. Wooster, S.E. Kentish, M. Ashokkumar, Minimising oil droplet size using ultrasonic emulsification, Ultrasonics Sonochemistry 16 (2009) 721–727.

17. A. Shanmugam, M. Ashokkumar,Characterization of Ultrasonically Prepared Flaxseed oil Enriched Beverage/Carrot Juice Emulsions and Process-Induced Changes to the Functional Properties of Carrot Juice Food Bioprocess Technol8 (2015) 1258-1266.

18. V. Ghosh, A. Mukherjee, and N. Chandrasekaran, Ultrasonic emulsification of food-grade nanoemulsion formulation and evaluation of its bactericidal activity." Ultrasonics Sonochemistry 20(1) (2013) 338-344.

19. I. Alzorqi, M. R. Ketabchi, S. Sudheer, S. Manickam, Optimization of ultrasound induced emulsification on the formulation of palm-olein based nanoemulsions for the incorporation of antioxidant β-d-glucan polysaccharides, Ultrasonics Sonochemistry 31 (2016) 71-84.

20. K. W. Tan, S. Y. Tang, R. Thomas, N. Vasanthakumari, S. Manickam, Curcumin-loaded sterically stabilized nanodispersion based on non-ionic colloidal system induced by

ultrasound and solvent diffusion-evaporation. Pure and Applied Chemistry, 88 (2016) 43-60.

21. S. Y. Tang, M. Sivakumar, A. M. H. Ng, P. Shridharan, Anti-inflammatory and analgesic activity of novel oral aspirin-loaded nanoemulsion and nano multiple emulsion formulations generated using ultrasound cavitation. International journal of pharmaceutics 430(1) (2012) 299-306.

22. T. K. Wei, S. Manickam, Response Surface Methodology, an Effective Strategy in the Optimization of the generation of Curcumin-loaded Micelles, Asia-Pacific Journal of Chemical Engineering 7(S1) (2012) S125-S133.

23. S. Y. Tang, M. Sivakumar, Design and Evaluation of Aspirin-loaded Water-in-Oil-Water Nano Multiple Emulsions prepared using Two-stage Ultrasonic Cavitational Emulsification Technique, Asia-Pacific Journal of Chemical Engineering 7(S1) (2012) S145-S156.

24. V. Ghosh, A. Mukherjee, and N. Chandrasekaran, "Influence of process parameters on droplet size of nanoemulsion formulated by ultrasound cavitation." Journal of Bionanoscience 7(5) (2013) 580-584.

25. V. Ghosh, A. Mukherjee, and N. Chandrasekaran, "Optimization of process parameters to develop nanoemulsion by ultrasound cavitation. J. Pure Appl. Ultrason. 37 (2015), 53-56.

26. R. P. Yadav, B. Kumari, Ultrasonic Studies on Mustard Oil: A Critical Review, International Journal of Science and Research 4(8), 517-531.

27. M. Mazza, M. Pomponi, L,Janiri, P.Bria, S.Mazza, Omega-3 fatty acids and antioxidants in neurological and psychiatric diseases: an overview. Progress in Neuro-Psychopharmacology & Biological Psychiatry 31 (2007)12-26.

28. V. Ghosh, A. Mukherjee, and N. Chandrasekaran, Mustard oil microemulsion formulation and evaluation of bactericidal activity, Int J Pharm PharmSci, 4 (2012) 497-500.

29. R. Pichot, F. Spyropoulos, I.T. Norton, Competitive adsorption of surfactants and hydrophilic silica particles at the oil–water interface: Interfacial tension and contact angle studies, Journal of Colloid and Interface Science 377 (2012) 396–405.

30. A. J. Jadhav, C. R. Holkar, S. E. Karekar, D. V. Pinjari, A. B. Pandit, Ultrasound assisted manufacturing of paraffin wax nanoemulsions: Process optimization, Ultrasonics Sonochemistry 23 (2015) 201–207.

31. C. Li, Z. Mei, Q. Liu, J. Wang, J. Xu, D. Sun, Formation and properties of paraffin wax submicron emulsions prepared by the emulsion inversion point method, Colloids and Surfaces A: Physicochem. Eng. Aspects 356 (2010) 71–77.

32. T. F. Tadros, Applied Surfactants: Principles and Applications, Wiley-VCH Verlag GmbH & Co. KGaA, Weinheim, 2005.

33. H. Silva, M. Cerqueira, A. Vicente, Influence of surfactant and processing conditions in the stability of oil-in-water nanoemulsions. Journal of Food Engineering 167 (2015) 89-98.

34. J. O. Sullivan, B. Murray, C. Flynn, I. Norton, Comparison of batch and continuous ultrasonic emulsification processes, Journal of Food Engineering 167 (2015), 114-121.

35. P. R. Gogate, P. A. Tatake, P. M. Kanthale, A. B. Pandit, Mapping of Sonochemical reactors: review, analysis, and experimental verification. AIChE Journal 48 (2002) 1542-1560.

36. P. R. Gogate, A. B. Pandit, Sonochemical reactors: scale up aspects. Ultrasonics Sonochemistry 11 (2004) 105-117.

37. P. Walstra, Principles of emulsion formation, Chem. Eng. Sci. 48 (2) (1993) 333–349.

38. S. Abbas, K. Hayat, E. Karangwa, M. Bashari, X. Zhang, An overview of ultrasound-assisted food-grade nanoemulsions. Food Eng. Reviews, 5 (2013), 139-157.

39. M. Ashokkumar, R. Bhaskaracharya, S. Kentish, J. Lee, M. Palmer, B. Zisu, The ultrasonic processing of dairy products e an overview, Dairy Science & Technology 90 (2010) 147-168.

40. A. B. Pandit, J. B. Joshi, Hydrolysis of fatty oils: effect of cavitation. Chemical Engineering Science 48(19) (1993) 3440-2.

41. F. Chemat, I. Grondin, P. Costes, L. Moutoussamy, A. Shum Cheong Sing, J. Smadja, High power ultrasound effects on lipid oxidation of refined sunflower oil. Ultrasonics Sonochemistry 11 (2004) 281–285.

42. S. Y. Tang, M. Sivakumar, A novel and facile liquid whistle hydrodynamic cavitation reactor to produce submicron multiple emulsions, AIChE Journal 59(1) (2013) 155-167.

43. S.S. Galooyak, and B. Dabir, Three-factor response surface optimization of nano-emulsion formation using a microfluidizer. Journal of food science and technology 52 (2015) 2558-2571.

44. S. Hosseini, B.G. Tarzi, M. Gharachorloo, M. Ghavami, H. Bakhoda, Optimization on the stability of linseed oil-in-water nanoemulsions generated by ultrasonic emulsification using response surface methodology (RSM). Oriental Journal of Chemistry 31(2015) 1223.

45. D. McClements,. Food Emulsions: Principles, Practice, and Techniques, (2005) 2nd ed. CRC Press, Boca Raton, Florida.

46. J.M. Morais Diane, J. Burgess, Vitamin E nanoemulsions characterization and analysis. Int. J. Pharm. 465 (2014), 455–463.

CHAPTER 3

FORMATION AND STABILITY OF O/W NANOEMULSION USING HYDRODYNAMIC CAVITATION: EFFECT OF GEOMETRY AND CAVITATION NUMBER
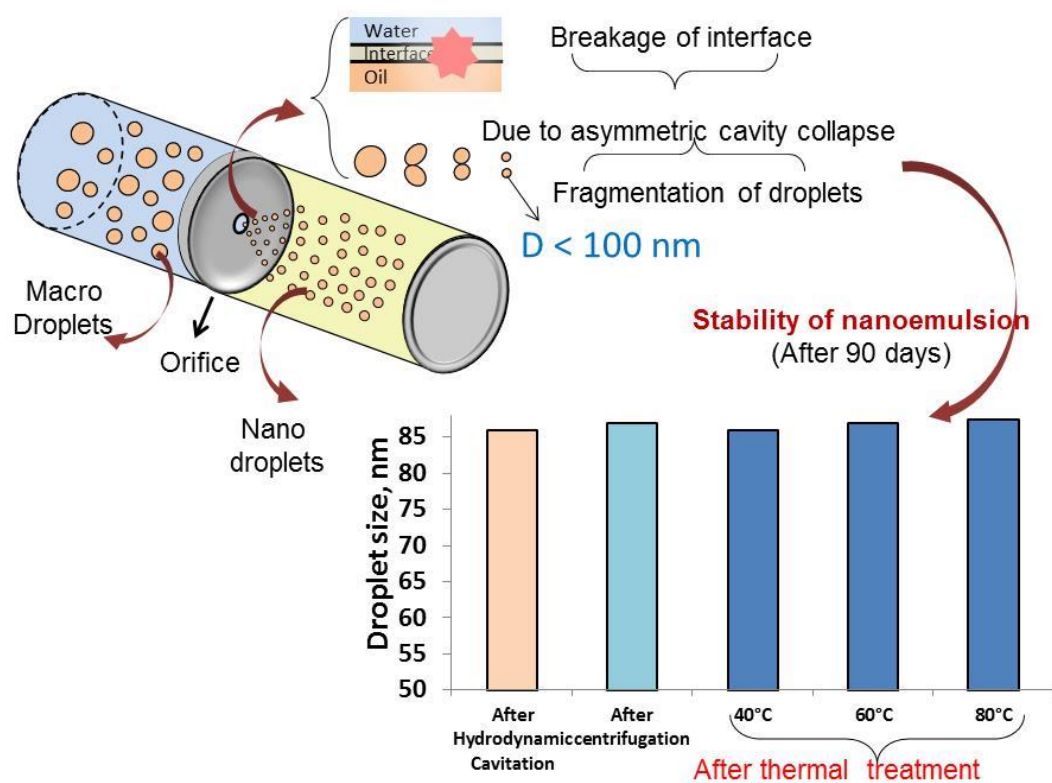
3.1 Introduction

Nanoemulsions are thermodynamically unstable systems and thus require adequate amount of energy either in the form of agitation or mechanical disturbances to achieve the emulsion droplet size on a nanoscale [1-4]. In past decades, many researchers studied high energy methods for the formation of nanoemulsions [5, 8-10]. High energy methods include using high speed homogenizers [11], high pressure homogenizers [12], colloid mills [13], microfluidizer [14, 15], and ultrasound processors [7, 14, 16 - 18] for agitation. High pressure homogenizers and microfluidizer are usually operated at high pressure in the order of ~1000 bar or higher [12, 14, 15], whereas high speed rotors are operated at high speed in order of ~10^4 RPM [11]. These equipments consume high energy and therefore are not found to be economical for large scale operations. Ultrasound processors are also efficient for nanoemulsion synthesis as found in our previous work reported in Chapter 2 but it is only suitable for small scale and batch operations [7, 16-18]. Thus, to overcome high energy consumption, and also to improve the throughput capacity, low energy methods or devices needs to be design for the synthesis of nanoemulsion which can be scaled up in an economical manner for the production of nanoemulsions on a large scale.

In recent years, hydrodynamic cavitation (HC) was developed as an emerging technique capable of intensifying the emulsification process on a large scale. As discussed earlier, HC is typically caused by affecting pressure variations in a flowing liquid as it passes through a constriction in a pipe. The variation of pressure through the constriction channel such as venturi and orifice plate with different geometry leads to the generation of cavities and hot spots as a result of subsequent cavity collapses [19-21]. These generated hot spots can induce physical effects such as micro jet streaming and high intensity local turbulence that acts as main driving force for the droplet size reduction in an emulsion. The energy released as a result of asymmetric cavity collapse dissipates at the molecular levels which enhance the mixing of two immiscible phases by reducing the interfacial tension and also causing fragmentation of the droplets into smaller sizes [5, 20]. Moreover, formation of emulsion also depends on intensity of micro-turbulence generated by cavitation bubbles in both oil and aqueous phase [22]. The intensity of micro-turbulence caused by cavity collapse depend on the physical properties of liquid such as density, viscosity etc. and as well as on the extent of shear applied. Therefore the intensity of micro-turbulence in oil and aqueous phase is

different. At lesser viscosity, the cavity collapse in oil phase creates high micro-turbulence that increases the interfacial area between immiscible phases and thereby forms an emulsion [22]. The other advantages associated with HC are that it is easy to handle, requires less energy inputs than high energy methods, can be used for continuous emulsification process [5, 10, 20, 23], and it can process large volume as compared to other techniques such as ultrasound processors, homogenizers, etc. Apart from that, HC has been successfully established as an intensifying technology for a variety of applications such as wastewater treatment, chemical synthesis, nanomaterials synthesis, etc. [20, 24].

The above phenomenon of HC has been well applied in previous studies for the formation of different emulsions [5, 10, 23]. But previously reported works were focused only on the preparation of oil in water emulsion using single hole orifice based HC devices. There is no work reported in the literature on the design and optimization of different cavitating devices such as orifice plate and venturi for the preparation of nanoemulsion. It is only recently that Ramisetty et al. [23] reported the effect of geometry of venturi (slit and circular) on the extent of coconut oil in water emulsification but the design of orifice plates based on several parameters such as α (ratio of throat perimeter to its cross sectional area) and β (throat area to pipe cross sectional area) are not reported yet. Moreover the significance of cavitation number for design and operation of a cavitating device was not discussed in any of the reported studies. The geometry of a cavitating device significantly influences the cavitational activities (inception, growth and collapse) inside a cavitating device [21, 25]. Thus, the present study was carried out with an objective to study the effect of geometry (venturi and orifice plate of different shapes) and geometrical parameters (flow area, perimeter, etc.) of cavitating devices on the formation and stability of mustard oil in water nanoemulsion. Additionally, other parameters such as inlet pressure, cavitation number and number of passes were studied to evaluate their effect on the droplet size reduction of an emulsion. Another objective of this study was to evaluate the kinetic stability of emulsion under centrifugal and thermal stress conditions. The energy efficiency of HC was also compared with ultrasonication for the formation of mustard oil in water nanoemulsion to validate the potential of HC over ultrasonication for large scale operations.

3.2 Materials and methods

3.2.1 Materials

The refined mustard oil, surfactants Tween 80 and Span 80 and deionized water of same make and grades were used as reported in section 2.2.1 of Chapter 2.

3.2.2 HC reactor

The schematic of a HC reactor experimental setup for carrying out the emulsification process is shown in Fig. 3.1. The setup comprised a vessel of capacity 10 liters, a positive displacement pump of power rating 1.1 kW, a pressure gauge and control valves which were connected at the desired places in the main and bypass line. The base of the vessel was connected to the suction side of the pump which discharged the solution from the vessel in two lines; main and bypass line. The solution from the pump was circulated through the main line which housed the cavitating device. The dimensions of all cavitating devices utilized in the experiment such as venturi and orifice plate of different designs and shapes are given in Table 3.1. The flow rate in the main line was controlled by varying the number of piston strokes of the pump per unit time through VFD system (Variable Frequency Drive), while keeping the bypass line fully closed. The bypass line was provided only to control the flow through main line in case of a breakdown of VFD. A cooling jacket was provided surrounding the vessel to control the temperature of the solution by circulating cold water through the jacket. Experiments were conducted at different inlet pressures ranging from 5 to 15 bar (gauge). The inlet pressure was monitored using a pressure gauge which was mounted at the inlet of the cavitating device in the main line. The flow rate was measured using a flow meter that was placed in the main line. The number of passes was varied by varying the flow through the main line and was estimated as per the following equation:

Number of passes (P) = (Volumetric flow rate /total volume of emulsion) x processing time

Since flow rates were different and therefore power dissipation per pass was not same for all devices. Hence in order to compare different devices based on the size reduction per pass, numbers of passes were normalized as given in Eq. (3.1):

$$P' = a + \frac{(X-A)(b-a)}{(B-A)}$$ (3.1)

Where P' is the value of normalized pass. The data were normalized on a scale of 31 to 248 (Fixed for all devices based on the passes obtained in OP1). Where "a" and "b" are the minimum and maximum value of the normalized scale, A and B are the minimum and maximum value of actual number of passes, and X is the actual pass for which the normalized value was calculated.
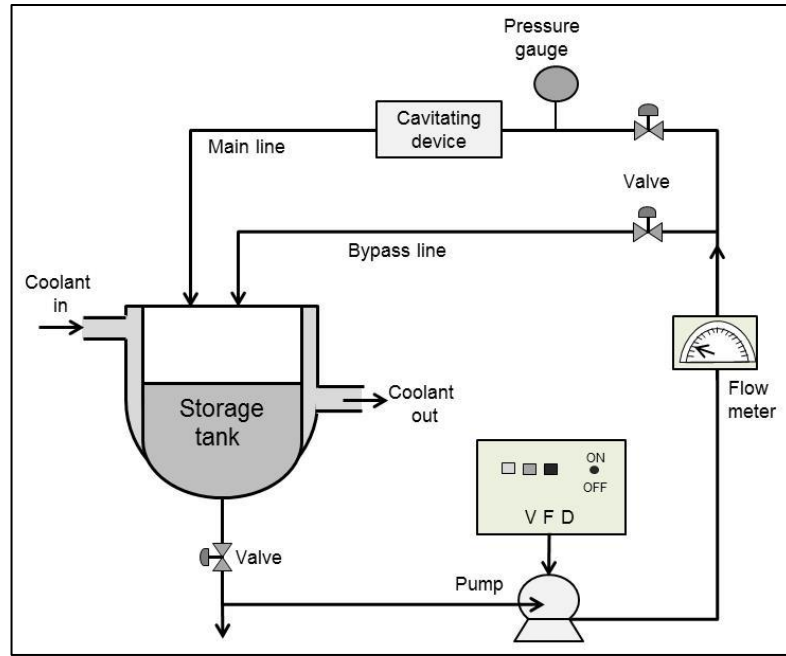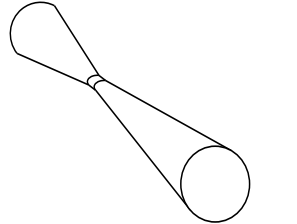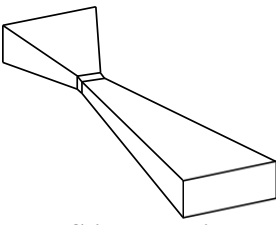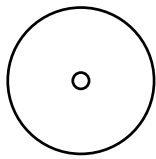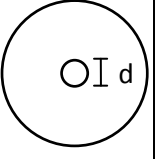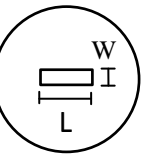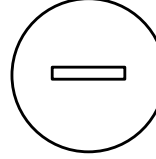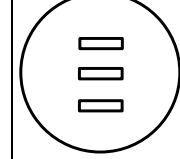
Fig. 3.1 Schematic of HC Reactor

The cavitating conditions inside the cavitating devices were characterized using a dimensionless number, known as cavitation number (C_V), which can be defined by Eq. (3.2)

$$C_V = \frac{(P_2 - P_V)}{\frac{1}{2}\rho V^2}$$ (3.2)

Where P_2 is the downstream pressure, P_V is vapor pressure of the liquid, ρ is density of the liquid at operating temperature and V is the velocity at the throat of a device. Usually the cavities are generated at $C_V \leq 1$ but if the solution contains dissolved gases or suspended particles, the cavity inception may occur at $C_V > 1$ [20, 25].

Table 3.1 Geometrical configuration and dimensions of hydrodynamic cavitating devices

Parameters	Circular Venturi (CV)	Slit venturi (SV)	Orifice plate-1 (OP1)	Orifice plate-2 (OP2)	Orifice plate-3 (OP3)	Orifice plate-4 (OP4)	Orifice plate-5 (OP5)
Throat dimensions	2 mm throat diameter Half convergent angle: 23° Half divergent angle: 6.5°	Throat width (W) – 1 mm Throat length (L) – 3.14 mm Half convergent angle: 23° Half divergent angle: 6.5°	2 mm diameter	3 mm diameter	L – 7.06 mm W – 1 mm	L – 14.14 mm W – 0.5 mm	L – 4.71 mm W – 0.5 mm of single cut
Flow area, (mm^2)	3.14			7.06			
Perimeter, (mm)	6.28	8.28	6.28	9.42	16.13	29.28	31.26
α, mm^{-1}	2.00	2.63	2.00	1.33	2.28	4.14	4.42
β,	0.011			0.025			
Pipe diameter, (mm)	19						
Pipe flow area, (mm^2)	283.385						

86

3.2.3 Preparation of emulsion

The emulsion was prepared using mustard oil as the dispersed phase in deionized water and the formulation was stabilized by the addition of two surfactants Tween 80 and Span 80. Primarily the surfactant Tween 80 (hydrophilic) was mixed with water and Span 80 (lipophilic) was mixed with oil and thereafter these mixtures were separately heated up to 40°C for complete dissolution of surfactants. After cooling, both the mixtures were added into the storage tank of the experimental setup and pumped through the cavitating device at different operating pressures ranging from 5 to 15 bar for 120 minutes. The total volume of the solution processed in the experimental set up was 3 liters. Experiments were carried out repeatedly using all cavitating devices (as shown in Table 3.1) at 5, 10 and 15 bar to optimize the geometrical and operating conditions. To prevent overheating of the solution, cold water was circulated through the jacket provided in the set up surrounding the vessel. The temperature of the solution was maintained at $30 \pm 2°C$. In all experiments, the HLB value of surfactant mixtures, concentration of oil (φ_O) and surfactant (φ_S) were fixed at 10, 10% (v/v) and 8% (v/v) respectively. The above parameters i.e. HLB value, oil and surfactant concentrations were optimized earlier using ultrasonication and reported in Chapter 2. In order to prepare the emulsion of HLB 10, surfactants Tween 80 and Span 80 were mixed in a volume ratio of 0.535:0.465. The cavitation number, flow rate through the cavitating device and energy dissipation at different inlet pressures for different cavitating devices are presented in Table 3.2. The samples were collected at every 15 minutes interval and then analyzed for the droplet size and Poly Dispersity Index (PDI) measurements.

Table 3.2 Flow and energy characteristics at different operating pressure for different HC devices

Devices	Pressure (bar)	Flow rate V_O (L/min)	Velocity, V (m/s)	Cavitation number, Cv	Power dissipation (J/s)
Slit venturi (SV)	5	4.5	23.89	0.34	37.50
	10	6.4	33.97	0.17	106.67
	15	7.8	41.40	0.11	195.00
Circular venturi (CV)	5	5	26.54	0.28	41.67
	10	6.2	32.91	0.18	103.33
	15	7	37.15	0.14	175.00
Orifice plate-1 (OP1)	5	3.5	18.58	0.57	29.17
	10	5.5	29.19	0.23	91.67
	15	6.8	36.09	0.15	170.00
Orifice plate-2 (OP2)	5	10	23.59	0.35	83.33
	10	13.6	32.08	0.19*	226.67*
	15	16.5	38.92	0.13	412.50
Orifice plate-3 (OP3)	5	10	23.58	0.35	83.33
	10	13.3	31.36	0.20	221.67
	15	16.3	38.44	0.13	407.50
Orifice plate-4 (OP4)	5	9.5	22.40	0.39	79.17
	10	12	28.29	0.25	200.00
	15	15.3	36.07	0.15	382.50
Orifice plate-5 (OP5)	5	9.6	22.65	0.38	80.00
	10	12.5	29.49	0.22	208.33
	15	15.3	36.09	0.15	382.50

*Sample calculation for C_V and power dissipation is given Appendix A.1 and A.2 respectively

3.2.4 Droplet size measurements

Droplet size of the prepared emulsions was determined using Zetasizer Nano ZS (Malvern Instruments, UK) provided with dynamic light scattering and electrophoresis facility for the analysis. Before carrying out the measurements, all the formulations were diluted to the ratio of 1:1000 in deionized water to prevent multiple scattering effects during size analysis. The Zetasizer gave the Z-average diameter which is represented as droplet size (nm) in this study. Duplicate samples along with three measurements were considered for ensuring repeatability of the analysis.

3.2.5 Kinetic stability analysis

The kinetic stability analysis of the emulsions was conducted using centrifugal and thermal stress tests to observe any possible breakage in emulsions such as creaming and/or coalescence. All the formulations were initially centrifuged at 3520 RCF (5000 RPM) for 15 minutes and also subjected to heating cycles at 40°C, 60°C and 80°C to observe any change in droplet size. The kinetic stability tests were also carried out after 7, 30, 60, and 90 days of storage. The stability of the emulsion after these tests was evaluated based on the observed droplet size. The emulsion was considered to be stable when no change was observed in the droplet size after a predetermined period. Samples prepared at the optimum conditions were stored at room temperature for up to 3 months and droplet size was measured at different intervals of time.

3.2.6 Theoretical insight into the Hydrodynamically cavitated emulsion for droplet size prediction

Different correlations were developed for the droplet size prediction under the turbulent inertial and turbulent viscous regimes during the homogenization [26]. It has been well established that droplet break-up and their sizes significantly depend on the shear stress applied to the system and the viscosity effects of the dispersed phase. Emulsification under the cavitation occurs basically in two stages. In initial stages, the primary droplets are formed due to the phenomena of Rayleigh-Taylor instability mechanism caused by the disturbance created at the interface. Thereafter, these primary droplets require high inertial forces to overcome the surface tension force ($2\sigma/R$) which causes the disruption of droplets

into fine sizes. Therefore, cavitation plays an important role at this stage when desired level of shear is required for the droplet disruption. The turbulent eddies created along with the shockwaves of cavity collapse, contributes to the droplet deformation and disruption [27]. Therefore, in the case of HC, the dependency of the flow characteristic parameters is significant which could alter the cavitating conditions inside the device.

At the throat section of HC device, the operating flow rate and velocity caused by the throttling are useful to predict the flow conditions. The extent of turbulence at the throat can be described by Reynolds number as the ratio of inertial to viscous forces.

$$Re = \frac{l\,V\rho}{\mu} \qquad\qquad (3.3)$$

Where l, is the characteristics length of the throat, V is the velocity (m/s) at the throat of HC device, $\rho,$ is the density of emulsion (kg/m³), and $\mu,$ is the viscosity of the emulsion (kg/m.s).

The cavitation condition inside the device is characterized using cavitation number which is described in Eq. (3.1). Moreover, the Weber number (We) which is the ratio of inertial to interfacial force, is associated with the shear stress generated for the droplet break up and it depends on the operating flow conditions. Taylor suggested that a droplet will not break unless the applied stress ($\tau_{applied}$) deforming the droplet exceeds the interfacial stress holding the droplet in the same shape [26]. The $\tau_{applied}$ is governed by the flow dynamics at the throat section which indicates that at higher shear generation, droplet size obtained would be lesser. The We number can be described as:

$$We = \frac{\tau_{applied}\rho}{\sigma} = \frac{l\,V^2\rho}{\sigma} \qquad\qquad (3.4)$$

Where, $\sigma,$ is the interfacial tension (mN/m).

All of the above flow characteristic parameters are affected by the variation of either geometry or operating conditions of HC devices or both. Therefore, the objective of this work was to develop a correlation to predict the droplet size under the influence of above hydraulic parameters during cavitation. The proposed correlation is based on the turbulent regimes generated at the throat section of the device. Since the flow dynamics in the HC device are mainly governed by the inertial stress generated at the throat to cause the droplet

disruption, and therefore the contribution of viscosity effects of the dispersed phase is assumed to be negligible and hence not considered.

3.3 Results and Discussions

3.3.1 Effect of inlet pressure and Cavitation number

Inlet pressure and cavitation number are the two major parameters that affect the cavitational conditions inside the cavitating device. In present work, all the cavitating devices as shown in Table 3.1 were operated at pressures of 5, 10 and 15 bar. The optimization of cavitating device and cavitation number was carried out based on the minimum droplet size of emulsion obtained after 120 minutes of processing. It can be seen from Table 3.1 that the devices SV (slit venturi), CV (circular venturi), and OP1 (orifice plate-1) possesses same flow area i.e. 3.14 mm^2 whereas orifice plates OP2, OP3, OP4 and OP5 have flow area of 7.06 mm^2. The effect of inlet pressure and cavitation number on the droplet size is shown in Fig. 3.2. It was observed that for all devices, on increasing the pressure from 5 to 10 bar, a significant reduction in the droplet size was observed but on further increasing the pressure from 10 to 15 bar, only a marginal or no further reduction in the droplet size was observed. On increasing the inlet pressure, the flow rate through the cavitating device increased and consequently the velocity at the throat increased which subsequently decreased the cavitation number (C_V) as per the definition in Eq. (3.1). At lower C_V, numbers of generated cavities were more resulting in higher cavitational yield and hence the droplet size reduced more rapidly due to enhanced turbulence and shear at lower C_V. But beyond an optimum C_V the droplet size remained almost constant at a fixed concentration of oil and surfactant in an emulsion. From Fig. 3.2, it was observed that on increasing pressure from 10 to 15 bar, there was no further reduction in droplet size using the devices with higher flow area (7.06 mm^2). However the droplet size was marginally decreased from that obtained at 10 bar for devices with lower flow area (3.14 mm^2) on increasing the pressure up to 15 bar. Thus, it was observed that the maximum cavitational effects were obtained at an optimum inlet pressure of 10 bar for all devices. It can be concluded from Fig. 3.2 that to achieve an emulsion of droplet size less than 100 nm, the optimum C_V was found to be in the range of 0.17 to 0.20 for all the devices. The minimum droplet size of about 87 nm was obtained using circular orifice plate (OP2) having throat size of 3 mm at C_V of 0.19 in 90 min of processing time.

Moreover, the PDI value of the emulsion was also improved at lower C_V. It was observed that for all the cavitating devices, on decreasing the C_V from 0.5 to an optimum value, the PDI was decreased from 0.6 to 0.1 which indicated that higher cavitational intensity was induced at lower C_V and thereby achieved narrow size distribution of the droplets in an emulsion. Therefore, it can be said that C_V is an important parameter which would help in designing a suitable cavitating device. Once the required C_V is known, the throat area of the device can be decided based on the velocity at the throat and volumetric flow rate that needs to be processed through HC. Thus, cavitation number is a significant factor which should be considered during the scale up of HC.

Apart from the shear forces applied for the reduction in emulsion size, surfactants also influence the formation of emulsion as it reduces the droplet size significantly by reducing the interfacial tension between two immiscible phases. At HLB 10, Tween 80 and Span 80 showed a good packing strength that maintained the hydrophobicity and hydrophilicity of the emulsion system under the cavitation conditions [18]. Thus, steric hindrance provided by the surfactants maintains the repulsion between the droplets and the cavitation effects causes the fragmentation of droplets and controls the size distribution based on the extent of shear applied. In overall, the combined effect of surfactant and HC not only reduced the emulsion size but also enhanced the stability of the emulsion.
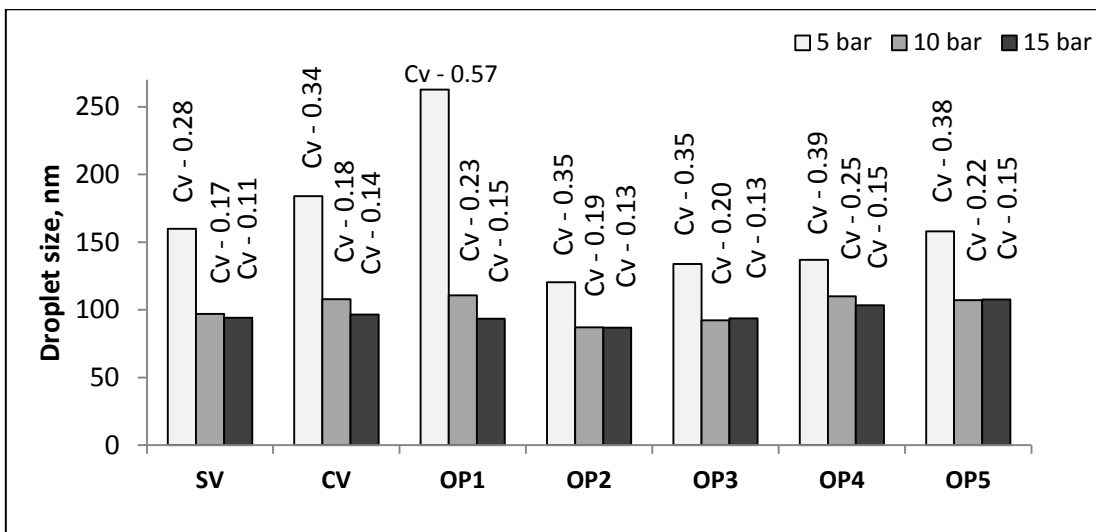
Fig. 3.2: Effect of inlet pressure and cavitation number on emulsion droplet size for all cavitating devices (emulsion compositions: HLB 10; φ_O: 10% (v/v), φ_S: 8% (v/v), 120 min)

Similar observation was also made by Ramisetty et al. [23] for the preparation of coconut oil in water emulsion using circular venturi as a cavitating device. It was observed that on increasing the inlet pressure from 5 to 10 bar, the droplet size was significantly reduced to 215 nm from 300 nm and remained almost constant thereafter. The optimum C_V reported in their work was in the range of 0.16 to 0.23 for circular and slit venturi.

The geometry and geometrical parameters of the cavitating device also affect the cavitating conditions which can be observed from the data presented in Table 3.2. Thus, the effects of geometrical parameters on the emulsion droplet size are discussed in further sections in detail.

3.3.2 Effect of various geometrical parameters

3.3.2.1 Effect of α (ratio of throat perimeter to its cross sectional area)

The parameter α, is the ratio of throat perimeter to its cross sectional area of any cavitating device. A change in α (i.e. perimeter at fixed cross section) caused either by varying the number of openings or by varying the shape of the throat (circular or rectangular), can alter the number of cavitational events occurring at the throat and thereby the cavitational yield. Many studies have reported on the effect of α in different applications using HC [28–31]. Sivakumar and Pandit [26] observed that on increasing α from 0.8 to 4, the degradation rate of Rhodamine B dye increased by 2 fold. Ghayal et al. [29] also reported that on increasing the value of α from 0.4 to 2, the conversion of triglycerides to methyl esters increased from 77% to 94%. Some other studies [30, 31] had also reported similar observations that higher cavitational yield for different applications was achieved by using the device having higher value of α. It can be understood by this fact that the higher value of α enhanced the shear layer perimeter at the throat which increased the number of cavitational events and hence increased the cavitational yield.

In present study, results obtained were contradictory to the previous findings. The effect of α on the droplet size of emulsion is shown in Fig. 3.3. Initially, the perimeter of the orifice plate was increased by changing the shape of throat from circular (OP2; α – 1.33) to rectangular (OP3; α – 2.28 and OP4; α – 4.14) but the droplet size increased from 87 nm to 110 nm on increasing α. Moreover, with an aim of reducing the droplet size than that obtained using orifice plate OP2, the perimeter of rectangular orifice plate (OP4; α – 4.14)

was further increased by increasing the number of openings i.e. 3 rectangular cuts of smaller size (OP5; α − 4.42), but again the droplet size was not reduced and remained almost constant. The rate of droplet size reduction per unit pass was found to be higher in case of lower α i.e. using orifice plate OP2. It can be seen from Fig. 3.3(A) that the droplet size reduction per unit pass was faster up to 200 passes using all orifice plates. The reduction in droplet size per unit pass was higher using orifice plate OP2 as the droplet size obtained was 93 nm using orifice plate OP2 and 109 nm using orifice plate OP5 after 200 passes. Afterwards, the droplet size remained almost constant and only a slight reduction in the droplet size was observed. This can also be evident from the curve of normalized passes as shown in Fig. 3.3(B) that the rate of size reduction per pass was higher in the case OP2 having lower α. The higher rate of droplet size reduction per pass in the case of OP2 is attributed to the higher energy dissipation per pass as shown in Fig. 3.3(C). Since at the given pressure drop, the velocity obtained was higher in case of OP2 as compared to that obtained using orifice plate OP5 having higher α as shown in Table 3.2. This resulted into the generation of higher shear at the throat of OP2 and thus produced the higher rate of droplet size reduction per pass as compared to other orifice devices. This is also evident from the calculated weber number as shown in Appendix A.5. The weber number was found to be higher in the case of OP2 (We=122.6) as compared to OP5 (We=93.57). Therefore, it can be concluded that a single hole orifice plate having circular hole is quite enough to produce the emulsion of droplet size less than 100 nm, provided the required cavitation number is achieved by varying the velocity at the throat of the cavitating device. Thus, it can be established that α has an insignificant effect on the droplet size reduction and rather C_V is more important parameter that should be considered for the design of a cavitating device.
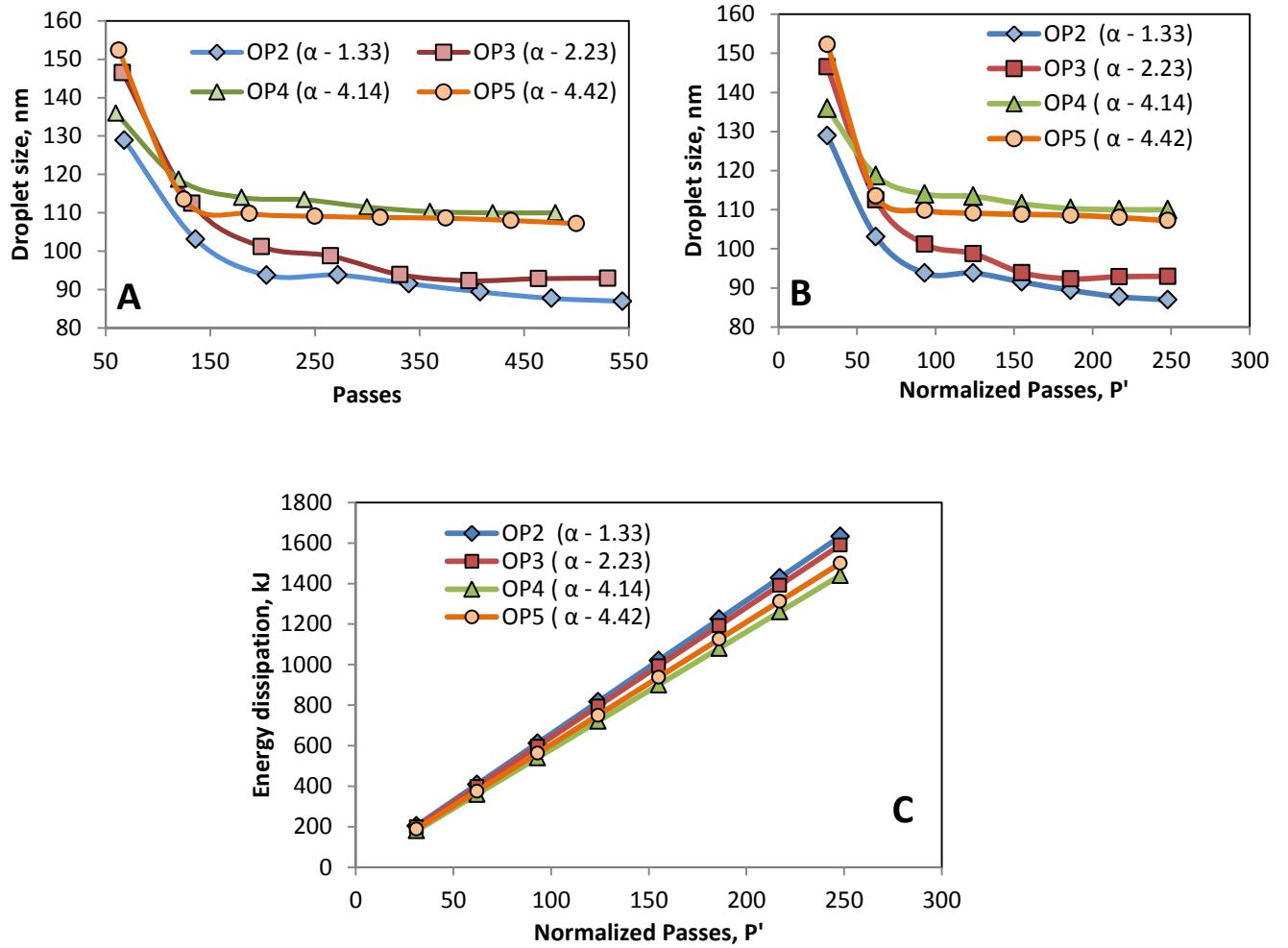
Fig. 3.3 Effect of α on droplet size (A) at different number of actual passes, and (B) at different number of normalized passes (P') and (C) Effect of normalized passes on energy dissipation (10 bar, HLB 10; φ_O: 10% (v/v), and φ_S: 8% (v/v))

3.3.2.2 Effect of β (ratio of throat area to cross sectional area of pipe)

The parameter β is the ratio of flow area of a cavitating device to cross sectional area of pipe. It is also an important parameter that could alter the frequency of turbulence and also affects the magnitude of turbulent pressure fluctuations inside the cavitating device [20, 28, 29]. In present work, two circular orifice plates OP1 (β - 0.011) and OP2 (β - 0.025) of different flow area have been compared to study the effect of β on the droplet size of an emulsion. Fig. 3.4 represents the effect of β on the droplet size of emulsion with different

number of passes at an optimum inlet pressure of 10 bar. It was observed that on increasing β from 0.011 to 0.025, the droplet size decreased from 122 nm to 87 nm after 90 min. Moreover, the minimum droplet size was obtained in case of orifice plate OP2 (β – 0.025) as compared to orifice plate OP1 (β – 0.011) for the same number of passes. From Fig. 3.4(A), it can be seen that at higher β, the droplet size reduced to 100 nm just after 136 passes (30 min) whereas at lower β, the droplet size reduced to 134 nm after 137 passes (75 min). Therefore, it has been established that the reduction in droplet size per unit pass was higher in case of orifice plate OP2. This may be attributed to the fact that the orifice plate having large value of β provided larger shear layer area and as a result generated more number of cavities. This is also evident from Fig. 3.4(B) that the rate of size reduction per pass was higher in the case of OP2 because of the higher energy dissipation per pass obtained in OP2 as compared to OP1 as shown in Fig. 3.4(C). The same can also be understood from the fact that the Weber number (We; ratio of inertial force to interfacial force) obtained in the case of OP2 was higher (We = 122) as compared to that obtained in OP1 (We = 67) at the same pressure drop (Appendix A.5). This emphasized that higher shear forces were generated in OP2 than OP1 which caused the higher rate of droplet size reduction. Also, it can be noted from Table 3.2 that power dissipated into the system per unit power supplied was higher for the orifice plate (OP2) having higher β value which enhanced the mixing of immiscible phases and reduced the droplet size to nano scale. The power dissipated into the system for orifice plate OP2 was 2.5 times higher than orifice plate OP1 (Table 3.2). Therefore, it is better to use a cavitating device having higher β because at lower β value, the pressure drop across the cavitating device as well as energy required for pumping would be higher to achieve the required cavitation number. Moreover at lower β value with sufficiently low C_V, flashing of liquid started which caused the cavity cloud formation in the cavitation zone and thereby reduced the cavitational intensity [33, 34].
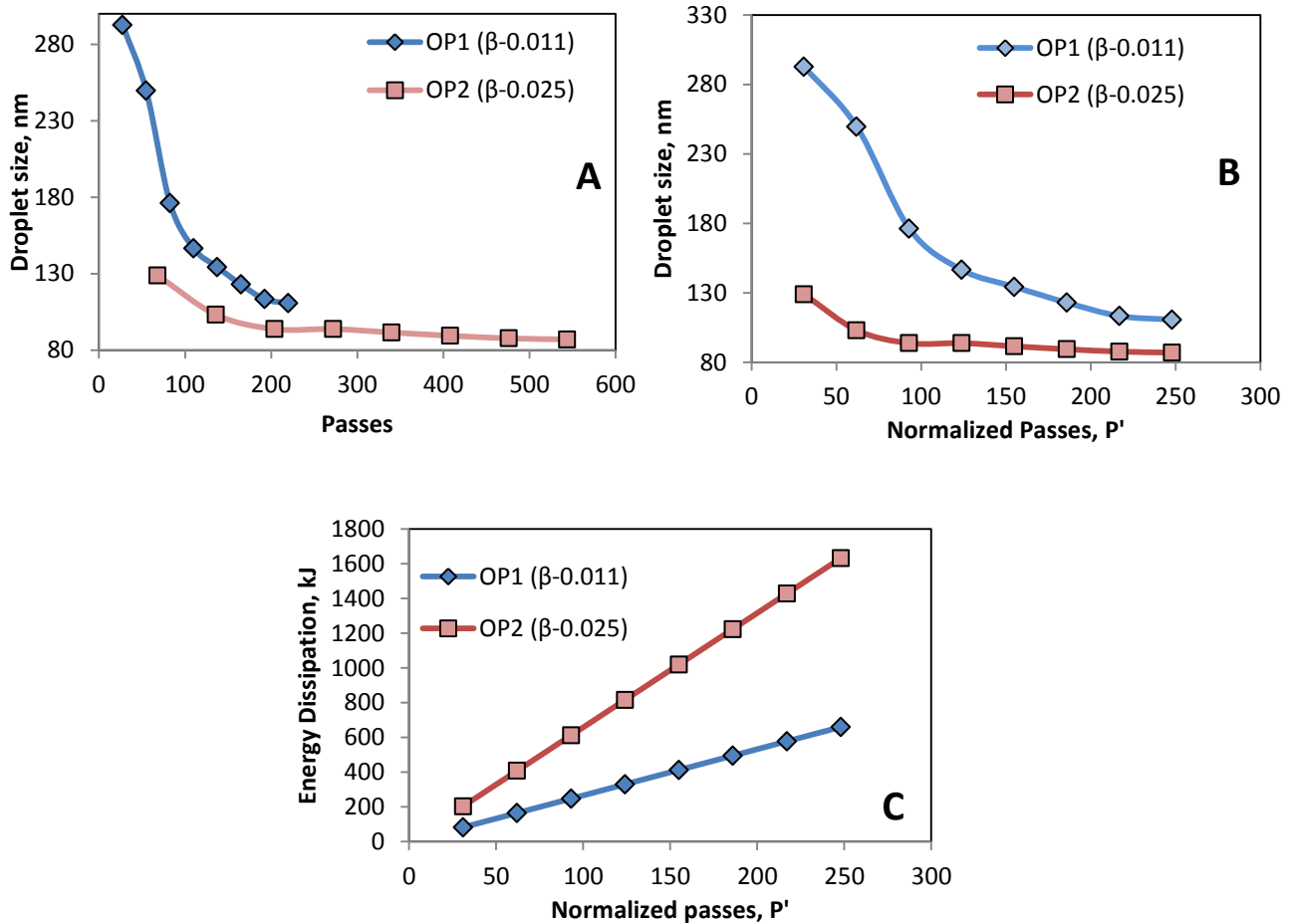
Fig. 3.4 Effect of β on droplet size (A) at different number of actual passes, and (B) at different number of normalized passes, P' and (C) Effect of normalized passes on energy dissipation (Condition: 10 bar, HLB 10; φ_O: 10% (v/v), and φ_S: 8% (v/v))

3.3.3 Effect of geometrical configurations of the cavitating device

The geometry of a cavitating device can be configured in different ways such as with a venturi or an orifice. The difference in the geometry brought the variation in flow dynamics inside the device in a considerable manner. A venturi having an upstream and downstream section at some angles prevents sudden contraction and expansions unlike what happens with an orifice plate. The divergent section of a venturi prevents the early cavity collapse and provides adequate time for a cavity to remain in low pressure region and thus allows it to grow to a maximum size before its collapse [35-37]. On the other hand due to smooth

97

convergent section, higher flow is obtained in a venturi as compared to orifice plate for the same pressure drop across the device which resulted into lower C_V (Table 3.2). Hence, the numbers of cavities generated are more in case of a venturi than an orifice plate. In a venturi device, stable cavities are formed which are beneficial for many physical, chemical and biological transformations [20, 21, 25].

In present work, ventures and orifice plates of same flow area (3.14 mm^2) were used as a cavitating device and compared to study the effect of their geometry on the extent of droplet size reduction. Fig. 3.5 shows droplet size obtained using orifice plate (OP1), slit (SV) and circular venturi (CV) at a constant pressure of 10 bar. It was observed that venturi based cavitating devices were more efficient as compared to the performance of an orifice plate device. Using slit venturi (SV), the droplet size obtained was 97 nm at C_V of 0.17 which was lower than that obtained i.e. 107.9 nm at C_V of 0.18 using circular venturi (CV) and 110.7 nm at C_V of 0.23 obtained using orifice plate OP1 after 120 min. Since, there was only a slight change in the final droplet sizes using all these devices, efficiencies of these devices were tested based on the reduction in droplet size per unit pass. It can be seen from Fig. 3.4(A) that initially up to 155 passes, the rate of droplet size reduction per unit pass was higher in case of both ventures than orifice plate OP1. To obtain similar droplet size for e.g. 133 nm, the number of passes required using orifice plate OP1 was higher (i.e. 138) than that required using both the ventures (94 passes). Beyond a certain optimum number of passes, the droplet size remained constant and the same can be observed from Fig. 3.4(A). It can be observed from Fig. 3.5(B) that the rate of droplet size reduction per pass was higher in the case of SV and CV as compared to orifice plate (OP1). As shown in Fig. 3.5(C) that the energy dissipation per pass was higher in the case of ventures than orifice plate and therefore higher rate of droplet size reduction was obtained using ventures. Because of smooth divergent sections in a venturi, the generation of cavities and their life span was higher in venturi than that obtained in an orifice plate. This can be clearly understood from the C_V obtained for all three devices at the same pressure drop. Since a lower C_V was obtained for ventures than orifice plate and therefore higher cavitational yield was obtained in ventures which can be assessed based on the lower droplet size obtained. However, no significant difference was observed in the droplet size and its reduction rate for both slit and circular venturi as shown in Fig. 3.5(A) & (B). This again proved that the throat perimeter to

area ratio (α) had no significant effect on the droplet size reduction. Therefore, it can be concluded that for the same β value, venturi based devices are found more suitable than orifice plate cavitating device.
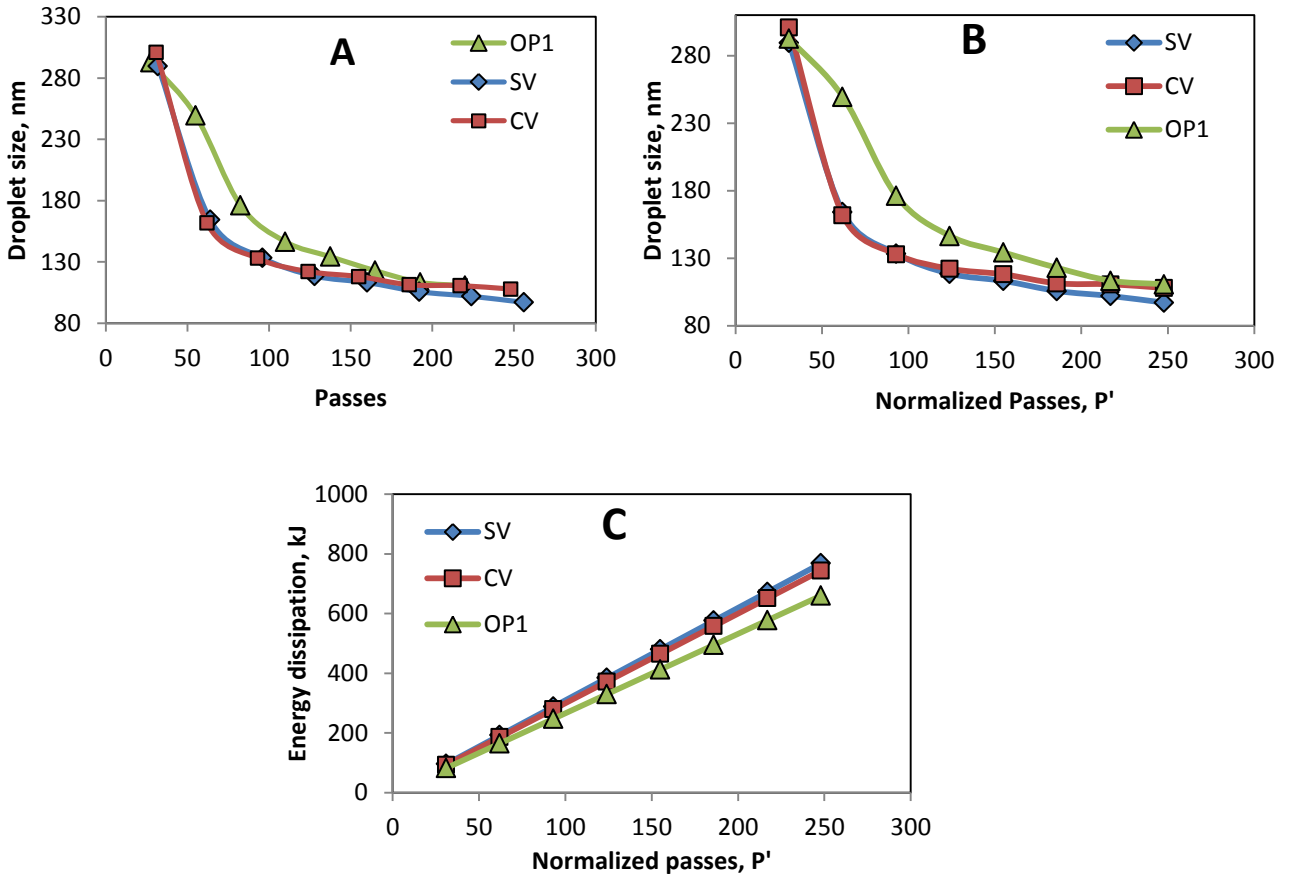
Fig. 3.5 Effect of geometry of cavitating device on the (A) droplet size vs. actual passes, (B) droplet size vs. normalized passes, and (C) Energy dissipation vs. normalized passes (Condition: HLB 10; φ_O: 10% (v/v), φ_S: 8% (v/v), flow area: 3.14 mm^2, 10 bar, 120 min)

3.3.4 Development of mathematical correlation for the prediction of droplet size of emulsion prepared using HC: Dimensionless analysis approach

From the above results obtained, it has been observed that the droplet size of emulsion was affected by the operating and geometrical parameters of hydrodynamic cavitation. Based on the Kolmogorov and Hinze theories [26], droplet breakup is caused by large shear and pressure gradients associated with eddies generated in turbulent flow field. In HC, the extent

of turbulence depends on the operating flow rate and characteristic dimension (diameter/hydraulic mean diameter) of the throat which can be expressed using various dimensionless numbers such as cavitation number (C_V), Reynold number (R_e) and weber number (W_e).

Therefore, based on the above aspects, dimensionless analysis was used to develop the correlation for the droplet size as a function of hydraulic parameters of HC. It has been observed that the droplet size of an emulsion (d_P, nm) is a function of velocity at the throat (v, m/s), density of emulsion (ρ, kg/m^3), viscosity (μ, cP), size of the throat (defined as characteristic length, l, m), interfacial tension (σ, mN/m) and pressure drop (ΔP, Pa) across the throat as shown below.

$$d_P = f(l, v, \rho, \sigma, \mu, \Delta P)$$

Where l, is the characteristics length of the throat (in case of circular shaped throat it is diameter of throat i.e. l = d, whereas for the case of non-circular it was calculated as:

$$l = \frac{(w \: x \: h)}{2(w + h)} * 4$$

'w' is width (m) and 'h' is height (m) of throat, v is the velocity (m/s) at the throat of HC device, ρ, is the density of emulsion (kg/m^3), σ, is the interfacial tension (mN/m), and μ, is the viscosity of the emulsion (kg/m.s).

To obtain a mathematical expression, the Buckingham Pi theorem was used. The number of variables are 7 and the dimensionless quantities are 3 i.e. Mass (M), Length (L) and Time (T) which are the primary dimensions used to describe the system.

As per the Buckingham Pi-theorem, the number of dimensionless groups that can be formed is,

$$g(7\text{-}3) = g(4)$$

With six primary dimensions and the method of repeating variables, it would be defined as:

$$\pi_1 = f(\pi_2, \pi_3, \pi_4)$$

With, π_1 = Dependent π group, and π_2 ... π_4 = Independent π groups,

Selecting $l, v, a \; nd\rho$ as repeating variables,

$$\pi_1 = (l^a v^b \rho^c . d_P)$$

Where, dimensions of $l, v, \rho,$ and d_P are L, LT^{-1}, ML^{-3}, L respectively. Therefore, by equalizing the exponents of each quantity, the final equation obtained is as follows.

$$\pi_1 = (\frac{d_P}{l})$$

Similarly,

$$\pi_2 = (l^a v^b \rho^c . \mu) \text{ will give, } \pi_2 = \left(\frac{\mu}{l.v.\rho}\right) = \frac{1}{R_e}$$

$$\pi_3 = (l^a v^b \rho^c . \sigma) \text{ will give, } \pi_3 = \left(\frac{\sigma}{l.v^2.\rho}\right) = \frac{1}{W_e}$$

$$\pi_4 = (l^a v^b \rho^c . \Delta P) \text{ will give, } \pi_4 = \left(\frac{\Delta P}{v^2.\rho}\right) = C_V$$

The above relations will yield the following function:

$$(\frac{d_P}{l}) = f(\frac{1}{R_e}, \frac{1}{W_e}, C_V) \tag{3.5}$$

The final expression will be

$$\left(\frac{d_P}{l}\right) = C . R_e^{-a} W_e^{-b} C_V^c \tag{3.6}$$

Where, C is constant.

The above correlation describes the effect of operating and geometrical parameters on the droplet size of emulsion under the turbulent regimes. As per the theory of Taylor, sufficient shear stress is required for the droplet disruption/breakup and hence local viscous forces generated by the dispersed phase are assumed to be negligible and therefore not accounted. Since, flow conditions used for this particular study was at the throat of HC device where the extreme turbulent in the flow was observed. Based on the experimental flow conditions, R_e was found to be in the range of 20000 to 10^5. Therefore, the proposed correlation describes the droplet size under turbulent regimes only.

3.3.4.1 Determination of exponents and constants

The correlation was established by using experimental results obtained with all HC devices, as presented in the previous sections. For each HC device, the parameters such as W_e, R_e and

C_v were calculated at different operating pressure ranging from 5 to 20 bar. The experimental data and the calculated parameters are shown in Appendix A.4.

Based on the Buckingham Pi-theorem, different algebraic equations were formed with unknown exponents and constants. The unknown exponents were then calculated by fitting these equations into experimental data by using MATLAB R2014b using the "fmincon" MATLAB function (coding shown in Appendix A.5). The model simulation starts with initial guess value of exponents. The error function Marquardt's Percent Standard Deviation (MPSD) was used to evaluate the model predicted error as shown below [38].

$$MPSD \quad = 100 \sqrt{(\frac{1}{p-n}\sum_{i=1}^{p}[\frac{(q_{e,meas}-q_{e,calculated})^2}{q_{e,means}}])} \qquad (3.7)$$

Where, p is number of experimental measurements; n: number of variables, and $q_{e,meas}$ and $q_{e,calculated}$ are the measured and calculated values of response (d_P/L). The objective of the error function was to minimize the sum of squares error of the difference between the experimental and predicted value of d_P/L.

The results obtained are shown in Table 3.3. The correlations were established by using experimental results obtained at different operating pressure in HC devices. The values of constants as shown in Table 3.3 were obtained by linear regression analysis. The corresponding values of MPSD indicated the error between experimental and predicted data. It can be seen from Table 3.3 that the values of the exponents obtained for different HC devices were not significantly different. This indicated that the geometrical conditions have insignificant effect on the droplet size however the role of operating conditions is crucial in order to achieve the desired level of homogenization and the subsequent emulsion size. To achieve the emulsion droplet size below 100 nm, the hydraulic Cv must be varied between 0.17 to 0.20, corresponding to hydraulic W_e ranging from 68 to 103 and Re ranging from 51000 to 72000. These correlations are useful for predicting the droplet size at different flow conditions. These correlations indicated that the droplet size is directly proportional to the cavitation number (C_v) and inversely proportional to the Reynolds number (R_e) and weber number (W_e). This indicated that higher inertial force generated at the throat of the cavitating device is beneficial to achieve the lower droplet size. Similar observation was also

noted with C_V that the droplet size decreased with decrease in the C_V, until a minimum threshold size is achieved.

Table 3.3 Correlations of droplet size with hydraulic parameters obtained for the different HC devices along with MPSD values

Devices	Correlation	MPSD values
SV	$\left(\dfrac{d_P}{l}\right) = 0.305. R_e^{-0.4604} W_e^{-0.8091} C_V^{0.9344}$	4.28×10^{-6}
CV	$\left(\dfrac{d_P}{l}\right) = 0.316. R_e^{-0.4398} W_e^{-0.7926} C_V^{0.9335}$	3.45×10^{-8}
OP1	$\left(\dfrac{d_P}{l}\right) = 0.465. R_e^{-0.4969} W_e^{-0.8335} C_V^{0.9638}$	5.70×10^{-8}
OP2	$\left(\dfrac{d_P}{l}\right) = 0.188. R_e^{-0.4693} W_e^{-0.7922} C_V^{0.9402}$	3.86×10^{-6}
OP3	$\left(\dfrac{d_P}{l}\right) = 0.224. R_e^{-0.4728} W_e^{-0.8097} C_V^{0.9380}$	5.98×10^{-6}
OP4	$\left(\dfrac{d_P}{l}\right) = 0.138. R_e^{-0.4993} W_e^{-0.8427} C_V^{0.9429}$	3.607×10^{-7}
OP5	$\left(\dfrac{d_P}{l}\right) = 0.372. R_e^{-0.4469} W_e^{-0.7902} C_V^{0.9415}$	2.52×10^{-9}

Therefore, the general equation based on the simulation results can be proposed as shown below, which can be used to predict the required emulsion droplet size using HC.

$$\left(\frac{d_P}{l}\right) = C. R_e^{-0.46} W_e^{-0.81} C_V^{0.94} \tag{3.8}$$

Where C is constant.

3.3.5 Kinetic stability of nanoemulsions

Apart from the formation of the nanoemulsion, it is necessary to determine the stability of nanoemulsion because after a certain time limit, the nanoemulsion gets disrupted under different breakdown conditions such as creaming, coalescence, flocculation, Ostwald ripening, etc. The stability of nanoemulsion depends on the droplet size. Lesser the droplet size, lesser would be the coalescence and creaming rate, and hence the emulsion would be stable for a longer time. The extent of stability of the nanoemulsion is determined using

different stability tests. The kinetic stability measurements help in predicting the short-term as well as long-term stability and also ensure the applicability of nanoemulsion in different fields [18, 39]. In present work, the kinetic stability tests were performed to evaluate the possible breakdowns in the nanoemulsion such as creaming and coalescence. The tests were performed using centrifugation and thermal stress treatment. Under the effect of centrifugal force and high temperature, the Brownian motion of droplets increases and as a result droplets approach each other which consequently increase the rate of coalescence and droplet size [18, 39]. The nanoemulsion is said to be physically stable if the droplet size of oil phase remains constant under these tests whereas unstable if there is a macroscopic change in their appearance and/or significant change in their droplet size. Nanoemulsion obtained using OP2 was stored for 7, 30, 60 and 90 days at ambient conditions. The stability of the stored nanoemulsion was assessed by subjecting the emulsion to centrifugation at 3520 RCF (5000 RPM) for 15 minutes and heating cycles at 40°C, 60°C, and 80°C for 30 min.

The droplet size obtained after stability tests at a predetermined period is given in Table 3.5. It was observed that there was no macroscopic sign of instability of emulsion after centrifugation. Even the droplet size was almost constant against the centrifugal force which indicated that the nanoemulsion maintained their droplet size and hence found to be stable under these stresses. Steric hindrance provided by the surfactants maintained the repulsion between the individual droplets whereas HC caused breaking the interface in order to obtain smaller droplet size. These combined effects of HC and surfactants improved the stability of an emulsion.

In case of thermal stress conditions, when the nanoemulsion was subjected to heating cycle for 30 min at the temperature of 40°C, 60°C and 80°C, the stability of nanoemulsion was unaffected as the droplet size was found to be similar to that obtained after production using HC. Increase in temperature had no significant effect on the emulsion characteristics as there was no evidence of phase separation or any major change in the droplet size as evident from the data reported in Table 3.4. Furthermore, the stability of the stored sample was also evaluated at lower temperature condition i.e. at 10°C and it was observed that decrease in temperature did not affect the emulsion characteristics as there was no significant difference in the droplet size. Therefore, it was concluded that the stability of prepared nanoemulsion

was less sensitive to temperature variations in the range of 10°C to 80°C. In overall, nanoemulsion produced with HC remained kinetically stable up to 90 days as there was no significant change in the droplet size observed after normal storage, centrifugal and thermal stress conditions.

Table 3.4 Kinetic stability evaluation of nanoemulsions

Time (days)	Droplet size after stability tests in nm				
	Without stability tests (normal storage)	After centrifuge	After thermal stress tests		
			40°C	60°C	80°C
After production using HC – 86.97 nm					
7	87.01	87.32	87.01	87.47	87.68
30	87.60	88.37	87.76	88.49	88.73
60	87.78	87.74	87.97	89.20	89.45
90	88.15	87.99	87.81	89.90	89.98

3.3.6 Energy efficiency evaluation of HC and Ultrasonication

In present work, the efficiency of hydrodynamic cavitation was studied in comparison of the ultrasonication process as reported in Chapter 2 for the formation of mustard oil in water emulsion. The comparison was made based on the energy efficiency of both the techniques. In our earlier work as presented in Chapter 2, the same nanoemulsion was prepared by ultrasonication process using the same composition i.e. at HLB 10, 10% (v/v) of oil concentration and 8% (v/v) of surfactant concentration. It was observed that the droplet size reduced up to sonication time of 25 min and thereafter it remained constant. The droplet size obtained at 25 min was around 90 nm and hence the same was considered for the energy calculations (as shown in Appendix A.3). It was observed that using HC (OP2 cavitating device), the maximum reduction in droplet size was obtained in 200 passes which corresponds to 45 min processing time and thereafter remained almost constant. The droplet size obtained after 45 min (200 passes) using HC was around 93 nm and the same was used for the energy calculations (Appendix A.3). The energy estimations were done based on the total energy delivered to the system (detailed calculation is shown in Appendix A). It was

observed that in case of HC, the energy required (kJ/ (m^3.nm)) to treat unit volume of emulsion with unit reduction in the droplet size was found to be low as compared to ultrasonication. Based on the energy calculations, HC was found to be 11 times more energy efficient than ultrasonication. Thus, it can be concluded that HC is more efficient than ultrasonication for the preparation of nanoemulsions of similar droplet size and can be scaled up on a large scale for the synthesis of oil in water nanoemulsion.

3.4   Summary

It has been studied that HC is a viable and energy efficient technique for the preparation of oil in water nanoemulsions. The efficiency of HC for the emulsification process was found to be dependent on C_V. It was found that to prepare emulsions of droplet size below 100 nm; it is desired to operate a cavitating device at C_V value in the range of 0.17-0.20. It was also found that the throat perimeter to cross sectional area ratio (α) had no significant effect on the droplet size reduction and an orifice plate cavitating device having single circular hole is quite sufficient to achieve the required droplet size. However it was observed that higher throat area to pipe area ratio (β) is beneficial to achieve an emulsion of smaller droplet size provided the required C_V is achieved. The maximum reduction in droplet size was achieved in 200 passes and thereafter the droplet size remained almost constant. Moreover the mustard oil in water nanoemulsion prepared using HC was found to be kinetically stable for up to 3 months under centrifugal and thermal stress conditions. Energy analysis of HC and ultrasonication showed that HC is 11 times energy efficient than ultrasonication. These advantages make hydrodynamic cavitation an economically feasible technology for the preparation of stable nanoemulsions on a large scale.

Appendix A

A.1 Sample calculation of cavitation number

Since,

$$C_V = \frac{(P_2 - P_V)}{\frac{1}{2}\rho V^2}$$

P_2 = downstream pressure, 101325 Pa

P_V = vapor pressure of water (as the majority of phase is water), 4242 Pa (assumed)

ρ = Density of emulsion = 993 kg/m^3

V = velocity of liquid, 32.08 m/s at 10 bar in OP1 device

$$C_V = \frac{(101325 - 4242)}{\frac{1}{2} \, x \, 993 \, x \, 32.08^2} = 0.19$$

Therefore, C_V of OP1 at 10 bar is 0.19.

A.2 Sample calculation for power dissipation in HC as shown in Table 3.2

(Device: OP2, Operating pressure: 10 bar (10 x 10^5 Pa), volumetric flow rate: 13.6 LPM = 0.00022667 m^3/s)

Mechanical power dissipation,

Power dissipated = Pressure drop across the device x volumetric flow rate

$\qquad$ = (10 x 10^5) Pa x 0.000226 m^3/s

$\qquad$ = 226.67 W = 226.67J/s

A.3 Energy efficiency of HC and ultrasonication based on total energy delivered

A.3.1.Hydrodynamic cavitation

(Pump power: 1.1 kW, operating pressure: 10 bar, processing time: 45 min, volume: 3L)

The droplet size obtained after 45 min was 93 nm using HC at an optimum pressure of 10 bar

Electrical energy supplied to pump in 45 min

$\qquad$ = 1.1 kW = 1100 J/s x 45 min x 60 s

$\qquad$ = 2970000 J = 2970 kJ

Processing volume = 3 L = 3 x 10^{-3} m^3

Energy density = Electrical energy supplied / volume

$= 2970 \text{ (kJ)}/0.003(\text{m}^3)$

$= 990000 \text{ kJ/m}^3 = 9.9 \text{ x } 10^5 \text{ kJ/m}^3$

Change in droplet size = (Initial size – size obtained after 45 min at 10 bar)

$= (1000 \text{ nm} - 93 \text{ nm}) = 907 \text{ nm}$

Energy utilized = Energy density / change in droplet size

$= 9.9 \text{ x } 10^5 \text{ (kJ/m}^3) / 907 \text{ (nm)} = \textbf{1091.51 kJ/ (m}^3\textbf{.nm)}$

A.3.2 Energy efficiency evaluation of ultrasonication based on total energy delivered

(Power of horn: 750W, operating frequency: 20 kHz, processing time: 25 min, processing volume: 100 ml)

The droplet size obtained after 25 min was 90 nm using ultrasonication in 25 min

Electrical energy supplied to horn in 25 min

$= 750 \text{ J/s x } 25 \text{ min x } 60 \text{ s } = 1125 \text{ kJ}$

Processing volume $= 100 \text{ mL} = 100 \text{ x } 10^{-6} \text{ m}^3$

Energy density = Electrical energy supplied / volume

$= 1125 \text{ (kJ)}/100 \text{ x } 10^{-6} \text{ (m}^3) = 1.125 \text{ x } 10^7 \text{ kJ/m}^3$

Change in droplet size = (Initial size – size obtained after 30 min)

$= (1000 \text{ nm} - 90 \text{ nm}) = 910 \text{ nm}$

Energy utilized = Energy density / change in droplet size

$= 1.125 \text{ x } 10^7 \text{ (kJ/m}^3) / 910 \text{ (nm)} = \textbf{12362.63 kJ/ (m}^3\textbf{.nm)}$

Appendix A.4: Coding of MATLAB

```
function [MPSD qe1] = jitendra(Um)

[qe1] = model(Um);

qe1_fexp = [0.000078982 0.000039528 0.000039712 0.000039933];

sum1 = 0;
nm = 4; np = 3;

    MPSD = 100*sqrt(1/(nm-np) * ((sum(qe1(1:4)) -
sum(qe1_fexp(1:4)))/sum(qe1_fexp(1:4)))^2);

end

function[qe1] = model(Um)
C = 1;
We = [55.226 93.58 140.25 179.33];
Re = [60988 79390 97191 109902];
Cv = [0.38 0.22 0.15 0.12];
a = Um(1);
b = Um(2);
c = Um(3);

syms qe11 qe12 qe13 qe14
eq(1) = -qe11 + C*(Re(1)^(-a))*(We(1)^(-b))*(Cv(1)^c);
eq(2) = -qe12 + C*(Re(2)^(-a))*(We(2)^(-b))*(Cv(2)^c);
eq(3) = -qe13 + C*(Re(3)^(-a))*(We(3)^(-b))*(Cv(3)^c);
eq(4) = -qe14 + C*(Re(4)^(-a))*(We(4)^(-b))*(Cv(4)^c);


QE1 = solve(eq(1:4),[qe11 qe12 qe13 qe14]);
qe1 = [double(QE1.qe11) double(QE1.qe12) double(QE1.qe13)
double(QE1.qe14)]


end


X_guess = [];
 Um_guess = [1 1 1];

 [Um MPSD qe1] = fminunc(@jitendra,Um_guess);
Um
[MPSD qe1] = jitendra(Um)
```

Appendix A.5: Experimental datas used for the development of correlation

Devices	Pressure, Pa	Vo, m³/s	Velocity, m/s	Ch. Length, L (m)	Density, ρ (kg/m3)	I.T., σ (mN/m)	ΔP, Pa	Viscosity, μ, kg/m.s	Cv	Re	We	d, nm	Size, d, m	d/L
SV	5	0.000075	23.88	0.001517	993	25.01	97083	0.001	0.34	35972.38	34.34708	159.8	1.598E-07	0.000105339
	8	9.16667E-05	29.19	0.001517	993	25.01	97083	0.001	0.23	43971.26	51.32032	110	0.00000011	7.25115E-05
	10	0.000106667	33.97	0.001517	993	25.01	97083	0.001	0.169	51171.76	69.50439	97.05	9.705E-08	6.3975E-05
	15	0.00013	41.4	0.001517	993	25.01	97083	0.001	0.114	62364.17	103.2338	94.2	9.42E-08	6.20962E-05
CV	5	8.33333E-05	26.54	0.002	993	25.01	97083	0.001	0.28	47445.54	45.32083	184	0.000000184	0.000092
	10	0.000103333	32.91	0.002	993	25.01	97083	0.001	0.18	65359.26	86.00453	107.9	1.079E-07	0.00005395
	15	0.000116667	37.15	0.002	993	25.01	97083	0.001	0.14	73779.9	109.5931	96.56	9.656E-08	0.00004828
	20	0.000133333	42.46	0.002	993	25.01	97083	0.001	0.108	84325.56	143.1613	102.7	1.027E-07	0.00005135
OP1	5	5.83333E-05	18.58	0.002	993	25.01	97083	0.001	0.57	36899.88	27.41303	262.8	2.628E-07	0.0001314
	8	7.83115E-05	24.94	0.002	993	25.01	97083	0.001	0.32	49527.76	49.38606	138.2	1.382E-07	0.0000691
	10	9.16667E-05	29.19	0.002	993	25.01	97083	0.001	0.23	57977.71	67.67514	110.7	1.107E-07	0.00005535
	15	0.000113333	36.09	0.002	993	25.01	97083	0.001	0.15	71681.53	103.4479	93.49	9.349E-08	0.000046745
OP2	5	0.000166667	23.59	0.003	993	25.01	97083	0.001	0.35	70276.01	66.28725	120.4	1.204E-07	4.01333E-05
	8	0.000205933	29.02	0.003	993	25.01	97083	0.001	0.23	86450.58	100.3117	106	0.000000106	3.53333E-05
	10	0.000226667	32.08	0.003	993	25.01	97083	0.001	0.19	95575.37	122.6049	87.72	8.772E-08	0.00002924
	15	0.000275	38.92	0.003	993	25.01	97083	0.001	0.13	115955.4	180.467	87.08	8.708E-08	2.90267E-05
OP3	5	0.000166667	23.58	0.00175	993	25.01	97083	0.001	0.35	40976.94	38.63474	133.9	1.339E-07	7.65143E-05
	8	0.000203915	28.84	0.00175	993	25.01	97083	0.001	0.24	50116.71	57.79152	110.95	1.1095E-07	0.0000634
	10	0.000221667	31.36	0.00175	993	25.01	97083	0.001	0.20	54499.33	68.341	92.96	9.296E-08	0.00005312
	15	0.000271667	38.44	0.00175	993	25.01	97083	0.001	0.13	66792.41	102.6486	93.77	9.377E-08	5.35829E-05
OP4	5	0.000158333	22.40	0.000966	993	25.01	97083	0.001	0.39	21482.23	19.23617	129.5	1.295E-07	0.000134058
	8	0.000190114	26.87	0.000966	993	25.01	97083	0.001	0.27	25774.73	27.6916	112.05	1.1205E-07	0.000115994
	10	0.0002	28.29	0.000966	993	25.01	97083	0.001	0.25	27135.45	30.69261	110	0.00000011	0.000113872

	15	0.000255	36.07	0.000966	993	25.01	97083	0.001	0.15	34597.69	49.89468	103.3	1.033E-07	0.000106936
OP5	5	0.00016	22.65	0.002712	993	25.01	97083	0.001	0.38	60988.33	55.22565	214.2	2.142E-07	7.89823E-05
	10	0.000208333	29.48	0.002712	993	25.01	97083	0.001	0.22	79390.11	93.57939	107.2	1.072E-07	3.9528E-05
	15	0.000255	36.09	0.002712	993	25.01	97083	0.001	0.15	97190.95	140.2488	107.7	1.077E-07	3.97124E-05
	20	0.000288333	40.81	0.002712	993	25.01	97083	0.001	0.12	109902	179.3323	108.3	1.083E-07	3.99336E-05

References

1. W. Liu, D. Sun, C. Li, Q. Liu, J. Xu, Formation and stability of paraffin oil-in-water nano-emulsions prepared by the emulsion inversion point method, J. Colloid. Interface Sci. 303 (2006) 557–563.

2. C. Solan, P. Izuierdo, J. Nolla, N. Azemar, M.J. Garcia, Nanoemulsions, Curr. Opin. Colloid. Interface Sci.10 (2005) 102-110.

3. J. Gutierrez, C. Gonzalez, A. Maestro, I. Sole, C. Pey, J. Nolla, Nano-emulsions: new applications and optimization of their preparation, Curr. Opin. Colloid Interface Sci. 13 (2008) 245-251.

4. Wang, X.Y.; Wang, Y.W; Huang, R. Enhancing stability and oral bioavailability of polyphenols using nanoemulsions. In: Micro/Nanoencapsulation of Active Food Ingredients. Q. R. Huang, P. Given and M. Qian (Editors). (2009) ACS Symposium Series 1007. Washington, DC.

5. S. Parthasarathy, S. Y. Tang, S. Manickam, Generation and optimization of palm oil-based oil-in-water (O/W) submicron-emulsions and encapsulation of curcumin using a liquid whistle hydrodynamic cavitation reactor (LWHCR), Ind. Eng. Chem. Res. 52 (34) (2013) 11829–11837.

6. D. K. Sarker, Engineering of nanoemulsions for drug delivery, Current Drug Delivery. 2 (2005) 297-310.

7. A. Shanmugam, M. Ashokkumar, Ultrasonic preparation of stable flax seed oil emulsions in dairy systems physicochemical characterization, Food Hydrocolloids 39 (2014) 151-162.

8. A. Gupta, H. B. Eral, T. A. Hattona, P. S. Doyle, Nanoemulsions: formation, properties and applications, Soft Matter 12(11) (2016) 2826-2841.

9. S. M. Jafari, Y. He, B. Bhandari, Production of sub-micron emulsions by ultrasound and microfluidization techniques, Journal of Food Engineering, 82(4) (2007) 478-488.

10. Z. Zhang, G. Wang, Y. Nie, J. Ji, Hydrodynamic cavitation as an efficient method for the formation of sub-100 nm O/W emulsions with high stability, Chin. J. Chem. Eng. 24(10) (2016) 1477-1480.

11. W. He, Y. Tan, Z. Tian, L. Chen, F. Hu, W. Wu, Food protein-stabilized nanoemulsions as potential delivery systems for poorly water-soluble drugs: preparation, in vitro characterization, and pharmacokinetics in rats, Int. J. Nanomedicine 6 (2011) 521-533.

12. J. Peng, W. Dong, L. Li, J. Xu, D. Jin, X. Xia, Y. Liu, Effect of high-pressure homogenization preparation on mean globule size and large-diameter tail of oil-in-water injectable emulsions, J. food and drug analysis 23(4) (2015) 828-835.

13. J.M. Perrier-Cornet, P. Marie, P. Gervais, Comparison of emulsification efficiency of protein-stabilized oil-in-water emulsions using jet, high pressure and colloid mill homogenization, J. Food Eng. 66 (2) (2005) 211–217.

14. S. Y. Tang, P. Shridharan, M. Sivakumar, Impact of process parameters in the generation of novel aspirin nanoemulsions–comparative studies between ultrasound cavitation and microfluidizer, Ultrason. Sonochem. 20(1) (2013) 485-497.

15. S. S. Galooyak, B. Dabir, Three-factor response surface optimization of nano-emulsion formation using a microfluidizer, J. food sci. tech. 52(5) (2015) 2558-2571.

16. K. A. Ramisetty, A. B. Pandit, P. R. Gogate, Ultrasound assisted preparation of emulsion of coconut oil in water: Understanding the effect of operating parameters and comparison of reactor designs, Chem. Eng. Process. 88 (2015) 70–77.

17. T.S.H. Leong, T.J. Wooster, S.E. Kentish, M. Ashokkumar, Minimising oil droplet size using ultrasonic emulsification, Ultrason. Sonochem. 16 (2009) 721–727.

18. J. Carpenter, V. K. Saharan, Ultrasonic assisted formation and stability of mustard oil in water nanoemulsion: Effect of process parameters and their optimization, Ultrason. Sonochem. 35PA (2017) 422-430.

19. P. R. Gogate, A. M. Kabadi, A review of applications of cavitation in biochemical engineering/biotechnology, Biochem Eng J 44 (2009) 60-72.

20. J. Carpenter, M. P. Badve, S. Rajoriya, S. George, V. K. Saharan, A. B. Pandit, Hydrodynamic cavitation: An emerging technology for the intensification of various chemical and physical processes in a chemical process industry, Rev. Chem. Eng. 33 (2016), 433-468.

21. V. S. Moholkar, A. B. Pandit, Modeling of hydrodynamic cavitation reactors: a unified approach, Chemical Engineering Science 56 (2001) 6295–6302.

22. A. Kalva, T. Sivasankar, V. S. Moholkar, Physical mechanism of ultrasound-assisted synthesis of biodiesel, Ind. Eng. Chem. Res. 48(1) (2008) 534-54.

23. K. A. Ramisetty, A. B. Pandit, P. R. Gogate, Novel approach of producing oil in water emulsion using hydrodynamic cavitation reactor, Ind. Eng. Chem. Res. 53(42) (2014) 16508-16515.

24. S. Rajoriya, J. Carpenter, V. K. Saharan, A. B. Pandit, Hydrodynamic cavitation: an advanced oxidation process for the degradation of bio-refractory pollutants, Rev. Chem. Eng. 32 (2016) 379–411.

25. V. K. Saharan, M. A. Rizwani, A. A. Malani, A. B. Pandit, Effect of geometry of hydrodynamically cavitating device on degradation of orange-G, Ultrason. Sonochem. 20(1) (2013) 345-353.

26. A. Gupta, V. Narsimhan, T. Hatton, and P. S. Doyle. "Kinetics of the change in droplet size during nanoemulsion formation. Langmuir 32(44) (2016) 11551-11559.

27. S. Mujumdar, P.S. Kumar, A.B. Pandit, Emulsification by ultrasound: Relation between intensity and emulsion quality, Indian Journal of Chemical Technology 4 (1997) 277-284.

28. M. Sivakumar, A. B. Pandit, Wastewater treatment: a novel energy efficient hydrodynamic cavitational technique, Ultrason. Sonochem. 9 (3) (2002) 123-131.

29. D. Ghayal, A. B. Pandit, V. K. Rathod, Optimization of biodiesel production in a hydrodynamic cavitation reactor using used frying oil, Ultrason. Sonochem. 20 (2013) 322–328.

30. Balasundaram B, Harrison STL. Optimising orifice geometry for selective release of periplasmic products during cell disruption by hydrodynamic cavitation, Biochem. Eng. J. 2011; 54: 207-209.

31. S. S. Sawant, A. C. Anil, V. Krishnamurthy, C. Gaonkar, J. Kolwalkar, L. Khandeparker, D. Desai, A. V. Mahulkar, V. V. Ranade, A. B. Pandit, Effect of hydrodynamic cavitation on zooplankton: a tool for disinfection, Biochem. Eng. J. 42(3) (2008) 320-328.

32. V. K. Saharan, M. P. Badve, A. B. Pandit, Degradation of Reactive Red 120 dye using hydrodynamic cavitation, Chem. Eng. J. 178 (2011) 100-107.

33. V. S. Moholkar, A. B. Pandit, Bubble behavior in hydrodynamic cavitation: effect of turbulence. AIChE 43(6) (1997) 1641-1648.

34. P. Kumar, S. Khanna, V. S. Moholkar, Flow regime maps and optimization thereby of hydrodynamic cavitation reactors. AIChE 58(12) (2012) 3858-3866.

35. T. A. Bashir, A. G. Soni, A. V. Mahulkar, A. B. Pandit, The CFD driven optimization of a modified venturi for cavitation activity, Can. J. Chem. Eng. 89 (2011) 1366–1375.

36. Kuldeep, V. K. Saharan, Computational study of different venturi and orifice type Hydrodynamic Cavitating devices, J. Hydrodynamic. 28(2) (2016) 293-305.

37. T. Jain, J. Carpenter, V. K. Saharan, CFD Analysis and Optimization of Circular and Slit Venturi for Cavitational Activity, J. Mat. Sci. Mech. Eng. 1 (2014) 28-33.

38. K. V. Kumar, K. Porkodi, F. Rocha, Comparison of various error functions in predicting the optimum isotherm by linear and non-linear regression analysis for the sorption of basic red 9 by activated carbon. Journal of hazardous materials *150*(1) (2008) 158-165.

39. H. Silva, M. Cerqueira, A. Vicente, Influence of surfactant and processing conditions in the stability of oil-in-water nanoemulsions. J. Food Eng. 167 (2015) 89-98.

CHAPTER 4

FORMATION AND STABILITY OF MULTILAYER O/W EMULSIONS: COMPARISON BETWEEN BATCH AND RECIRCULATING FLOW ULTRASONICATION PROCESS

4.1 Introduction

Oil in water (O/W) emulsions consisting of the dispersion of small lipid droplets in a continuous phase have been utilized in variety of food, pharmaceutical and cosmetic products[1−6]. Among all the functional bioactive compounds, mono and poly unsaturated fatty acids are found to be the essential compounds that provide several health benefits [7,8]. Their incorporation into O/W emulsions provide a perfect microencapsulating atmosphere for lipids to prevent them from the lipid auto-oxidation as well as to maintain their nutritional quality [1,9]. These essential fats are highly susceptible to the attack of oxidative radicals and get oxidized under various environmental stresses such as air, light and thermal processing [9,10].

The major challenge in this area is to produce emulsions with high stability against the various instability factors such as creaming, coalescence, flocculation, and oxidation during storage [11]. Two major deciding factors for producing a highly stable O/W emulsion are the choice of suitable emulsifier(s) and intensity of shear supplied for homogenization. Relying only on one of them would pose a great challenge in terms of technical and economic feasibility of food emulsions. Protein, an amphiphilic emulsifier has an ability to get dispersed during the emulsification process by rapidly adsorbing at the oil-water interface, reducing the interfacial tension and prevents the oil droplets against coalescence and flocculation [9]. But the protein stabilized emulsions are highly sensitive to the pH and temperature variations [1,10,12].

In the recent decade, many studies reported the utilization of protein-polysaccharide combinations for stabilizing the emulsions [8,10,13,14]. The preparation of such emulsions using layer by layer (LbL) approach attracted more interest in recent years because of many advantages such as perfect encapsulation for lipids, preventing them from the attack of peroxides and the controlled release of bioactive compounds. In LbL method, primary emulsion stabilized with a charged emulsifier (protein) is produced by homogenization and thereafter diluted with oppositely charged polysaccharide, to form a double layer or secondary emulsion. The formation of an electrostatically charged double layer of protein and polysaccharide forms a thicker interfacial membrane at the oil-water interface which consequently increases the electrostatic repulsion between the droplets thereby stabilizing the emulsions against coalescence. However to produce highly stable multilayer emulsion, it

becomes necessary to select an appropriate process condition such as the concentration of biopolymers, level of homogenization, charge density by varying pH, and dispersed phase (oil) characteristics to overcome the problem of droplet aggregations which is usually known as bridging and depletion flocculation [2,8,10,13,14].

On the other hand, to minimize the use of emulsifiers and in order to achieve the high stability of emulsion against flocculation, food emulsions are prepared using high shear homogenizers. Numerous studies on the formation of conventional (single layer) and multilayer emulsion reported the use of high energy methods including high speed blender, mixers, high pressure homogenizers, microfluidizer to produce stable emulsions [1,7,8,10,13–16]. These methods require high energy inputs (pressure ~1000 bar or more and speed ~1000s of RPM) and are found to be costly on a large scale for making food emulsions.

In recent years, ultrasonication is considered as a promising, efficient and environmentally acceptable technique for the preparation of different emulsions mainly monolayered emulsions having applications in food, pharmaceutical, and cosmetic products [4,17,18][19]. However, particularly in multilayer emulsions, only few studies have reported the use of ultrasonication for the formation of secondary emulsions [1,13,20]. These studies reported the use of ultrasonication as an ancillary process for removing flocs (bridging/depletion flocculation) after the formation of multilayer emulsions using homogenizers. These previous studies had not reported on the effect of sonication time on the extent of flocculation, rather concluded that the flocs disrupted during sonication were sometimes again reforming back to flocs after sonication (depending on the conditions such as pH and biopolymer concentration). Therefore, it becomes necessary to know that what extent of sonication should be given so that the stability of emulsions against flocculation can be enhanced for a longer time. Moreover, ultrasonication generates highly reactive free radicals during the intense cavity collapse in the liquid medium. These radicals can migrate to the surface or inside the oil droplets which in turn oxidize the oil molecules. Hence, it is necessary to optimize the sonication time such that the emulsion physical stability can be improved without compromising the chemical characteristics of oil molecules or emulsions.

Therefore, one of the aims of the present work was to study the effect of ultrasonication time on the multilayer emulsion's physicochemical properties such as droplet size, zeta potential,

morphology, physical and oxidative stability of emulsions prepared using olive oil, water, WPI and SA. Additionally, the effects of other parameters such as pH and SA concentration on the above mentioned parameters were studied to find out the best conditions for obtaining multilayer emulsion.

Previous studies reported in literature were carried out in batch mode only with low processing volume for the synthesis of conventional and multilayer emulsions using ultrasonication. And utilization of ultrasonic irradiations for treating large volume required more energy [21]. Therefore, this approach would not be sustainable when scaled up to large scale operations. Hence, looking at this aspect, the conceptual design of a recirculating flow configuration (RFC) has been developed for emulsification process with an objective to process larger volume with minimal amount of energy. For this purpose, the efficacy of ultrasonication based batch and recirculation flow mode for the production of multilayer emulsion was evaluated for energy efficiency and processing volumes to establish the scale up aspect.

4.2 Materials and Methods

4.2.1   Materials

Refined olive oil and whey protein isolate (WPI, > 90% protein) were purchased from the local market. Sodium alginate (SA) as a secondary biopolymer and Cumene hydroperoxide (CHP) for peroxide value calculations were obtained from Sigma Aldrich (India). Deionized water (Ultrapure, Thermofisher) was used for the preparation of all dispersions and dilutions. All the materials were used in the experiments without any further purification.

4.2.2   Preparation of emulsions

Stock solutions of 1 wt% WPI and SA of desired concentrations were prepared and kept for stirring for 2 h to promote their complete dissolution in water and then stored for overnight at room temperature. Sodium azide (0.04 wt %) was also added to these dispersions in order to avoid the formation of microbial species. Primary emulsion (PE) was prepared by mixing olive oil (10 wt %) with WPI aqueous solution (90 wt %) in a batch ultrasonication process. The mixture was sonicated for up to 15 min in order to reduce the oil droplet size. The pH of PE formed using sonication was found to be 6.5. Further in order to observe the interaction

between WPI and SA molecules, pH of emulsion was adjusted to different values ranging from 4 to 7 using 0.1N H_2SO_4 or NaOH. The secondary emulsions (SE) were then prepared by mixing PE with SA aqueous solution in a ratio of 1:1 (by volume) and keeping the same pH as that of PE. The prepared SE was subjected to sonication in batch mode for 60 sec. The final compositions of all constituents in SE formed were: 4.93 wt % oil, 0.443 wt % WPI, 0.0381 wt% sodium azide and 0.1-0.3 wt % SA. All prepared emulsions were stored at room temperature for further analysis.

4.2.3 Experimental set up

Batch studies with processing volume of 100 mL were carried out in a glass beaker of capacity 150 mL using an ultrasonic horn (power output of 750 W, operating frequency of 20 kHz and 40% amplitude). As shown in Fig. 4.1(a), the tip of ultrasonic horn having diameter of 13 mm was immersed up to 25 mm depth in the emulsion mixture. Initially, PE was sonicated up to 15 min and then the SE was sonicated for 30, 60 and 90 sec in order to optimize the sonication time. The glass beaker was placed in a cold water bath to maintain the temperature at 30±2°C during the ultrasonication process.

In case of RFC, emulsification was carried out in the sonication cell provided with a recirculating flow line with processing volume of 1500 mL. The schematic of recirculating flow configuration is represented in Fig. 4.1(b). It mainly consists of (i) a sonication cell made up of SS316 and having capacity of 600 mL, (ii) a storage tank of capacity of 2 L for holding the emulsion mixture, (iii) a pump with capacity of 20 W with a maximum flow rate of 2 L/min, and (iv) Inlet and outlet flow valves. The dimensions of sonication cell are: diameter - 8 cm, Thickness of jacket- 1.5 cm, total height of the cell -16 cm, height of outlet valve- 12 cm (from bottom). During emulsification, the emulsion mixture in the storage tank was circulated through the sonication cell using pump at different flow rates. The flow rate was adjusted using the bottom inlet flow valve connected at the discharge side of the pump. A cooling jacket was provided for the sonication cell to control the temperature of the emulsion by circulating cold water through the jacket. Experiments were conducted at different flow rates ranging from 0.5 to 1.5 L/min with different number of passes. The number of passes in the sonication cell was determined as:

Number of passes = (Volumetric flow rate/total volume of emulsion) x sonication time
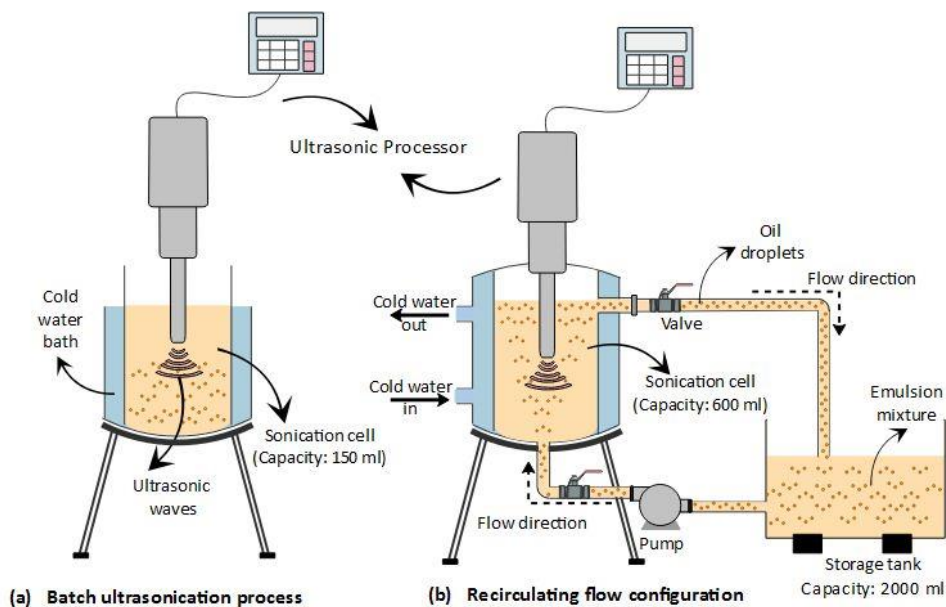
Fig. 4.1 Ultrasonication based experimental set up for emulsification process

4.2.4 Droplet size and zeta potential measurements

Droplet size and zeta potential of the prepared emulsions were determined using Zetasizer Nano ZS (Malvern Instruments, UK) provided with dynamic light scattering and electrophoresis facility for the analysis. All the formulations were diluted to the ratio of 1:1000 in deionized water at the same pH as of the prepared emulsions in order to prevent multiple scattering effects during size analysis. The Zetasizer gave the Z-average diameter which is represented as droplet size (nm) in this study. Duplicate samples along with three measurements were considered for ensuring repeatability of the analysis.

4.2.5 Separation and creaming index measurements

The separation index (SI) was used to measure the extent of non-emulsified oil or oil layer obtained at the top of PE. The % SI was measured after 7 days of storage. The % SI was determined as:

$$\% \text{ SI} = \frac{H_C}{H_T} \; x \; 100 \qquad\qquad (4.1)$$

Where, H_C represent the height of the oil layer obtained at the top and H_T represents the total height of the PE.

The creaming index (CI) was determined by measuring the extent of separation of cream and serum phase after a storage time of 7 days at room temperature. The cloudy and/or transparent phases seen at the bottom of storage bottles were considered as serum phase. The %CI was measured as [10]:

$$\% \, CI = \frac{H_S}{H_T} \, x \, 100 \qquad (4.2)$$

Where, H_S and H_T represent the height of the serum phase and total height of the emulsion, respectively. The % CI provides the information on the extent of droplet aggregation and/or separation of emulsion phases. Higher the % CI, higher will be the droplet aggregation and faster will be the creaming.

4.2.6 Optical microscopic analysis

Emulsions microstructure was analyzed using optical microscope (Leica Microsystems). A small drop of emulsion was placed on a glass slide and then covered with a cover slip. The emulsion drop between the slide and slip got spread and was analyzed through the microscope. All images of emulsions were analyzed at 50 X magnification and were acquired through the computer interfaced to the microscope via digital image processing software.

4.2.7 Oxidative stability: Evaluation of peroxide value

The concentration of hydroperoxide (primary lipid oxidation products) present in pure oil and all emulsions was evaluated using method reported by Shantha & Decker [22] and Chen et. al.[23]. Lipids present in emulsions were extracted by adding a small volume of emulsion (0.3 mL) to a mixture of isooctane/2-propanol (1.5 mL, 3:1 v/v) and then vortexed for 30 s, followed by centrifugation for 5 min at 3500 RPM. Thereafter, 0.2 mL of top solvent layer containing extracted lipids was taken and mixed with 2.8 mL of methanol/1-butanol (2:1 v/v) mixture and 30 μL of 3.94 M ammonium thiocyanate/Fe^{2+} (1:1 v/v) solution. The Fe^{2+} solution was prepared by mixing equal amounts of 0.132 M barium chloride and 0.144 M

ferrous sulfate. The barium sulfate gets precipitated and a clear solution of Fe^{2+} was obtained. The complete mixture of extracted lipids was kept for 20 min in the dark. The peroxides present in the solution oxidized the Fe^{2+} into Fe^{3+} and a faint yellow color was appeared in the end. The absorbance was measured at 510 nm using a UV-visible spectrophotometer (Shimadzu). The concentration of hydroperoxide in the emulsion mixture was determined using a standard curve of Cumene Hydroperoxide (CHP) and measured as µM of CHP per gram of oil. All solutions were prepared freshly on a day to day basis for analysis.

4.3 Results and Discussions

4.3.1   Formation of primary emulsion (PE): optimization of sonication time

Initially, PE was formulated through batch experiments in the sonication cell at pH 7 in order to optimize the required sonication time for minimum droplet size and separation index. The results obtained are shown in Fig. 4.2. It was observed that on increasing the sonication time from 3 to 10 min, the droplet size significantly got reduced from 473 to 312 nm and further slightly reduced to 308 nm after 15 min sonication. The reduction in droplet sizes can be attributed to the physical effects of sonication within the emulsion mixture such as the liquid microjets and high intensity turbulence caused as a result of cavity collapse are capable of disrupting the droplets. These effects uniformly distribute the protein molecules within the dispersed phase and facilitate their adsorption at the oil-water interfaces. Moreover the %SI was decreased from 20% to almost 0% on increasing the sonication time from 3 to 15 min. At 10 min sonication time, the %SI was 10% and an oil layer was observed at the top. Though there was no significant change in the droplet size beyond 10 min of sonication, but the higher stability and perfect dispersion was achieved in 15 min of sonication time and therefore 15 min of sonication time was considered for further experiments.
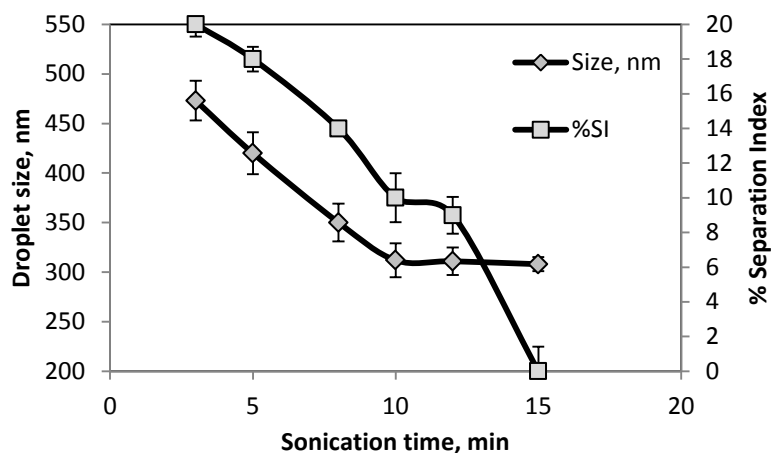
Fig. 4.2 Effect of sonication time on droplet size and %SI of PE

(10 t% oil, 0.9 wt% WPI, pH 7)

4.3.2 Formation of secondary emulsion (SE): effect of process parameters

4.3.2.1 Influence of pH and SA concentration on zeta potential of emulsions

The interaction between SA and WPI coated droplets was monitored using ζ- potential measurements. To establish the interaction between SA molecules and WPI coated droplets, the SA concentration was varied in the range of 0.1-0.3 wt% at the different pH values (4-7). The results obtained are shown in Fig. 4.3(A) & (B). In the primary emulsion (PE), ζ- potential of the droplets was varied in the range of +14 mV to -57 mV on increasing pH from 4 to 7. It has been well established that because of the amphiphilic behavior of WPI molecules, the surface charge density changed from positive to negative on varying the pH below its isoelectric point (pI = 4.5 to 4.7) to 7. However, when SA were incorporated into PE, the surface charge density over the WPI coated droplets varied from -39 mV to -59 mV (at 0.2 wt% of SA) in the pH range of 4 to 7.

At pH 6 & 7, for all SA concentrations, there was no significant difference in ζ- potential of PE and SE indicating that limited interaction occurred between WPI coated droplets and SA molecules because of similar charge (Δζ~ 0) as shown in Fig. 4.3(B). Therefore at pH 6 and 7, because of the strong electrostatic repulsion between the WPI coated droplets and SA molecules, SEs were destabilized. On decreasing the pH value towards the pI (isoelectric point) of WPI i.e. at pH 5, the ζ- potential of WPI coated surfaces i.e. PE decreased to –13 mV whereas it increased to -43 mV for SE (0.1 wt% SA). Because of the higher net negative

124

charge over droplets (Δζ = -30 mV) at 0.1 wt% of SA concentration, a strong electrostatic interaction between SA molecules and WPI coated droplets existed. At pH 5, SA molecules contain sufficient anionic carboxylate groups (–COO⁻) which gets adsorbed on the cationic amino groups ($-NH_3^+$) of the protein molecules. Moreover, on increasing the SA concentration from 0.1 to 0.3 wt%, the net charge on the droplet surfaces was remained almost constant. However on further reducing the pH value to 4, the ζ-potential of PE and SE was found to be +14.8 mV and -31 mV, respectively. The net charge over the droplets (Δζ) was significantly increased on decreasing the pH from 5 to 4 indicating the formation of double layer emulsion because of strong electrostatic interaction between WPI coated droplets and SA molecules. However at pH 4, the extent of interaction was so high that SA started bridging with more than one droplet at a time. As a result of this, droplets came closer leading to the formation of flocs by the bridging mechanism and ultimately destabilized the bilayer emulsion (Described in detail in further sections). Similar trends between the interaction of protein and SA molecules during the formation of multilayer emulsions have been reported earlier in the literature [10,13,14]. Thus based on the observed behavior, it was concluded that at pH 5, the interaction between the biopolymers SA and WPI was strong enough to form a bilayer emulsion.
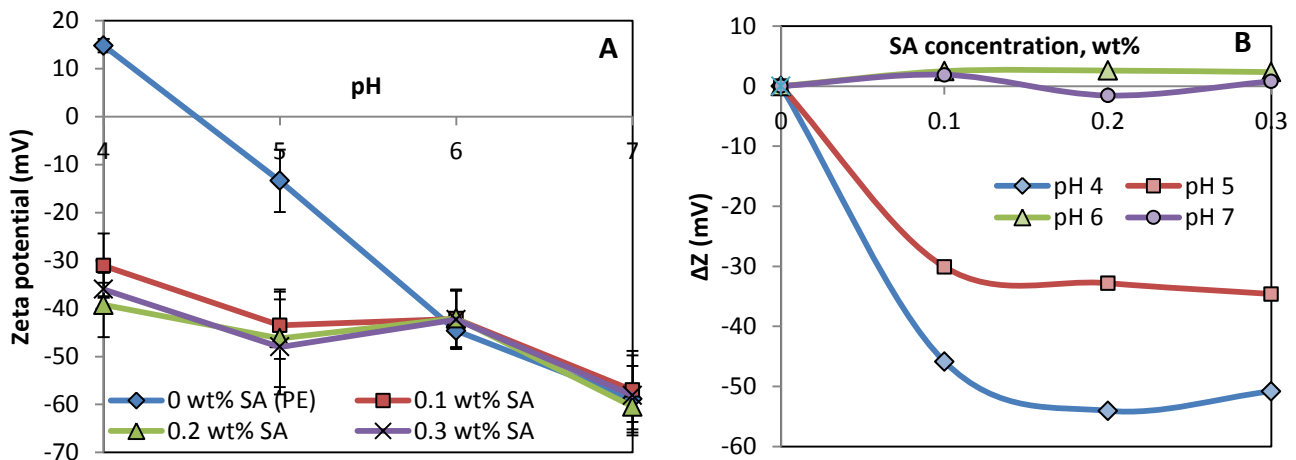
Fig. 4.3 Effect of pH and SA concentration on (A) Zeta potential & (B) Net charge of PE and SE

4.3.2.2 Influence of pH and SA concentration on stability of emulsions

The stability of PE and SE was evaluated using droplet size, creaming index and optical microscopy measurements at different pH from 4 to 7 and SA concentration in the range of 0 – 0.3 wt %.

In PEs, at pH 6 and 7, it was observed that the droplet size was found to be relatively small i.e. 400 nm and 308 nm respectively indicating the formation of a stable emulsion as shown in Fig 4.4(A). The amino groups of WPI rapidly adsorbed at the oil-water interface and stabilized the PE against the flocculation. However at pH 6 and 7, SEs were found to be unstable as shown in Fig. 4.4 (A) & (B) and 4.5. On adding SA (at all concentrations) in PE, no change in the droplet size of SE was observed at pH 6 and 7 as shown in Fig. 4.4(A). Also, the %CI obtained in SE at all SA concentrations varying from 0.1 to 0.3wt% were higher as depicted in Fig. 4.4(B). This indicated that the adsorption of SA molecules over the WPI coated surfaces was ineffective because of weak interaction or the strong repulsive forces between the biopolymers at pH 6 and 7. Further, it can also be seen in Fig. 4.5 that the extent of flocculation was increased on increasing the SA concentration from 0.1 to 0.3 wt%. This showed that because of the weak interaction forces between both biopolymers, unadsorbed SA molecules were excluded from the vicinity of the PE droplets and resulted in flocs formation of SA molecules. Moreover the large osmotic attractive forces between the PE droplets ultimately resulted in larger flocs of PE droplets as well. This phenomena is known as the depletion flocculation[11,24].
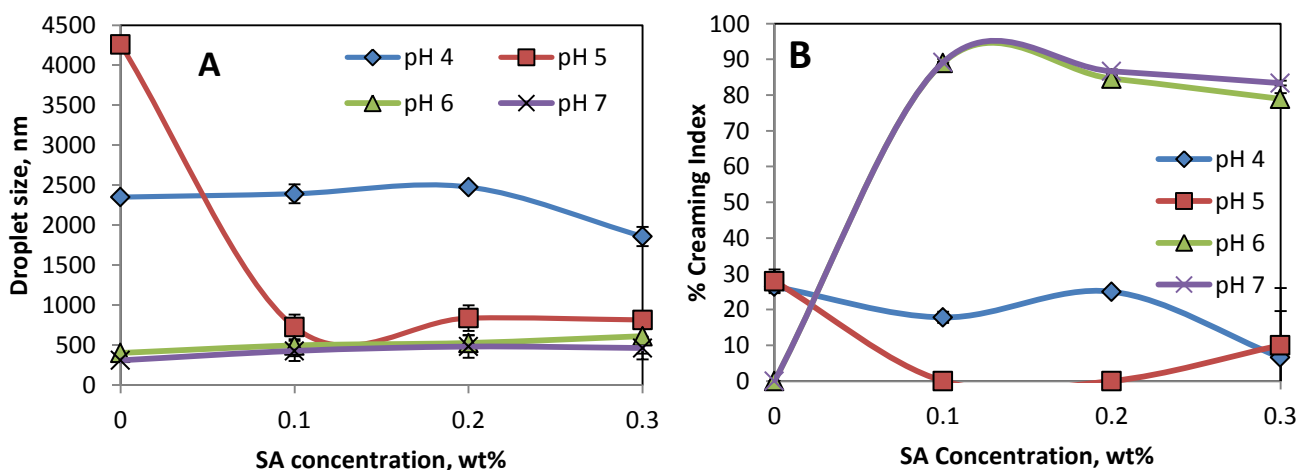
Fig.4.4 Effect of pH and SA concentration on (A) Droplet size, and (B) Creaming Index of multilayer emulsions

At pH 5 and 4, the PE was found to be unstable because of extensive droplet aggregation as indicating from the microscopic analysis, creaming index (Fig. 4.5) and droplet size obtained (Fig. 4.4(A)). It was observed that the droplet size of PE was drastically increased from 308 nm to 2349 nm when pH fell from 7 to 4. Since the droplet charge obtained at pH 5 and 4 (near the pI) was lesser and thus droplet aggregation occurs as a result of insufficient electrostatic repulsive forces between them leading to the formation of unstable PE. On contrary, the SE formed at pH 5 showed significant stability against the droplet aggregation as shown in Fig. 4.5 because of well-established interaction between the WPI coated droplets and SA molecules as discussed earlier. As shown in Fig. 4.4(A), the droplet size of SE at pH 5 was higher than that obtained at pH 6 and 7 for all the SA concentrations indicating the adsorption of SA molecules on the PE droplets. Whereas % CI of SE formed at pH 5 was found to be almost 0% as shown in Fig. 4.4(B). Also there was no phase separation or indication of any droplet aggregation as found in microscopic images of Fig. 4.5 for 0.1 and 0.2 wt% SA, which indicated the formation of stable bilayer system over the droplets. However at 0.3 wt% of SA, depletion flocculation occurred due to the presence of excess SA which can be clearly seen from Fig. 4.5. On comparing the PDI of SEs obtained at 0.1 and 0.2 wt% SA, it was observed that SE prepared using 0.2 wt% SA had more uniform droplet size distribution than that prepared with 0.1 wt% SA. The PDI of SE was found to be 0.5 and 0.68 when prepared with 0.2 and 0.1 wt% SA, respectively.

On the other hand at pH 4, the electrostatic interaction between SA and WPI coated droplets was quite high, since the net charge ($\Delta\zeta$) obtained was significantly higher than that obtained at pH 5. Thus due to the extreme interaction between the biopolymers, SA molecules bridge with multiple droplets of PE which leads to bridging flocculation [11,14]. As a result, the droplet size and % CI obtained at pH 4 was significantly higher at all concentration of SA as shown in Fig. 4.4(A) & (B). It can also be seen from microscopic images that the extent of flocculation was higher at pH 4. Therefore SE formed at pH 4 was found to be unstable as it showed more creaming and higher flocculation. The present results were found to be in accordance with the previous reports [10,13,14]. Therefore, the SE formed at pH 5 and 0.2 wt % SA was found to be more stable against the depletion and bridging flocculation and showed good physical stability against creaming.
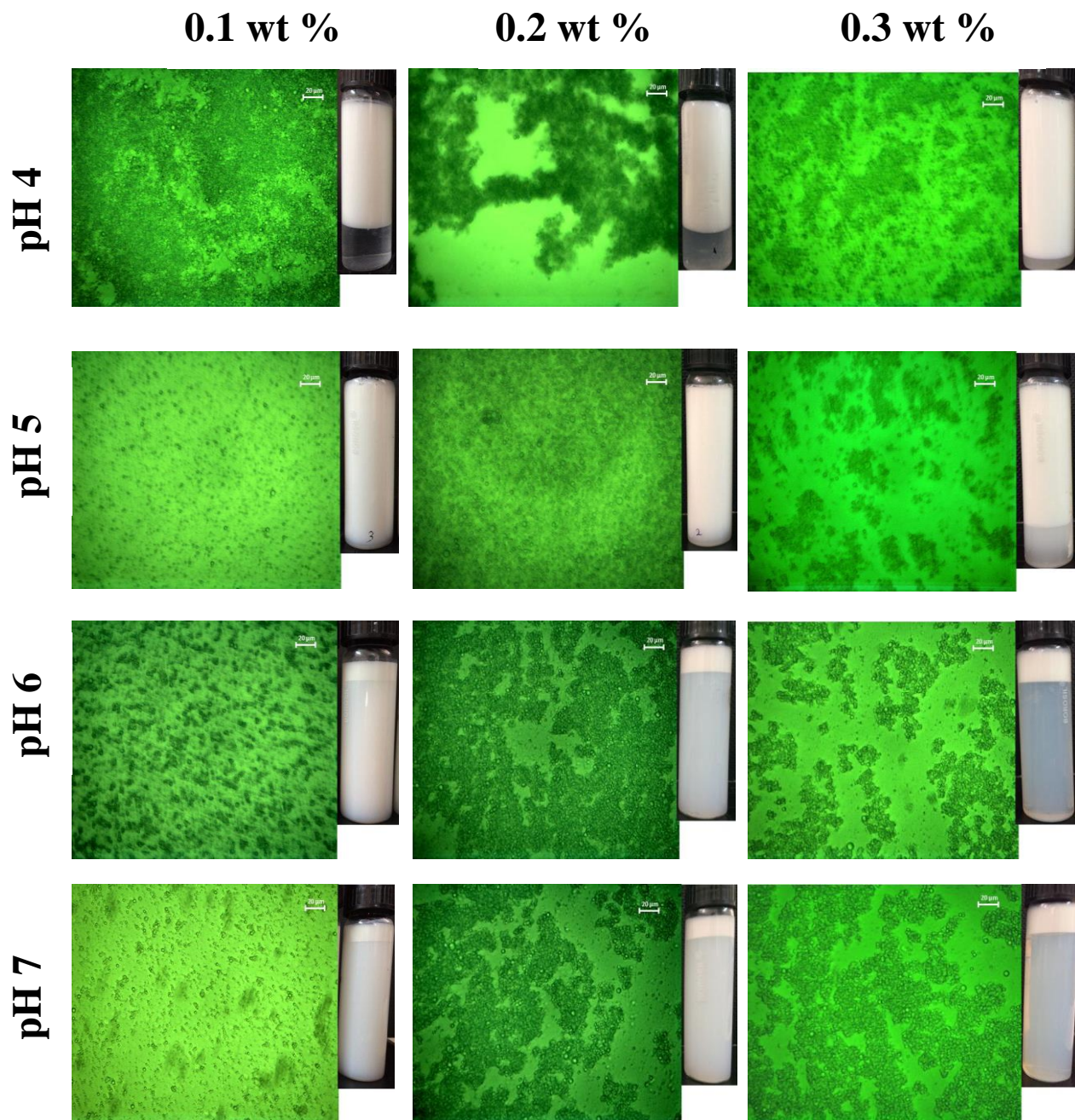
Fig. 4.5 Microscopic analysis of SEs at various pH and SA concentration (0.443 wt% WPI, 4.93 wt% oil, 60 sec sonication, 50 X magnifications, 20μm scale bar)

4.3.2.3 Effect of sonication on SE

Previous studies reported that SE prepared with biopolymers using the ultrasonication process was stable against the flocculation [1,13,20]. However the effect of sonication time on physical and oxidative stability of the multilayer emulsion over a long time period has not been reported. For this reason, we studied the effect of sonication time on the stability of SE prepared at optimum conditions (pH 5 and 0.2 wt% SA). The sonication time was varied in the range of 0 to 90 sec and the results obtained are shown in Fig. 4.6(A). Immediately after addition of SA into PE (without sonication), the droplet size obtained was significantly higher i.e. 6690 nm. Also, a clear serum phase (% CI = 60%) was observed in non sonicated secondary emulsion as shown in Fig. 4.6(A), which indicated that all of oil droplets were remained in creaming phase and unadsorbed biopolymers (WPI/SA) remained in the serum phase. In order to effectively distribute/adsorb SA molecules on the PE droplets, energy is required to overcome the mass transfer resistances caused by high viscous aqueous SA solution.

The stability of SE was improved on sonicating the emulsion. It was observed that the droplet size decreased by 7 fold, i.e. from 6690nm to 968nm on sonicating the emulsion for 30 sec. The sonication effects disrupt the flocs and disperse the SA molecules more uniformly into the system. On further increasing the sonication time i.e. beyond 30 sec, the droplet size was very slightly reduced from 968 nm to 836 nm at 60 sec and then remained constant. This indicated that sufficient energy was dissipated into the emulsion within 60 sec to get the minimum possible droplet size. Moreover, long term stability of the SEs against separation was also evaluated by measuring creaming index up to 21 days of storage time. It was observed that the SE prepared at various sonication time (60-90 sec) was found to be stable (%CI = 0) after the storage time of 21 days. This showed that SE prepared using sonication was kinetically stable for a period of 21 days. Moreau et al.,[20] also studied the effect of sonication on the formation of SE of corn oil stabilized with β-Lg and pectin complexes. It was reported that the mean particle size of SE was reduced by 4 times on sonicating the emulsion mixture for 30 sec (40% amplitude and 20 kHz frequency). The mean particle size of SE was reduced from 12.9 μm to 2.6 μm after 30 sec of sonication and then remained constant on further sonicating the mixture.
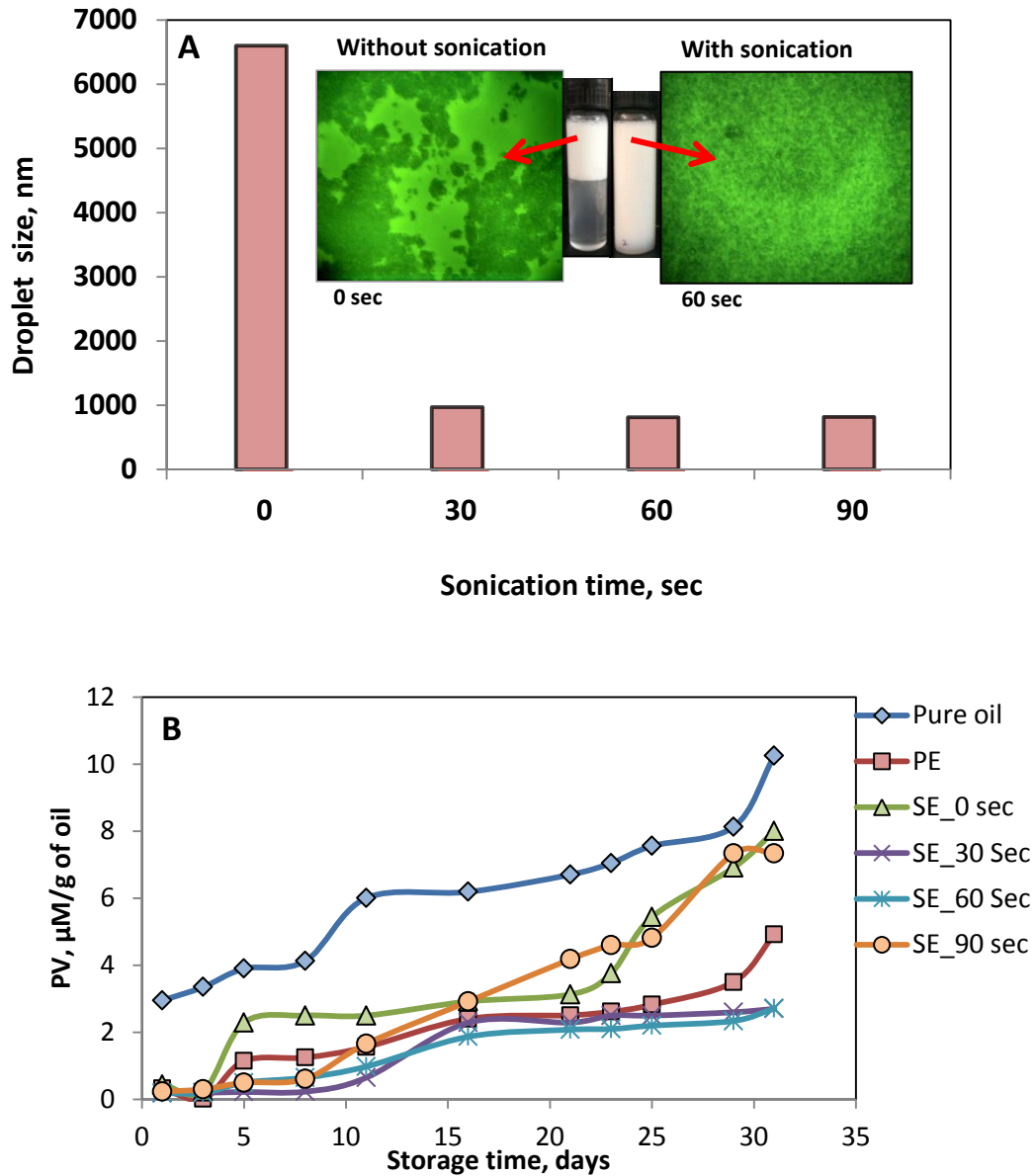
Fig. 4.6 Effect of sonication time on (A) physical stability, and (B) oxidative stability of secondary emulsions (4.93 wt% oil, 0.443 wt% WPI, 0.2 wt% SA, pH 5)

Apart from the physical stability, oil/lipids are susceptible to oxidation. The lipid oxidation occurs due to the residual or generated peroxides or radicals in the emulsion. It has been established that acoustic cavitation through ultrasound can generate highly reactive free radicals under extreme conditions of cavity collapse which are capable of oxidizing fatty acids present in oil [25,26]. Therefore, we examined the effect of ultrasonication on the

oxidative stability of emulsions. For this purpose, the peroxide value (PV) which is a direct measurement of concentration of primary oxidation products (lipid hydroperoxide) in emulsions was determined.

It can be observed from Fig. 4.6(B), that PV of pure oil was appreciably higher than that obtained for the oil droplets in the emulsions generated (PE and SE). This indicates that the biopolymers which encapsulate the oil act as a shield and thus prevent the attack of peroxides on the oil molecules. In PE, the PV obtained was lower during the first few days of storage but it moderately increased after 25 days. Moreover, the PV of PE was comparably higher than that of SE prepared in 30 and 60 sec of sonication. In case of SE, the PV of non sonicated SE (at 0 sec) was significantly higher than the sonicated samples. The PV obtained for non sonicated SE was increased from 0.23 to 6.28 µM CHP/g of oil during the storage time of 30 days. However, the PV of SE prepared at 30 and 60 sec of sonication time was found to be 2.4 and 2.7 µM CHP/g of oil respectively which was lower than that obtained for pure oil, PE and non sonicated emulsion. This indicates that the inherent antioxidant activity provided by the stable bilayer system inhibits the attack of peroxides and improved the oxidative stability of the emulsion. However, at higher sonication time of 90 sec, PV of SE was increased after 15 days. This can be attributed that on increasing the sonication time, free radicals may get generated which caused faster oxidation of lipid or oil molecules. Thus it can be concluded that based upon the droplet size and PV measurements, the sonication time of 60 sec was found to be optimum for the preparation of SE.

4.3.3   Comparison of layer by layer (LbL) and mixed approach

Apart from LbL method, mixed approach is an alternative way to prepare the multilayer emulsions. In the present study, the characteristics of emulsions obtained with LbL approach were compared with that prepared by mixed approach at the same optimized operating conditions (0.443 wt % WPI, 4.93 wt% oil and 0.2 wt% SA and pH 5). In mixed approach, WPI and SA aqueous solutions were mixed together until a clear solution was obtained, which was kept overnight for complete solubilization. The pH of the mixture was set to pH 5 and then olive oil was added to it and further subjected the solution for sonication.

The results obtained are shown in Fig. 4.7. It was observed that the droplet size obtained using mixed approach was relatively higher i.e. 2231 nm in 5 min sonication as compared to

that obtained using LbL approach (836 nm) in 60 sec as shown in Fig. 4.7(A). It may be due to the highly viscous nature of SA that decelerated the homogenization process during emulsification because high viscosity of polysaccharide can reduce the cavitation intensity [12]. It can be seen from the microscopic images (Fig. 4.7(B)) that the clusters of unadsorbed biopolymers and oil droplets were formed. Due to these larger flocs, acoustic energy was not effectively transmitted through the emulsion mixture and therefore produced emulsion of poor characteristics. Moreover, it was observed that on increasing the sonication time from 5 to 15 min for mixed emulsions, the droplet size increased to 4508 nm.
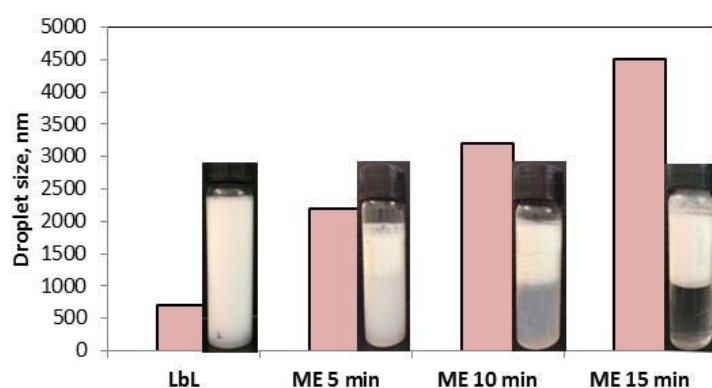
(A)
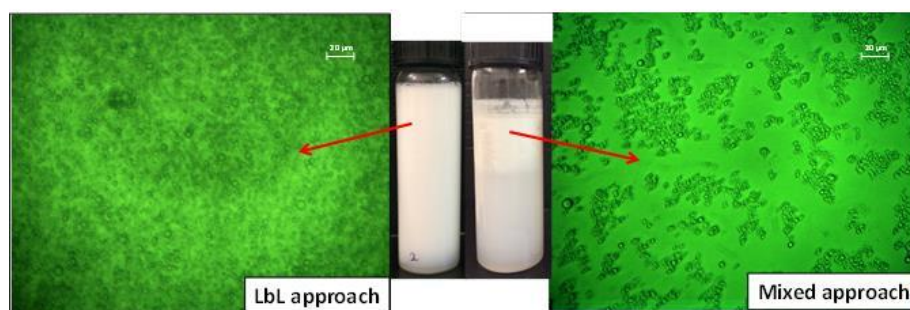
(B)

`

Fig. 4.7 Comparison of LbL vs. mixed emulsion approach based on (A) droplet size, creaming stability at different sonication time and (B) microstructure analysis (4.93 wt% oil, 0.443 wt% WPI, 0.2 wt% SA, 50 X magnifications)

In addition to that on increasing the sonication time, the extent of phase separation was also increased. As shown in Fig. 4.7(A), at 5 min sonication, a cloudy serum phase was obtained but at higher sonication time i.e. at 10 and 15 min, transparent serum phase was obtained. This indicated that the degree of droplet aggregation was higher at higher sonication time as shown in the microscopic images in Fig. 4.7(B). In LbL technique ultrasonication was given in two stages; firstly, PE was prepared by sonicating a mixture of olive oil and WPI aqueous solution for 15 min. This caused the uniform dispersion of oil droplets within the aqueous solution with adsorption of WPI at the interface. While, during the preparation of SE at pH 5, a higher electrostatic repulsion force and mild sonication for 60 sec leads to the perfect adsorption of SA on the WPI coated droplets. The LbL approach produced stable emulsion of smaller droplet size and without any flocculation.

4.3.4 Formation of PE and SE using recirculating flow configuration

Most of the studies related to the preparation of mono and multilayer emulsions using ultrasonication were carried out in batch processes on a laboratory scale. Because of the low processing capacity with high energy consumption, the use of ultrasonication on an industrial scale has not been adopted. Therefore, with an aim of processing larger volume with minimal energy consumption, PE and SE were prepared using recirculating flow configuration (RFC) at the optimum process conditions obtained from batch studies. Experiments were carried out at different flow rates with different number of passes in order to form stable emulsions of similar characteristics. Moreover, the energy efficacy of the RFC technique in comparison with the batch ultrasonication process was evaluated in order to develop the scale up aspects.

4.3.4.1 Effect of residence time/flow rate

The ultrasonication cell was operated with flow in the recirculating mode for a processing volume of 1500 mL at the optimized parameters from the batch studies. Experiments were carried out at different flow rates such as 0.5, 1 and 1.5 L/min with number of recirculation passes varying from 0 to 60 passes. The flow rate indicates the residence time of emulsion mixture in the sonication cell which can be calculated as:

Residence time (sec) = (Volume of sonication cell, ml) / Operating flow rate (ml/min)

The results obtained are shown in Fig. 4.8(A) & (B).

Primary emulsion: From Fig. 4.8(A), it was observed that for the same number of recirculation passes (30), minimum droplet size of around 421 nm was obtained at 0.5 L/min whereas droplet sizes of 934 nm and 1500 nm were obtained at 1 and 1.5 L/min respectively at pH 7. Since the residence time of PE was higher at lower flow rate which allowed the mixture to be exposed for a longer time in the ultrasonic irradiation zone, the droplet size obtained was lower [27]. At higher residence time (72 sec at 0.5 L/min), it was assumed that every fraction of emulsion was exposed to the cavitating conditions near the tip of horn. As a result of asymmetric cavity collapse and subsequent physical effects, WPI molecules and oil droplets were uniformly dispersed in the system which facilitated the effective adsorption of WPI on droplet surfaces. However at lower residence time (<72 sec) or higher flow rate, acoustic energy was not properly utilized due to insufficient exposure under ultrasonic zone resulting in increased droplet size.

Meanwhile, it was also observed from Fig. 4.8A that on increasing the number of passes, the droplet size was reduced up to a certain number of passes and thereafter remained constant. It can be seen from Fig. 4.8(A) that at 0.5 L/min, there was significant reduction in droplet size up to 20 passes whereas at 1 and 1.5 L/min, the droplet size was decreased up to 40 passes and further became constant.

Secondary emulsion: Prior to the formation of SE using RFC, pH of PE was set to 5 and then diluted with SA aqueous solution in 1:1 volume ratio followed by pH adjustment. The results obtained are shown in Fig. 4.8(B). Similar observation was also made during the preparation of SE using RFC. The SE prepared without sonication (0 passes) was found to be unstable. The droplet size obtained was around 6600 nm and the % CI obtained was 68% which indicated the formation of droplet aggregation. However, the stability of SE was improved on sonicating the mixture in the RFC. The droplet size was found to be lower at lower flow rate. The minimum droplet size was achieved at 0.5 L/min i.e. 812 nm as compared to that obtained at 1 and 1.5 L/min i.e. 1263 nm and 1517 nm respectively after 6 passes. The stability of SE prepared using RFC at different number of passes was also tested and it was found that no phase separation occurred during the storage time of 21 days as shown in Fig. 4.9. Thus it was concluded that SE prepared using RFC was kinetically stable for a period of 21 days.
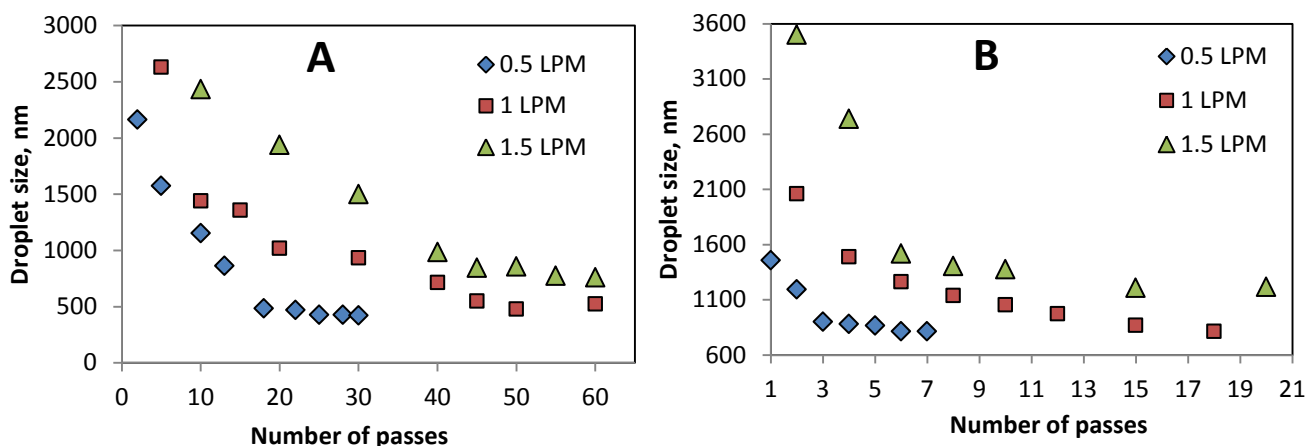
Fig. 4.8 Effect of flow rate and recirculation passes on droplet size of (A) PE (10 wt% oil, 0.9 wt% WPI, pH 7) and (B) SE (4.93 wt% oil, 0.443 wt% WPI, 0.2 wt% SA, pH 5)

The PV of SE formed using RFC was also determined as a function of storage time. As shown in Fig. 4.10, it was observed that the PV of SE was found to be lower using RFC during 20 days of storage as compared to that obtained in batch study. As discussed earlier, in the batch process, the acoustic energy was mostly dissipated to a fixed fraction of emulsion mixture rather than the entire volume. Thus it could be possible that because of continuous sonication to a fixed amount of emulsion mixture, the surfactants bilayer over the droplet could be disrupted and as a result the droplets become more susceptible to the attack of radicals produced during sonication. However in case of RFC, due to uniform distribution of the acoustic energy in the entire volume, the bilayer coated droplets were stable for a longer duration and hence less amenable to the attack of peroxides or radicals. Hence, SE prepared using RFC was stable against physical separation and oxidation than that obtained using batch process.

135

After
7 days

H_T

H_S

After
21 days

0   1   2   3   4   5   6   7

Number of recirculation passes
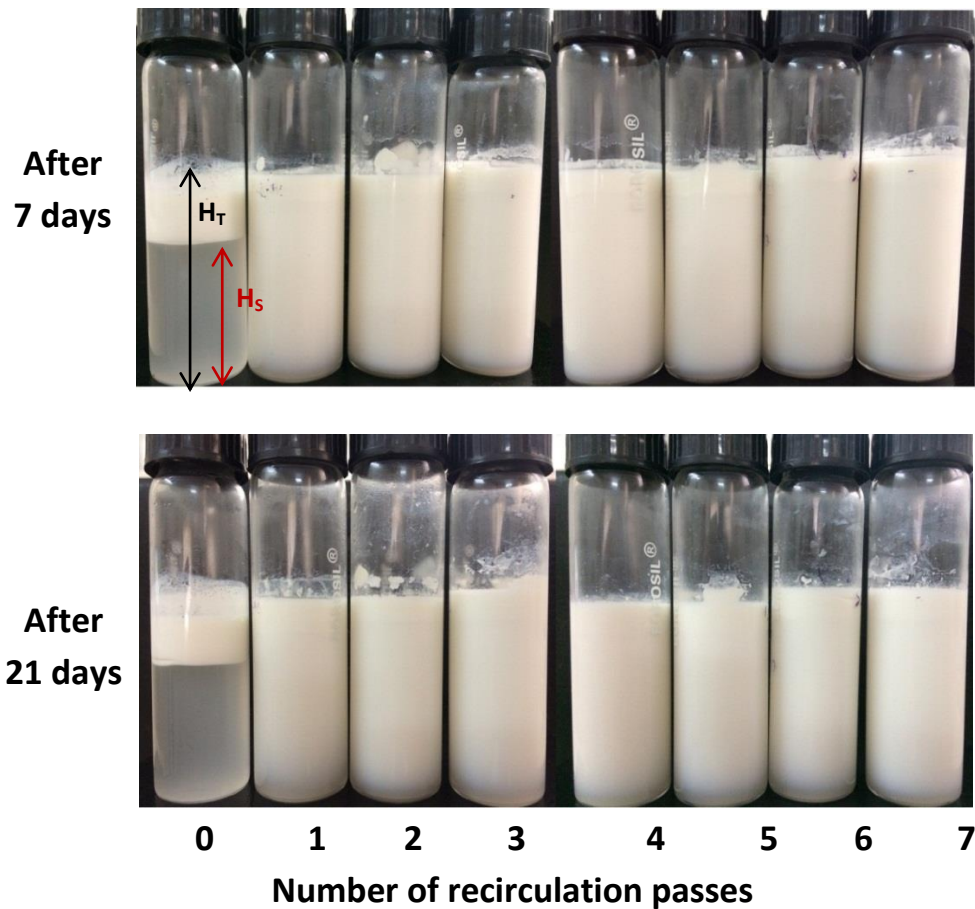
Fig. 4.9 Creaming stability of SE prepared using RFC at different number of passes

(4.93 wt% oil, 0.443 wt% WPI, 0.2 wt% SA, pH 5, 0.5 LPM)
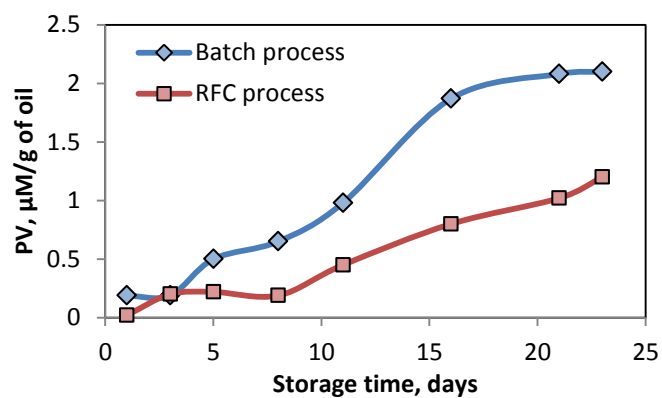
Fig. 4.10 Evaluation of peroxide value (PV) of SE prepared using batch and RFC process

(4.93 wt% oil, 0.443 wt% WPI, 0.2 wt% SA, pH 5, 60 sec sonication for batch and 0.5 LPM

after 6 passes in RFC mode)

4.3.5 Energy efficiency of batch and RFC process

The energy efficiency of both the processes was calculated based on (1) the total energy delivered to the system, and (2) calorimetric energy dissipated to the system. The basis of the energy calculations was the amount of energy required to process a unit volume of emulsion in order to achieve the required droplet size (J/ml.nm) of SE. In the batch study, the minimum droplet size of SE was 836 nm obtained in 60 sec of sonication time whereas in case of RFC, the droplet size of 812 nm was achieved after 6 recirculation passes at 0.5 L/min. Thus these operating conditions were considered for the energy calculations for obtaining SE (Calculations are shown in Appendix A). It was observed that in RFC, the energy required to process a unit volume of emulsion in order to achieve the required droplet size (J/ml.nm) of SE was found to be low as compared to batch ultrasonication process. Based on the total energy delivered to the system, RFC was found to be 2.5 times more energy efficient whereas based on the calorimetric energy dissipation, RFC was found to be 1.4 times efficient than the batch mode of ultrasonication process. Thus, it is recommended to use RFC rather than the batch process for preparation of multilayer food O/W emulsions.

In the batch mode of operation, the maximum reduction in the droplet size of PE was obtained within the initial 10 min and thereafter it remained almost constant. This indicated that maximum amount of acoustic energy was wasted in disrupting the smaller fraction of larger droplets left out after 10 min. However in RFC; the droplet size was reduced gradually over the entire processing time. Due to the recirculation process, biopolymers were uniformly dispersed into the mixture and the droplet size distribution was also improved. Therefore, operating the ultrasonication process in recirculating mode offers several advantages such as capability of processing large volumes, effective utilization of ultrasonic power, and the major advantage is its energy efficiency which is comparably higher than the batch process.

4.4 Summary

Ultrasonication process has been employed for the preparation of multilayer olive oil in water emulsion using batch and recirculating flow mode processes. Batch studies proved that the stability of multilayer emulsion was strongly dependent on the pH, SA concentration and ultrasonication. SE prepared at pH 5 and 0.2 wt % of SA was found to be more stable against bridging and depleting flocculation. At pH 5, the electrostatic interaction between biopolymers was strong enough for the formation of a stable bilayer system and thus overcoming bridging and depletion flocculation. The effect of sonication on the stability of SE was also evaluated. It was observed that the droplet size was reduced by 7 times and the extent of flocculation was diminished on sonicating the SE. The SEs prepared under various sonication time (60-90 sec) were found to be kinetically stable and no phase separation occurred during 21 days of storage. However SE emulsion prepared at highest sonication time (90 sec) was not stable against oxidation. Thus based upon the oxidative and physical stability of SE, the optimum sonication time was considered to be 60 sec.

Additionally, in order to maximize the processing volume capacity with minimal energy consumption; RFC based ultrasonication process was used. RFC process was found to be almost 2.5 times more energy efficient than the batch process and found to be a viable option to be used on an industrial scale due to its ability to process larger volume with lower energy consumption than the batch mode especially for the preparation of emulsions in food industry.

Appendix A

A.1 Energy efficiency based on total energy delivered to the system

A.1.1 Energy efficiency evaluation of batch ultrasonication process

(Power of horn: 750W, operating frequency: 20 kHz, processing time: 15 min, processing volume: 100 mL)

a) Electrical energy supplied for PE = Power of horn (J/s) x time of operation (s)

$$= 750 \text{ J/s x 15 min x 60 s } = 675000 \text{ J}$$

Energy density = Electrical energy supplied / processing volume

$$= 675000 \text{ (J)}/100 \text{ (mL)} = 6750 \text{ J/ml}$$

(b) Electrical energy supplied for SE

$$= 750 \text{ J/s x 60 s } = 45000 \text{ J}$$

Energy density = Electrical energy supplied / processing volume

$$= 45000 \text{ (J)}/100 \text{ (mL)} = 450 \text{ J/ml}$$

Therefore, Total energy supplied per unit volume,

$$= 6750+450 = 7200 \text{ J/mL}$$

Since the droplet size of SE obtained after 60 sec was 836 nm in batch study

Therefore, Energy utilization = Energy density / final droplet size achieved

$$= 7200 \text{ (J/mL)} / 836 \text{ (nm)} = \textbf{8.61 J/ (mL. nm)}$$

A.1.2 Energy efficiency evaluation of RFC process

(Power of horn: 750W, operating frequency: 20 kHz, power of pump: 20 W, processing time: 75 min, processing volume: 1500 mL)

(a) Electrical energy supplied for the PE= {Power of horn + power of pump} (J/s) x time of operation (s)

$$= (750 + 20) \text{ J/s x 75 min x 60 s } = 3465000 \text{ J}$$

Energy density = Electrical energy supplied / processing volume

$$= 3465000 \text{ (J)}/1500 \text{ (mL)} = 2310 \text{ J/mL}$$

(b) Electrical energy supplied for SE

$$= 770 \text{ J/s x 18 min x 60 s } = 831600 \text{ J}$$

Energy density = Electrical energy supplied / processing volume

$$= 831600 \text{ (J)}/1500 \text{ (mL)} = 554.4 \text{ J/ml}$$

Therefore, Total energy supplied per unit volume,

$$= 2310+554.4 = 2864.4 \text{ J/mL}$$

Since the droplet size of SE obtained after 6 passes (18 min) was 812 nm using RFC

Therefore, Energy utilization = Energy density / final droplet size achieved

$$= 2864.4 \text{ (J/mL)} / 812 \text{ (nm)} = \textbf{3.52 J/ (mL. nm)}$$

A.2 Energy efficiency based on calorimetric energy dissipated to the system

A.2.1 Batch ultrasonication process

(Power of horn: 750W, operating frequency: 20 kHz, processing time: 15 min, processing volume: 100 mL, Water density, $\rho = 0.9962$ g/mL, heat capacity of water, $C_P = 4.18$ kJ/kg-^{o}C))

a) Calorimetric energy dissipation after 15 min for PE

$$= (\rho.V).Cp\Delta T = (0.9962*100*4.18*(50-31)^oC = 7911.82 \text{ J}$$

Energy density = Energy dissipated / processing volume

$$= 7911.82 \text{ (J)}/100 \text{ (mL)} = 79.11 \text{ J/ml}$$

b) Calorimetric energy dissipation after 1 min for SE

$$= (\rho V)Cp\Delta T = (0.9962*100*4.18*(33-31) = 832.82 \text{ J}$$

Energy density = Enegy dissipated / processing volume

$$= 832.82 \text{ (J)}/100 \text{ (mL)} = 8.32 \text{ J/ml}$$

Therefore, Total energy dissipated per unit volume to form SE,

$$= 79.11+8.32 = 87.43 \text{ J/mL}$$

Since the droplet size of SE obtained after 60 sec was 836 nm in batch study

Therefore, the actual energy consumed to process a unit volume in order to achieve a unit size of emulsion.

Energy utilization = Energy density / final droplet size achieved

$$= 87.43 \text{ (J/mL)} / 836 \text{ (nm)} = \textbf{0.1045 J/ (mL. nm)}$$

A.2.2 RFC ultrasonication process

(Power of horn: 750W, operating frequency: 20 kHz, processing time: 75 min, processing volume: 1500 mL, Water density, $\rho = 0.9962$ g/mL, heat capacity of water, $C_P = 4.18$ kJ/kg-^{o}C)

a) Calorimetric energy dissipation after 75 min for PE

$$= (\rho V).Cp\Delta T \quad = (0.9962*1500*4.18*(40\text{-}31) = 56215.6 \text{ J}$$

Energy density = Enegy dissipated / processing volume

$$= 56215.6 \text{ (J)}/1500 \text{ (mL)} = 37.47 \text{ J/ml}$$

b) Calorimetric energy dissipation after 18 min for SE

$$= (\rho V)Cp\Delta T \quad =(0.9962*1500*4.18*(36\text{-}31) = 31230.9 \text{ J}$$

Energy density = Enegy dissipated / processing volume

$$= 31230.9 \text{ (J)}/1500 \text{ (mL)} = 20.82 \text{ J/ml}$$

Therefore, Total energy dissipated per unit volume to form SE,

$$= 37.47 +20.82 = 58.29 \text{ J/mL}$$

Since the droplet size of SE obtained after 6 passes (18 min) was 812 nm using RFC

Therefore, the actual energy consumed to process a unit volume in order to achieve a unit size of emulsion will be,

Energy utilization = Energy density / final droplet size achieved

$$= 58.29 \text{ (J/mL)} / 812 \text{ (nm)} = \textbf{0.0717 J/ (mL. nm)}$$

Therefore, based on actual energy consumption, RF process was 1.45 time energy efficient than batch process for the synthesis of multilayer emulsion.

References

[1]   D. Guzey, H.J. Kim, D.J. McClements, Factors influencing the production of o/w emulsions stabilized by β-lactoglobulin-pectin membranes, Food Hydrocolloids. 18 (2004) 967–975. doi:10.1016/j.foodhyd.2004.04.001.

[2]   D. Guzey, D.J. McClements, Formation, stability and properties of multilayer emulsions for application in the food industry, Advances in Colloid and Interface Science. 128–130 (2006) 227–248. doi:10.1016/j.cis.2006.11.021.

[3]   S.Y. Tang, S. Manickam, T.K. Wei, B. Nashiru, Formulation development and optimization of a novel Cremophore EL-based nanoemulsion using ultrasound cavitation, Ultrasonics Sonochemistry. 19 (2012) 330–345. doi:10.1016/j.ultsonch.2011.07.001.

[4]   M. Sivakumar, S.Y. Tang, K.W. Tan, Cavitation technology - A greener processing technique for the generation of pharmaceutical nanoemulsions, Ultrasonics Sonochemistry. 21 (2014) 2069–2083. doi:10.1016/j.ultsonch.2014.03.025.

[5]   I. Alzorqi, M.R. Ketabchi, S. Sudheer, S. Manickam, Optimization of ultrasound induced emulsification on the formulation of palm-olein based nanoemulsions for the incorporation of antioxidant β-D-glucan polysaccharides, Ultrasonics Sonochemistry. 31 (2016) 71–84. doi:10.1016/j.ultsonch.2015.12.004.

[6]   S.Y. Tang, M. Sivakumar, A.M.H. Ng, P. Shridharan, Anti-inflammatory and analgesic activity of novel oral aspirin-loaded nanoemulsion and nano multiple emulsion formulations generated using ultrasound cavitation, International Journal of Pharmaceutics. 430 (2012) 299–306. doi:10.1016/j.ijpharm.2012.03.055.

[7]   Y.S. Gu, E. a Decker, D.J. McClements, Influence of pH and iota-carrageenan concentration on physicochemical properties and stability of beta-lactoglobulin-stabilized oil-in-water emulsions., Journal of Agricultural and Food Chemistry. 52 (2004) 3626–3632. doi:10.1021/jf0352834.

[8]   C. Sun, S. Gunasekaran, Effects of protein concentration and oil-phase volume fraction on the stability and rheology of menhaden oil-in-water emulsions stabilized by whey protein isolate with xanthan gum, Food Hydrocolloids. 23 (2009) 165–174. doi:10.1016/j.foodhyd.2007.12.006.

[9]   A.R. Taherian, M. Britten, H. Sabik, P. Fustier, Ability of whey protein isolate and/or

fish gelatin to inhibit physical separation and lipid oxidation in fish oil-in-water beverage emulsion, Food Hydrocolloids. 25 (2011) 868–878. doi:10.1016/j.foodhyd.2010.08.007.

[10] S.A. Fioramonti, M.J. Martinez, A.M.R. Pilosof, A.C. Rubiolo, L.G. Santiago, Multilayer emulsions as a strategy for linseed oil microencapsulation: Effect of pH and alginate concentration, Food Hydrocolloids. 43 (2015) 8–17. doi:10.1016/j.foodhyd.2014.04.026.

[11] D.J. McClements, Food Emulsions Principles, Practices, and Techniques Second Edition, Food Emulsions Principles, Practices, and Techniques. (2005). doi:10.1093/acprof:oso/9780195383607.003.0002.

[12] F. Azarikia, S. Abbasi, Efficacy of whey protein-tragacanth on stabilization of oil-in-water emulsions: Comparison of mixed and layer by layer methods, Food Hydrocolloids. 59 (2016) 26–34. doi:10.1016/j.foodhyd.2015.11.030.

[13] R. Pongsawatmanit, T. Harnsilawat, D.J. McClements, Influence of alginate, pH and ultrasound treatment on palm oil-in-water emulsions stabilized by β-lactoglobulin, Colloids and Surfaces A: Physicochemical and Engineering Aspects. 287 (2006) 59–67. doi:10.1016/j.colsurfa.2006.03.022.

[14] S. Pallandre, E.A. Decker, D.J. McClements, Improvement of stability of oil-in-water emulsions containing caseinate-coated droplets by addition of sodium alginate, Journal of Food Science. 72 (2007). doi:10.1111/j.1750-3841.2007.00534.x.

[15] D. Guzey, D.J. McClements, Impact of Electrostatic Interactions on Formation and Stability of Emulsions Containing Oil Droplets Coated by b-Lactoglobulin-Pectin Complexes, Journal of Agricultural and Food Chemistry. 55 (2007) 475–485. doi:10.1021/jf062342f.

[16] J. Zhang, T.L. Peppard, G.A. Reineccius, Double-layered emulsions as beverage clouding agents, Flavour and Fragrance Journal. 30 (2015) 218–223. doi:10.1002/ffj.3231.

[17] A. Shanmugam, M. Ashokkumar, Ultrasonic preparation of stable flax seed oil emulsions in dairy systems - Physicochemical characterization, Food Hydrocolloids. 39 (2014) 151–162. doi:10.1016/j.foodhyd.2014.01.006.

[18] S. Abbas, K. Hayat, E. Karangwa, M. Bashari, X. Zhang, An Overview of

Ultrasound-Assisted Food-Grade Nanoemulsions, Food Engineering Reviews. 5 (2013) 139–157. doi:10.1007/s12393-013-9066-3.

[19] S.Y. Tang, P. Shridharan, M. Sivakumar, Impact of process parameters in the generation of novel aspirin nanoemulsions - Comparative studies between ultrasound cavitation and microfluidizer, Ultrasonics Sonochemistry. 20 (2013) 485–497. doi:10.1016/j.ultsonch.2012.04.005.

[20] L. Moreau, H.-J. Kim, E.A. Decker, D.J. McClements, Production and characterization of oil-in-water emulsions containing droplets stabilized by beta-lactoglobulin-pectin membranes., Journal of Agricultural and Food Chemistry. 51 (2003) 6612–6617. doi:10.1021/jf034332+.

[21] J. Carpenter, V.K. Saharan, Ultrasonic assisted formation and stability of mustard oil in water nanoemulsion: Effect of process parameters and their optimization, Ultrasonics Sonochemistry. 35 (2017) 422–430. doi:10.1016/j.ultsonch.2016.10.021.

[22] N.C. Shantha, E.A. Decker, Rapid, Sensitive, Iron-Based Spectrophotometric Methods for Determination of Peroxides Values of Food Lipids, Journal of AOAC International. 77 (1994) 421–424.

[23] F. Chen, L. Liang, Z. Zhang, Z. Deng, E.A. Decker, D.J. McClements, Inhibition of lipid oxidation in nanoemulsions and filled microgels fortified with omega-3 fatty acids using casein as a natural antioxidant, Food Hydrocolloids. 63 (2017) 240–248. doi:10.1016/j.foodhyd.2016.09.001.

[24] D.J. McClements, Protein-stabilized emulsions, Current Opinion in Colloid and Interface Science. 9 (2004) 305–313. doi:10.1016/j.cocis.2004.09.003.

[25] A.B. Pandit, J.B. Joshi, Hydrolysis of Fatty Oils: Effect of Cavitation, Chemical Engineering Science. 48 (1993) 3440–3442. doi:10.1016/0009-2509(93)80164-L.

[26] F. Chemat, I. Grondin, P. Costes, L. Moutoussamy, A.S.C. Sing, J. Smadja, High power ultrasound effects on lipid oxidation of refined sunflower oil, Ultrasonics Sonochemistry. 11 (2004) 281–285. doi:10.1016/j.ultsonch.2003.07.004.

[27] J. O'Sullivan, B. Murray, C. Flynn, I. Norton, Comparison of batch and continuous ultrasonic emulsification processes, Journal of Food Engineering. 167 (2015) 114–121. doi:10.1016/j.jfoodeng.2015.05.001.

CHAPTER 5

CURCUMIN ENCAPSULATION IN MULTILAYER O/W EMULSION: SYNTHESIS USING ULTRASONICATION AND STUDIES ON STABILITY, ANTIOXIDANT AND RELEASE ACTIVITY
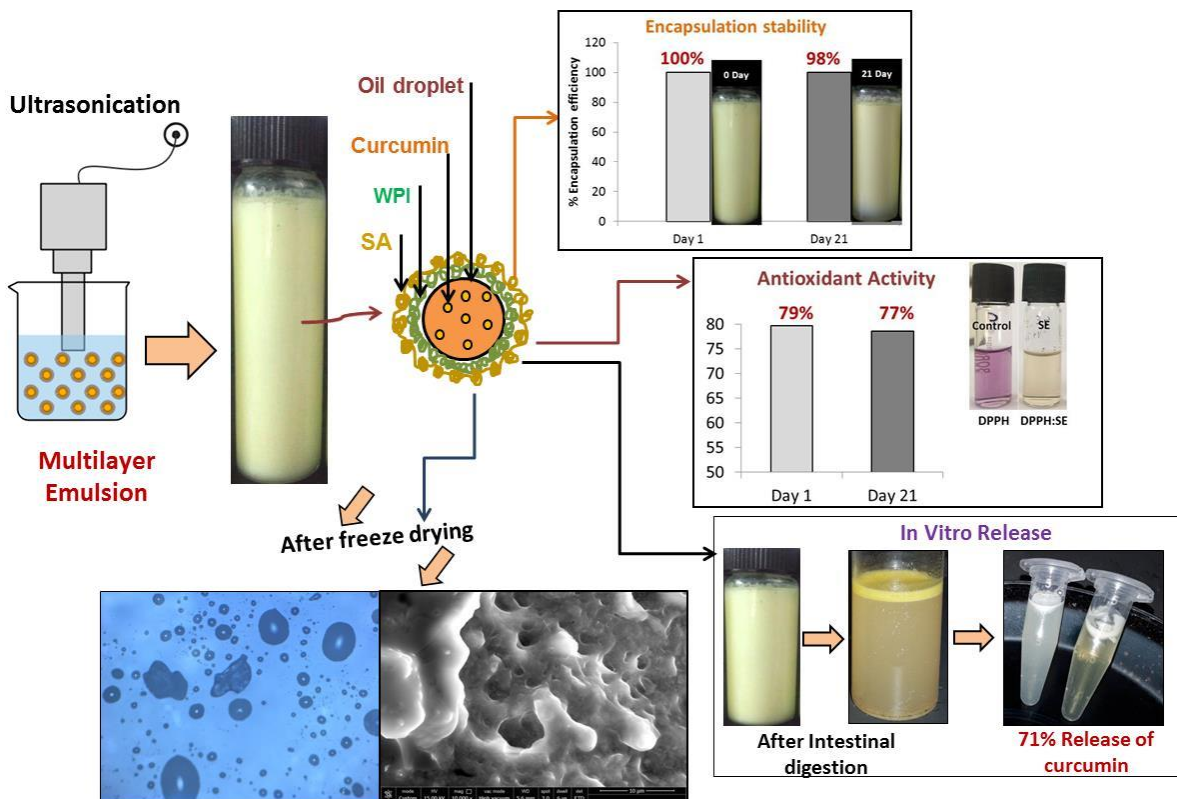
5.1 Introduction

Curcumin is a well-known nutraceutical polyphenol compound obtained from the turmeric plant and possesses various chemical and biological properties such as anticancer, antioxidant, anti-inflammatory, antibacterial and anticarcinogenic etc.[1,2]. Curcumin comprises various chemical reactive functional groups which are found to be effective against the cells of various diseases like cancer, arthritis, asthma, atherosclerosis, heart disease, etc.[3]. Recently, curcumin has gained significant interest among the researchers in the field of medicinal and pharmaceutical industries due to its health promising properties. However, there are challenges for its utilization in functional foods, medicines and other products because of poor water solubility, low bioavailability and chemical instability against physiological conditions such as pH [1,4,5]. In the last decade, lots of research works have been carried out to overcome these limitations using lipid based emulsification for encapsulating lipophilic compounds such as curcumin[6–9]. The encapsulation technique via O/W emulsification includes the incorporation of curcumin in the core (oil phase) of the emulsion matrix that improves the stability, functionality and facilitates their controlled release. Recently, the use of a novel emulsion matrix system prepared using layer by layer approach, known as multilayer emulsion for the encapsulation of lipophilic compounds has attracted researcher's interest to achieve this goal[10–14]. Multilayer emulsification is a potential strategy for the encapsulation of lipophilic compounds and this system has several advantages over other conventional nanoemulsions such as it enhances the physical and oxidative stability, provides protection against environmental conditions, promotes greater bioavailability and allows the controlled release in the GI tract of the body. In addition, the material and composition of the interfacial coating can be designed in such a way that the emulsion responds to specific triggers for the release of bioactive compounds [11,12].

Multilayer emulsions are formed using layer by layer approach which includes the deposition of alternative layers of oppositely charged biopolymers such as protein and polysaccharides over the oil droplets. The electrostatically charged layer of biopolymers forms a thick interfacial membrane at the oil-water interface that helps to inhibit the droplet coalescence and aggregation and thus enhances the physical stability of the emulsion. The multiple coating over the emulsion droplets also help to hinder the diffusion of various peroxides in the core (oil phase) of the emulsion and thus prevents the lipid oxidation. It has

146

been proved that the multilayer emulsions are found to be more stable for a longer storage time against the variation in the physico-chemical conditions such as solution pH, temperature, ionic strength, lipid auto-oxidation etc.[15–21]. Moreover, multilayer emulsions stabilized with food grade emulsifiers (mainly biopolymers) have advantages such as proper ingestion and consumption of constituents in the GI tract unlike the emulsions stabilized with synthetic surfactants and organic solvents which could adversely affect the biological conditions inside the human body. As per the author's knowledge, only few studies have been reported in the literature on the use of multilayer emulsion for the encapsulation of curcumin but most of these studies were mainly focused on evaluating the stability of curcumin loaded multilayer emulsions within the GI tract during the in vitro digestion process. In this regard, Silva et al.[22] reported the effect on the stability parameters of curcumin loaded single layer emulsion (SDS coated MCT droplet) and multilayer emulsion (SDS/chitosan/alginate/chitosan coated droplets) during the digestion under different GI systems such as stomach, duodenum, jejunum and ileum. Similarly in another study by Silva et al.[11], they have studied the formation of WPI/chitosan stabilized ME containing curcumin and reported the effect on stability parameters (particle size, zeta potential and morphology) during in vitro digestion in the same GI systems. Likewise, Pinheiro et al.[13] had carried out a similar work but prepared the multilayer emulsion with different wall materials i.e. lactoferrin/alginate layers. Despite the enormous potential of multilayer emulsion for the encapsulation of bioactives, there is still lack of information available in the literature on the kinetic stability of multilayer emulsion carrying curcumin and also on the physiochemical properties of curcumin encapsulated in emulsion during storage. Also, there is no major study reported in the literature which compares the performance of single layer and double layer emulsion for the encapsulation of bioactive compound like curcumin based on their encapsulation stability, antioxidant and release activity. It is only recently that Acevedo-Fani et al.[12] reported the effect of single, double and triple layer (lactoferrin/alginate/ε-poly-L-lysine) coating on the encapsulation stability and antioxidant activity of encapsulated resveratrol, a bioactive compound. It has been observed that the multiple layers of biopolymers formed over the oil droplets improved the antioxidant activity of resveratrol during the storage time of four weeks.

147

Therefore, based on the above aspects, the objective of this study was to evaluate the effect of single layer (whey protein isolate) and double layer (whey protein isolate/sodium alginate) coating on the stability, antioxidant activity, and release properties of curcumin under the intestinal conditions during a storage period of three weeks.

In the present work, ultrasonication has been employed for the preparation of multilayer emulsions containing curcumin in order to improve the stability of emulsions. It utilizes the immense power of cavity collapse to generate intense disruptive forces for dispersing the oil phase into the aqueous phase which helps to achieve a uniform size distribution with the minimum average droplet diameter[23–25][26][27]. In overall, this study provides detailed information on the formation of multilayer emulsion as a carrier system for the curcumin with an aim to enhance the stability and release of curcumin which could be used for various applications in the food and pharmaceutical industries.

5.2 Materials & Methods

5.2.1 Materials

Curcumin (95%) was received from M/s Aurea Biolabs Pvt. Ltd., Cochin, India. Cooking grade olive oil extra light (Sieaga, manufactured in Spain) containing 75% (w/w) unsaturated and 15% (w/w) saturated fats was obtained from market. Whey protein isolate (WPI, > 90% protein) was obtained from Bulk Amino, India. Sodium alginate (SA) was procured from Sigma Aldrich (India). The 1, 1-diphenyl-2-picrylhydrazyl (DPPH) radical (Molecular weight: 394.32 g/mol) and Pancreatin from porcine pancreas (Activity, 4 x JP i.e. 4 times higher than activities defined by Japanese Pharmacopoeia (JP)) were purchased from TCI Chemicals, India. Bile salt (Bile acids sodium salt, cholic acid Deoxycholic acid sodium salt mixture for bacteriology) containing minimum bile acid content of 45% was obtained from Lobachemie, India. Other chemicals and reagents used were of analytical grade. Deionized water (Ultrapure, Thermofisher) was used for the preparation of dispersions and emulsions. All the materials were used without any further purification.

5.2.2 Solubility and stability of curcumin in olive oil

The solubility of curcumin in olive oil was determined at room temperature. Prior to the preparation, different amounts of curcumin in the range of 2 to 6 mg was added in 20 mL of

olive oil and mixed in a vortex shaker to solubilize the curcumin. Afterwards, the mixture was heated to 80°C for 45 min in a water bath and sonicated for 10 min (750 W, 20% amplitude, 20 kHz frequency, Sonics USA) to dissolve the curcumin particles. The mixtures were then centrifuged at 3000 RPM for 5 min to remove any undissolved particles. The solubility of curcumin in oil was found to be 0.2 mg/mL equivalent to 0.022 % (w/w) of curcumin and it was found to be in agreement with the previously reported data [28].

The chemical stability of curcumin was also measured to ensure that there was no degradation of curcumin during heating and sonication as well as during storage. Curcumin degradation in the mixture was determined by measuring the change in absorbance at 428 nm (λ_{max}) over the storage time of 21 days using UV spectrophotometer [5]. It was observed that the absorbance of the curcumin oil mixture remained constant during the storage of 21 days. This also indicated that ultrasonication and heating didn't have any adverse effect on the curcumin oil mixture and therefore this preparation method was favorable for the effective solubilization of curcumin in oil. Similar observations have also been reported in the literature that the curcumin dissolved in various triglycerides remained chemically stable when subjected to heating and sonication[8,29]

5.2.3 Preparation of curcumin loaded multilayer emulsions (MEs)

After the preparation of the oil phase consisting of curcumin and olive oil, the multilayer emulsions were prepared in the same way (Fig. 5.1) as described in our previous work [20]. The curcumin loaded primary emulsion (PE) was prepared by mixing 10 g of oil phase containing 0.022 % (w/w) curcumin and 90 g of 1 % (w/w) WPI aqueous solution. The solution was sonicated for 15 min (40% Amplitude, 20 kHz, 750 W) in an ultrasonic processor while pH was maintained to 7. The emulsion vessel was placed in a cold water bath to avoid temperature rise and maintained at 30±2°C during the ultrasonication process. Prior to the preparation of secondary emulsion (SE), the pH of the PE was adjusted to 5 as the electrostatic interaction between PE and SE was found to be good at pH 5 as reported in our earlier work[20]. The SE was prepared by mixing PE with 0.4 % (w/w) SA aqueous solution in a ratio of 1:1 (by volume) and pH was adjusted to 5 with 0.1 N H_2SO_4. During the preparation of SE, ultrasonication was carried out for 60 seconds in order to disperse the SA molecules over the WPI coated droplets. The effect of sonication time on the

encapsulation efficiency of curcumin is also studied in both the emulsion by varying time in the range of 3 to 15 min for PE and 30 to 120 sec in the case of SE. The effects of pH, SA concentration and sonication time on the physical and chemical stability of PE and SE have been optimized and reported in our previous work[20]. These optimized conditions were used in the present study for the preparation of curcumin loaded emulsions. Thus in the present work, the PE and SE were prepared at pH 7 & 5 respectively.

The final composition of the constituents in PE are: 0.0022 % (w/w) curcumin, 9.99 % (w/w) oil, 0.9 % (w/w) WPI and composition of SE are: 0.00108 % (w/w) curcumin, 4.90 % (w/w) oil, 0.443 % (w/w) WPI, 0.2 % (w/w) SA, 0.0381 % (w/w) sodium azide, and the remaining was water. Sodium azide was added to the dispersions in order to prevent the microbial growth and all the prepared emulsions were stored at room temperature for further analysis.

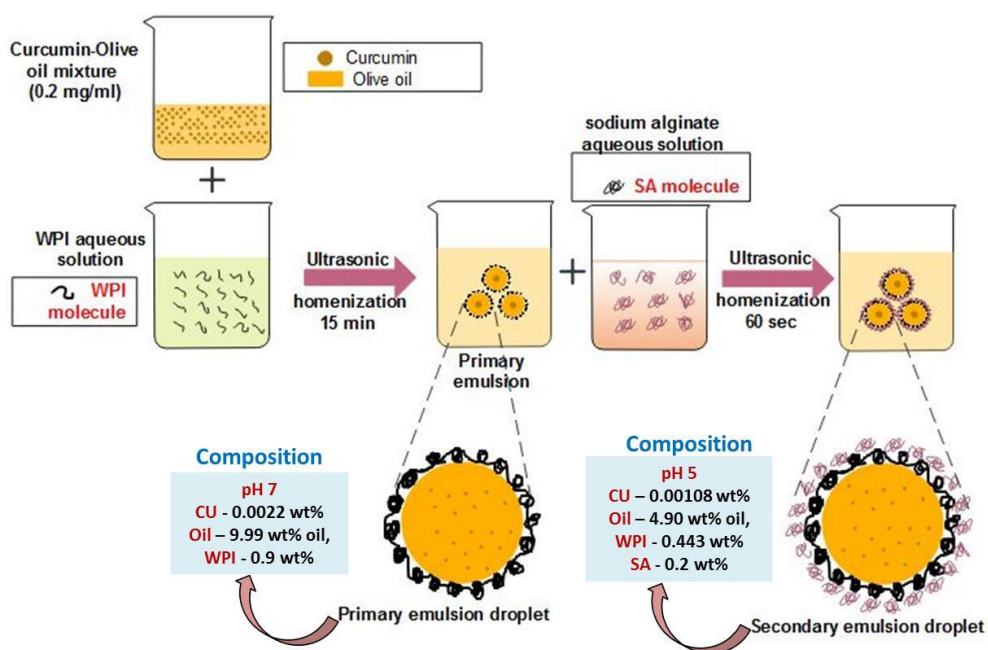Fig. 5.1 Experimental protocol for the preparation of curcumin loaded PE and SE

5.2.4 Droplet size and poly dispersity index (PDI) measurements

Droplet size and PDI values of the prepared emulsions were determined using Zetasizer Nano ZS (Malvern Instruments, UK) provided with dynamic light scattering and electrophoresis facility for the analysis. All the formulations were diluted 1000 times in

deionized water by keeping pH constant so as to prevent the multiple scattering effects during size analysis. Refractive indices of 1.45 for olive oil and 1.330 for water were used in the analysis. The Zetasizer gave the Z-average diameter of the droplets which is represented as droplet size (nm) in this study. Duplicate samples along with three measurements were considered for ensuring repeatability of the analysis.

5.2.5 Encapsulation efficiency

The encapsulation efficiency of curcumin in the multilayer emulsion was determined by analyzing the concentration of curcumin in the stable phase of emulsions by the UV Spectrophotometric method. 0.3 mL of emulsion (PE or SE) was mixed with 3.7 mL of ethanol and vortexed for one minute to promote the release of curcumin from the emulsion. The mixture was then centrifuged at 4000 RPM for 5 min. After centrifugation, the upper clear yellow phase containing curcumin was decanted and analyzed using UV spectrophotometer at 428 nm (λ_{max}). The concentration of curcumin in the emulsion was determined using a calibration curve which was prepared by mixing curcumin in the olive oil at different concentrations. The encapsulation efficiency (EE) of PE and SE was measured for different sonication time and also as a function of storage time for 21 days and it was determined using Eq.(1) as given below:

$$\% \, EE = \frac{Cu_e}{Cu_i} \, x \, 100 \qquad\qquad (5.1)$$

Where Cu_e is the concentration of curcumin in the stable phase of emulsions at specific condition and Cu_i is the initial concentration of curcumin added. Duplicate samples were prepared for ensuring the repeatability of analysis.

5.2.6 Freeze drying and morphological characterization of curcumin loaded emulsions

After preparation of stable emulsions under the optimized conditions based on the encapsulation efficiency and droplet size for different sonication time, the PE and SE were freeze dried in order to observe the effect of water vaporization on the stability of the multiple layer coated emulsion droplets. Prior to the morphological analysis, a small liquid layer of emulsion was placed on the glass petri plate such that the microstructures of the dispersed multilayer coated droplets are not disturbed during the freeze drying. The drying

was performed in a freeze drier (Operon) operated at -86°C for 48 h under vacuum of 1.33 mbar, which were performed in duplicate. The microscopic analysis of the freeze dried layers was carried out using optical microscopy (OM) and Scanning Electron Microscopy (SEM). In OM, the dried layer was placed on a microscopic slide and covered with a cover slip. The multiple images of dried emulsified layers were captured at 50X magnification and processed using the digital image processing software connected to the microscope (Leica Microsystems). The morphology was also analyzed using SEM technique with Energy Dispersive X-ray Detector (SEM) (Nova Nano SEM 450, EDX: X-flash 6TI30 Bruker). The freeze dried layers of PE and SE were sputter coated with gold and analyzed in a scanning electron microscope operated at an acceleration voltage of 15 kV. FTIR analysis were also performed for detecting the presence of all essential constituents (i.e. curcumin, protein, alginate, fatty acids of oil) of the freeze dried emulsion by evaluating the chemical bonds in the range of 400–4000 cm^{-1} wavenumbers. The FTIR spectra were recorded in a Perkin Elmer spectrophotometer.

5.2.7 Antioxidant activity of curcumin loaded emulsions

The antioxidant activity of curcumin encapsulated in PE and SE was measured by evaluating its scavenging activity against the DPPH radical using the method reported in literature [12] along with some modifications. The encapsulated curcumin was allowed to release from the stable phase of emulsions by mixing emulsions with ethanol. The mixture was shaken well and centrifuged in order to promote the release of curcumin in the ethanol. Since the curcumin concentrations in oil (0.2 mg/ml), PE (0.02168 mg/mL) and SE (0.0108 mg/mL) were different. Therefore in order to compare the antioxidant property of all the encapsulated systems, they were mixed with ethanol in such a way that the curcumin concentration in the clear yellow phase (ethanolic solution) obtained after mixing and centrifugation (4000 RPM, 5 min) remained same. For this, 1 mL of PE was mixed with 5 ml ethanol and 2 mL of SE was mixed with 4 mL of ethanol for total volume of 6 mL. Similarly the sample of curcumin-oil (CU-Oil) and curcumin-ethanol (CU-Ethanol) mixtures were prepared separately in a similar manner for comparisons with emulsions. After mixing and centrifugation, an aliquot of 2 mL of curcumin extracted solution (upper clear yellow phase) was mixed with 1 mL of DPPH solution (0.1 mM) for making the total volume of 3 mL. The

control solution was prepared by mixing ethanol with DPPH solution (0.1 mM). All solutions were kept in dark at room temperature for 45 min allowing the reaction between antioxidant (curcumin) and free radicals to get completed. After incubation, the absorbance of all the samples was measured at 518 nm (λ_{max}) using UV Spectrophotometer. The free radical scavenging activity of curcumin was determined as given in Eq. (5.2).

$$\% \ Radical \ scavenging \ activity = \frac{Absorbance_{control} - Absorbance_{sample}}{Absorbance_{control}} \ x \ 100$$

.... (5.2)

5.2.8 In vitro release of curcumin

In vitro release study was performed by simulating the intestinal condition inside the human body for the release of curcumin. Simulated intestinal fluid (SIF) was prepared by dissolving the pancreatin enzyme (4 mg/mL) and bile salt (25 mg/mL) in a phosphate buffer saline (PBS) followed by adjusting pH to 7.5 [6]. The emulsions (PE and SE) were mixed with SIF in a volume ratio of 1:2 (v/v) and the pH was further adjusted to 7.5 using NaOH solution. The mixtures were then incubated for 4 h in an incubator (Remi Lab, India) at 37°C with continuous shaking at 100 RPM. At every interval of 1 h, samples were taken and heated to 80°C in a water bath for 15 min in order to ensure the deactivation of enzyme before analysis. The samples were further mixed with PBS containing 0.5% (v/v) Tween 80 in a volume ratio of 1:2 (v/v) and maintain the pH at 7.5. The final mixture (1.5 mL) was centrifuged at 4000 RPM for 5 min and the clear yellow phase solution containing released curcumin obtained at the bottom of the centrifuge tube was analyzed using HPLC. The HPLC method of analysis reported by Chen et al.[30] and Peng et al.[2] was adopted. The analysis of curcumin present in the phase obtained after centrifugation was performed using C18 column (150 mm × 4.6 mm, 5 μm particle size) in a HPLC with PDA detector (Shimadzu) at the wavelength of 425 nm. The mobile phase used for the analysis contained the mixture of 0.3% (v/v) glacial acetic acid solution and acetonitrile at a ratio of 45:55 (v/v) while the flow rate of the mobile phase was maintained at 1.0 mL/min throughout the analysis. The % curcumin released was determined using Eq. (5.3) as given below:

$$\% \, Release = \frac{Concentration \; of \; curcumin \; released \; at \; specific \; time}{Initial \; concentration \; of \; curcumin} \; x \; 100$$

......(5.3)

To analyze release kinetics and mechanism, the following mathematical models were fitted to the experimental data as given in Eq. (5.4 to 5.6) [31,32].

Zero-order model, $C_t = C_{to} + k_o t$ (5.4)

First-order model, $ln \, C_t = ln \, C_{Ao} - k_1 t$ (5.5)

Higuchi model, $C_t = k_H t^{\frac{1}{2}}$ (5.6)

Where, C_t is the amount of drug released at time t, and k_O, k_1, and k_H represent zero-order release constant, first-order release constant, and Higuchi constant., respectively. The values of rate constants were determined by fitting the release data into respective equations.

5.2.9 Statistical analysis

All the experiments were performed twice using freshly prepared samples and the results of each parameter were reported as averages and standard deviations (SD). The statistical analyses was also performed in Minitab 17 (Trial version) using one-way Analysis of Variance (ANOVA) and the mean values of different responses such as the encapsulation efficiency, antioxidant activity and % release of curcumin for both the PE and SE were compared using Tukey's comparison test to determine significant difference ($p<0.05$) among the mean values.

5.3 Results & Discussion

5.3.1 Droplet size and poly dispersity index (PDI) analysis

The droplet size of curcumin loaded PE and SE was measured to examine the droplet stability. The droplet size provides information on the mean hydrodynamic diameter of the biopolymer coated droplets which further decide the stability of single and double layer emulsions. The electrostatic interaction between these biopolymers which depends on the pH can be examined by measuring the zeta potential and is well studied in our previous work [20]. It has been observed that at pH 5, the net surface charge of SE droplets (-46 mV ± 7.2) was much higher than that of PE (-13 mV ± 4.6) which suggested the adsorption of SA onto

the WPI coated droplets[20]. Therefore the electrostatic interaction between the WPI and SA layers was found to be good at pH 5 and thus the SE were prepared at the optimum pH 5 for getting stable emulsions. The droplet size distribution of ultrasonically prepared PE and SE is shown in Fig. 5.2A. It was observed that the size of PE droplet containing curcumin was 359 ± 5.6 nm whereas in the case of SE droplet, it was increased to 841 ± 13.4 nm. An increase in the droplet size of SE can be attributed to the increased mean hydrodynamic size of the droplet due to the formation of a secondary layer of SA over the WPI coated oil droplet containing curcumin. The higher droplet size indicated that the anionic carboxylate group of SA was effectively adsorbed over the cationic amino group of protein molecules. The droplet size of PE and SE in the absence of curcumin was found to be 308 and 836 nm respectively as reported in our previous article [20]. The droplet size obtained for the curcumin loaded PE and SE was found to be almost similar to that obtained for PE and SE without the curcumin loading. This indicated that the emulsion droplet size was not affected by the encapsulation of curcumin. Though the droplet size of PE droplet was lower as compared to SE but the size distribution was found to be better in case of SE as shown in Fig. 5.2A. The PDI value of the PE and SE was found to be 0.62 ± 0.035 and 0.49 ± 0.049 respectively which indicated that the size distribution was wider in the case of PE. The lower PDI value obtained in the case of SE may be attributed to the strong electrostatic attraction between oppositely charged SA and WPI molecules which caused uniform size distribution. The microscopic images also revealed the similar observation as shown in Fig. 5.2B. It can be seen in the microscopic image of PE that some of the droplets are bigger in size and hence size distribution obtained was wider. However in the case of SE, droplets were of uniform size and hence the size distribution was narrow (Fig. 5.2A).
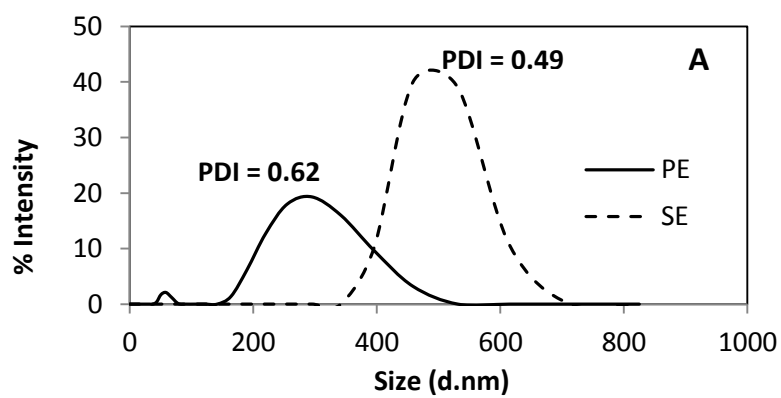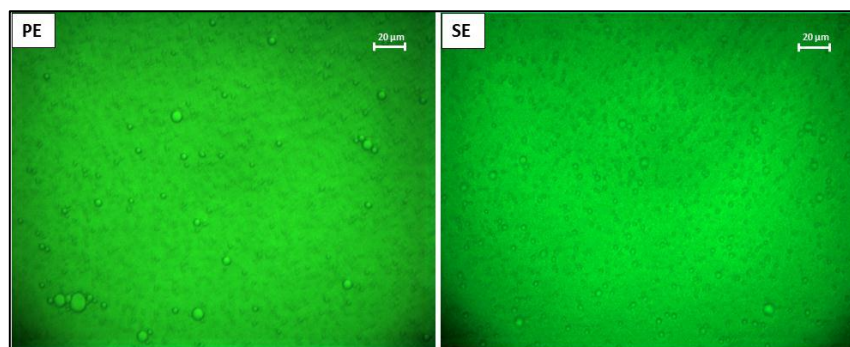
Fig. 5.2(A) Droplet size distribution, and (B) Optical microscopic images (50X magnifications, 20µm scale bar) of curcumin loaded PE and SE

5.3.2 Encapsulation efficiency of PE and SE

The encapsulation efficiency which is also an indication of the stability of curcumin in PE and SE was analyzed for the different sonication time as well as during the storage. As shown in Fig. 5.3(A-C), it has been observed that the encapsulation efficiency was found to be dependent on the sonication time. It can be seen from Fig. 5.3A that in the case of PE, the % EE was increased from 78 % to 100 % on increasing the sonication time from 3 to 15 min. An increase in the encapsulation efficiency can be attributed to the enhanced stability of emulsion at higher sonication time. Moreover, the statistical analysis conducted based on one-way ANOVA and Tukey comparisons test showed a significant difference ($p < 0.05$) in the encapsulation efficiency when carried out at different sonication time. The effect of increased sonication is the uniform dispersion of the protein molecules to facilitate their adsorption at the oil-water interface which subsequently increases the retention period of curcumin present in the emulsified droplets. As reported in our previous work [20], the PE was found to be unstable due to the separation of unemulsified oil from the emulsion which was measured as % separation index. The % separation index was found to be higher for lower sonication time and therefore the %EE obtained was correspondingly lower which can be attributed to the emulsion instability. Further, during the preparation of SE, it was necessary to homogenize the SE for the effective dispersion and adsorption of the SA molecules on the WPI coated droplets, carried out by ultrasonication. Fig. 5.3B presents the effect of sonication time on the %EE and it has been observed that the %EE of SE was found to be almost 100% for all the sonication time studied in the range of 30 to 120 sec. This can

be attributed to the double layer shield formed over the oil droplets containing curcumin as a result of electrostatic deposition of SA over WPI coated droplets. The double layer shield of biopolymers improved the emulsion stability as well as protected the curcumin against the variation in physico-chemical conditions.

It can be seen from Fig. 5.3A that sonication time has significant effect on the % EE in the case of PE. A higher sonication time of 15 min was required for the preparation of stable PE. However, during the preparation of SE, the main objective was only to disperse the SA molecules as the coating of SA over the WPI coated droplets is governed by strong electrostatic interaction between both the biopolymers and therefore only mild sonication for 30 sec was required to disperse the molecules. The %EE of SE prepared at different sonication time was further evaluated during the storage of 3 weeks and it was observed that the %EE of SE sonicated at 30 sec decreased to 86 % after 3 weeks, whereas beyond 30 sec, %EE remained higher and almost same (nearly 99%) for all the sonication time (60-120 sec). Thus it can be said that during the preparation of SE, the effect of sonication time is not significant and it is only required to disperse the molecules of SA more effectively in the solution.

The %EE of curcumin in PE and SE which was prepared at the optimized process conditions was also measured as a function of storage period and is presented in Fig. 5.3C. The statistical analysis conducted based on one-way ANOVA showed a significant effect ($p < 0.05$) on the encapsulation efficiency during the different storage time. It has been observed that the SE showed significantly higher encapsulation efficiency of curcumin than PE during the storage time of 21 days. Initially the %EE of SE was 100 %, and no significant change was observed during the storage of three weeks ($p < 0.05$). However, in the case of PE, the % EE significantly decreased to 56 $\pm$2.63 % from 100 $\pm$0.78 % after 21 days of storage. Further, the Tukey comparison test indicated a difference although not very significant (p-value = 0.058) between the mean values of % EE of PE and SE which confirmed that both the systems were different in terms of their stability behavior during the storage. In PE, a thick viscous layer was formed at the top of the emulsion as shown in Fig. 5.3D which was due to the inter droplet aggregation in the emulsion during the storage. The extent of aggregation increased during the storage period and hence the amount of curcumin encapsulated in the stable dispersed phase of emulsion decreased. The %EE was lower in the

case of PE after the storage time of 21 days, whereas in the case of SE, there was no formation of an aggregated layer during the storage period indicating the almost 100% encapsulation efficiency. Therefore, it can be concluded that SE possess higher stability than PE which makes it a suitable carrier for the encapsulation of curcumin.
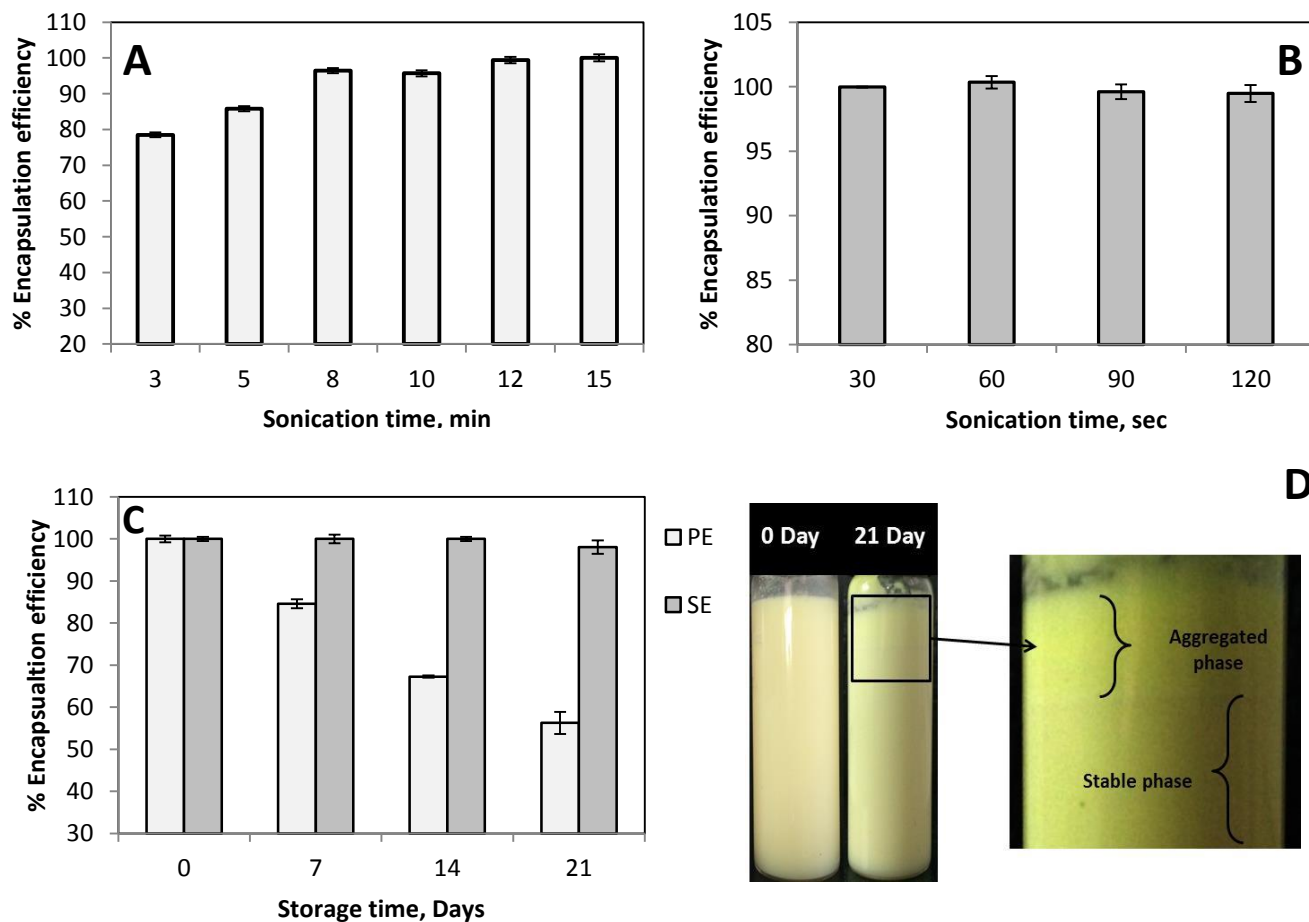

Fig. 5.3 Encapsulation efficiency of curcumin in (A) PE, (B) SE at different sonication time, (C) PE(15 min sonication, pH 7) and SE (60 sec sonication, pH 5) during the storage, and (D) Phase aggregation in PE after 21 days. (Means of both the systems were different from each other (p = 0.058))

5.3.3 Characterization of freeze dried curcumin loaded MEs

The O/W emulsion containing curcumin is formed using food grade ingredients that contain various functional constituents such as omega-3 polyunsaturated fatty acids and α-linolenic acid in olive oil, protein and carbohydrates in emulsifiers, and curcumin as an antioxidant. The O/W emulsion that contains encapsulated curcumin can easily be incorporated into various food products such as beverages, cereals, baked foods etc. in order to enrich them with multi-functional characteristics [5]. The incorporation of emulsion into food products can be done by converting the emulsion into powder and gel form[33]. Therefore in this work, the liquid emulsions were converted into the powder form by freeze drying and its morphology was evaluated. The emulsions were lyophilized using freeze drying technique in which the solution was first frozen at -86°C and the surrounding pressure was further reduced to allow the sublimation of frozen water from the mixture. The dried products were collected and characterized by FTIR and microscopic techniques.

5.3.3.1 FTIR Analysis

The FTIR analysis was carried out to determine the presence of the major components such as curcumin, olive oil, protein and sodium alginate in the emulsion powder. The results are shown in Fig. 5.4 and confirm the presence of all constituents in the freeze dried PE (FD-PE) and freeze dried SE (FD-SE) samples. In the FTIR spectra, the band observed at 3497.27 cm^{-1} represents the main characteristic peak of pure curcumin which corresponds to the phenolic O–H stretching of benzene ring [8]. However in the case of FD-PE and FD-SE, the peak of curcumin was shifted to 3478.6 and 3470.6 cm^{-1} respectively. The peak intensity of the phenolic group appeared to be low because of the overlapping effect by the amide group of WPI which was observed in the same range i.e. 3285-3286 cm^{-1}. The decrease in the wave number of peak indicates the strong interaction of curcumin with the WPI-SA coated droplets during the emulsification. The peaks observed at 3286.18 and 3285.76 cm^{-1} in the case of FD-SE and FD-PE respectively corresponds to the N–H stretching vibrations of amide group presents in the WPI. The bands obtained at 1643.79 and 1539.13 cm^{-1} in the case of PE corresponds to Amide-I and Amide-II respectively representing the polypeptide bond group present in the WPI. However in the case of FD-SE, the spectra of Amide-I and Amide-II were slightly shifted to 1634.60 and 1540 cm^{-1} respectively which could be due to

the interaction of WPI and SA molecules during the formation of SE. The band obtained at 1034.32 cm^{-1} in the case of FD-SE corresponds to the C–O–C stretching of ether group presents in the saccharide structure of sodium alginate (SA)[34]. Other major peaks obtained in the spectra of FD-PE and FD-SE at 2923 cm^{-1}, (C–H stretching (asymmetry)), 2854 cm^{-1} (C–H stretching (symmetry)), 1744 cm^{-1} (C=O stretching), 1454 cm^{-1} (C–H bending), 1151 cm^{-1} (C–O stretching), and 717 cm^{-1} (C–H bending) were similar in both the FD-PE and FD-SE samples as these peaks correspond to the functional groups of triglycerides present in the olive oil [35]. Thus, it can be concluded from the FTIR analysis that all the components were present in the freeze dried PE and SE, however the shifting of wavenumbers observed indicates the strong interaction between the emulsifier and curcumin loaded oil droplets. The FTIR analysis indicated that the curcumin was effectively loaded into the FD-PE and FD-SE.
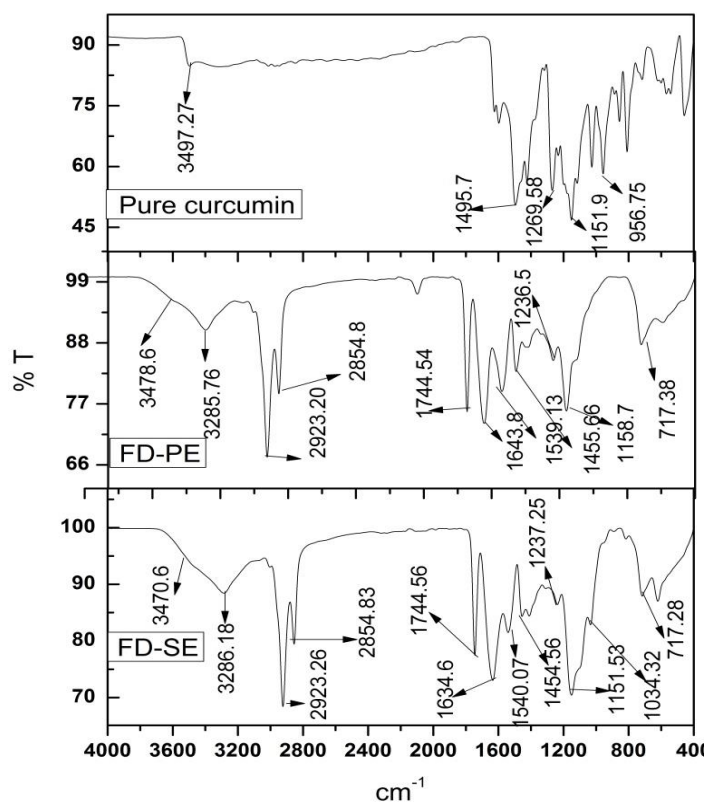

Fig. 5.4 FTIR analysis of pure curcumin, freeze dried PE and SE microparticles

160

5.3.3.2 Morphological analysis: Optical microscopy and SEM analysis

The morphological analysis of the FD-PE and FD-SE was performed using optical microscope and SEM. Before freeze drying, a thin layer of emulsion was spreaded carefully on a glass petri plate and then subjected to drying in order to observe the microstructure without any fissures or breakage of the multilayer coated droplets during vacuum drying. The microscopic images as shown in Fig. 5.5(A) clearly indicated that spherically shaped microparticles of PE and SE were obtained after drying. It can be seen that each microparticle comprises a tiny glowing hole indicating the presence of oil droplet and black shell formed over each hole indicates the adsorbed biopolymers. Moreover, it can also be seen that each microparticle consists a single hole and is uniformly dispersed into the system which clearly indicates that the emulsion droplets were stable against flocculation and agglomeration.

In the case of FD-PE, only few droplets were visible however more droplets of uniform size were observed in the FD-SE. This was attributed to the leakage of oil on the surface during the sublimation of ice crystals in the FD-PE [14,36]. However in the case of SE, due to the formation of a double layer system, the microstructure remained undisturbed and therefore the curcumin loaded oil droplets remained intact.

The SEM analysis was also performed in order to observe the surface topography of the FD-PE and FD-SE samples and is shown in Fig. 5.5(B). Both the samples showed the porous structure with widely distributed pores. The FD-PE microparticle showed regular surface whereas irregular surfaces adjoining the pores were observed in the case of FD-SE. It can be seen from Fig. 5.5(B) that pores are covered by a thick layer of emulsifiers in the case of SE. The irregular surface obtained in the case of FD-SE is attributed to the formation of composite of protein and polysaccharides due to the strong electrostatic interaction between them. The holes or cavities were formed due to the sublimation of ice crystals and a vacuum space surrounding the oil droplets was created as a result of water vaporization [14,36]. The formation of a double layer shield of biopolymers over the oil droplets caused a reduction in the leakage of oil from the emulsion droplets and thereby enhanced the encapsulation efficiency of SE. In overall, morphological results confirmed that spherically shaped SE droplets in a well dispersed stable form had enhanced encapsulation stability of curcumin than that of PE.
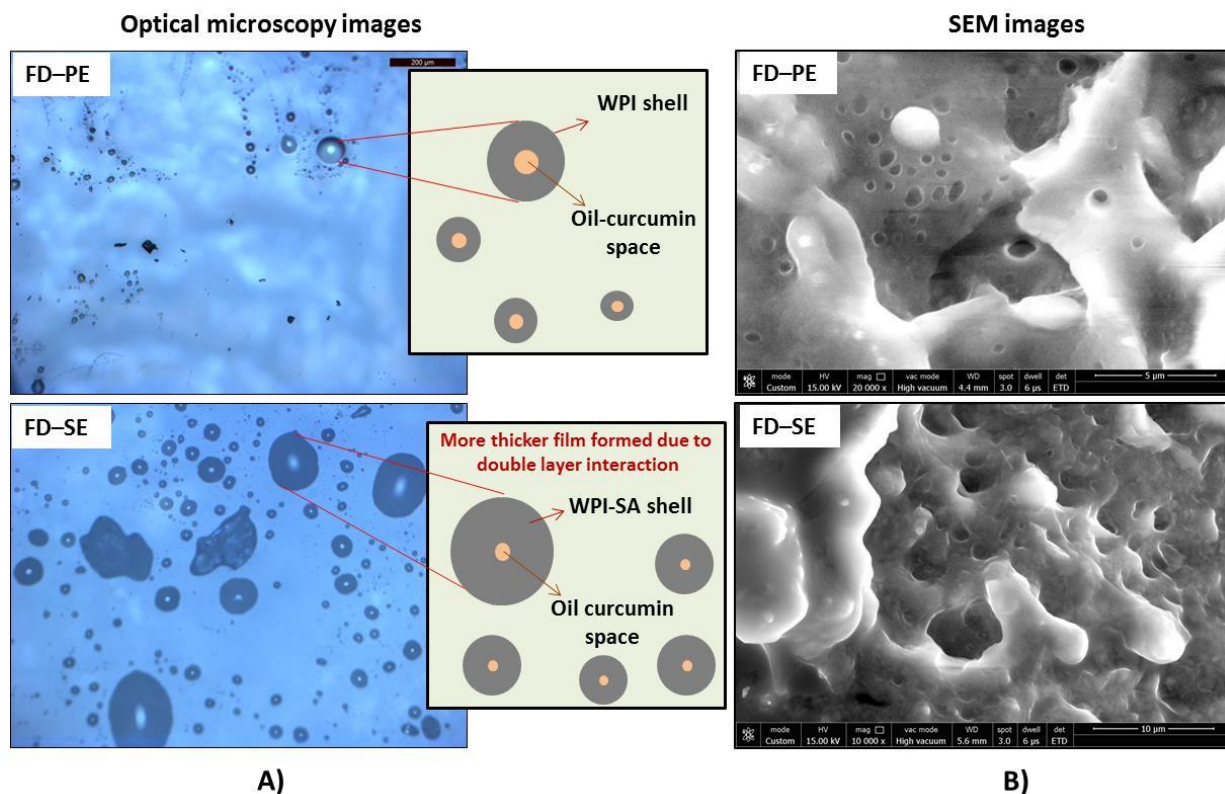
Fig. 5.5 Morphology of PE and SE microparticles using (A) optical microscope (*inside picture indicating the schematic representation of WPI-SA coated droplets encapsulating curcumin*) and (B) SEM technique

5.3.4 Free radical scavenging activity of curcumin encapsulated in MEs

The DPPH method is commonly used to evaluate the free radical scavenging activity of the antioxidant[37]. The DPPH is stable organic nitrogen radical and is mostly soluble in various solvents including water. It is purple in color and exhibits strong absorption at 517 nm, whereas in presence of antioxidant, it get reacted and its color disappears [38]. DPPH radical has the tendency to abstract the hydrogen atom from the antioxidant to become a stable diamagnetic molecule and subsequently the decolorization of the DPPH occurs which indicates the radical scavenging property of the antioxidant agent [37,38]. Therefore, antioxidant activity of curcumin can be evaluated by monitoring the decrease in the color intensity of DPPH using UV spectrophotometer. In the present work, the scavenging activity of the curcumin encapsulated in PE and SE was evaluated.

During the analysis, first, the antioxidant activity of the intact emulsion (PE and SE) was measured and both the emulsions showed significantly higher and similar scavenging activity (almost 75%). However, it was difficult to differentiate which component (either biopolymers or curcumin) was actually contributing in scavenging the DPPH radicals and therefore the antioxidant activity of the released curcumin was measured after separating it from the emulsion.

It can be observed from Fig. 5.6A that in case of curcumin loaded SE, the absorbance of the solution at the wavelength of 518 nm was reduced significantly, which is due to the reaction of DPPH with curcumin causing a reduction in the color. This also indicated that SE was capable to retain/encapsulate the curcumin to a greater extent than PE. In case of CU-Oil and CU-Ethanol, the curcumin got deteriorated under the surrounding environmental conditions and therefore as less amount of curcumin was available to react with DPPH, the absorbance was not reduced to the extent compared to the reduction achieved by CU-SE. The DPPH scavenging activity was also measured as a function of storage time for the samples and the results are shown in Fig. 5.6B. The statistical analysis conducted based on one-way ANOVA and Tukey comparisons test showed a significant difference ($p < 0.05$) in the scavenging activity during the different storage time for all the encapsulating systems. In case of curcumin oil (CU-Oil), it showed significantly ($p<0.05$) higher % scavenging activity than all other systems except SE but it gradually reduced during storage. The higher % scavenging activity in CU-Oil can be attributed to the additional antioxidant property of olive oil and its ingredients (vitamin E, carotenes, squalene, and phytosterols etc.) which may have contributed to the overall scavenging activity [39]. The initial concentration of olive oil in CU-Oil was also higher than all the other systems which also might be the reason for the difference in the antioxidant activity. Similarly in CU-Ethanol mixture, a significant reduction in the scavenging activity of curcumin was observed during the storage. The scavenging activity of CU-Ethanol and CU-Oil mixture decreased from 40 ±1.2% to 29 ±1.63% and 54 ±0.68% to 49 ±4.88% respectively after 21 days of storage. This indicated that the antioxidant activity of curcumin reduced during the storage which can be attributed to the chemical instability of curcumin under the environmental conditions. Some studies reported on the chemical instability of curcumin against the variation in pH and temperature. Moreover, the curcumin encapsulated in PE (CU-PE) showed lowest scavenging activity

which further decreased during the storage period. The maximum scavenging activity of curcumin in CU-PE was observed at 38 ±1.70% which decreased to 23 ±2.44% after 21 days of storage. The decrease in scavenging activity can be attributed to the decreased encapsulation efficiency of curcumin in PE. However specifically in case of PE (Fig. 5.6B), a significant reduction in the scavenging activity was observed after 7 days which was due to the decrease in its %EE as observed in Fig. 5.3C. Due to the poor encapsulation efficiency of PE, the amount of curcumin available in stable PE for the reaction with DPPH molecules was less and hence its scavenging activity was lower. However, the curcumin encapsulated in SE showed 79±0.34% scavenging activity which was higher than other encapsulated systems (PE, oil and ethanol). Also, no significant reduction in the scavenging activity of the curcumin was observed during the storage time of 21 days which may be attributed to the enhanced encapsulation efficiency of SE. Based on the Tukey comparison test, the scavenging activity of SE is significantly higher ($p < 0.05$) than all other encapsulating systems which confirm that the SE system is statistically different based on their means comparison. Hence, it can be stated that the presence of a double layer shield over the oil droplet containing curcumin helped in maintaining the antioxidant property of curcumin during the storage. Moreover, the biopolymers used to create the encapsulated systems may also act as an antioxidant agent and could contribute to the overall scavenging activity against the DPPH. Previous studies reported that polypeptides and polysaccharides exhibit certain antioxidant activity [12]. The results obtained in the present work are found to be in agreement with previous report[12]. Therefore it can be concluded that incorporation of secondary emulsifier not only enhanced the encapsulation efficiency but also helped to maintain the antioxidant properties of curcumin.
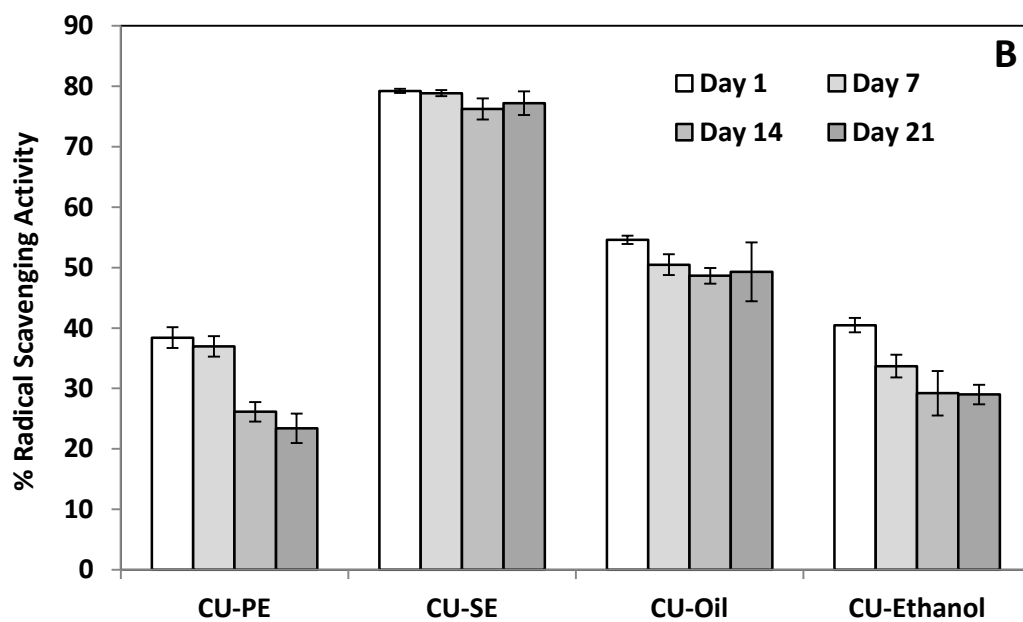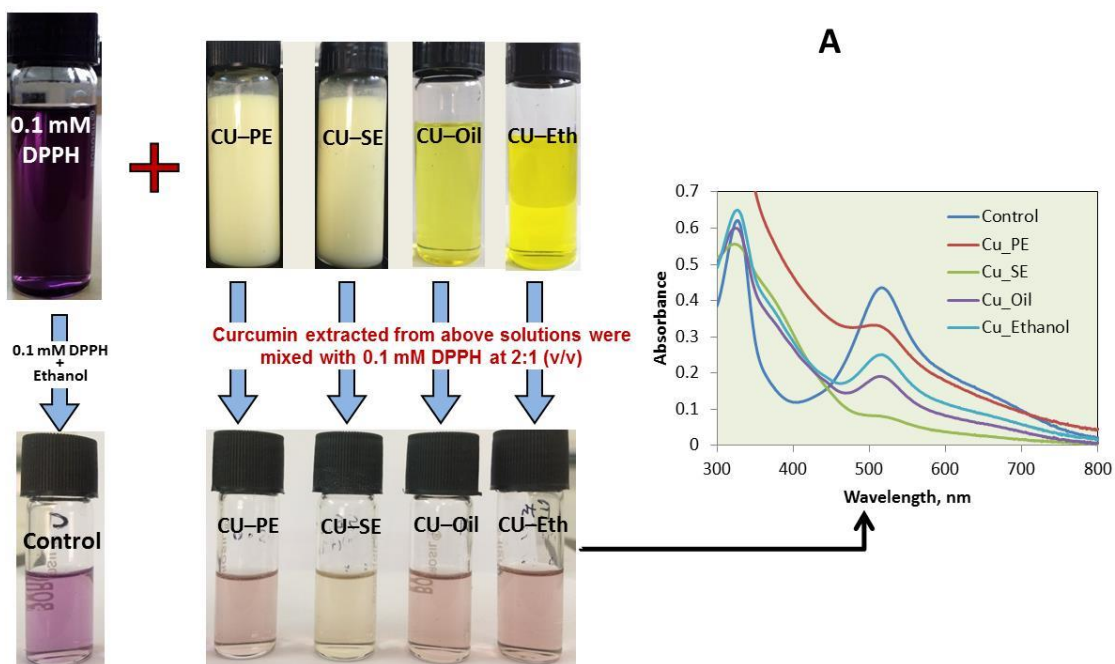
Fig. 5.6 Radical scavenging activity of curcumin encapsulated in emulsions, oil & ethanol solution (A) UV/vis spectra of all the solutions (B) Scavenging activity during the storage. (Means of all the systems were significantly different from each other ($p < 0.05$))

5.3.5 In vitro release of curcumin

After achieving the successful encapsulation of curcumin in PE and SE, a simulated intestinal system was created to perform the in-vitro release of curcumin into the intestinal tract of the body. Under the simulated intestinal conditions, the lipid and emulsifier gets digested and curcumin is released. To measure the quantity of released curcumin after digestion process, the SS method (Sample and separate) was employed in which the release of curcumin was assessed using centrifugation method [40]. This method provides a direct approach to monitor the drug release [40].

The release of curcumin was studied by initially digesting the curcumin loaded emulsion followed by dilution in phosphate buffer saline (pH 7.5) containing 0.5% (v/v) Tween 80 and further by mixing and centrifugation. Addition of Tween 80 promotes the release of curcumin from the digested solution. It can be clearly seen in Fig. 5.7A (sample b & b') that after centrifugation, a clear yellow phase containing curcumin was obtained at the bottom whereas the undigested constituents (lipid and emulsifier) formed a layer at the top. In order to further ensure the digestion of constituents, the entire procedure was carried out in the absence of pancreatin enzyme and bile salt. The turbid nature of the solution as observed in Fig. 5.7A (sample a & a') indicated that curcumin was not released from the emulsion mixture after centrifugation in the absence of pancreatin enzyme and bile salt. The curcumin released into the clear yellow phase obtained after centrifugation was analyzed using HPLC and % release of curcumin at various incubation periods is shown in Fig. 5.7B. Moreover, the in vitro digestion was also performed in the gastric conditions and it was observed that the emulsions remained stable under the gastric digestion process and thereby not allowing the curcumin to release from the emulsified droplets. Hence no release of curcumin was observed, which might be due to the high resistance of protein molecular chain against pepsin (gastric enzyme) under the gastric conditions. Therefore, it has been assumed that the emulsion system was stable before the intestinal digestion and therefore in-vitro release was further studied under the simulated intestinal conditions.

Statistical analysis conducted based on one-way ANOVA and Tukey comparisons test showed a significant difference ($p < 0.05$) in the % release of curcumin at different incubation time during in vitro digestion of PE and SE. The maximum release of almost 63 ±2.56% and 71 ±2.39% was attained after 2 h in PE and SE, respectively and thereafter it

remained constant. However, almost 90% of the total curcumin release was observed in the first 1 hour only. Both the emulsions showed significant release of curcumin after the in vitro digestion however the % release of curcumin in SE was significantly higher (p = 0.009) than the PE. The higher % release in the case of SE can be attributed to the lower initial concentration of oil phase present in the SE which rapidly digested under the similar intestinal condition. Under the intestinal conditions, the bile salt and pancreatin enzyme degrade the emulsion constituents and releases the encapsulated curcumin. The breakdown initiated by the lipolytic activity of pancreatin is activated in the presence of bile salt. The bile salt which acts as a surface active agent, preferentially get adsorbed at the biopolymer coated droplets or it may also displace the protein and polysaccharides from the interface thereby allowing the lipase present in the pancreatin to enter inside the lipid molecules [6,13]. This promotes the binding of the enzyme with the oil droplets which thereby accelerated the hydrolysis of lipid into monoglycerides and free fatty acids. Apart from the lipolysis, the simultaneous proteolysis of the adsorbed protein and polysaccharides resulted in the breakdown of the emulsions and caused the release of curcumin from the core of the lipid phase.

Similar observation has been reported by Sari et al.[6], that the majority of curcumin i.e. 72% was released within 2 h under in vitro intestinal digestion conditions. It has also been reported that the protein stabilized emulsion was found to be stable under the gastric digestion process and the release of curcumin was inhibited due to the high resistance of β-lactoglobulin (protein) against pepsin (gastric enzyme) digestion. However, they observed that pancreatin enzyme in presence of bile salt promoted the lipolysis and proteolysis which caused the destabilization of emulsion and release of curcumin. Other authors also reported that the maximum release of curcumin was in the intestinal tract of the body [9,41].
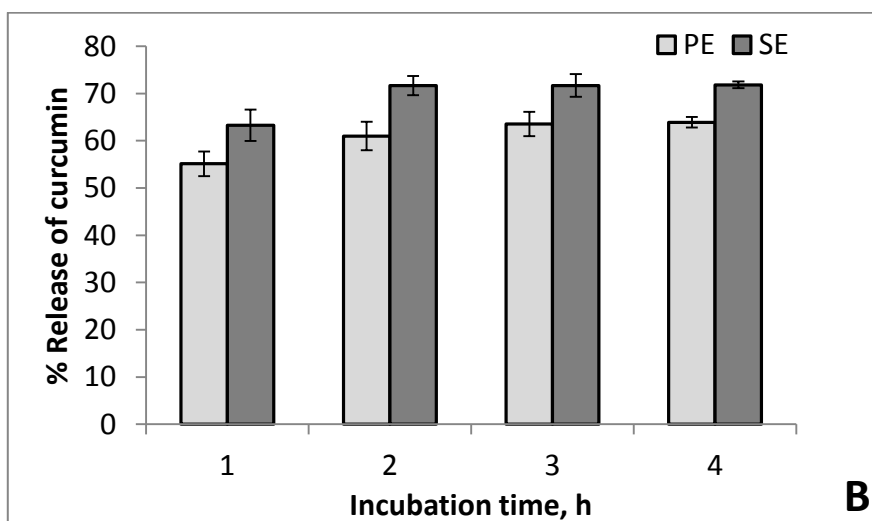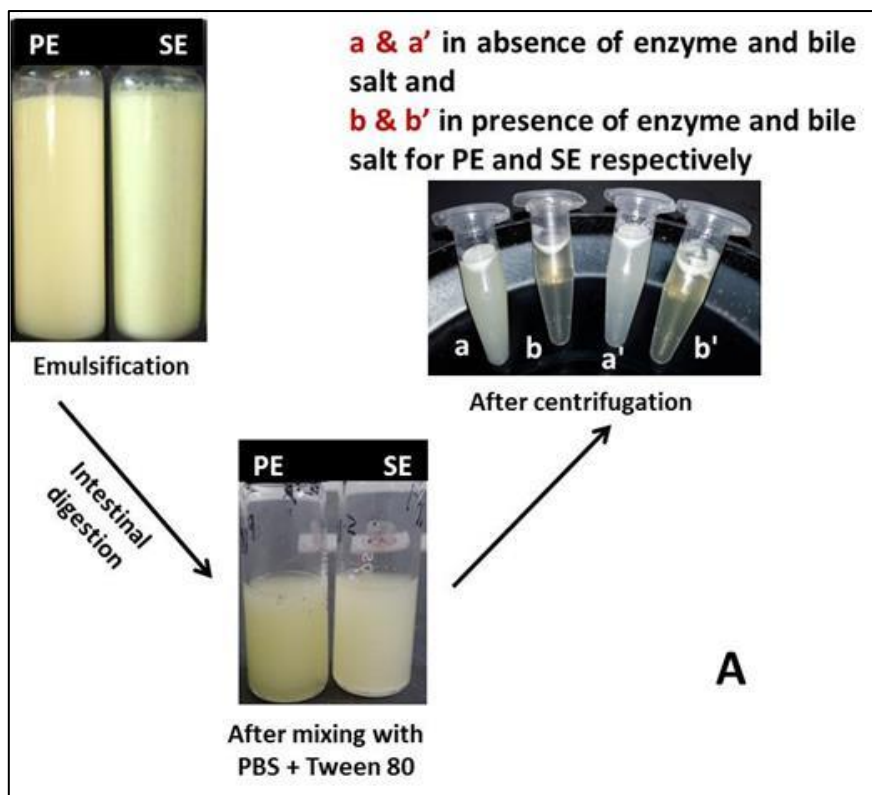
Fig. 5.7 Release of curcumin from PE and SE (A) Simulated intestinal digestion process, and (B) % curcumin release as a function of incubation time (Means of both the systems were significantly different from each other ($p < 0.05$))

5.3.6 Kinetics of In vitro release study

Different kinetic models such as zero order, first order and Higuchi model were fitted into experimental data to evaluate the kinetic rate of release of curcumin. The kinetic model showing highest correlation coefficient (R^2) was considered as the most appropriate model for the released data. The zeroth order rate describes systems when drug release is independent of initial concentration and is generally seen for poorly water soluble drugs in the matrix [42]. The first order describes the system in which the release is dependent on the concentration which is generally seen for water soluble drugs in porous matrix [42]. However, the Higuchi model describes the release of the drug from an insoluble matrix to be linearly related to the square root of time and is based on Fickian diffusion [31]. According to the Higuchi model, the drug release from nano- or micro-dispersions generally follows diffusion/degradation or a combination of diffusion and degradation mediated release phenomena [31].

As shown in Table 5.1, the best fit with the highest correlation coefficient (R^2) was observed in the zero-order release kinetic for both PE and SE. It can also be seen that the rate constant obtained for zero order kinetic model was almost same for both PE and SE which indicates that the initial concentration of curcumin has no effect on the release rate. Therefore it can be concluded that the process of breakdown of emulsion matrix system under the lipolytic activity of pancreatin in the presence of bile salt is concentration independent and followed the zero order kinetics. The data were also fitted in the Higuchi model in which a non-linear relationship was obtained which suggested that the release process is not a diffusion controlled.

Table 5.1 Kinetic analysis of curcumin release under the simulated intestinal condition

Emulsion	Zero-Order kinetic		First-Order kinetic		Higuchi Model	
	k_O, mg/min	R^2	K_1, 1/min	R^2	K_H, /min$^{1/2}$	R^2
PE	0.0007	0.98	0.0012	0.947	0.0656	0.91
SE	0.0008	0.936	0.0011	0.897	0.0356	0.871

5.4 Summary

Multilayer emulsion prepared using layer by layer approach was found to be a suitable microencapsulating system with higher encapsulation efficiency and improved chemical stability of the hydrophobic compound such as curcumin. The detailed conclusions of the study are summarized as follows:

➢ The encapsulation efficiency of curcumin in SE was found to be 100% even after a storage period of three weeks whereas it reduced to 55% in the case of PE during the storage. The double layer emulsion (SE) was found to be resistive against the phase separation during the storage which subsequently enhanced the encapsulation stability of curcumin.

➢ The freeze dried PE and SE containing curcumin were characterized using FTIR and microscopic techniques. FTIR results revealed that all the constituents of emulsions including curcumin were intact after freeze drying of the emulsions. The microstructure of the droplets coated with biopolymers remained stable in the case of SE during freeze drying.

➢ The antioxidant activity of curcumin encapsulated into different systems was also evaluated and it was found to be higher in the case of SE during storage up to three weeks, whereas it significantly reduced in the case of other encapsulating systems such as PE, oil and ethanol.

➢ A simulated intestinal digestive model was used to perform the release of curcumin during the digestion of PE and SE in presence of pancreatin enzyme and bile salt and maximum curcumin release of almost 71% and 63% was obtained in SE and PE, respectively.

➢ The release kinetic of curcumin under the simulated intestinal condition followed the zeroth order kinetic model indicated the independency of the initial concentration of curcumin in In vitro release study.

This study confirmed the successful formulation of curcumin encapsulated system for its effective applications involving the delivery of such a bioactive compound in the intestinal tract of the body.

References

(1) Araiza-Calahorra, A.; Akhtar, M.; Sarkar, A. Recent Advances in Emulsion-Based Delivery Approaches for Curcumin: From Encapsulation to Bioaccessibility. Trends Food Sci. Technol. 2018, 71, 155–169. https://doi.org/10.1016/j.tifs.2017.11.009.

(2) Peng, S.; Li, Z.; Zou, L.; Liu, W.; Liu, C.; McClements, D. J. Enhancement of Curcumin Bioavailability by Encapsulation in Sophorolipid-Coated Nanoparticles: An in Vitro and in Vivo Study. J. Agric. Food Chem. 2018, 66 (6), 1488–1497. https://doi.org/10.1021/acs.jafc.7b05478.

(3) Bar-Sela, G.; Epelbaum, R.; Schaffer, M. Curcumin as an Anti-Cancer Agent: Review of the Gap Between Basic and Clinical Applications. Curr. Med. Chem. 2010, 17 (3), 190–197. https://doi.org/10.2174/092986710790149738.

(4) Ahmed, K.; Li, Y.; McClements, D. J.; Xiao, H. Nanoemulsion- and Emulsion-Based Delivery Systems for Curcumin: Encapsulation and Release Properties. Food Chem. 2012, 132 (2), 799–807. https://doi.org/10.1016/j.foodchem.2011.11.039.

(5) Kharat, M.; Du, Z.; Zhang, G.; McClements, D. J. Physical and Chemical Stability of Curcumin in Aqueous Solutions and Emulsions: Impact of PH, Temperature, and Molecular Environment. J. Agric. Food Chem. 2017, 65 (8), 1525–1532. https://doi.org/10.1021/acs.jafc.6b04815.

(6) Sari, T. P.; Mann, B.; Kumar, R.; Singh, R. R. B.; Sharma, R.; Bhardwaj, M.; Athira, S. Preparation and Characterization of Nanoemulsion Encapsulating Curcumin. Food Hydrocoll. 2015, 43, 540–546. https://doi.org/10.1016/j.foodhyd.2014.07.011.

(7) Malik, P.; Ameta, R. K.; Singh, M. Preparation and Characterization of Bionanoemulsions for Improving and Modulating the Antioxidant Efficacy of Natural Phenolic Antioxidant Curcumin. Chem. Biol. Interact. 2014, 222, 77–86. https://doi.org/10.1016/j.cbi.2014.07.013.

(8) Malik, P.; Singh, M. Study of Curcumin Antioxidant Activities in Robust Oil-Water Nanoemulsions; New Journal of Chemistry. 2017, 41(21), 12506-19. https://doi.org/10.1039/c7nj02612a.

(9) Joung, H. J.; Choi, M. J.; Kim, J. T.; Park, S. H.; Park, H. J.; Shin, G. H. Development of Food-Grade Curcumin Nanoemulsion and Its Potential Application to Food

Beverage System: Antioxidant Property and In Vitro Digestion. J. Food Sci. 2016, 81 (3), N745–N753. https://doi.org/10.1111/1750-3841.13224.

(10) Huang, J.; Wang, Q.; Li, T.; Xia, N.; Xia, Q.; Multilayer Emulsions as a Strategy for Linseed Oil and Alpha-Lipoic Acid Micro-Encapsulation: Study on Preparation And in vitro characterization. Journal of the science of food and agriculture. 2018, 98(9), 3513-23. https://doi.org/10.1002/j.

(11) Silva, H. D.; Beldíková, E.; Poejo, J.; Abrunhosa, L.; Serra, A.T.; Duarte, C. M. M.; Brányik, T.; Cerqueira, M. A.; Pinheiro, A. C.; Vicente, A. A. Evaluating the effect of Chitosan Layer on Bioaccessibility and Cellular Uptake of Curcumin Nanoemulsions. J. Food Eng. 2019, 243, 89–100. https://doi.org/10.1016/j.jfoodeng.2018.09.007.

(12) Acevedo-Fani, A.; Silva, H. D.; Soliva-Fortuny, R.; Martín-Belloso, O.; Vicente, A. A. Formation, Stability and Antioxidant Activity of Food-Grade Multilayer Emulsions Containing Resveratrol. Food Hydrocoll. 2017, 71, 207–215. https://doi.org/10.1016/j.foodhyd.2017.05.007.

(13) Pinheiro, A. C.; Coimbra, M. A.; Vicente, A. A. In Vitro Behaviour of Curcumin Nanoemulsions Stabilized by Biopolymer Emulsifiers - Effect of Interfacial Composition. Food Hydrocoll. 2016, 52, 460–467. https://doi.org/10.1016/j.foodhyd.2015.07.025.

(14) Fioramonti, S. A.; Rubiolo, A. C.; Santiago, L. G. Characterisation of Freeze-Dried Flaxseed Oil Microcapsules Obtained by Multilayer Emulsions. Powder Technol. 2017, 319, 238–244. https://doi.org/10.1016/j.powtec.2017.06.052.

(15) Fioramonti, S. A.; Martinez, M. J.; Pilosof, A. M. R.; Rubiolo, A. C.; Santiago, L. G. Multilayer Emulsions as a Strategy for Linseed Oil Microencapsulation: Effect of pH and Alginate Concentration. Food Hydrocoll. 2015, 43, 8–17. https://doi.org/10.1016/j.foodhyd.2014.04.026.

(16) Guzey, D.; McClements, D. J. Formation, Stability and Properties of Multilayer Emulsions for Application in the Food Industry. Adv. Colloid Interface Sci. 2006, 128–130 (2006), 227–248. https://doi.org/10.1016/j.cis.2006.11.021.

(17) Guzey, D.; McClements, D. J. Impact of Electrostatic Interactions on Formation and Stability of Emulsions Containing Oil Droplets Coated by Β-Lactoglobulin-Pectin

Complexes. J. Agric. Food Chem. 2007, 55 (2), 475–485. https://doi.org/10.1021/jf062342f.

(18) McClements, D. J. Food Emulsions Principles, Practices, and Techniques Second Edition. Food Emuls. Princ. Pract. Tech. 2005. https://doi.org/10.1093/acprof:oso/9780195383607.003.0002.

(19) Pongsawatmanit, R.; Harnsilawat, T.; McClements, D. J. Influence of Alginate, PH and Ultrasound Treatment on Palm Oil-in-Water Emulsions Stabilized by β-Lactoglobulin. Colloids Surfaces A Physicochem. Eng. Asp. 2006, 287 (1–3), 59–67. https://doi.org/10.1016/j.colsurfa.2006.03.022.

(20) Carpenter, J.; George, S.; Saharan, V. K. A Comparative Study of Batch and Recirculating Flow Ultrasonication System for Preparation of Multilayer Olive Oil in Water Emulsion Stabilized with Whey Protein Isolate and Sodium Alginate. Chem. Eng. Process. 2018, 125, 139–149. https://doi.org/10.1016/j.cep.2018.01.006.

(21) Sun, C.; Gunasekaran, S. Effects of Protein Concentration and Oil-Phase Volume Fraction on the Stability and Rheology of Menhaden Oil-in-Water Emulsions Stabilized by Whey Protein Isolate with Xanthan Gum. Food Hydrocoll. 2009, 23 (1), 165–174. https://doi.org/10.1016/j.foodhyd.2007.12.006.

(22) Silva, H. D.; Poejo, J.; Pinheiro, A. C.; Donsì, F.; Serra, A. T.; Duarte, C. M. M.; Ferrari, G.; Cerqueira, M. A.; Vicente, A. A. Evaluating the Behaviour of Curcumin Nanoemulsions and Multilayer Nanoemulsions during Dynamic in Vitro Digestion. J. Funct. Foods 2018, 48, 605–613. https://doi.org/10.1016/j.jff.2018.08.002.

(23) Sivakumar, M.; Ying, S.; Wei, K. Ultrasonics Sonochemistry Cavitation Technology – A Greener Processing Technique for the Generation of Pharmaceutical Nanoemulsions. Ultrason. Sonochem. 2014, 21 (6), 2069–2083. https://doi.org/10.1016/j.ultsonch.2014.03.025.

(24) Shanmugam, A.; Ashokkumar, M. Ultrasonic Preparation of Stable Flax Seed Oil Emulsions in Dairy Systems - Physicochemical Characterization. Food Hydrocoll. 2014, 39, 151–162. https://doi.org/10.1016/j.foodhyd.2014.01.006.

(25) Carpenter, J.; Saharan, V. K. Ultrasonic Assisted Formation and Stability of Mustard Oil in Water Nanoemulsion: Effect of Process Parameters and Their Optimization.

Ultrason. Sonochem. 2017, 35, 422–430. https://doi.org/10.1016/j.ultsonch.2016.10.021.

(26) Tang, S. Y.; Shridharan, P.; Sivakumar, M. Impact of Process Parameters in the Generation of Novel Aspirin Nanoemulsions - Comparative Studies between Ultrasound Cavitation and Microfluidizer. Ultrason. Sonochem. 2013, 20 (1), 485–497. https://doi.org/10.1016/j.ultsonch.2012.04.005.

(27) Leong, T.S.; Manickam, S.; Martin, G.J.; Li, W.; Ashokkumar, M. Springer Briefs In Molecular Science, Ultrasonic Production of Nano-Emulsions for Bioactive Delivery in Drug and Food Applications, 2018. https://doi.org/10.1007/978-3-319-73491-0.

(28) Sari, T. P.; Mann, B.; Sharma, R.; Kumar, R. Process Optimization for the Production of Nanoencapsulated Curcumin and Analysis for Physicochemical Characteristics and Antioxidant Mechanism. Int. J. Biotechnol. Bioeng. Res. 2013, 4 (6), 581–586.

(29) Ahmed, K. Encapsulation of Curcumin in O / w Nanoemulsions and Its Bioaccessibility After In Vitro Digestion., Master thesis. 2014. University of Massachusetts Amherst.

(30) Chen, X.; Zou, L. Q.; Niu, J.; Liu, W.; Peng, S. F.; Liu, C. M. The Stability, Sustained Release and Cellular Antioxidant Activity of Curcumin Nanoliposomes. Molecules 2015, 20 (8), 14293–14311. https://doi.org/10.3390/molecules200814293.

(31) Piotrowska, U., Oledzka, E., Kamysz, W., Białek, S., & Sobczak, M. The Effect of Polymer Microstructure on Encapsulation Efficiency and Release Kinetics of Citropin 1.1 from the Poly (ε-caprolactone) Microparticles. Nanomaterials, 2018, *8*(7), 482.

(32) Elmeshad, A. N., S. M. Mortazavi, and M. R. Mozafari. Formulation and characterization of nanoliposomal 5-fluorouracil for cancer nanotherapy. Journal of liposome research, 2014, 24(1), 1-9.

(33) Adelmann, H.; Binks, B. P.; Mezzenga, R. Oil Powders and Gels from Particle-Stabilized Emulsions. Langmuir 2012, 28 (3), 1694–1697. https://doi.org/10.1021/la204811c.

(34) Li, P.; Dai, Y.; Zhang, J.; Wang, A.; Wei, Q. Chitosan-Alginate Nanoparticles as a Novel Drug Delivery System for Nifedipine. Int. J. biomedical science. 2008, 4 (3), 221–228.

(35) Yang, H.; Irudayaraj, J.; Paradkar, M. M. Food Chemistry Discriminant Analysis of Edible Oils and Fats By FTIR, FT-NIR and FT-Raman spectroscopy. Food Chemistry. 2005, 93, 25–32. https://doi.org/10.1016/j.foodchem.2004.08.039.

(36) Silva, E. K.; Zabot, G. L.; Meireles, M. A. A. Ultrasound-Assisted Encapsulation of Annatto Seed Oil : Retention and Release of a Bioactive Compound with Functional Activities. Food Res. Int. 2016, 78, 159–168. https://doi.org/10.1016/j.foodres.2015.10.022.

(37) Ak, T. Chemico-Biological Interactions Antioxidant and Radical Scavenging Properties of Curcumin. Chem.-Bio. Int., 2008, 174, 27–37. https://doi.org/10.1016/j.cbi.2008.05.003.

(38) Aksoy, L.; Kolay, E.; Ağılönü, Y.; Aslan, Z.; Kargıoğlu, M.; Free Radical Scavenging Activity , Total Phenolic Content, Total Antioxidant Status, and Total Oxidant Status of Endemic Thermopsis Turcica. Saudi Journal of Biological Sciences, 2013, 235–239. https://doi.org/10.1016/j.sjbs.2013.02.003.

(39) Sabatini, N.; Perri, E.; Rongai, D. Olive Oil Antioxidants and Aging; Elsevier Inc., 2018. https://doi.org/10.1016/B978-0-12-811442-1/00004-3.

(40) Souza, S. D. A Review of In Vitro Drug Release Test Methods for Nano-Sized Dosage Forms. Adv. Pharm. 2014, 2014 (304757), 1–12. https://doi.org/10.1155/2014/304757.

(41) Tikekar, R. V; Pan, Y.; Nitin, N. Fate of Curcumin Encapsulated in Silica Nanoparticle Stabilized Pickering Emulsion during Storage and Simulated Digestion. Food Res. Int. 2013, 51 (1), 370–377. https://doi.org/10.1016/j.foodres.2012.12.027.

(42) Najib, N., and M. S. Suleiman. The kinetics of drug release from ethylcellulose solid dispersions." Drug Development and Industrial Pharmacy, 1985, 11(12), 2169-2181.

CHAPTER 6

CONCLUSIONS AND

SCOPE FOR FUTURE WORK

6.1 Conclusions

It has been concluded that the ultrasonication and hydrodynamic cavitation can be effectively used for the synthesis of oil water emulsions that are utilized in variety of food, pharmaceutical and cosmetic products. This thesis work shows that both techniques have a potential to produce emulsion of desired sizes, while their successful implementation on an industrial scale depends on several conditions such as emulsion compositions, operating parameters and physicochemical properties of ingredients of emulsions (density, viscosity and pH of the solution) to be produced. The following conclusion can be drawn from this work.

It has been found that the ultrasonication and hydrodynamic cavitation is capable of producing the emulsion having the size on nano scale. The work reported in chapter 2 indicates that ultrasonication process was found to be effective to produce the emulsion of size 87 nm with enhanced kinetic stability up to 3 months. Apart from that it was also established that the ultrasonication process didn't affect the oil molecular structure as observed in the FTIR analysis. Moreover hydrodynamic cavitation was also employed to prepare the same nanoemulsion with the same ingredients and it has been found that HC process has capability to produce emulsion of size below 100 nm. It was observed that at a moderate operating pressure of 10 bar with orifice device, the minimum droplet size of 87 nm was achieved and it was concluded that the droplet size below 100 nm can be achieved by operating HC devices at cavitation number in the range of 0.17 to 0.20. Moreover, the detailed geometrical investigation of orifice and venturi based cavitating device was also carried out and it was found that the single hole orifice plate of circular shape having lower perimeter was found to be efficient for producing the emulsion with enhanced kinetic stability of 3 months. Based up on the energy efficiency comparison with ultrasonication, hydrodynamic cavitation was found to be more cost effective technique.

Further the potential of ultrasonication process for the synthesis of multilayer emulsion and the process intensification was explored in which the detailed investigation on the physical and oxidative stability of ultrasonically prepared multilayer emulsions with protein and polysaccharide biopolymers was done. Initially, to establish a double layer formation, the electrostatic interaction between WPI and SA was evaluated by measuring the zeta potential and it was found that in the basic condition (pH 6 and 7), emulsions were flocculated by

means of depletion mechanism whereas under acidic condition (pH 4), emulsions were destabilized by bridging flocculation. However, at an intermediate pH 5, the interaction was good and emulsion formed was found to be stable without any separation observed during the storage. It has been also observed that the controlled sonication not only improved the stability of multilayer emulsion against flocculation but also helped to prevent the oxidation of lipid which was measured by evaluating the peroxide value of emulsion. The ultrasonication process was also employed in a recirculating flow mode for the formation of similar emulsion and it was found that the recirculating approach was found to be more effective than batch ultrasonication process indicating its potential for the large scale operation.

The study reported in chapter 5 was focused on the effective utilization of the synthesized multilayer emulsions for the encapsulation of curcumin. This study investigated the comparison of single layer and double layer emulsion prepared using ultrasonication based on their encapsulation efficiency, antioxidant activity and release properties of curcumin during storage. It has been observed that the formation of a double layer coating over the primary coated droplets enhanced the encapsulation efficiency as well as antioxidant activity of curcumin during the storage of 3 weeks. Moreover, multilayer emulsions encapsulating curcumin were freeze dried in order to see the effect of dehydration on the stability of multilayer coated droplets. FTIR and morphological analysis revealed that the microstructure of emulsion droplets was found to be stable in case of SE. In vitro release of curcumin from the multilayer emulsion was carried out under simulated intestinal condition in the presence of pancreatin enzyme and bile salt and it was found that the curcumin was released in a controlled manner as a result of the digestion of lipids and biopolymers in the simulated intestinal conditions. In overall this study provides the useful information on the formation of multilayer emulsion as a carrier system for the better protection and controlled release of curcumin which could be useful and relevant in food and pharmaceutical applications.

6.2 Scope of future work

There is further scope for the improvement to make the ultrasonication and hydrodynamic cavitation as more cost effective and energy efficient techniques for the emulsification process on the large scale of operation. The future work can be carried out on the:

1. Development of hybrid cavitation i.e. combination of US and HC for the synthesis of food emulsions in order to see the effect of combination of low and high frequency cavitation on the various emulsification process parameters such as rate of size reduction, stability etc.

2. Design of higher perimeter hydrodynamic cavitating devices with different geometries in order to achieve the desired rate of size reduction and high stability especially in the case of emulsions stabilized using biopolymers.

3. Use of high power ultrasonicator to process large volumes in batch and recirculating mode.

4. Incorporation of other pharmaceutical drugs which are highly susceptible to the environmental stresses and study of the encapsulation stability, bioavailability and release kinetics of different drugs.

5. Modeling and simulation of formation and deformation of emulsion droplets (such as coalescence and Ostwald ripening) prepared at different operating conditions of ultrasonication and HC. Development of mathematical correlations and model equations using the parameters such as droplet size and shear generated (in case of ultrasonication, power density and in case of HC, throat size, cavitation number) such that required droplet size can be correlated to the geometrical and operating parameters of a cavitating device.

6. Rheological assessment of the emulsions prepared using cavitation to see the variation in the viscosity of the emulsions under different stresses.

PUBLICATIONS

Curcumin Encapsulation in Multilayer Oil-in-Water Emulsion: Synthesis Using Ultrasonication and Studies on Stability and Antioxidant and Release Activities

Jitendra Carpenter, Suja George, and Virendra Kumar Saharan*

Department of Chemical Engineering, Malaviya National Institute of Technology, Jaipur 302017, India

ABSTRACT: Curcumin is a natural polyphenol compound obtained from the turmeric plant, having numerous promising health benefits. To deliver curcumin into the human body, it is necessary to develop an efficient carrier system for its encapsulation such that the physicochemical properties of curcumin can be preserved during storage. In this study, the encapsulation stability, antioxidant activity, and release properties of curcumin encapsulated in the primary emulsion (PE: 0.0022% (w/w) curcumin, 9.99% (w/w) oil, 0.9% (w/w) whey protein isolate, pH 7) and secondary emulsion (SE: 0.00108% (w/w) curcumin, 4.90% (w/w) oil, 0.443% (w/w) WPI, 0.2% (w/w) sodium alginate, pH 5) prepared using ultrasonication were analyzed. It was observed that the formation of a double-layer coating of secondary biopolymer over the primary coated droplet enhanced the encapsulation efficiency and antioxidant activity of the curcumin during storage for 3 weeks. Moreover, the multilayer emulsions were freeze-dried to see the effect of dehydration of emulsion on the stability of multilayer-coated droplets. Fourier transform infrared analysis indicated the presence of all of the constituents, including curcumin, after the freeze drying of the emulsions. Scanning electron microscopy images showed that the microstructure of emulsion droplets was found to be uniformly distributed in the case of SE. The antioxidant activity of curcumin encapsulated in SE was found to be higher during storage, whereas it was significantly reduced in other encapsulated systems like PE, olive oil, and ethanol. In vitro release of curcumin from the multilayer emulsion was carried out under the simulated intestinal conditions of pancreatin enzyme and bile salt. Maximum releases of 71 and 63% were obtained in SE and PE, respectively, within 2 h of digestion. Overall, this study provides useful information on the formation of multilayer emulsion as a carrier system for the better protection and release of curcumin useful for food and pharmaceutical applications.
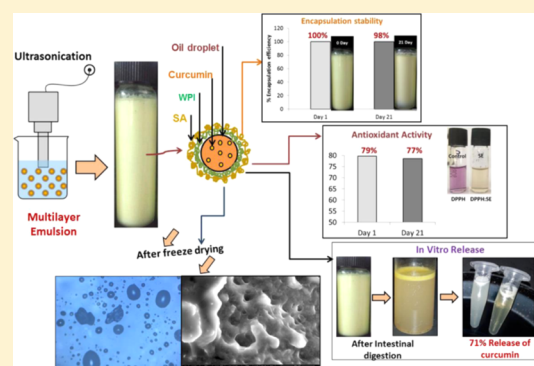
INTRODUCTION

Curcumin is a well-known nutraceutical polyphenol compound obtained from the turmeric plant that possesses various chemical and biological properties such as anticancer, antioxidant, anti-inflammatory, antibacterial, anticarcinogenic activities, and so on.[1,2] Curcumin comprises various chemical-reactive functional groups that are found to be effective against cells of various diseases like cancer, arthritis, asthma, atherosclerosis, heart disease, etc.[3] Recently, curcumin has gained significant interest among the researchers in the field of medicinal and pharmaceutical industries due to its promising health properties. However, there are challenges for its utilization in functional foods, medicines, and other products because of poor water solubility, low bioavailability, and chemical instability against physiological conditions such as pH.[1,4,5] In the last decade, several research works have been carried out to overcome these limitations using lipid-based emulsification for encapsulating lipophilic compounds such as curcumin.[6−9] The encapsulation technique via O/W emulsification includes the incorporation of curcumin in the core (oil phase) of the emulsion matrix that improves the stability and functionality and facilitates their controlled release. Recently, the use of a novel emulsion matrix system prepared using layer-

by-layer approach, known as multilayer emulsion for the encapsulation of lipophilic compounds, has attracted researcher's interest to achieve this goal.[10−14] Multilayer emulsification is a potential strategy for the encapsulation of lipophilic compounds, and this system has several advantages over other conventional nanoemulsions; for example, it enhances the physical and oxidative stability, provides protection against environmental conditions, promotes greater bioavailability, and allows controlled release in the GI tract of the body. In addition, the material and composition of the interfacial coating can be designed in such a way that the emulsion responds to specific triggers for the release of bioactive compounds.[11,12]

Multilayer emulsions are formed using layer-by-layer approach, which includes the deposition of alternative layers of oppositely charged biopolymers such as protein and polysaccharides over the oil droplets. The electrostatically charged layer of biopolymers forms a thick interfacial membrane at the oil−water interface that helps to inhibit the

Ultrasonic assisted formation and stability of mustard oil in water nanoemulsion: Effect of process parameters and their optimization

CrossMark

Jitendra Carpenter, Virendra Kumar Saharan *

Chemical Engineering Department, Malaviya National Institute of Technology, Jaipur 302017, India

A B S T R A C T

The present work reports the ultrasound assisted preparation of mustard oil in water nanoemulsion stabilized by Span 80 and Tween 80 at different operating conditions. Effects of various operating parameters such as HLB (Hydrophilic Lipophilic Balance) value, surfactant volume fraction (φ_S), oil volume fraction (φ_O) and power amplitude were investigated and optimized on the basis of droplet size and stability of nanoemulsions. It was observed that minimum droplet size of about 87.38 nm was obtained within 30 min of ultrasonication at an optimum HLB value of 10, φ_S of 0.08 (8%, v/v), φ_O of 0.1 (10%, v/v) and ultrasonic power amplitude of 40%. The stability of the nanoemulsion was measured through visual observation and it was found that the unstable emulsions got separated within 24 h whereas, stable emulsions never showed any separation until 90 days. In addition to that, the kinetic stability of the prepared nanoemulsions was also assessed under centrifuge and thermal stress conditions. The emulsion stability was found to be unaffected by these forces as the droplet size remained unchanged. The ultrasound prepared emulsion was found to be long term stable even after 3 months of storage at ambient conditions without any visual evidence of creaming and phase separation and also remained kinetically stable. FTIR analysis of the emulsions at different sonication conditions was carried out to examine the possible impact of ultrasonically induced chemical effects on oil structure during emulsification and it was found that the oil molecular structure was unaffected by ultrasonication process. The present work illustrates the formation and stability of mustard oil in water nanoemulsion using ultrasound cavitation which may be useful in food and cosmetic based applications.

© 2016 Elsevier B.V. All rights reserved.

1. Introduction

Nanoemulsions are gaining more interest due to their wide applications in food industries, pharmaceuticals, cosmetics, etc. because of their several benefits. Due to the nano droplet size, nanoemulsions retain long term stability i.e. up to several months and years [1] as compared to other conventional emulsions. Prior to the application of nanoemulsions, their characteristics and stability are to be well established. Mainly the emulsion stability against the various breakdown processes including coalescence, flocculation, creaming and Ostwald ripening, pose a great limitation against its use and synthesis [2].

In food applications, nanoemulsions are found as a novel system for delivery of various nutraceuticals. Nanoemulsions have potential to improve the solubility and bioavailability of many food active compounds and therefore serve as a carrier for the delivery of lipophilic active compounds in food applications [3,4]. In

pharmaceuticals, nanoemulsion is suitable for drug delivery because of its ability in solubilizing the non-polar active compounds [5–7]. In cosmetics, nanoemulsions can be used for synthesis of skin and hair care products.

A nanoemulsion is a non-equilibrium system (i.e. thermodynamically unstable) and hence cannot be formed spontaneously [2]. Also, large amounts of emulsifiers are avoided in food, pharmaceuticals, and cosmetics based nanoemulsions. Therefore nanoemulsions require some desired amount of energy either in the form of agitation or mechanical disturbances to assist the emulsification process thus breaking the interface and reducing the emulsion droplet size [8]. Generally, high speed agitators and high pressure homogenizers are preferred for the preparation of nanoemulsions but these techniques consume high energy and have less control over the particle size distribution and stability of emulsions [8,9]. On the other side, Ultrasound method is found to be an efficient technique for the preparation of nanoemulsions that has better control over the characteristics of emulsions [9–12]. When ultrasound waves are transferred through the liquid medium, they create cavitation phenomena which comprise of the

---

* Corresponding author.
  E-mail address: vksaharan.chem@mnit.ac.in (V.K. Saharan).
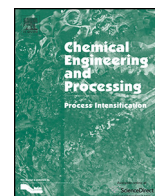
Low pressure hydrodynamic cavitating device for producing highly stable oil in water emulsion: Effect of geometry and cavitation number

Jitendra Carpenter, Suja George, Virendra Kumar Saharan*

Chemical Engineering Department, Malaviya National Institute of Technology, Jaipur, 302017, India

A B S T R A C T

In present work, the detailed geometrical analysis of hydrodynamic cavitating devices was carried out to investigate the effect of geometry (orifice and venturi of different shapes) and geometrical parameters on the formation and stability of mustard oil in water nanoemulsion. The optimization of geometrical parameters was carried out based on the lowest droplet size obtained and droplet size reduced per unit pass. It was observed that the single hole orifice plate of circular shape having lower perimeter and higher flow area than other orifice devices, was found to be an efficient device which produced emulsion of lowest droplet size i.e. 87 nm at an optimum C_V of 0.19 (10 bar optimum operating pressure) in 90 min of processing time. Moreover, it was found that the kinetic stability of the nanoemulsion assessed under centrifugal and thermal stress conditions remained unaffected by these forces. The prepared nanoemulsion using hydrodynamic cavitation (HC) was found to be physically stable up to 3 months indicating the potential of HC over high energy techniques for producing highly stable emulsion with droplet size below 100 nm on a large scale. Furthermore HC was found to be 11 times energy efficient than acoustic cavitation/ultrasonication for the preparation of nanoemulsion.

© 2017 Elsevier B.V. All rights reserved.

1. Introduction

Nanoemulsions exhibit long-term stability as compared to the conventional emulsions (macroemulsion) because they possess droplet size in the range of 50–100 nm as evident in several studies [1–7]. Macroemulsions possesses droplet size more than 1 μm and thus they lose their kinetic stability more rapidly under different breakdown conditions such as creaming, coalescence, flocculation, Ostwald ripening etc [8]. Although nanoemulsions are non-equilibrium systems (thermodynamically unstable), they are found to be kinetically stable for several months/years against its separation into constituent phases [1–3,6]. Therefore, because of its high stability, nanoemulsions have enormous potential in a wide range of applications such as in foods, pharmaceuticals, cosmetics, paints, and synthesis of other nanomaterials, etc. [3–7].

Nanoemulsions require adequate amount of energy either in the form of agitation or mechanical disturbances to achieve the emulsion droplet size on a nanoscale [8]. In past decades, many researchers studied high energy methods for the formation of nanoemulsions [5,8–10]. High energy methods include using high speed homogenizers [11], high pressure homogenizers [12], colloid mills [13], microfluidizer [14,15], and ultrasound processors [7,14,16–18] for agitation. High pressure homogenizers and microfluidizer are usually operated at high pressure in the order of ~1000 bar or higher [12,14,15], whereas high speed rotors are operated at high speed in order of ~10^4 RPM [11]. These equipments consume high energy and therefore are not found to be economical for large scale operations. Ultrasound processors are also efficient for nanoemulsion synthesis but they are only suitable for small scale and batch operations [7,16–18]. Thus, to overcome high energy consumption, low energy methods have been used which can be scaled up in an economical manner for production of nanoemulsions on a large scale.

In recent years, hydrodynamic cavitation (HC) was developed as an emerging technique capable of intensifying the emulsification process on a large scale. HC is typically caused by affecting pressure variations in a flowing liquid as it passes through a constriction in a pipe. The variation of pressure through the constriction channel such as venturi and orifice plate with different geometry leads to the generation of cavities [19–21]. These generated cavities undergo a subsequent adiabatic collapse resulting in the formation of a supercritical state of localized high temperature zones in the range of 1000–5000 K and pressure in the range of 100–1000 bar, known as a hot spot [20]. These generated hot spots can induce

A comparative study of batch and recirculating flow ultrasonication system for preparation of multilayer olive oil in water emulsion stabilized with whey protein isolate and sodium alginate

Jitendra Carpenter, Suja George, Virendra Kumar Saharan*

Chemical Engineering Department, Malaviya National Institute of Technology, Jaipur, 302017, India

ABSTRACT

The present study reports process intensification by ultrasonication of multilayer oil in water (O/W) emulsion stabilized with whey protein isolate (WPI) and sodium alginate (SA). Ultrasonication was employed in both batch and recirculating flow configurations. The effect of process parameters such as pH, SA concentration, and sonication time on droplet size, zeta potential, morphology, physical and oxidative stability of the multilayer emulsion was studied using batch process. It was observed that the emulsion prepared at pH 5, 0.2 wt% SA and 60 s sonication had good bilayer interaction between WPI and SA molecules. Moreover, it was found that sonication if given for a controlled time period can improve the physical and oxidative stability of the emulsion. Further, the ultrasonication based recirculating flow configuration (RFC) was utilized for the preparation of multilayer emulsion at the optimum operational conditions obtained in the batch studies. The emulsions prepared using RFC were found to have better physical and oxidative stability than using batch ultrasonication at the optimum flow rate of 0.5 L/min with 6 recirculation passes. RFC was found to be 2.5 times more energy efficient than batch ultrasonication process for the synthesis of multilayer emulsions.

1. Introduction

Oil in water (O/W) emulsions consisting of the dispersion of small lipid droplets in a continuous phase have been utilized in variety of food, pharmaceutical and cosmetic products [1–6]. Among all the functional bioactive compounds, mono and poly unsaturated fatty acids are found to be the essential compounds that provide several health benefits [7,8]. Their incorporation into O/W emulsions provide a perfect microencapsulating atmosphere for lipids to prevent them from the lipid auto-oxidation as well as to maintain their nutritional quality [1,9]. These essential fats are highly susceptible to the attack of oxidative radicals and get oxidized under various environmental stresses such as air, light and thermal processing [9,10].

The major challenge in this area is to produce emulsions with high stability against the various instability factors such as creaming, coalescence, flocculation, and oxidation during storage [11]. The two major deciding factors for producing a highly stable O/W emulsion are the choice of suitable emulsifier(s) and intensity of shear supplied for homogenization. Relying only on one of them would pose a great challenge in terms of technical and economic feasibility of food emulsions. Protein, an amphiphilic emulsifier has an ability to get dispersed

during the emulsification process by rapidly adsorbing at the oil-water interface, reducing the interfacial tension and prevents the oil droplets against coalescence and flocculation [9]. But the protein stabilized emulsions are highly sensitive to the pH and temperature variations [1,10,12].

In the recent decade, many studies reported the utilization of protein-polysaccharide combinations for stabilizing the emulsions [8,10,13,14]. The preparation of such emulsions using layer by layer (LbL) approach attracted more interest in recent years because of many advantages such as perfect encapsulation for lipids, preventing them from the attack of peroxides and the controlled release of bioactive compounds. In LbL method, primary emulsion stabilized with a charged emulsifier (protein) is produced by homogenization and thereafter diluted with oppositely charged polysaccharide, to form a double layer or secondary emulsion. The formation of an electrostatically charged double layer of protein and polysaccharide forms a thicker interfacial membrane at the oil-water interface which consequently increases the electrostatic repulsion between the droplets thereby stabilizing the emulsions against coalescence. However to produce highly stable multilayer emulsion, it becomes necessary to select an appropriate process condition such as the concentration of biopolymers, level of

Jitendra Carpenter, Mandar Badve, Sunil Rajoriya, Suja George, Virendra Kumar Saharan*
and Aniruddha B. Pandit

Hydrodynamic cavitation: an emerging technology for the intensification of various chemical and physical processes in a chemical process industry

Abstract: Hydrodynamic cavitation (HC) has been explored by many researchers over the years after the first publication on hydrolysis of fatty oils using HC was published by Pandit and Joshi [Pandit AB, Joshi JB. Hydrolysis of fatty oils: effect of cavitation. Chem Eng Sci 1993; 48: 3440–3442]. Before this publication, most of the studies related to cavitation in hydraulic system were concentrated to avoid the generation of cavities/cavitating conditions. The fundamental concept was to harness the energy released by cavities in a positive way for various chemical and mechanical processes. In HC, cavitation is generated by a combination of flow constriction and pressure-velocity conditions, which are monitored in such a way that cavitating conditions will be reached in a flowing system and thus generate hot spots. It allows the entire process to operate at otherwise ambient conditions of temperature and pressure while generating the cavitating conditions locally. In this review paper, we have explained in detail various cavitating devices and the effect of geometrical and operating parameters that affect the cavitation conditions. The optimization of different cavitating devices is discussed, and some strategies have been suggested for designing these devices for different applications. Also, various applications of HC such as wastewater treatment, preparation of nanoemulsions, biodiesel synthesis, water disinfection, and nanoparticle synthesis were discussed in detail.

Keywords: biodiesel synthesis; hydrodynamic cavitation; microbial cell disruption; nanomaterials; wastewater treatment.

*Corresponding author: Virendra Kumar Saharan, Department of Chemical Engineering, Malaviya National Institute of Technology, Jaipur 302017, India, e-mail: vksaharan.chem@mnit.ac.in
Jitendra Carpenter, Sunil Rajoriya and Suja George: Department of Chemical Engineering, Malaviya National Institute of Technology, Jaipur 302017, India
Mandar Badve and Aniruddha B. Pandit: Department of Chemical Engineering, Institute of Chemical Technology, Mumbai 400019, India

1 Introduction

In the last decade, cavitation technique has been extensively studied, and it has been successfully applied for the various physical, chemical, and biological processes. This novel technique not only produces the desirable transformation but also reduces the total processing cost and is found to be more energy efficient than many other conventional techniques. Cavitation offers immense potential for the intensification of various physical and chemical processes in an energy efficient manner (Gogate and Kabadi 2009).

Cavitation is defined as a phenomenon of formation, growth, and collapse of microbubbles or cavities, occurring in a few milli- to microseconds at multiple locations in the reactor and thus releases large magnitude of energy in a short span of time (Mahulkar and Pandit 2010). Cavitation is initiated with the formation of vapor cavities (bubbles or voids) when liquid enters into the low-pressure region, and subsequently these cavities attain a maximum size under the conditions of isothermal expansion. In the successive compression cycle, an immediate adiabatic collapse occurs, resulting in the formation of supercritical state of high local temperature and pressure, known as hot spot. The chemical and physical transformations required for the process occur because of these intense temperature and pressure conditions that are generated in these hot spots. The mechanical or physical effects of cavitation, such as the microjet streaming and high-intensity local turbulence, are mainly responsible for the intensification of physical processes such as synthesis of nanoemulsion, nanoparticle formation, microbial disruption, and disinfection. By contrast, its chemical effects, such as the generation of highly reactive free radicals in the aqueous environment, are mainly responsible for the intensification of chemical processes such as synthesis of chemicals, degradation of the water pollutants, etc.

Cavitation can be generated in a liquid medium either through flow variation in a flowing liquid known as hydrodynamic cavitation (HC) or by passing ultrasonic waves through the liquid known as acoustic

Sunil Rajoriya, Jitendra Carpenter, Virendra Kumar Saharan* and Aniruddha B. Pandit

Hydrodynamic cavitation: an advanced oxidation process for the degradation of bio-refractory pollutants

Abstract: In recent years, water pollution has become a major problem for the environment and human health due to the industrial effluents discharged into the water bodies. Day by day, new molecules such as pesticides, dyes, and pharmaceutical drugs are being detected in the water bodies, which are bio-refractory to microorganisms. In the last two decades, scientists have tried different advanced oxidation processes (AOPs) such as Fenton, photocatalytic, hydrodynamic, acoustic cavitation processes, etc. to mineralize such complex molecules. Among these processes, hydrodynamic cavitation (HC) has emerged as a new energy-efficient technology for the treatment of various bio-refractory pollutants present in aqueous effluent. In this review, various geometrical and operating parameters of HC process have been discussed emphasizing the effect and importance of these parameters in the designing of HC reactor. The advantages of combining HC with other oxidants and AOPs such as H_2O_2, ozone, Fenton process, and photocatalytic process have been discussed with some recommendation for large-scale operation. It has been observed that the geometry of the HC device and other operating parameters such as operating pressure and cavitation number are the key design parameters that ultimately decide the efficacy and potentiality of HC in degrading bio-refractory pollutants on an industrial scale.

Keywords: cavitation number; cavitational yield; hybrid methods; hydrodynamic cavitation; industrial wastewater treatment.

*Corresponding author: Virendra Kumar Saharan, Department of Chemical Engineering, MNIT, Jaipur-302017, India, e-mail: vksaharan.chem@mnit.ac.in
Sunil Rajoriya and Jitendra Carpenter: Department of Chemical Engineering, MNIT, Jaipur-302017, India
Aniruddha B. Pandit: Chemical Engineering Department, Institute of Chemical Technology, Matunga, Mumbai-400019, India

1 Introduction

The treatment of wastewater containing bio-refractory pollutants (which have the tendency to resist the conventional biological treatment) from various industries has been a major environmental problem. Water is being polluted by industrial and commercial actions, agricultural practices, and day-to-day human activities. Human health is affected by water pollution typically due to the contamination of drinking water from waste streams. Several industries such as pesticides, dyes, textiles, and many other industries are continuously polluting water as they contain large quantities of organic pollutants. These organic molecules are bio-refractory or very toxic to microorganisms. Hence, conventional biological methods are not capable of completely degrading such complex compounds due to high toxicity and carcinogenicity (Saharan et al. 2011, 2013). In the past years, many researchers have developed various methods for the degradation of organic pollutants such as carbon bed adsorption, biological methods, oxidation using chlorination and ozonation, electrochemical methods, membrane processes, and many other advanced oxidation processes (AOPs) (Mrowetz et al. 2003, Gogate and Pandit 2005, Martin et al. 2008, Rajoriya and Kaur 2014, Secondes et al. 2014, Dai et al. 2015). Most of the AOPs such as Fenton process, photocatalytic, hydrodynamic, and acoustic cavitation (AC) have been established in research laboratories effectively, but several challenges are faced by many industries to scale them up. In general, AOPs are a set of processes that involve the generation of highly reactive and non-selective hydroxyl radicals ($^\bullet OH$), which have high oxidation potential (2.80 eV) and are capable of oxidizing toxic organic/inorganic compounds and non-biodegradable pollutants (Behnajady et al. 2008a, Mendez-Arriaga et al. 2009, Wang and Zhang 2009, Bagal and Gogate 2012). Among all the AOPs, hydrodynamic cavitation (HC) process is found to improve the treatment ability to a greater extent and gives better energy efficiency for the removal/degradation of bio-refractory pollutants on an industrial